Technical Report

RENEWABLE ENERGY
POWER SYSTEM
MODULAR
SIMULATOR

RPM-SIM

User's Guide

By

Jan T. Białasiewicz, Ph.D., P.E.
Eduard Muljadi, Ph.D.
R. Gerald Nix, Ph.D., P.E.
Stephen Drouilhet, P.E.

NREL

Contents

PART I

SIMULATOR DESCRIPTION

PART II

CASE STUDIES
AND
VALIDATION TESTS

Appendix A

How to Set-up and Run the Simulation

Appendix B

Synchronous Generator Model E7201L1 Data Sheet

Appendix C

Wales Control System Dump Load Dispatch at the HPTB

Appendix D

Documentation for RPM-S<small>IM</small> at NREL's
National Wind Technology Center

Purpose and General Characteristics

The advantage of hybrid power systems is the combination of the continuously available diesel power and locally available, pollution-free wind energy. With the hybrid power system, annual diesel fuel consumption can be reduced and pollution can be minimized at the same time. To take full advantage of the wind energy when it is available and to minimize diesel fuel consumption, a proper control strategy must be developed. The control system is subject to the specific constraints of a particular application. It has to maintain power quality, measured by the quality of electrical performance, meaning that both the voltage and the frequency must be controlled. Because of this, a simulation study of each new system is needed to confirm that a control strategy results in desired system performance.

Using the VisSim™[1] visual environment, we developed a modular simulation system to facilitate an application-specific and low-cost study of the system dynamics for wind–diesel hybrid power systems. The simulation study can help in the development of control strategies to balance the system power flows under different generation/load conditions. Using the typical modules provided, it is easy to set up a particular system configuration.

In this manual, we present the principal modules of the simulator. Using case studies of a hybrid system, we also demonstrate some of the benefits that can be gained from understanding the effects of the designer's modifications to these complex dynamic systems. In these systems, the diesel generator, working as a master, controls the voltage and the frequency. The wind speed varies with time, as does the village load. Therefore, we regard the diesel generator as a controlled energy source, whereas the wind is an uncontrolled energy source and the village load is an uncontrolled energy sink. The diesel generator balances the difference between the power consumed by the village load and the power generated by the wind turbine. On occasion, the wind speed can be very high, resulting in energy generation that exceeds the energy demand of the village load. Under such circumstances, the power from the diesel becomes very low, and the wind may try to drive the diesel engine. Should the wind turbine override the diesel, the frequency control could be lost, and the system would become unstable. To avoid this, the dump load is controlled so that the power generated by the diesel will always be higher than a minimum value. In addition, the energy surplus can be saved for future use by utilizing the rotary converter/battery assembly. Therefore, the dump load should be regarded as a controlled energy sink. When the battery is being discharged, the rotary converter/battery assembly should be viewed as a controlled energy source. On the other hand, when the battery is being charged, it should be seen as a controlled energy sink. By properly choosing the sequence of events programmed for our case studies, we demonstrate that all operation aspects of the hybrid power system, briefly discussed above, can be easily taken into consideration. The single-line diagram of a typical hybrid power system, which involves all modules available in the simulator, is shown in Figure 1-1. The user must include the point of common coupling (PCC) module, as a

---

[1] VisSim is the trademark of Visual Solutions.

node where all power sources and power sinks are connected, in every simulation diagram. The other principal modules shown in Figure 1-1 are the diesel generator (DG), the AC wind turbine (WT) with the induction generator and the wind speed time series as the input, the rotary converter (RC) with the battery bank (BB), the village load (VL), the dump load (DL), the inverter, and the PV array (PV). In addition, R+jX represents the transmission-line impedance and PFC represents the power factor-correcting capacitors. In all electrical simulations, we use the d-q axis convention and synchronous reference frame. In particular, in the PCC module, the q-axis and d-axis components v_{qs1} and v_{ds1} of the line voltage V_s are defined.
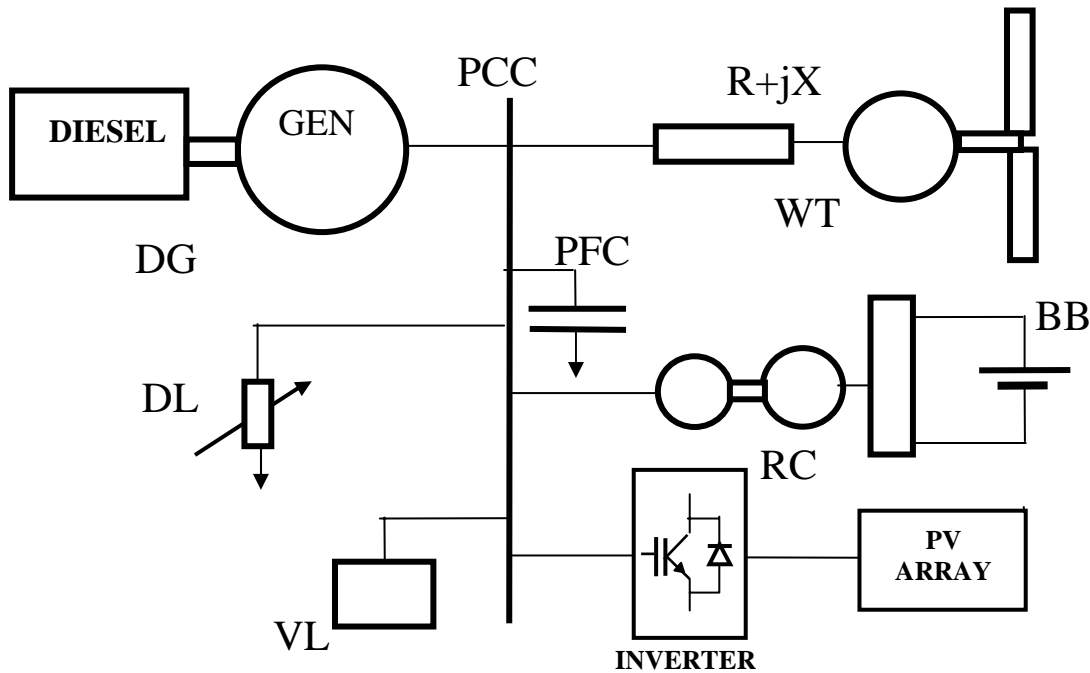
Figure 1-1. A typical hybrid power system

Using the typical modules provided, it is easy to set up a system of a desired configuration. The Add command on the File menu is used to place all the required modules (provided in the RPMSim_DST subdirectory of VisSim) on the simulation screen. VisSim's multilevel programming concept, along with the ability to create compound blocks, facilitates presentation of simulation modules, their submodules, or both, at different levels of "resolution."

Clicking the mouse on the block that represents a module reveals, where appropriate, its block diagram. This reveals the submodules with their connections, inputs and outputs, and possibly a short explanatory note. This note lists parameters that the user will set, outlines system variables generated by this particular module, and gives a general description of the module. Clicking on any submodule of a given block diagram brings up a screen that contains blocks simulation diagram and parameter module as well as a note of explanation. The parameter module contains application-specific parameters that are set by the user. The simulation diagram shows the equation-level representation of a particular device using the simulation blocks available in VisSim menus. An explanatory note can also be attached if appropriate.

The user can attach a display block to any simulation variable to obtain its numerical value or attach a plot block to acquire its graphical representation as a function of time. These blocks are available under the Signal Consumer menu and can be used at any level of the simulation diagram. VisSim menus list commands that automate many tasks and blocks that correspond to numerous linear and nonlinear functions.

General Characteristics of Principal Modules

Here are the principal modules and their file names currently available in the simulator subdirectory:

- PCC, file PCC_m.vsm

- DG, file DG_m.vsm

- AC WT/wind speed, file wtg_base_mod.vsm (used to represent a single or the first of multiple wind turbines; includes the wind speed module), file WTG_mod.vsm (used to represent additional wind turbines; does not include the wind speed module), and file WIND_SPEED.vsm (represents wind speed)

- RC/BB assembly, file BB_RC.vsm

- VL, file VL.vsm

- DL, file DL.vsm

- Battery, file BAT.vsm

- Inverter, file INV.vsm

- PV array, file PV_ARRAY.vsm.

The PCC module, which is a node where all power sources and sinks are connected, must be included in every simulation diagram. The top simulation diagram of the PCC module displays a button used to turn the village load on or off by clicking the mouse. This switching can also be performed while the simulation is running. Its top simulation diagram also includes two basic system parameters: the voltage set point and the frequency set point.

The DG module includes a model of a diesel engine, a synchronous generator, an engine speed control block (which generates a fuel/air ratio [represented by the $\%_{FUEL}$ variable]) required to keep the frequency constant, and a voltage regulator, which determines the field current to keep the line voltage constant.

The AC WT module simulates the two-step conversion of wind power to electrical power. In the first step, the wind power is converted to mechanical power represented by the torque developed by the wind turbine rotor and transmitted to the induction generator through the gearbox. In the second step, the electrical power is obtained. This module includes a model of a transmission line that connects the induction generator with the synchronous generator at the PCC. The PFC

capacitors, which are located at the induction generator, are also included. For the designer's convenience, the AC WT module is included in two files. The file wtg_base_mod.vsm consists of the AC WT module, the PCC WT-GEN block (included to enable simulation of multiple wind turbine systems), and the wind speed module. The file WTG_mod.vsm contains the wind turbine module and is used to represent additional wind turbines in simulation diagrams of power systems with multiple wind turbines. If the multiple wind turbines with different wind profiles are simulated, the wind speed module (or modules) must be added (with the Add command) to the simulation screen, as illustrated in Figure 1-2. The user must connect (click and drag) its output to the input of the AC WT module on the top-view simulation diagram of a hybrid power system. If, in the multiple wind turbine simulation, the same wind profile is used for all wind turbines, the variable *V_wind* must be added and connected to the input of each additional wind turbine, as illustrated in Figure1-3.
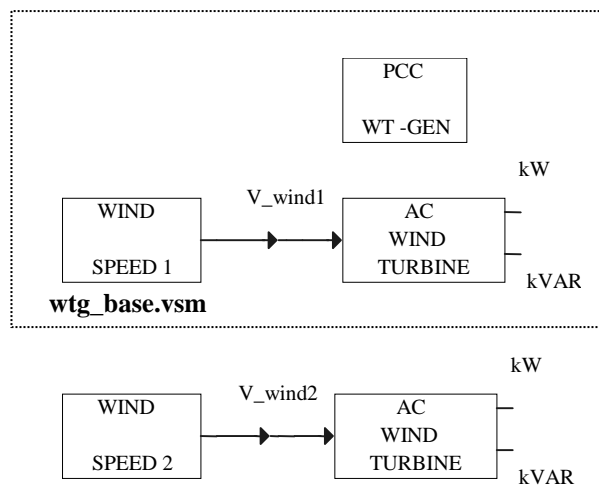
Figure 1-2. Multiple wind turbines with different wind profiles

The wind speed module is implemented with the import data file block provided in VisSim. It imports data points from a specified wind speed file and translates them into the output wind speed signal. The user can change the wind speed file. It is a two-column ASCII file: first column is the time data column and the second is the wind speed column.

The rotary converter/battery bank assembly consists of a BB block and an RC block. The rotary converter consists of two machines: the DC motor and the synchronous generator. It performs the AC/DC conversion while charging the battery and the DC/AC conversion while discharging the battery. It can also be set up to work as a synchronous condenser while you control the level of reactive power generated or absorbed. The BB block represents energy storage designed to work with the rotary converter. It can be either charged or discharged depending on the sign of the reference power P_{BAT_ref}. If this sign is negative, the DC motor of the rotary converter works as a generator and charges the battery. If the sign of P_{BAT_ref} is positive, the battery is discharged and provides power to the system through the rotary converter. The BB block model is also available as a stand-alone battery module.
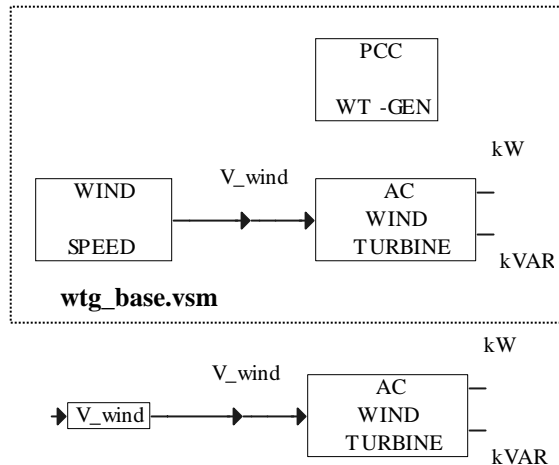
Figure 1-3. Multiple wind turbines with the same wind profile

The VL module represents the load specified by the real power consumption and the village load power factor. The village load profile is programmed and stored in a file, which must be available before the program can be run.

The dump load is an adjustable resistive load controlled in the steps of dissipated power to be defined by the user. The DL module is used to load the diesel engine by selecting the number of active load elements (i.e., the number of power steps applied). This selection is done automatically through one of the following control strategies chosen by the user:

- The diesel power control strategy maintains the minimum diesel load so that the power delivered by the diesel engine is greater than a certain percentage of its rated power.
- The frequency control strategy controls the number of the load elements active to keep the frequency within the limits set by the user.

The user can elect to activate either one of these control strategies by clicking on a button (available in the VisSim's Signal Producers menu) that, when activated, turns red and generates the signal 1.

The inverter can work in one of two modes—the master mode or the slave mode. It may be used to connect the PV array or the battery to the system. In the master mode, the inverter controls the system's frequency and voltage. In this case, the power exchange is determined by the system's power balance. In the slave mode, the user specifies the real and the reactive power that must be generated or absorbed. The transfer from slave mode to master mode is determined based on the control strategy designed by the hybrid power plant ì¥Á   %

¿   ö9
ÿjͅbjbjÞøÞø   ÿÿ   ÿÿ   ]   š
ÿ   ˜   ½ͅÿ   ¼'   D3   0 ÿÿ 9   ±]   š ÿÿ
          š   š   ¤

d   d   d $ ^   ^   ^
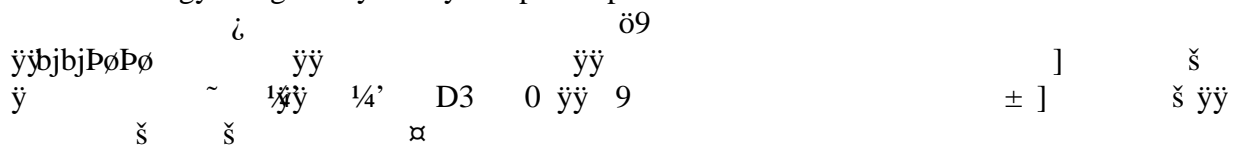
^   P   Ø   ental conditions that are available in the Sandia IVTracer Program. In the PV array model, the generated power depends on insolation and temperature, which can be downloaded from the Internet for a given geographical location and selected time period. The PV array can be connected to the PCC using the inverter or the rotary converter.

For all modules included in the simulator, we assumed (for both real and reactive power) a general power sign convention: the power absorbed is displayed as negative and the power generated is displayed as positive. A village load (as an inductive load) always absorbs both the real and the reactive power and both powers are always negative. The real power of a diesel generator is always positive and its reactive power may be positive or negative. The real power of the wind turbine generator is negative during motoring and positive during generation. Its reactive power is always absorbed, meaning that it is displayed as a negative quantity.

Chapter 2

Point of Common Coupling

The PCC module, the node where all power sources and power sinks are connected, must be included in every simulated power system. In Figure 2-1, we show a single-line diagram (as in Figure 1-1) of a hybrid power system where we dot-framed the PCC portion of the diagram.
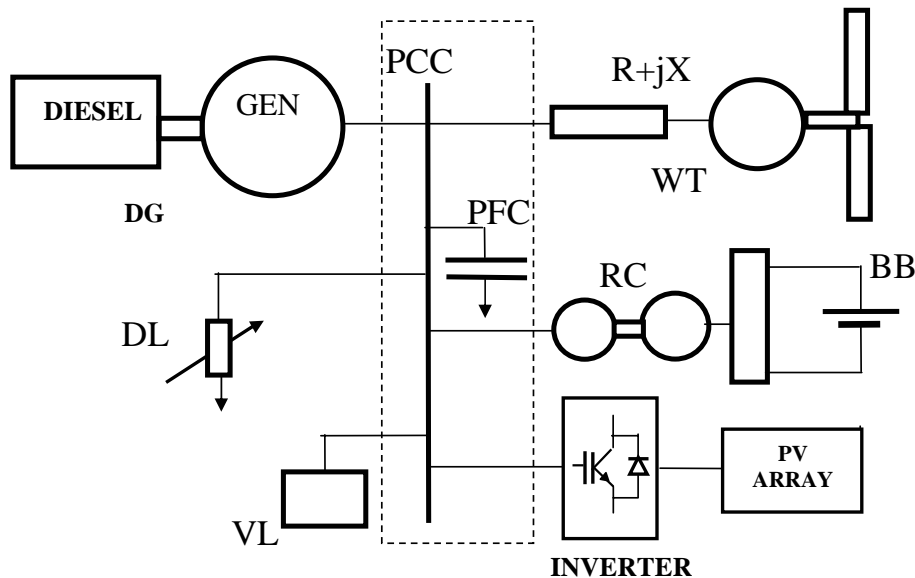

Figure 2-1. A single-line hybrid power system diagram with the PCC portion dot-framed

The user brings the PCC module to the simulation screen using the Add command and selecting file PCC_m.vsm. Next, the user obtains top-view diagram of the PCC module (shown in Figure 2-2) by clicking the mouse on the rectangle representing this module. This view features three elements: (1) the mouse-controlled button used to turn on [red button, variable *VillageLoad* = value logic 1] and off [white button, variable *VillageLoad* = value logic 0] the village load; (2) the parameter module compound block; and (3) the simulation diagram compound block.

Figure 2-3, which is the expansion of the parameter module, shows the parameters that can be set by the user. In addition, the base frequency w_b in rad/sec is calculated in this module. A special binary variable *DGS* is introduced and defined in the DG module if the DG is part of the simulated system. Otherwise the variable *DGS* is defined in the NO_DIESEL module (added to the simulation screen of systems with the inverter and without the DG). Its value is 1 in two cases: (a) the system starts its operation with the diesel generator start-up, and (b) the switching

from the inverter as a master to the diesel as a master was commanded and the diesel was synchronized. In both cases the diesel generator controls the system's voltage and frequency. On the other hand, $DGS = 0$ if there is no DG on the system or if the inverter operates in the master mode. As Figure 2-3 shows, it is assumed in this case that the current value of the system's frequency $w = w_b$. Such assumption is justified because this frequency value is enforced by the power electronics. Otherwise, when the DG is in control, $w = w_d$ is the frequency enforced by the DG's engine speed control system. This switch is needed to ensure that all the grid-connected sources or sinks will be synchronized to the appropriate frequency.

Figure 2-4 represents the expansion of the simulation diagram compound block. Recall that in all simulations we use the d-q axis convention. Therefore, each voltage and current has two components. Consequently, Figure 2-4(a) represents the relationship between the d-axis components of the currents of all system modules, and it shows how the d-axis component of the line voltage is obtained. The same is repeated in Figure 2-4(b) for the q-axis components. To make the relationships between the currents and voltages involved readily apparent, the circuit diagrams (corresponding to the simulation diagrams of Figure 2-4) are shown in Figure 2-5.
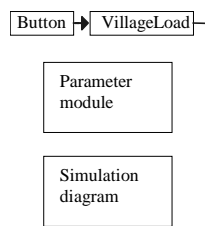

**Figure 2-2. Top-view diagram of the PCC module**
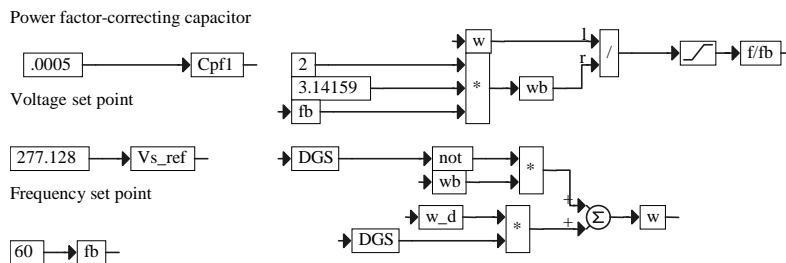

Figure 2-3. Parameter module of the PCC
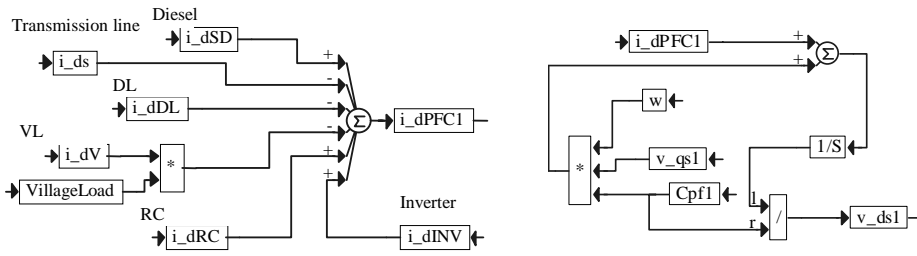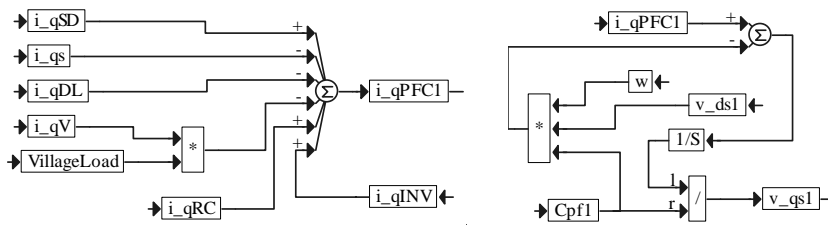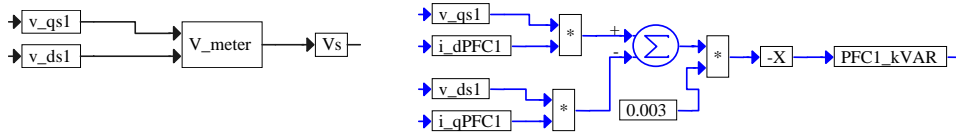
Figure 2-4. PCC module simulation diagram: (a) d-axis, (b) q-axis, and (c) calculation of the system voltage and the reactive power generated by the PFC capacitors

The denotations for q-axis and d-axis components of the currents involved are shown in Table 2-1.

Table 2-1. Denotations for q-axis and d-axis Components of Currents Involved

i_{qSD}, i_{dSD} -	Current provided by the synchronous generator/diesel module
i_{qRC}, i_{dRC} -	Current provided by the rotary converter
i_{qINV}, i_{dINV}	Inverter current
i_{qs}, i_{ds}	Transmission line current (to asynchronous machine/wind turbine)
i_{qDL}, i_{dDL}	Dump load current
i_{qV}, i_{dV}	Village load current.

Note that if the current representing a given module enters the top node in the circuit diagram of Figure 2-5 (or is added at the summing junction in Figure 2-4), its power is positive when it is generating power and negative when it is absorbing power. On the other hand, if the current representing a given module leaves the top node in the circuit diagram of Figure 2-5 (or is subtracted at the summing junction in Figure 2-4), its calculated power is positive when it is absorbing power and negative when it is generating power. To follow the general convention that the power generated is positive and the power absorbed is negative, we invert the sign of the power calculated for the modules represented by the currents leaving the top node in the diagram shown in Figure 2-5.

Let us consider some examples. The diesel generator always generates the real power. Therefore, its real power is always positive, or we say that it follows the assumed current sign convention. On the contrary, the diesel generator may generate or absorb the reactive power; the diesel reactive power may be positive or negative, depending on the load demand. The wind turbine generator during the motoring period absorbs real power, meaning that it draws the current from the PCC junction. The direction in which this current flows is the same as the direction assumed. Therefore, the calculated (absorbed) real power is positive. It requires the change of sign to follow the general convention. For the same reason, we must change the sign of the real power calculated when the wind turbine is generating. According to the circuit diagrams in Figure 2-5, we define the following currents:

$$i_{qPFC1} = i_{qSD} + i_{qRC} + i_{qINV} - i_{qs} - i_{qDL} - i_{qV},$$

$$i_{dPFC1} = i_{dSD} + i_{dRC} + i_{dINV} - i_{ds} - i_{dDL} - i_{dV}.$$

Using the same circuit diagram, we write the following equations defining q-axis and d-axis components v_{qs1} and v_{ds1} of the line voltage (V_s):

$$v_{qs1} = \frac{1}{C_{pf1}} \int (i_{qPFC1} - \omega C_{pf1} v_{ds1}) dt,$$

$$v_{ds1} = \frac{1}{C_{pf1}} \int (i_{dPFC1} + \omega C_{pf1} v_{qs1}) dt \, ,$$

where C_{pf1} is the PFC capacitor of the value to be designated by the user in the parameter module shown in Figure 2-3, and ω is the real system frequency calculated in the DG module that must be a part of every simulated power system. These equations are implemented in the right-side parts of Figure 2-4(a) and Figure 2-4(b).
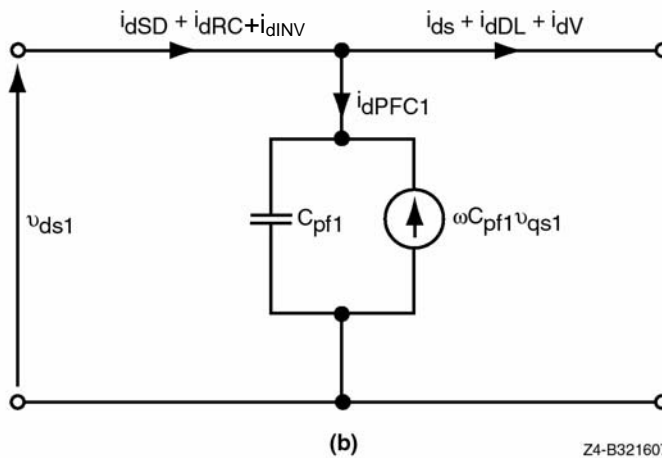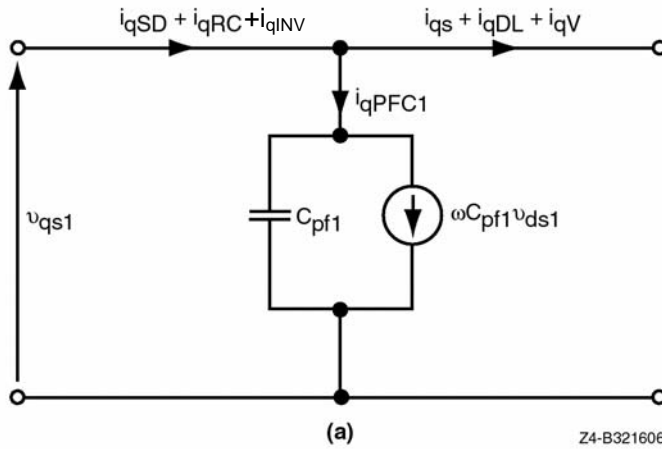

**Figure 2-5. PCC module circuit diagram: (a) q-axis and (b) d-axis**

V_s is calculated in the compound block V_meter, shown in Figure 2-4(c), according to the following equation:

$$V_s = \sqrt{v_{qs1}^2 + v_{ds1}^2} \ .$$

The calculation of the reactive power generated by the PFC capacitor is also shown in Figure 2-4(c). According to our convention, the reactive power generated must be positive. If the power is generated, the currents i_{qPFC1} and i_{dPFC1} should be entering the summing junction. The user can check to see that the currents are leaving the junction. In other words, the calculated reactive power is negative, so we introduce the inversion of sign in the calculation of the reactive power shown in Figure 2-4(c).

Diesel Generator

In Figure 3-1, we show a single-line diagram (as in Figure 1-1) of a hybrid power system where we dot-framed the portion of the diagram that represents the diesel generator. As shown in this figure, the system consists of two machines: (1) a diesel engine and (2) a synchronous generator. The user brings the DG module to the simulation screen by using the Add command and selecting the file DG_m.vsm. In addition, the user must add the DG/inverter control block to the simulation screen by selecting the file DG_INV_CTRL.vsm. This block is used to program diesel/inverter operation and is required if either the DG or the inverter, or both, are involved in the simulated power system. This block is described, along with the inverter, in Chapter 8.
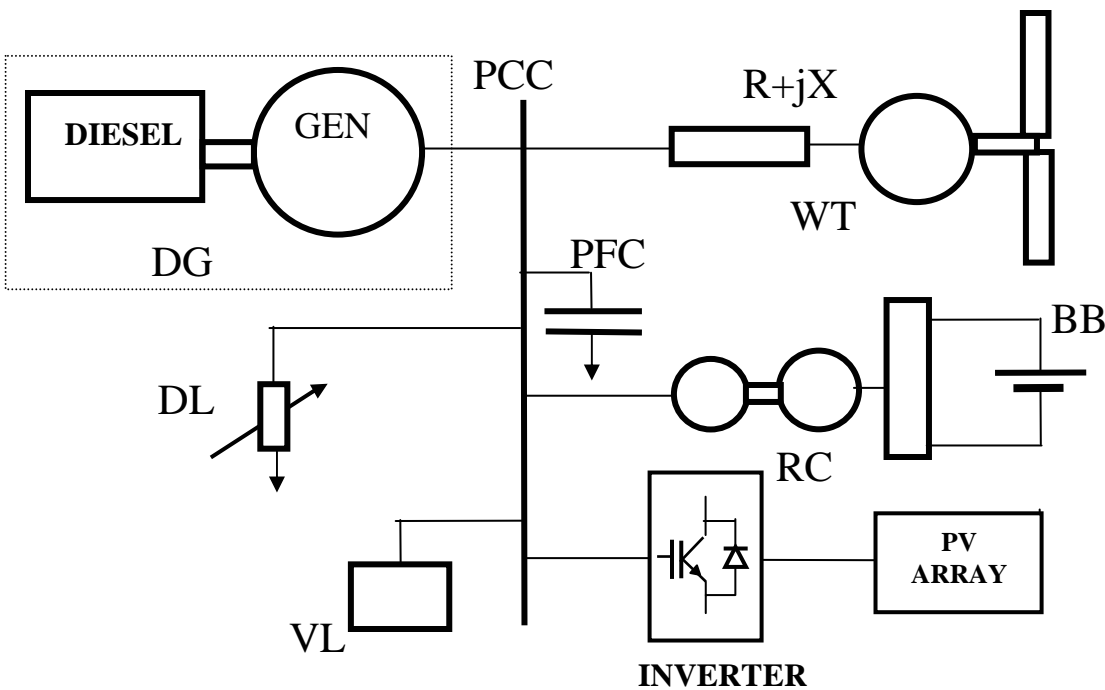

Figure 3-1. A single-line power system diagram with the DG portion dot-framed

Figure 3-2(a) represents the top-view diagram of the DG module. Two outputs— SD_{kW} and SD_{kVAR} —make the real and reactive power available for monitoring with either a display or plot block that the user chooses and connects by clicking and dragging. Clicking the mouse will bring up the second-level block diagram, such as the one in Figure 3-2(b), which represents the principal functional blocks of the diesel generator with their interconnections and in which all inputs and outputs are clearly shown. At this level, an additional control block called DG/inverter switch appears; it generates several binary signals to properly control diesel/inverter operation. Again, we describe this along with the inverter in Chapter 8. According to the block diagram in Figure 3-2(b), the speed control block generates a proper fuel/air ratio (represented by the variable

$\%_{FUEL}$) for the diesel engine. This enables the engine to generate the proper torque to drive the synchronous generator. The voltage regulator (with the proper adjustment of the field current of the synchronous generator) controls the line voltage V_s.
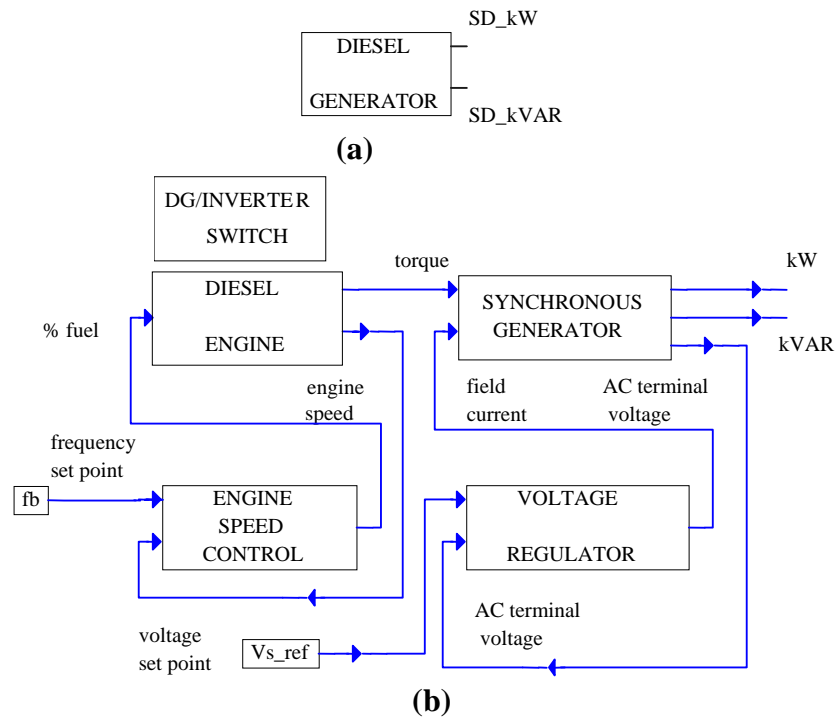
Figure 3-2. Block diagrams of the DG module: (a) top-view and (b) second-level showing principal functional modules and their interconnections

The first denominator coefficient in this transfer function represents the first order dynamics between %FUEL and T_diesel.

%_FUEL

+
− (Σ)

* POWER

Gen_m_rad/sec +
1 + (Σ)

1/r /

$\dfrac{1}{1\ \dfrac{}{.0001\ s+1}}$ T_diesel torque

2000
Diesel slope

5
minimum value of the %FUEL

100
100%_FUEL

* Pdiesel_rated

0.25

* Pdiesel_min

Minimum Diesel Load

Gen_m_rad/sec engine speed
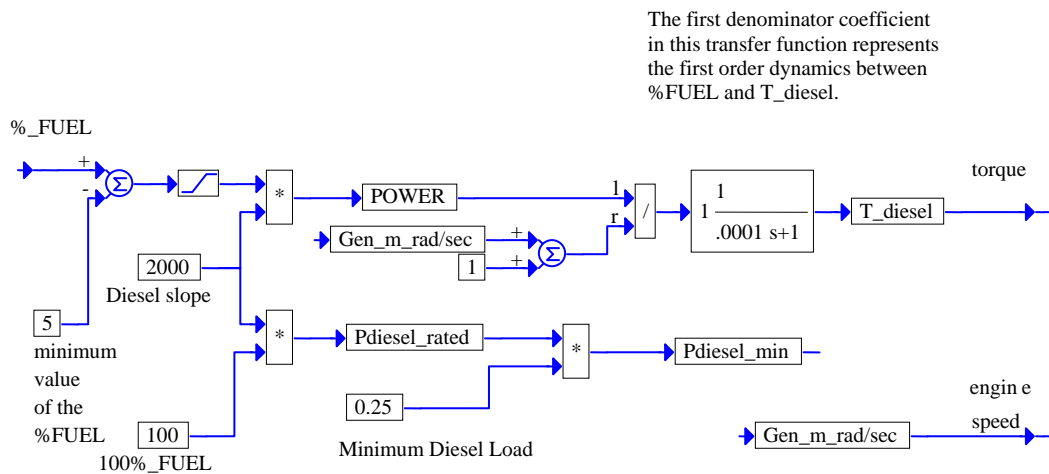
Figure 3-3. Simulation diagram of the diesel engine module

Figure 3-3 represents a simple simulation diagram of a diesel engine. Its *POWER = f(%$_{FUEL}$)* characteristic is represented as a straight line with the slope and the minimum value of the *%$_{FUEL}$* (the dead zone) that the user defines based on the data from the diesel engine manufacturer, so that it will approximate the engine modeled. As we can see in Figure 3-3, the rated power for the simulated diesel engine is 200 kW. Using the generated power and angular velocity *Gen$_{m\_rad/sec}$*, the torque *T$_{diesel}$* is generated assuming the first-order dynamics[1]. The user can specify the time constant. The minimum diesel load *P$_{diesel\_min}$* (chosen in Figure 3-3 as 25% of the rated power) is calculated. Diesel power is controlled to generate above-minimum power. This objective is accomplished by connecting the right number of dump load resistors (for more information, see Chapter 7).

The first- and second-level expansions of the synchronous generator module are shown in Figure 3-4. The first level, presented in Figure 3-4(a), consists of two compound blocks (parameter module and simulation diagram) and shows two control inputs—*T$_{diesel}$* and the field current *i$_f$*—and three outputs—*SD$_{kW}$* , *SD$_{kVAR}$* , and *V$_s$*. Note that for clarity of presentation, the output *V$_s$* is calculated in the PCC module as shown in Figure 2-4(c). Figure 3-4(b) lists all machine parameters set by the user. Figure 3-4(c) shows the first-level expansion of the synchronous generator simulation diagram with the following compound blocks: torque equation, power calculations (where the outputs *SD$_{kW}$* and *SD$_{kVAR}$* are generated), and the Q-generator and the D-generator. This block diagram also shows that the electromotive force generated is assumed as a reference (i.e., its phase is assumed to be zero). Consequently, its d-axis component is zero, which is symbolically shown as a zero input to the D-generator. Under this assumption, the input to the Q-generator is defined by the following equation:

---

[1] The first-order dynamics of the form *K*/(*sT*+1) is implemented with the transfer function block provided by VisSim. In the dialog box of this block, the user declares the gain *K* and the coefficients of the numerator and the denominator polynomial of the transfer function.

$$E_{q\_D} = K_{e\_D}\omega\Phi = K_{e\_D}\omega L_f i_f \ ,$$

where Φ is the flux proportional to the field current (i_f). The other parameters are explained in Figure 3-4(b). The Q-generator and D-generator, shown in Figure 3-5, generate the current i_{qSD} and i_{dSD}, respectively, contributed by the diesel generator to the system at the PCC module. These currents are calculated according to the following equations:

$$i_{qSD} = \frac{1}{L_{qSD}} \int (E_{q\_D} - v_{qs1} - R_{SD}i_{qSD} - \omega L_{dSD}i_{dSD})dt \ ,$$

$$i_{dSD} = \frac{1}{L_{dSD}} \int (-v_{ds1} - R_{SD}i_{dSD} + \omega L_{qSD}i_{qSD})dt \ .$$

We also show in this figure that these currents are contributed to the system through the PCC when $DGS = 1$. The binary variable DGS is defined in the DG/Inverter Switch included in the DG model and is described in Chapter 8.

Figure 3-6(b) shows the power calculation block in an expanded form. The electrical power generated is calculated according to the following equation:

$$P_{Egen\_D} = 3\ i_{qSD}E_{q\_D} \ .$$

Then the real power provided to the system is calculated as

$$P_{gen} = 3(v_{qs1}i_{qSD} + v_{ds1}i_{dSD}) \ \ [\text{W}] \quad \text{or} \quad SD_{kW} = 10^{-3}P_{gen} \ \ [\text{kW}] .$$

The apparent power SD_{kVA} and the reactive power SD_{kVAR} are also calculated in this block according to the following equations:

$$SD_{kVA} = 3\times10^{-3}\sqrt{v_{qs1}^2 + v_{ds1}^2}\sqrt{i_{qSD}^2 + i_{dSD}^2} \ ,$$

$$SD_{kVAR} = 3\times10^{-3}(v_{qs1}i_{dSD} - v_{ds1}i_{qSD}) \ .$$

Finally, in Figure 3-6(a) the torque equation is simulated to obtain the angular velocity of the diesel generator $Gen_{m\_rad/sec}$. This brings us to the following equation:

$$Gen_{m\_rad/\sec} = \frac{1}{J_{SD}} \int (T_{diesel} - T_{gen} - B_{SD}Gen_{m\_rad/\sec})dt \ ,$$

where T_{gen} represents the generated electrical power P_{Egen_D}; i.e.,

$$T_{gen} = \frac{P_{Egen\_D}}{Gen_{m\_rad/\sec}} \ .$$

(a)

PARAMETER MODULE

SIMULATION DIAGRAM

T_diesel
i_f

SD_kW
SD_kVAR
Vs

(a)

voltage-flux constant
0.0032 → Ke_D

field winding resistance
50 → Rf

field winding inductance
20 → Lf

stator resistance
0.0001 → R_SD

stator inductance, q component
5.1e-005 → L_qSD

stator inductance, d component
0.0001 → L_dSD

synchronous generator moment of inertia
2 → J_SD

4 → pole_SD

viscous friction coefficient of the synchronous generator
0.0003 → B_SD

(b)

T_diesel → TORQUE EQUATION

POWER CALCULATIONS

Ke_D
w
* → Eq_D → Q-generator

0 → D-generator

i_f → Lf
* → Flux

(c)

Figure 3-4. First- and second-level expansion of the synchronous generator module: (a) first-level expansion, (b) parameter module expansion, and (c) simulation diagram expansion

Q-generator
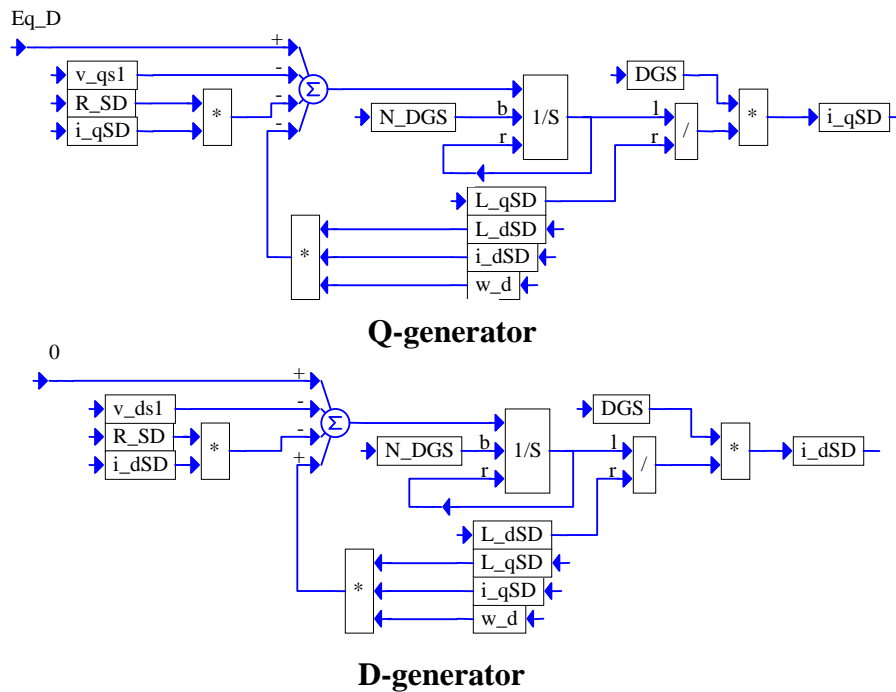
D-generator

Figure 3-5. Simulation diagram of the synchronous generator (DG module): Q-generator and D-generator

Two more blocks in the second-level simulation diagram of the diesel generator module are shown in Figure 3-2(b): the engine speed control block and the voltage regulator. They are fully expanded in Figures 3-7 and 3-8, respectively.

In Figure 3-7, using the angular velocity $Gen_{m\_rad/sec}$, we find the value of the ratio f/f_{b_d} along with an important system variable, the angular frequency $\omega_d = 2\pi f$. Then the frequency f is found.

The speed of the diesel engine is controlled by the control variable $\%_{FUEL}$ generated by the governor (represented in the simulation by the proportional + integral [PI] controller) so that the relative frequency error $1 - f/f_{b\_d}$ is driven to zero.
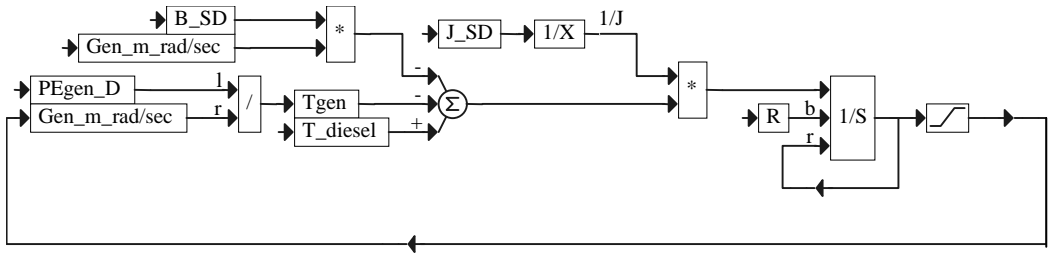
(a)
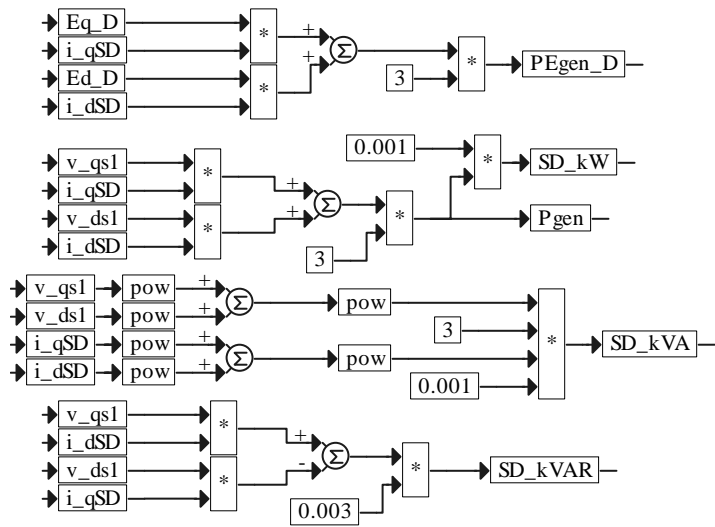
(b)

Figure 3-6. Simulation diagram of the synchronous generator (DG module):
(a) torque equation and (b) power calculations
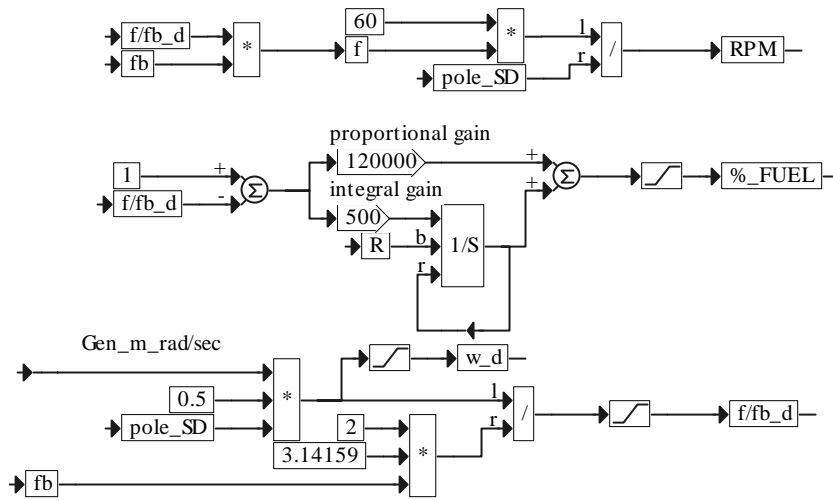
Figure 3-7. Simulation diagram of the engine speed control system
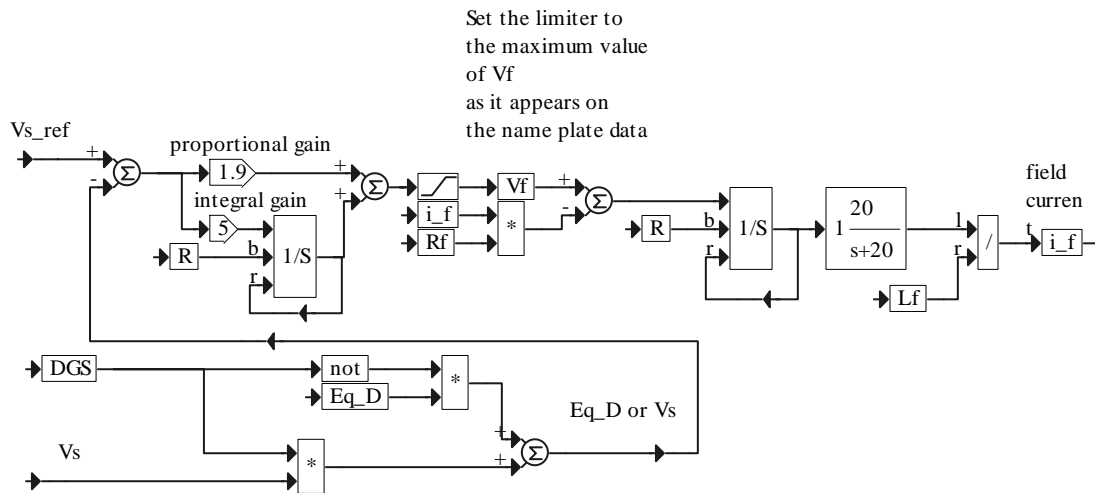
Figure 3-8. Simulation diagram of the voltage regulator

In Figure 3-8, the field current i_f of the synchronous generator is calculated according to the equation

$$i_f = \frac{1}{L_f} \int (V_f - R_f i_f) dt \,,$$

where the voltage V_f is defined as the output of the PI controller determined to drive the line voltage error $V_{s\_ref} - V_s$ to zero or (when $DGS = 0$, while switching the master function from the inverter to diesel) to drive to zero the error $V_{s\_ref} - Eq\_D$ during the synchronization process. To smooth the field current, the low-pass filter with the cut-off frequency of 20 rad/sec is added. The limiter must be set to the value of V_f as it appears on the nameplate data of the machine. The user should adjust proportional and integral gain to avoid saturating the field current. The practical solution is to make proportional gain slightly smaller than $(V_f)/(V_{s\_ref})$ and then to set the largest possible integral gain to avoid saturation.

AC Wind Turbine

In Figure 4-1, we show a single-line diagram (as in Figure 1-1) of a hybrid power system where we dot-framed the portion of the diagram representing the AC WT. As shown in this figure, the WT consists of two machines: (1) a wind turbine and (2) an asynchronous generator. In addition, the PFC capacitor (although not shown at this presentation level) and the line impedance R+jX are also included. The user brings the WT modules to the simulation screen by using the Add command and selecting the file wtg_base_mod.vsm. If more than one AC WT is on the system the user selects one WTG_mod.vsm block for each additional wind turbine. In the multiple wind turbine system, the PFC capacitors are included in the PCC module and in every WT block.
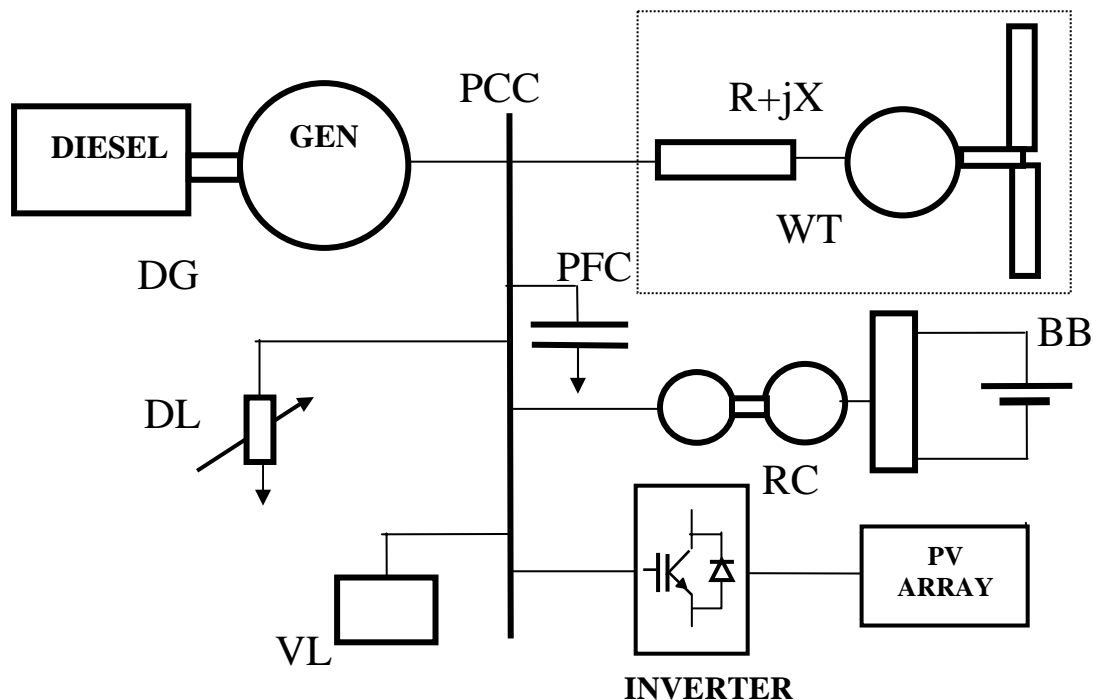

Figure 4-1. A single-line power system diagram with the WT module dot-framed

Figure 4-2 presents the top-view block diagram of the AC WT module implemented by the file wtg_base_mod.vsm. It consists of three blocks, shown in Figure 4-2(b), which are WT, PCC of the wind turbine generators (PCC WT-GEN; included to enable simulation of multiturbine systems), and wind speed. In this second-level simulation diagram, we included specific instructions about how to append the simulation diagram of the PCC WT-GEN block, shown in Figure 4-2(d), when multiple wind turbines are involved in the system. The WT module has two outputs labeled kW and kVAR, which make the real and reactive power available for monitoring. In Figure 4-2(c), we present the expansion of the WT block, showing the interconnections of its

principal components and their inputs and outputs. In this simulation, the reactive power has two components: (1) one absorbed by the induction generator and (2) one contributed by the PFC capacitor block.

(a)

Start-up time in the INDUCTION GENERATOR block to be declared by the user.

For each additional WTG block added, the user has to find (in the POWER FACTOR CORRECTION CAPACITOR block/Simulation Diagram) the variable names assigned by the system to q- and d-components of the transmission line current.

Transmission line current components are to be added to the proper summing junctions in the PCC_WT-GEN block.

(b)

Start-up time in the induction generator block to be declared by the user.

(c)

summing junction for q-components of the transmission line current

summing junction for d-components of the transmission line current

PCC_WTG

(d)

Figure 4-2. AC WT module implemented by the file wtg_base_mod.vsm: (a) top-view diagram, (b) second-level diagram, (c) expansion of the AC WT block, and (d) expansion of the PCC WT-GEN block
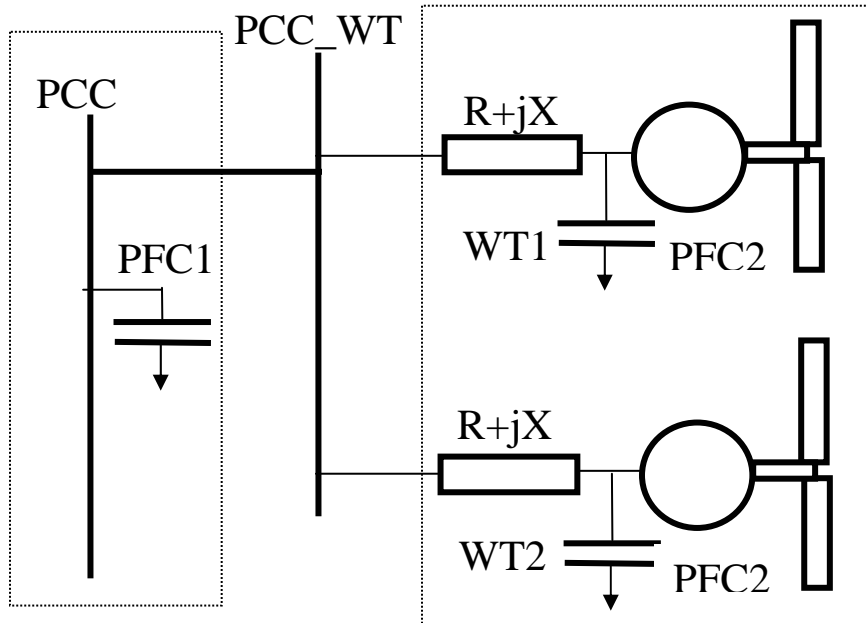
Figure 4-3. Two wind turbines connected to the power system

This slider is used to offset the limit. The limit is set between 0 and 20. Thus to change the impact of the limit between 2 to 22, the slider must be set to 2.

This slider is used to offset the wind speed. Thus the wind speed data is reduced by the offset from the slider.
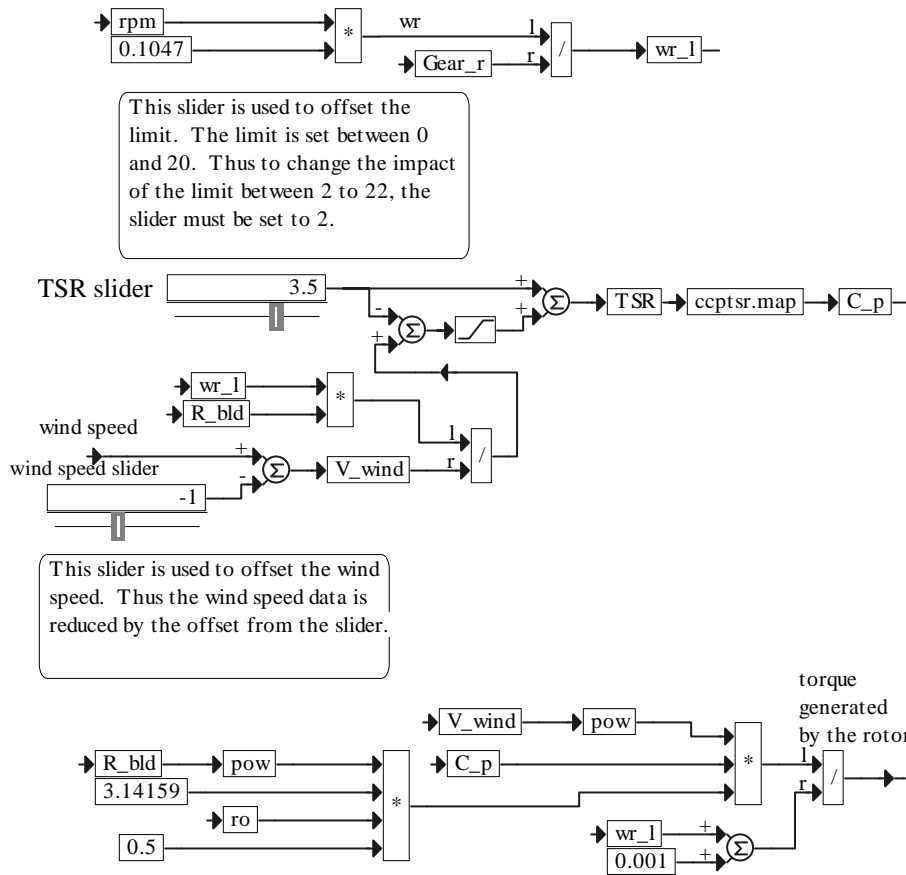
Figure 4-4. Simulation diagram of the wind turbine rotor

In Figure 4-3, we show a part of the power system with two wind turbines. In this figure, the wind turbine generators are connected to the PCC_WT, which is connected to the PCC of the system. PFC capacitors PFC2 represent capacitors included in the WT1 and WT2 AC wind turbine blocks.

By clicking the mouse on any of the blocks shown in Figure 4-2(c), the user obtains its lower level expansion. Such expansion of the wind turbine rotor block consists of: (1) the parameter module and (2) the simulation diagram. The parameter module contains two parameters: the air density ρ and the blade radius R_{bld}. By clicking the mouse on the simulation diagram, the user can retrieve its expansion as shown in Figure 4-4. In the simulation diagram the velocity *rpm* of the induction machine is converted to the angular velocity ω_r in radians/second, which in turn is divided by the gear ratio $Gear_r$. This results in the angular velocity of the blade ω_{r_l}, i.e.,

$$\omega_{r\_l} = \frac{\omega_r}{Gear_r} = \frac{0.1047rpm}{Gear_r} \ .$$

Then, the tip-speed ratio *TSR* is calculated using the relation

$$TSR = \frac{\omega_{r-l}R_{bld}}{V_{wind}} \ .$$

The nonlinear relation between *TSR* and the performance coefficient C_p is encapsulated in the map block, which performs piecewise linear interpolated look-ups. An ASCII data file is used for this mapping. The C_p, generated by the map block is then used to calculate the wind power P_{wind}, from which the torque generated by the wind turbine T_{wt} is determined. These calculations, shown in Figure 4-4, are represented by the following equations:

$$P_{wind} = 0.5\rho\pi R_{bld}^2 C_p V_{wind}^3 \ ,$$

$$T_{wt} = \frac{P_{wind}}{\omega_{r-l}} \ .$$

Included in this simulation diagram also are two sliders called the TSR slider and the wind speed slider. The TSR slider is used to set as necessary the low limit of the *TSR*. However, this has the window effect. The window effect of the use of this slider is shown in Figure 4-5, in which, because of the adjustment of the slider to the value of 3, we obtain $TSR_{min}= 3$ (we set the initial value of C_p to a small positive number) and $TSR_{max} = 23$. The width of the window is adjusted by the settings of the limiter.

The wind speed slider is used to offset the standard wind speed (increasing or decreasing its mean value). This effect is illustrated in Figure 4-6.

(a)   **(b)**
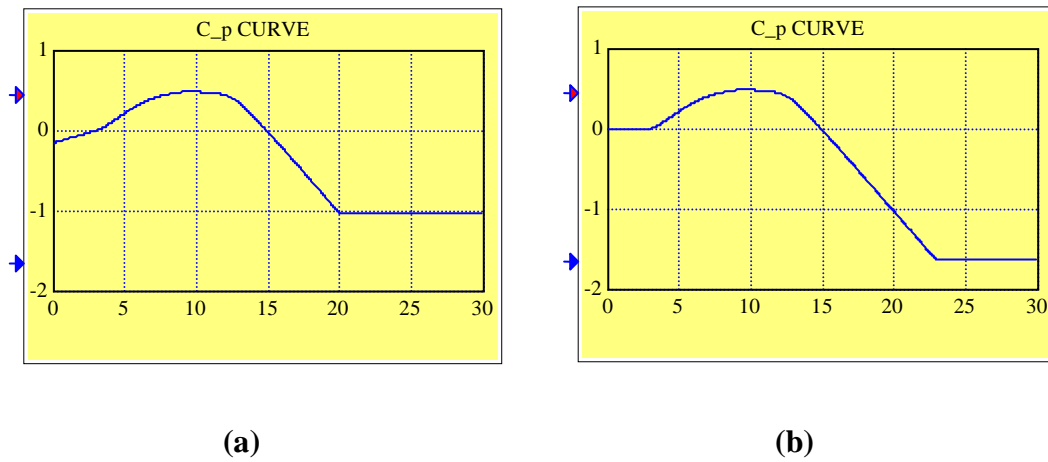
Figure 4-5. Moving window effect of the slider on $C_p = f(TSR)$ **characteristics: (a)** $TSR_{min} = 0$**,** $TSR_{max} = 20$ **(these are the settings of the limiter),** **(b) the slider set to** 3 **comes into play and** $TSR_{min} = 3$**,** $TSR_{max} = 23$
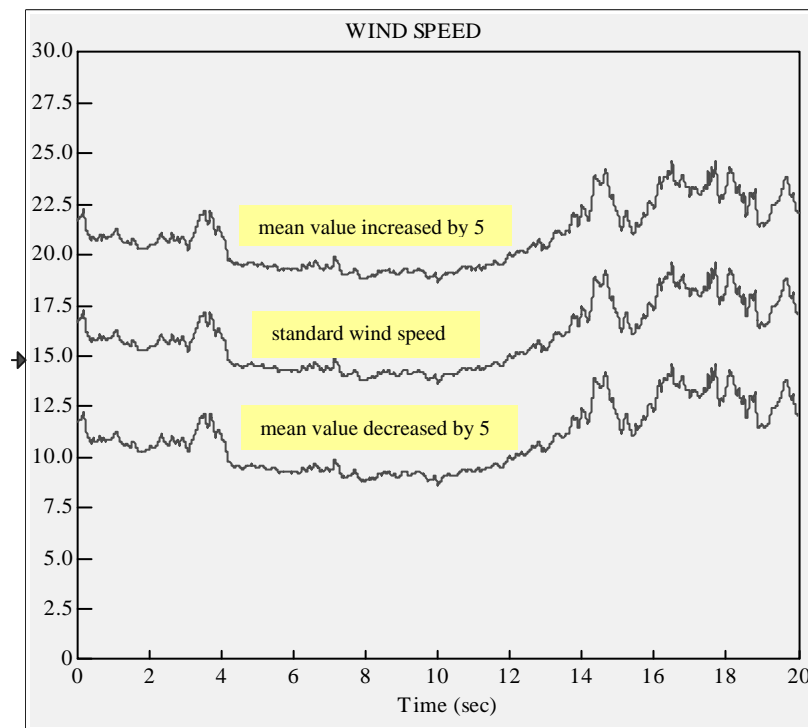
Figure 4-6. Effect of the slider on the standard wind speed

In Figure 4-7, the expansion of the gearbox block is shown, in which the gear ratio is declared and the high-velocity torque is calculated, appended with a negative sign for future calculations, and denoted by T_{wind}.

gear ratio

3 → Gear_r

(a)

torque generated
by the wind turbine

torque at the output
of the gearbox

Gear_r

-X → T_wind

(b)
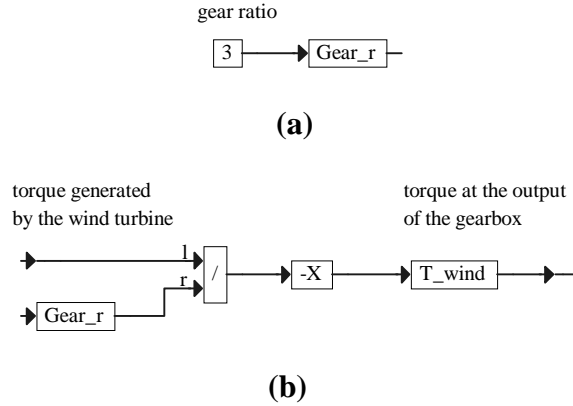
Figure 4-7. Gearbox: (a) parameter module expansion and (b) expansion of the simulation diagram

Figure 4-8 shows the first-level expansion of the induction generator block. The parameters of the machine, which are set by the user, are listed in the parameter module as shown in Figure 4-8(a). In addition, the calculations of a set of constants in terms of these parameters, which simplify the simulation of induction generator, are also placed in the parameter module. This part of the parameter module is not shown in Figure 4-8(a). The following equations, implemented in the parameter module, specify these constants:

$$a^{-1} = 1 + X'_{lr} / (X_m + X_{ls}), \; b^{-1} = 1 + X_{ls} / (X_m + X'_{lr}),$$

$$c = \frac{r_s \omega_b}{X_{ls}} \;, \; d = \omega_b \;, \; e = \frac{r'_r \omega_b}{X'_{lr} X} \;, \; f^{-1} = X_{ls} \;, \; g^{-1} = X'_{lr} \;, \; h = \frac{P}{2J\omega_b} \;, \; k = \frac{3P}{4\omega_b} \;,$$

where $\omega_b = 377$ (in radians per second or rad/sec) is the base speed.

The first-level expansion of the simulation diagram of the induction machine is shown in Figure 4-8(b). Let us concentrate on the two main blocks labeled ds_axis and qs_axis. Clicking the mouse will bring up the expansions of these blocks. They implement the following equations describing the induction machine:

$$\Psi_{qs} = \omega_b \int [v_{qs2} - \frac{\omega}{\omega_b} \Psi_{ds} + \frac{r_s}{X_{ls}} (\Psi_{mq} - \Psi_{qs})] dt \;,$$

$$\Psi_{ds} = \omega_b \int [v_{ds2} - \frac{\omega}{\omega_b} \Psi_{qs} + \frac{r_s}{X_{ls}} (\Psi_{md} - \Psi_{ds})] dt \;,$$

$$\Psi'_{qr} = \omega_b \int [v'_{qr} - \frac{\omega - \omega_r}{\omega_b} \Psi'_{dr} + \frac{r'_r}{X'_{lr}} (\Psi_{mq} - \Psi'_{dr})] dt \;,$$

$$\Psi'_{dr} = \omega_b \int [v'_{dr} - \frac{\omega - \omega_r}{\omega_b} \Psi'_{qr} + \frac{r'_r}{X'_{lr}} (\Psi_{md} - \Psi'_{dr})] dt \;,$$

$$\Psi_{mq} = a\Psi'_{qr} + b\Psi_{qs} \;,$$

4-6

$$\Psi_{md} = a\Psi'_{dr} + b\Psi_{ds},$$

$$i_{qi} = f(\Psi_{qs} - \Psi_{mq}),$$

$$i_{di} = f(\Psi_{ds} - \Psi_{md}),$$

$$i'_{qr} = g(\Psi'_{qr} - \Psi_{mq}),$$

$$i'_{dr} = g(\Psi'_{dr} - \Psi_{md}),$$

where v_{qs2} and v_{ds2} are defined in the PFC Capacitor block described below.

(a)

(b)
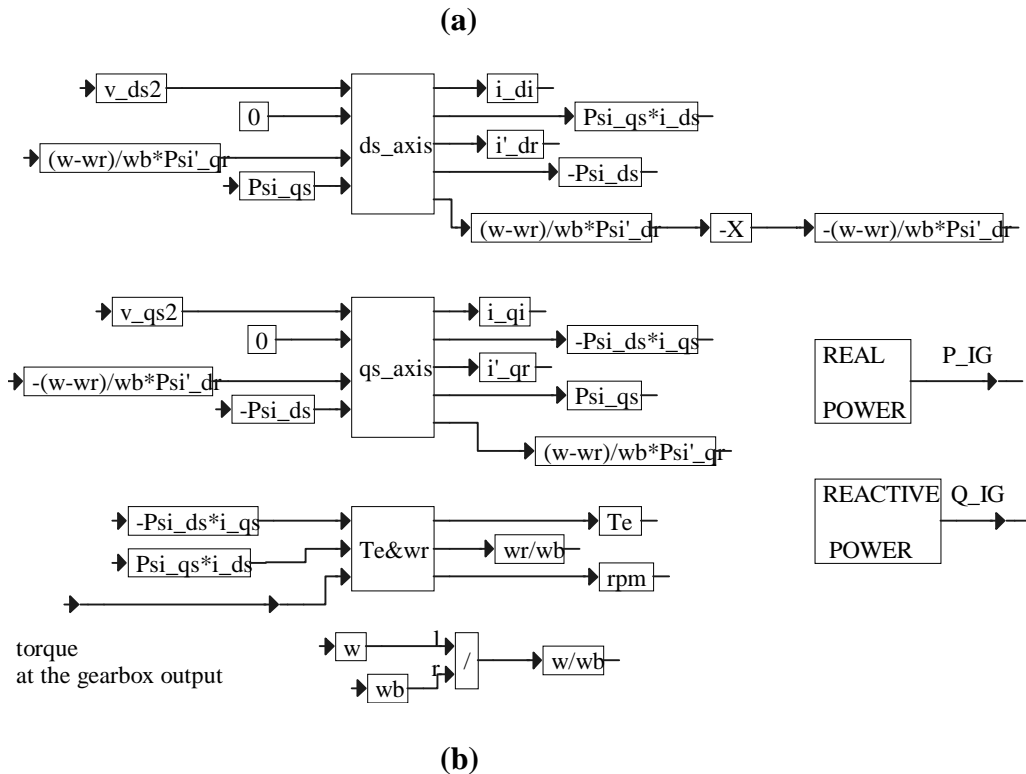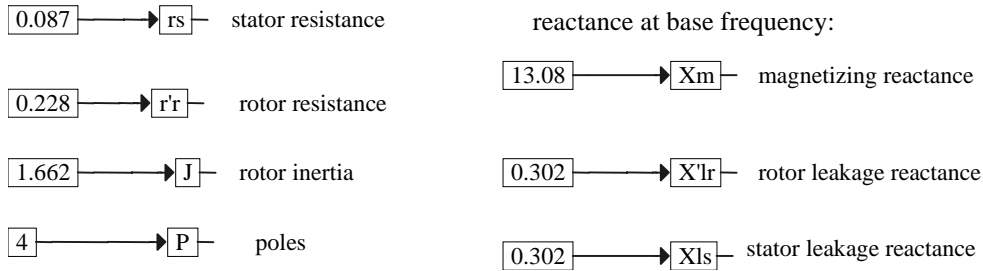
**Figure 4-8. First-level expansion of the induction generator block:
(a) parameter module and (b) simulation diagram**

Note that according to the model assumed (as best seen in Figure 4-9) the induction generator current components, i_{di} and i_{qi}, equal to the respective transmission line currents, i_{ds} and i_{qs}, minus

the respective components, i_{dPFC2} and i_{qPFC2}, of the PFC capacitor current. The block labeled Te&wr implements the following equations:

$$T_e = k(\Psi_{ds} i_{qi} - \Psi_{qs} i_{di}),$$

$$\frac{\omega_r}{\omega_b} = h \int (T_e - T_{wind}) dt,$$

$$rpm = 9.54929 \frac{\omega_r}{P/2}.$$

Inside this block we added the slider with the range from -1 to 0, which sets the initial condition on $-\omega_r / \omega_b$ with –1 corresponding to the synchronous speed. The user can use this slider to reduce the start-up time or the duration of the motoring mode of operation.

The equation implemented in the real power block is

$$P_{IG} = 3 \times 10^{-3} (v_{qs2} i_{qi} + v_{ds2} i_{di}) [\text{kW}].$$

The equations implemented in the reactive power block are

$$Q_{IG} = 3 \times 10^{-3} (v_{qs2} i_{di} - v_{ds2} i_{qi}) [\text{kVAR}],$$

$$S_{IG} = 3 \times 10^{-3} \sqrt{v_{qs2}^2 + v_{ds2}^2} \sqrt{i_{qi}^2 + i_{di}^2} [\text{kVA}].$$

Figure 4-10 presents the PFC capacitor and transmission line model block. Its parameter module is expanded in Figure 4-10(a) and shows the following parameters set by the user:

C_{pf2} PFC capacitor at the wind turbine site

R_{LN} Transmission line resistance

L_{LN} Transmission line inductance.
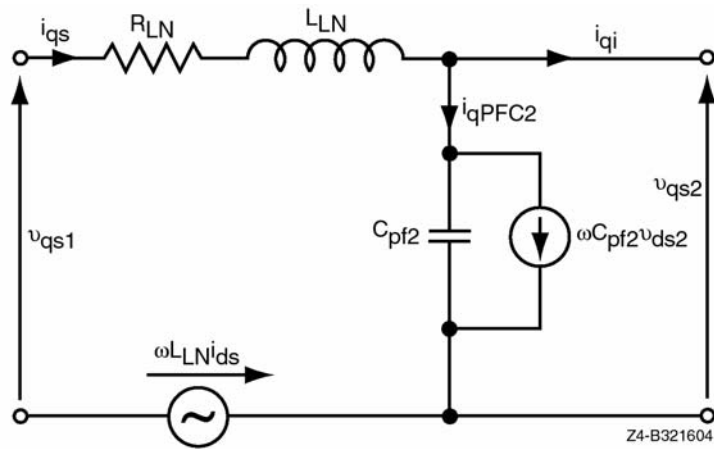
(a)
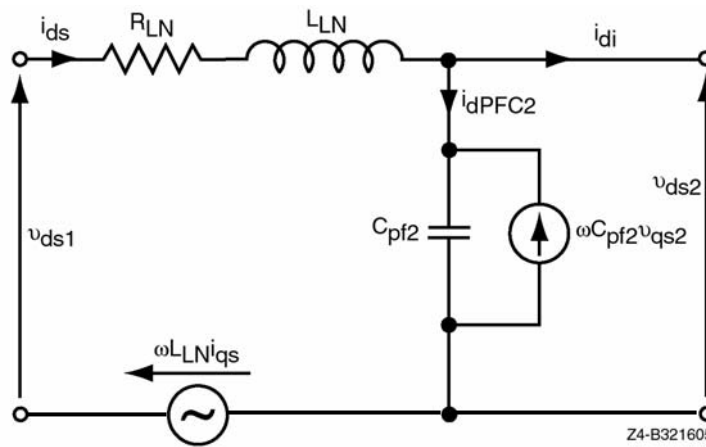
(b)

Figure 4-9. Circuit diagram of the PFC capacitors and transmission line model block: (a) q-axis circuit representation and (b) d-axis circuit representation

power factor correction capacitor

0.0002 → Cpf2

transmission line resistance

0.01 → R_LN

transmission line inductance

0.0002 → L_LN
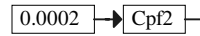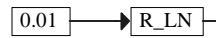
(a)
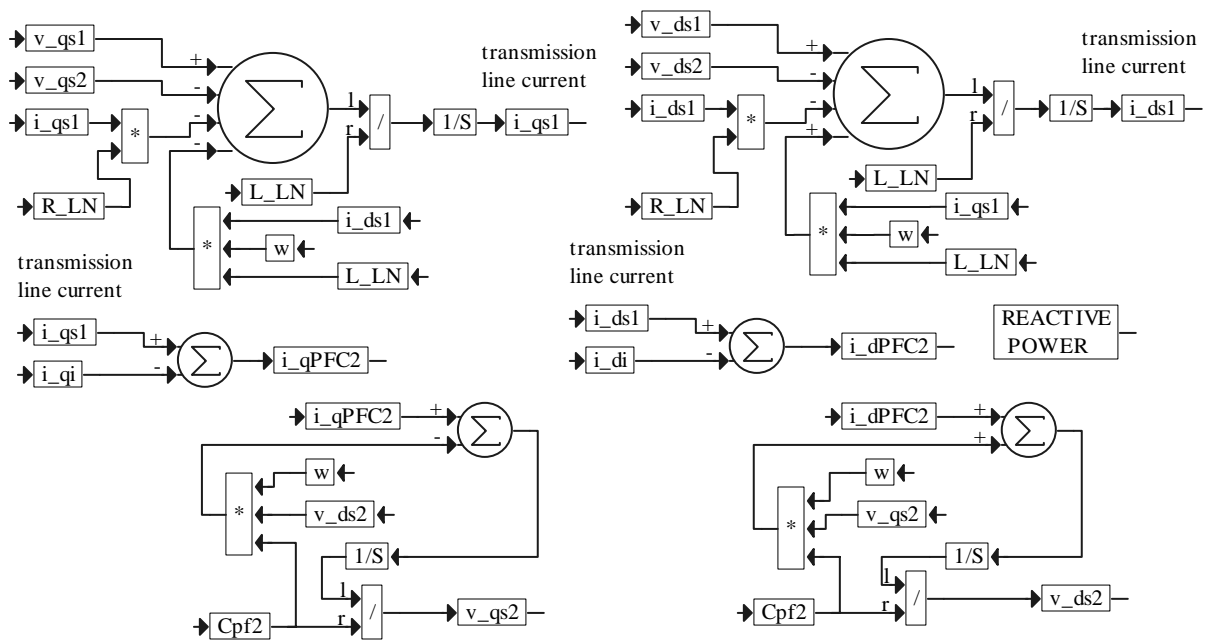
(b)
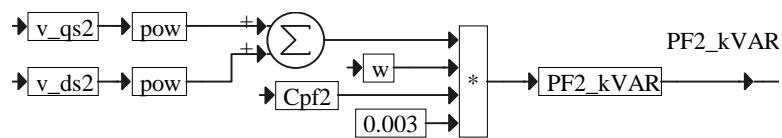
(c)

Figure 4-10. PFC capacitors and transmission line model block: (a) parameter module, (b) simulation diagram, and (c) expansion of the reactive power block

The simulation diagram is expanded in Figure 4-10(b) and its corresponding circuit diagram is shown in Figure 4-9. The transmission line connects the diesel generator with the induction generator. According to the circuit diagram, the d-q axis equations involved follow:

$$i_{qPFC2} = i_{qs1} - i_{qi},$$

$$i_{dPFC2} = i_{ds1} - i_{di},$$

$$v_{qs2} = \frac{1}{C_{pf2}} \int (i_{qPFC2} - \omega C_{pf2} v_{ds2}) dt,$$

$$v_{ds2} = \frac{1}{C_{pf2}} \int (i_{dPFC2} + \omega C_{pf2} v_{qs2}) dt,$$

$$i_{qs1} = \frac{1}{L_{LN}} \int (v_{qs1} - v_{qs2} - \omega L_{LN} i_{ds1} - R_{LN} i_{qs1}) dt,$$

$$i_{ds1} = \frac{1}{L_{LN}} \int (v_{ds1} - v_{ds2} + \omega L_{LN} i_{qs1} - R_{LN} i_{ds1}) dt.$$

The variables, i_{qs1} and i_{ds1}, used in these equations to account for a multiple wind turbine system [as explained in Figure 4-3(d)] correspond to the currents, i_{qs} and i_{ds} in Figure 4-9.

Finally, Figure 4-10(c) shows the expansion of the reactive power block, which implements the equation

$$PF2_{kVAR} = 3 \times 10^{-3} \omega C_{pf2} (v_{qs2}^2 + v_{ds2}^2).$$

The file WTG_mod.vsm, used as we mentioned to simulate multiple wind turbine generator systems, is identical to the AC WT block shown in Figure 4-2(b). However, when this file is added to the simulation screen to represent additional wind turbines, VisSim will automatically rename the variables generated in this simulation diagram. The user will be particularly interested in the new names of the d and q component of the transmission line current for the added wind turbine generator. The user must add the components of this current at the summing junctions in the simulation diagram of the PCC WT-GEN block shown in Figure 4-2(d).

After addition of the file WTG_mod.vsm the block AC WIND TURBINE appears in the simulation screen. Now, (as illustrated in Figures 1-2 and 1-3) the user must add and connect to its input the variable *V_wind* or generate a new WIND SPEED block and connect its output to the input of the newly added AC WIND TURBINE block. Then the user must click on the AC WIND TURBINE block, the POWER FACTOR CORRECTION CAPACITORS block, and the SIMULATION DIAGRAM block. The simulation diagram shown in Figure 4-10(b) will appear on the screen. The names of the transmission line current components for the added wind turbine

generator will be visible. Now, the user must open the PCC WT_GEN block shown in Figure 4-2(d) and add these variables at the proper summing junctions. If more than two wind turbines are on the system, the user must first (with the click of the mouse) add connectors to the summing junctions in Figure 4-2(d) (as a default there are connectors provided for only one additional wind turbine generator).

Rotary Converter/Battery Bank Assembly

In Figure 5-1, we show a single-line diagram (as in Figure 1-1) of a hybrid power system where we dot-framed the portion of the diagram that represents the RC/BB assembly. As shown in this figure, the RC consists of a battery bank and two machines: (1) a DC machine and (2) a synchronous machine. In this chapter, we will present the DC machine in detail and briefly discuss the synchronous machine. For a complete discussion of the synchronous machine, see Chapter 3. The user brings the RC to the simulation screen by using the Add command and selecting the file BB_RC.vsm.
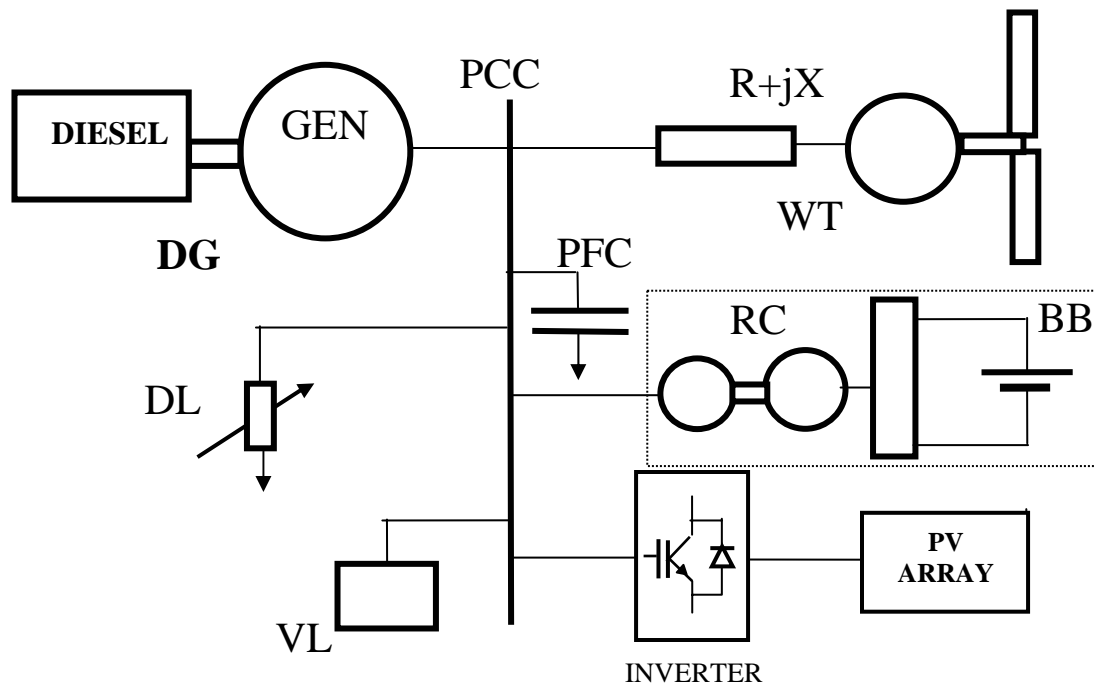
Figure 5-1. A single-line diagram of a hybrid power system with the RC portion dot-framed

Figure 5-2(a) presents the top-view block diagram representing the rotary converter. The RC module has two outputs—labeled RC_{kW} and RC_{kVAR}—that make the real and the reactive power, respectively, available for monitoring. Figure 5-2(b), obtained by clicking the mouse on the battery module, shows the fully expanded simulation diagram of the battery, including the parameters that the user can set. By clicking the mouse, the user also obtains the second-level block diagram of the rotary converter, shown in Figure 5-2(c). This represents its principal functional blocks with their interconnections and all inputs and outputs are clearly shown and labeled. As shown in Figure 5-2(c), the rotary converter simulation diagram consists of the following principal blocks:

- DC motor/generator
- Synchronous generator/motor
- DC machine field controller
- Voltage regulator.
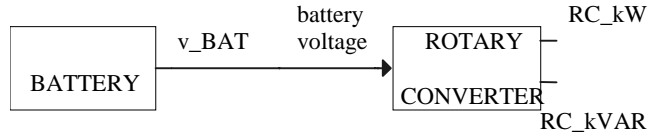
(a)
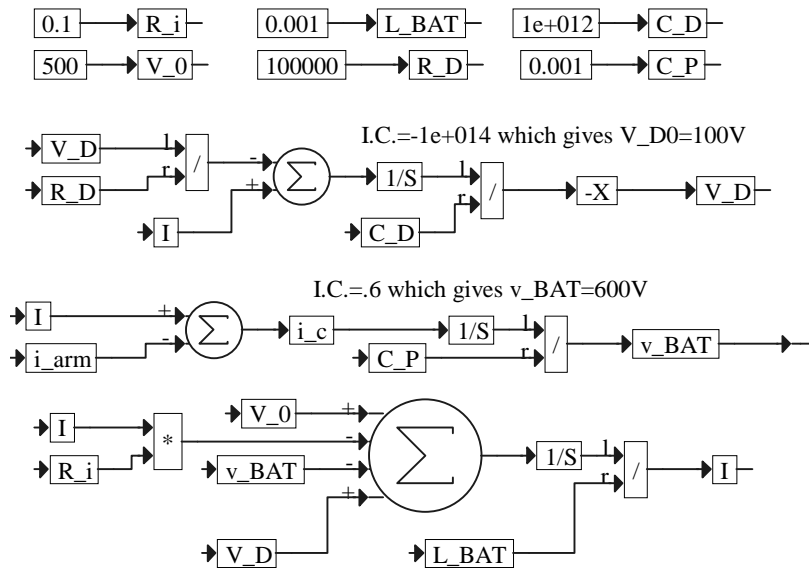
(b)
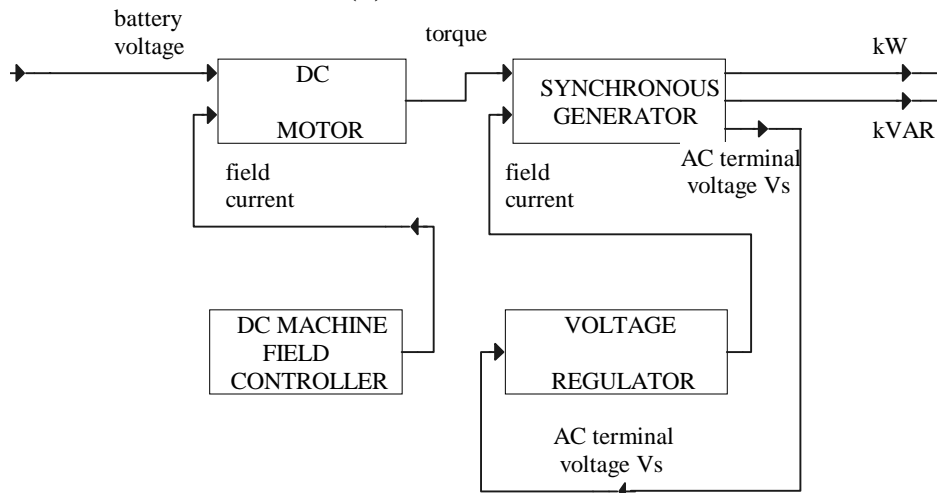
(c)

Figure 5-2. Block diagrams of the RC/BB assembly: (a) top-view block diagram, (b) expansion of the battery module, and (c) second-level diagram showing principal functional blocks of the rotary converter
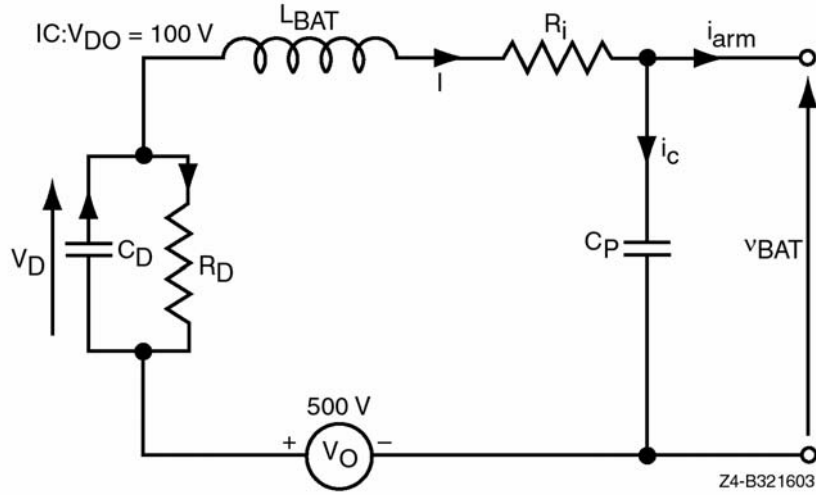
**Figure 5-3. Circuit diagram of the battery**

Note that this simulation diagram of the rotary converter module is very similar to that of the DG module shown in Figure 3-2(b). We will take advantage of this when describing its operation. Let us first concentrate on the description of the simulation diagram of the battery module shown in Figure 5-2(b). Its circuit diagram is shown in Figure 5-3. In this diagram, the voltage source V_0 = 500 V represents the minimum battery voltage to which the battery can be discharged without damage. The other part of the voltage of the fully charged battery is represented by the initial value V_{D0} of the voltage V_D across the capacitor C_D, which together with the parallel resistor R_D models the battery leakage. It is assumed for this particular simulation that the fully charged and unloaded battery has a voltage of 600 V. To make sure that this voltage is kept practically constant, as the power flow in/out of the battery fluctuates, a large capacitor (C_P= 1000 µF) is connected as shown in this circuit diagram. With such a capacitor, the voltage drops on the inner resistance R_i and the inner inductance L_{BAT}, when the battery is loaded, can be practically neglected.

Following this explanation, we are ready to write the equations describing the assumed battery model represented by both the circuit diagram in Figure 5-3 and the simulation diagram in Figure 5-2(b). These equations are

$$V_D = V_{D0} - \frac{1}{C_D} \int (I - \frac{V_D}{R_D}) dt ,$$

$$v_{BAT} = \frac{1}{C_P} \int (I - i_{arm}) dt ,$$

$$I = \frac{1}{L_{BAT}} \int (V_0 - IR_i + V_D - v_{BAT}) dt .$$

field inductance

2 ──→ Lf_DC

field resistance

120 ──→ Rf_DC

stator resistance

0.1 ──→ Ra_DC

stator inductance

0.12 ──→ La_DC

(a)

v_BAT

v_BAT ──→ V_DC

Battery_ON

not

if_DC

Lf_DC

w   ✱ Ea

Kf_Lf

I_DC

Ra_SR

Ea

La_DC

1/r / 1/S I_DC

PE_DC 1/r / T_DC

I_DC

v_BAT   ✱ P_BAT

Gen_m_rad/sec

BATTERY
POWER
CONTROL

Kf_Lf

CALCULATION

(b)

P_BAT_ref slider

20000   ✱ P_BAT_ref

E_R   1/r >

and

RC turn-on
threshold slider

225   Vs 1/r >

or Battery_ON

1/Z b x

RC TURN-ON CONDITION   **TURN-ON STATE LATCH**

(c)

**Figure 5-4. First-level expansion of the DC motor block: (a) parameter module,
(b) simulation diagram, and (c) expansion of the battery power control block**

5-4

Now, we are ready to describe the rotary converter module. Clicking on any of the blocks shown in Figure 5-2(c)brings up its lower level expansion. Such expansion of the DC motor block consists of: (1) the parameter module and (2) the simulation diagram. These blocks in an expanded form, again obtained by clicking the mouse, are shown in Figure 5-4(a) and (b), respectively. The parameter module specifies the following parameters, which are set by the user:

L_{f_DC} Field inductance

R_{f_DC} Field resistance

R_{a_DC} Stator resistance

L_{a_DC} Stator inductance.

In the simulation diagram in Figure 5-4(b), the back emf E_a is proportional to the field current i_{f_DC} generated by the DC machine field controller. It is given by the following equation:

$$E_a = K_{f\_Lf} \Phi_f \omega = K_{f\_Lf} i_{f\_DC} L_{f\_DC} \omega .$$

The conversion constant K_{f_Lf} is calculated for every i_{f_DC} value (in the compound block shown in this figure) according to the following equation:

$$K_{f\_Lf} = \frac{E_{anl}}{i_{f\_DC} L_{f\_DC} \omega_{DC\_rated}} .$$

It is assumed that the nonlinear characteristic of the no load voltage E_{anl} versus i_f at a constant speed ω_{DC_rated}, resulting from the saturation of the magnetic path in the DC machine, is given. We represent this relation as a table. For each value of i_{f_DC} (in the first column of the table) we read E_{anl}, which we put in the second column of this table. Next, we represent this table as an ASCII file with the extension .map. This file is then used to define the VisSim map block used in the simulation. If this nonlinear characteristic is not given, we must use the nameplate parameters on the DC machine to calculate the elements of the second column of this table. Using the rated parameters $I_a = 350$ A, $V_t = 600$ V and $R_a = 0.1\Omega$, we calculate the rated value of $E_a = 565$ V from the equation

$$V_t = E_a + I_a R_a .$$

From the rated rpm value of 1800, we obtain $\omega_{DC\_rated} = 188.495$ rad/sec. Then, assuming the linear relation $E_{anl} = k \, i_{f\_DC}$ and substituting the rated $E_a = 565$ V for E_{anl} and the rated value of i_f =1.49 A for i_{f_DC}, we find that $k = 379.2$. Now we can calculate the entries of the second column of our table. This approach is used in the standard simulation block of the battery/rotary converter. An example, which considers the field saturation curve for the real system, is presented as the Case Study 8 in Chapter 10.
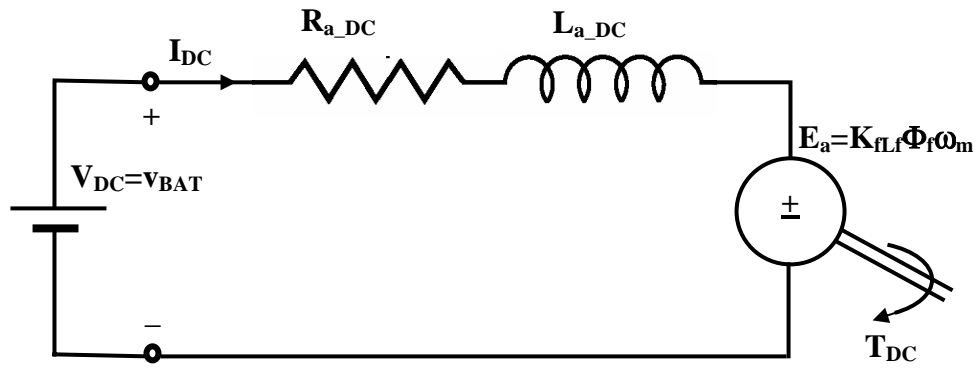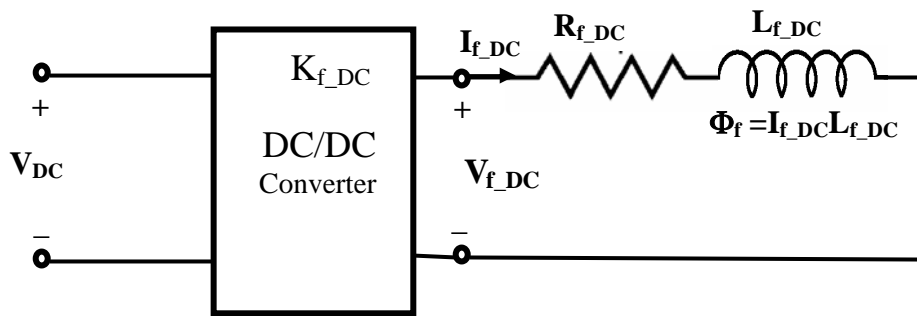
**Figure 5-5. Circuit diagrams of the DC motor: (a)
armature winding circuit diagram and
(b) field winding circuit diagram**

The field current i_{f_DC} is calculated so that the battery power

$$P_{BAT} = v_{BAT} I_{DC}$$

follows the battery reference power P_{BAT_ref}, which can be changed with a slider as shown in
Figure 5-4(c). The variable P_{BAT_ref} can also be preprogrammed using the VisSim blocks or can be
declared as a file. It may be chosen negative, which means that it is desired to charge the battery.
In this case, the DC machine works as a generator. It may be chosen positive, which means that
it is desired to discharge the battery. However, as we can see in Figure 5-4(c), the battery
reference power will be set to zero (irrespective of its adjusted value), during the start-up phase
of the simulation, as long as the binary variable $Battery_{ON}$ remains equal to zero. As seen in
Figure 5-4(c), the binary variable $Battery_{ON}$ switches to 1 when both the per phase voltage V_s and
the emf E_R (generated in the synchronous generator block of the rotary converter module) are
close enough to the reference per phase voltage V_{s_ref}. This RC turn-on threshold condition can be
changed with a slider. The RC turn-on condition implementation diagram, dot-framed in Figure
5-4(c), is introduced for performance stability of the power system in the start-up phase and,
once fulfilled, is removed by the turn-on state latch circuit, which is dot-framed in Figure 5-4(c).
In other words, the binary variable $Battery_{ON}$ remains equal to 1.

Returning to Figure 5-4(b), we can see that as long as $Battery_{ON} = 0$, the DC motor remains still. As soon as the condition $Battery_{ON} = 1$ is fulfilled, the DC motor starts operating. It works as a generator for negative P_{BAT_ref}; i.e., it generates negative torque T_{DC} or is driven by the synchronous machine that, because of this condition, is forced to operate as a synchronous motor. On the other hand, with positive P_{BAT_ref}, the battery is being discharged, and the DC motor produces a positive torque T_{DC}, which in turn drives the synchronous generator. The DC power from the battery is being converted into AC power supplied to the grid. The equations describing the simulation diagram in Figure 5-4(b), under the condition $Battery_{ON} = 1$, follow:

$$I_{DC} = \frac{1}{L_{a\_DC}} \int (v_{BAT} - E_a - R_{a\_DC} I_{DC}) dt \ ,$$

$$P_{E\_DC} = E_a I_{DC} \ , \quad T_{DC} = \frac{P_{E\_DC}}{Gen_{m\_rad/\sec}} = K_{fLf} L_{f\_DC} i_{f\_DC} I_{DC} \ ,$$

where E_a has already been defined.

For better understanding of the interaction between the armature winding and the field winding of the DC machine, the relevant circuit diagrams are presented in Figure 5-5. This interaction is realized through the field winding flux Φ_f, which is proportional to the field current i_{f_DC}. We can use the DC/DC converter or AC/DC phase-controlled rectifier to control this current. In particular, as shown in Figure 5-6, the DC/DC conversion constant is controlled by the PID controller. Figure 5-7 represents the first- and the second-level expansion of the synchronous generator compound block. This figure has the same structure as Figure 3-4 because they both represent the synchronous generator. The essential difference is between parts (c) of these figures. The generation of the voltage E_{qD} in Figure 3-4(c) and the generation of the voltage E_R in Figure 5-7(c) are both governed by the same equation. However, we chose E_{qD} to be a reference; i.e., we assumed that its phase is zero (so we have the input to the d-generator $E_{dD} = 0$). Consequently, we cannot make the same assumption for the voltage E_R. This is accounted for in Figure 5.7(c) by calculating the angle

$$\gamma = \int (\omega_{RC} - \omega) dt \ .$$
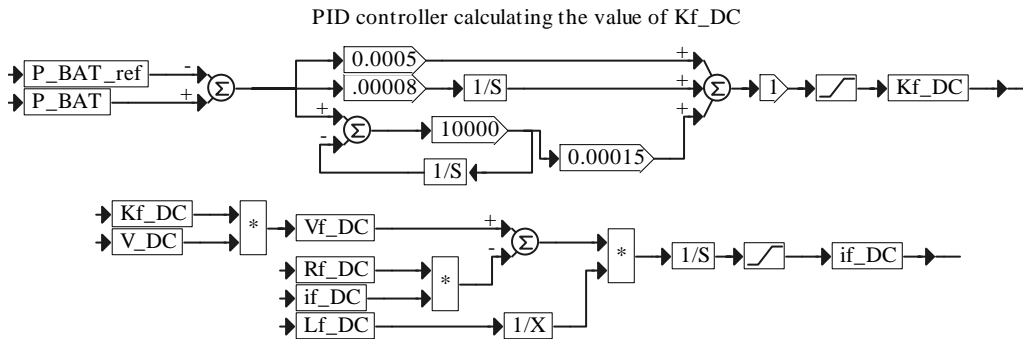
**Figure 5-6. Simulation diagram of the DC machine field controller**

(a)

voltage-flux constant

$\boxed{1.0232} \longrightarrow \boxed{\text{Ke\_RC}}$

stator resistance

$\boxed{0.061} \longrightarrow \boxed{\text{R\_SR}}$

stator inductance, q component

$\boxed{.00494} \longrightarrow \boxed{\text{L\_qSR}}$

stator inductance, d component

$\boxed{.0068} \longrightarrow \boxed{\text{L\_dSR}}$

$\boxed{4} \longrightarrow \boxed{\text{pole\_RC}}$

field winding resistance

$\boxed{30} \longrightarrow \boxed{\text{Rf\_RC}}$

field winding inductance

$\boxed{1.7} \longrightarrow \boxed{\text{Lf\_RC}}$

synchronous generator moment of inertia

$\boxed{2} \longrightarrow \boxed{\text{J\_SR}}$

viscous friction coefficient of the synchronous generator

$\boxed{0.003} \longrightarrow \boxed{\text{B\_SR}}$

(b)

(c)
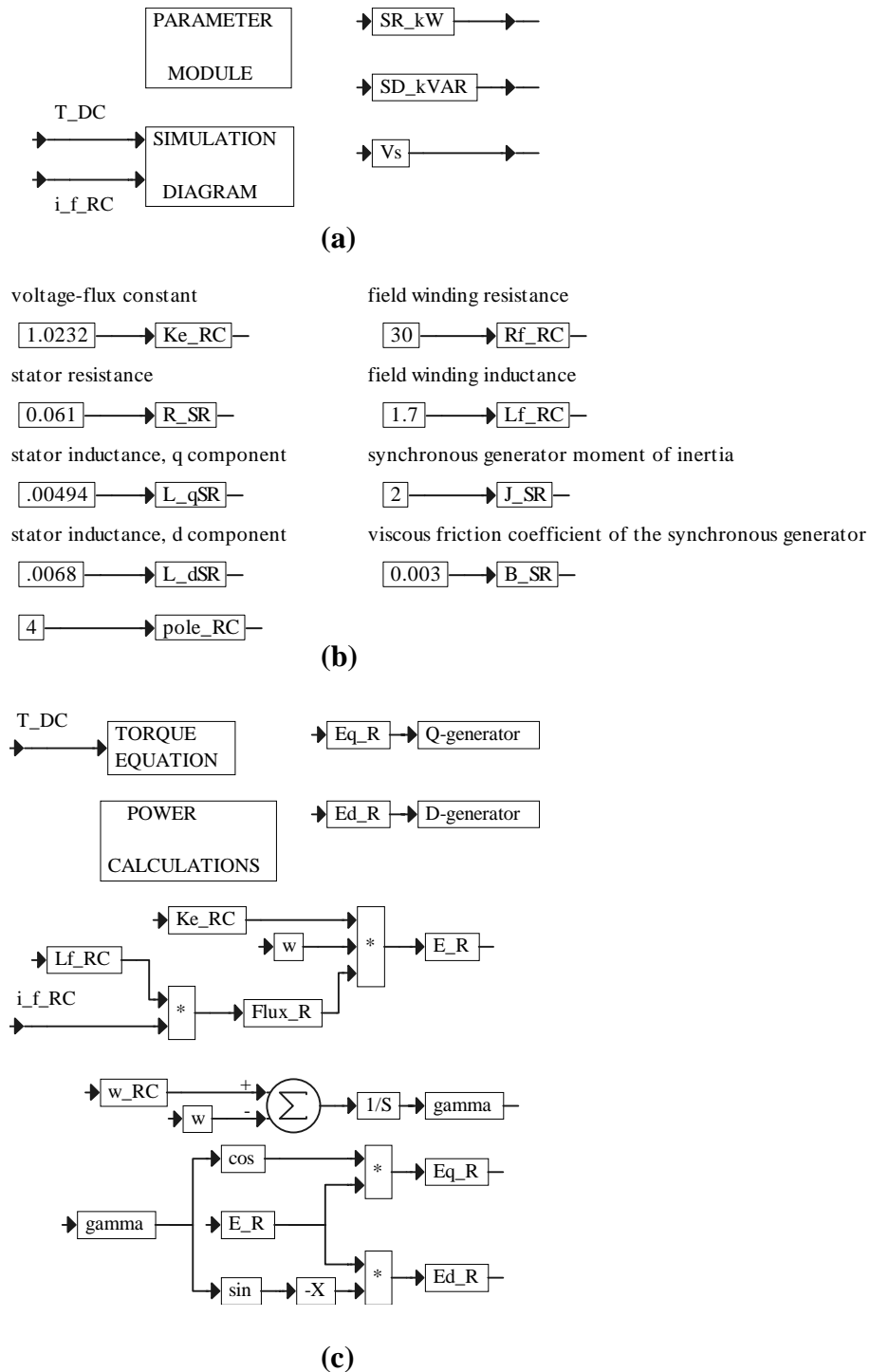
Figure 5-7. First- and second-level expansion of the synchronous generator block used as a part of the rotary converter module: (a) first-level expansion, (b) parameter module expansion, and (c) simulation diagram expansion
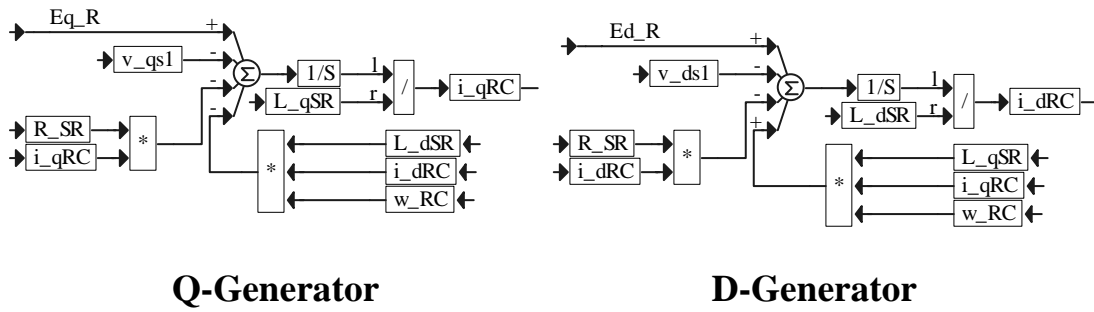
Q-Generator **D-Generator**

(a)
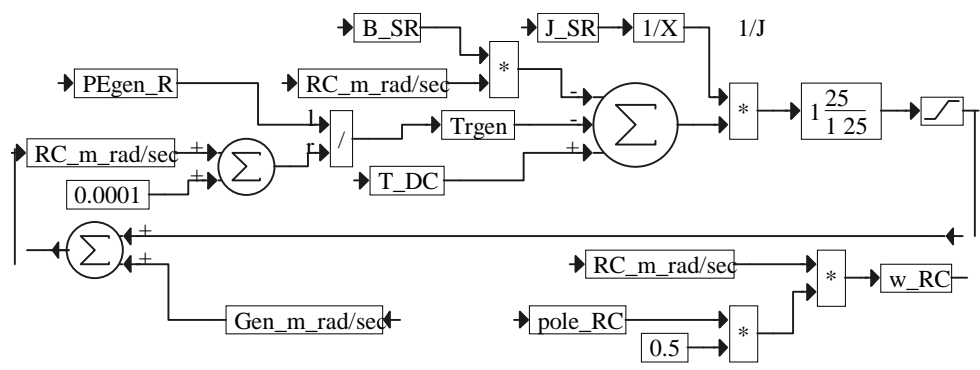
(b)
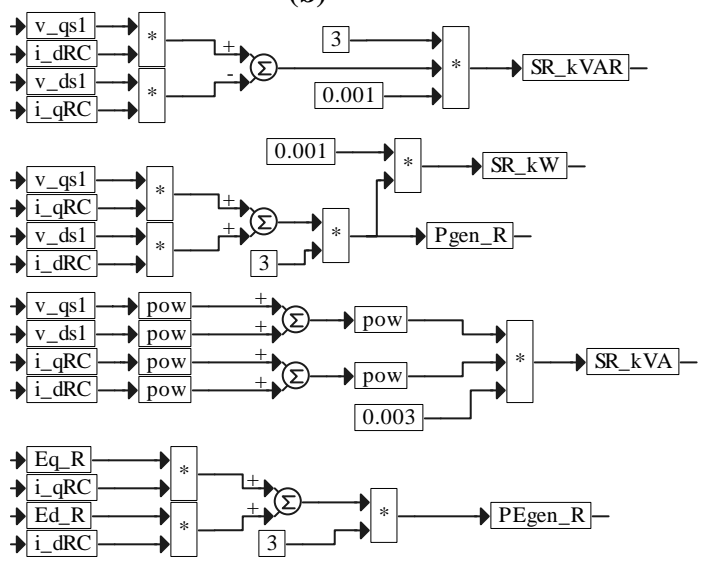
(c)

Figure 5-8. Simulation diagram of the synchronous generator (rotary converter module):
(a) Q-generator and D-generator, (b) torque equation, and (c) power calculations

and generating q and d components of E_R according to the following equations:

$$E_{q\_R} = E_R \cos \gamma,$$
$$E_{d\_R} = -E_R \sin \gamma,$$

where ω_{RC} is the angular frequency calculated in Figure 5-8(b) based on the angular velocity of the rotary converter $RC_{m\_rad/sec}$ which, in turn, is obtained from the simulation of the torque equation in Figure 5-8(b). Note that the difference $\omega_{RC} - \omega$ is nonzero only in the transient and is used here to establish the angle γ, which in steady state remains constant or $\omega_{RC} = \omega$. The equation simulated in Figure 5-8(b) reads

$$RC_{m\_rad/sec} - Gen_{m\_rad/sec} = \frac{1}{J_{SR}}(T_{DC} - T_{rgen} - B_{SR}RC_{m\_rad/sec}),$$

where

$$T_{rgen} = \frac{P_{Egen\_R}}{RC_{m\_rad/sec}}$$

and P_{EgenR} is the electrical power generated and calculated in Figure 5-8(c). In the simulation of this equation, a low-pass filter with the transfer function $25/(s+25)$ is added to filter out the higher harmonics. Power calculations in Figure 5-8(c) are self-explanatory. The Q-generator and the D-generator, shown in Figure 5-8(a), are the same as those in Figure 3-5(b).

Refer to Figure 5-6 for the simulation diagram of the DC machine field controller.. The field current i_{f_DC} is generated to drive the error $P_{BAT\_ref} - P_{BAT}$ to zero. First, recall that in Figure 5-4(b) we renamed the variable v_{BAT} as follows:

$$V_{DC} \equiv v_{BAT}.$$

In the simulation diagram of Figure 5-6, the name V_{DC} is used for the battery voltage. The simulation diagram in the lower part of this figure is described by the following equations:

$$i_{f\_DC} = \frac{1}{L_{f\_DC}} \int (V_{f\_DC} - R_{f\_DC}i_{f\_DC})dt,$$

$$V_{f\_DC} = K_{f\_DC}V_{DC},$$

and i_{f_DC} is controlled by the DC/DC conversion coefficient K_{f_DC}.

Figure 5-9 presents the simulation diagram of the voltage regulator, which was designed as a voltage/reactive power controller. The purpose of control action **during the start-up period of the simulation** (of the duration chosen by the user and set up to be 2 sec in the simulation diagram in Figure 5-9), generated in this regulator, is to drive the difference

$$err = V_{s\_ref} - E_R$$

to zero.
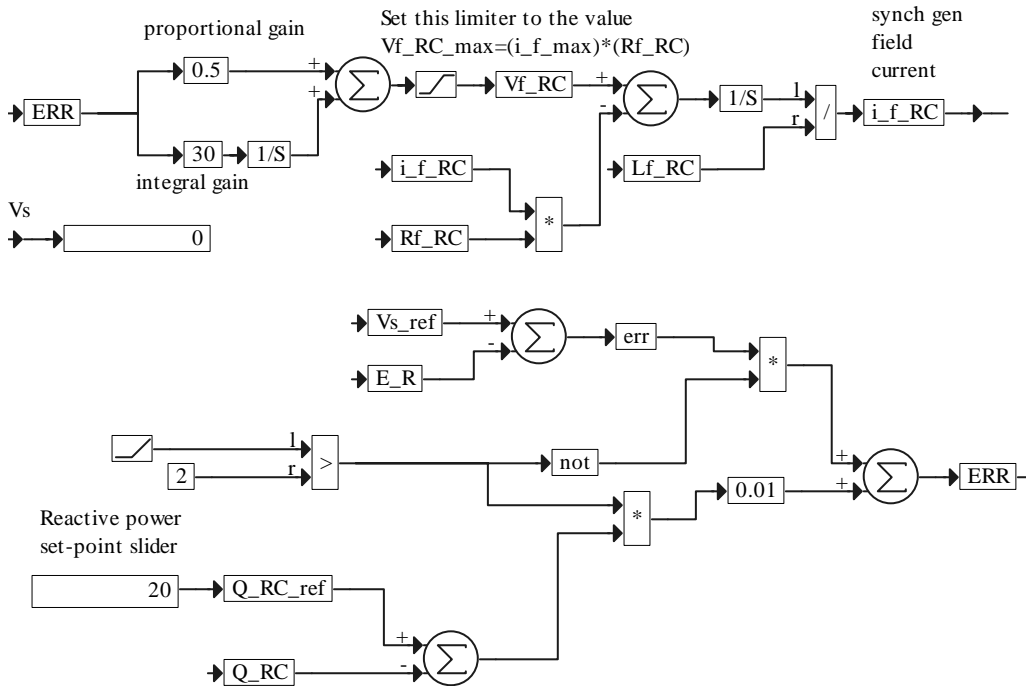
Figure 5-9. Simulation diagram of the voltage regulator

The emf E_R is, according to simulation diagram in Figure 5-7(c), given by the following equation:

$$E_R = K_{e-RC} \, Flux_R \, \omega,$$

where

$$Flux_R = L_{f\_RC} i_{f\_RC},$$

i_{f_RC} is the field current (DC) of the synchronous generator, and K_{e_RC} is the voltage-flux constant. Therefore, the field current i_{f_RC} is used to control E_R. Consequently, as a result of the PI's action, the field voltage V_{f_RC} is generated. Then, as shown in Figure 5-9, the simulation of the following equation results in the field current i_{f_RC}:

$$i_{f\_RC} = \frac{1}{L_{f\_RC}} \int (V_{f\_RC} - R_{f\_RC} i_{f\_RC}) dt \ .$$

After the start-up period of the simulation, the signal *err* is replaced by the difference

$$Q_{RC\_ref} - Q_{RC},$$

where Q_{RC} is the reactive power generated (if positive) or absorbed (if negative) by the rotary converter and Q_{RC_ref} is its reference value, which can be varied with a slider. Therefore, the user can control the reactive power Q_{RC}. In other words, with *P_BAT_ref* set to zero, the rotary converter becomes a reactive power source or the reactive power sink. The rotary converter operating in this mode is called a synchronous condenser.

Note that the limiter for V_{f_RC} should be properly set before running the program. The relevant instruction is given in the simulation diagram of Figure 5-9.

Village Load

In Figure 6-1, we present a single-line diagram (as in Figure 1-1) of a hybrid power system where we dot-framed the portion of the diagram that represents the village load. The user brings the village load to the simulation screen by using the Add command and selecting the file VL.vsm.
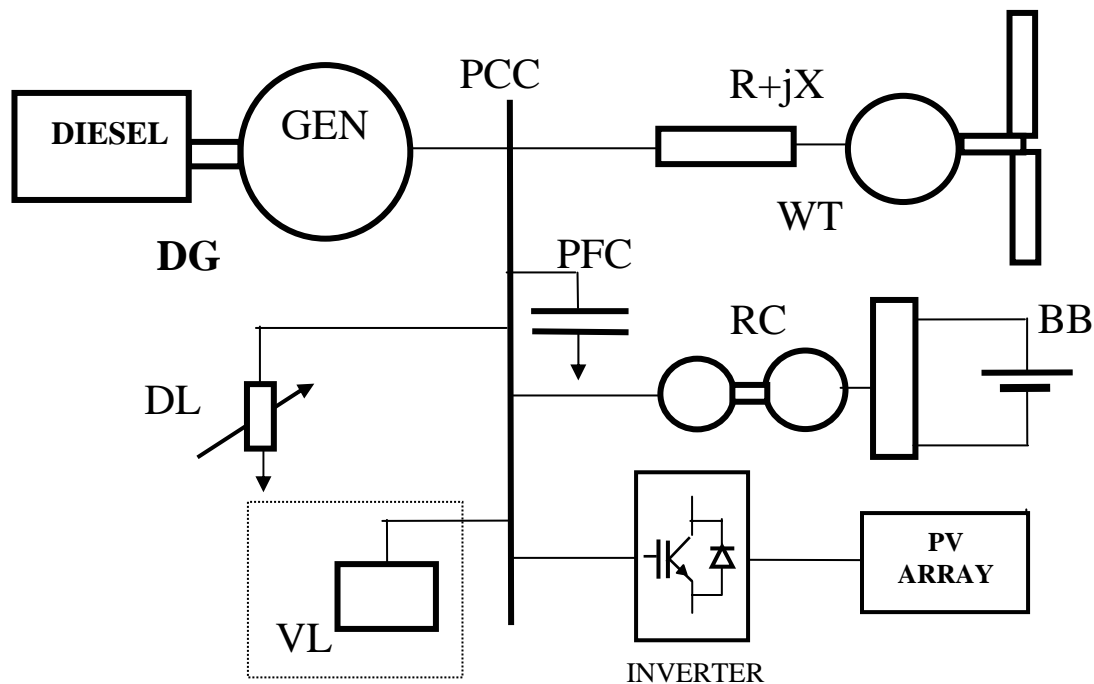
Figure 6-1. A single-line diagram of a hybrid power system with the VL module dot-framed

Figure 6-2(a) represents the block diagram of the VL module as it appears in simulation diagrams. Its first-level expansion, shown in Figure 6-2(b), has two output variables, available for direct monitoring; i.e., the real power load P_V in [kW] and the reactive power load Q_V in [kVAR]. The expansion of its simulation diagram block is shown in Figure 6-2(c) and consists of three compound blocks: (1) power calculations, (2) q-axis, and (3) d-axis representations of the load. The output variables of the last two blocks are the component i_{qV} and i_{dV} of the load current. These current components enter the PCC node if the user activates village load by clicking the mouse on the button in the top-view diagram of the PCC module. The parameter module in the first-level expansion is further expanded in Figure 6-2(d). The parameters defined by the user, specific to the application considered, are the rated real power consumption P_v and the power factor pf. The user has a choice between fixed load, declaring the values of variables P_{v1} and pf_1, and the load profile, declaring P_{v2} and pf_2 in a form of time series. The user makes the choice by clicking on the button in the parameter module of the VL. Button on (red) corresponds to fixed

village load and button off corresponds to the village load profile. In Figure 6-3, we show an example of a village load profile represented by the two time series
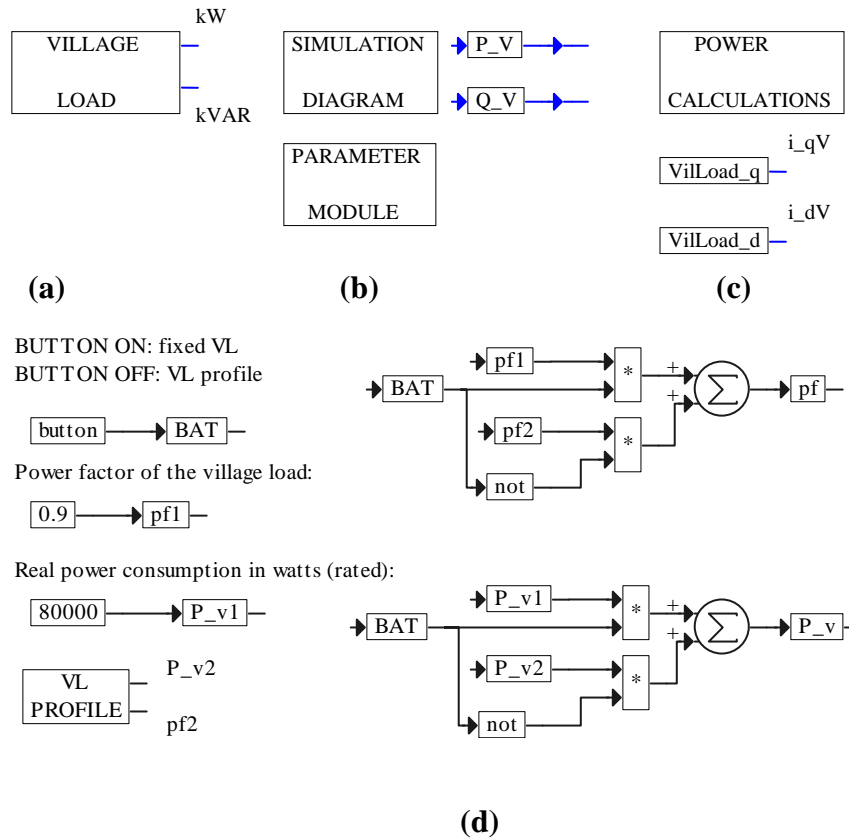
Figure 6-2. Block diagrams of the VL module: (a) representation of the VL module in simulation diagrams, (b) first-level expansion, (c) second-level expansion of the simulation diagram, and (d) second-level expansion of the parameter module

contained in the ASCII data files power.dat and pf.dat. The user can modify these data files according to the load profile to be represented or set up his or her own import block in VisSim. To open these files the user must click on VL Profile [Figure 6-2(d)] and then on the blocks shown in Figure 6-3. The dialog box Import Setup comes up with a button Browse Data. Clicking on this button opens the data files in Notepad. The data files involved must have the format shown in Figure 6-3, where the first column is the time and the second column is the value of the variable.

In Figure 6-4, the compound blocks, which appear in Figure 6-2(c), are expanded. Figure 6-4(a) shows how both components of the load current are calculated. These calculations are realized by implementation of the equations describing the circuit diagram presented in Figure 6-5. First, however, it is necessary to determine the equivalent rated village load parameters: the resistance R_v and the inductance L_v. These, as shown in the upper part of Figure 6-4(a), are found by simulation of the following equations:

$$\frac{P_v}{3} = \frac{V_{s\_ref}^2}{R_v}, \qquad \frac{Q_v}{3} = \frac{V_{s\_ref}^2}{X_v}, \qquad L_v = \frac{X_v}{\omega_b},$$

where the rated reactive power Q_v is defined as

$$Q_v = \sqrt{S_v^2 - P_v^2} = \sqrt{\left(\frac{P_v}{pf}\right)^2 - P_v^2}$$

with $S_v = P_v / pf$ being the apparent power. The equations mentioned above, describing the circuit diagram in Figure 6-5, are implemented here to generate the components of the load current, and are listed below separately for each component. For the q-axis component, the equations read

$$i_{qv} = i_{qV1} + i_{qV2},$$

$$i_{qV1} = \frac{v_{qs1}}{R_v},$$

$$i_{qV2} = \frac{1}{L_v} \int (v_{qs1} - \omega i_{dv} L_v) dt .$$

power.dat
0.0000000e+000 2.0000000e+004
0.9999999e+000 2.0000000e+004
1.0000000e+000 5.0000000e+004
2.4999999e+000 5.0000000e+004
2.5000000e+000 2.0000000e+004
2.0000000e+001 2.0000000e+004

pf.dat
0.0000000e+000 0.5000000e+000
0.9999999e+000 0.5000000e+000
1.0000000e+000 1.0000000e+000
2.4999999e+000 1.0000000e+000
2.5000000e+000 0.7500000e+000
2.0000000e+001 0.7500000e+000

Figure 6-3. An example of a village load profile represented graphically and by ASCII data files power.dat and pf.dat
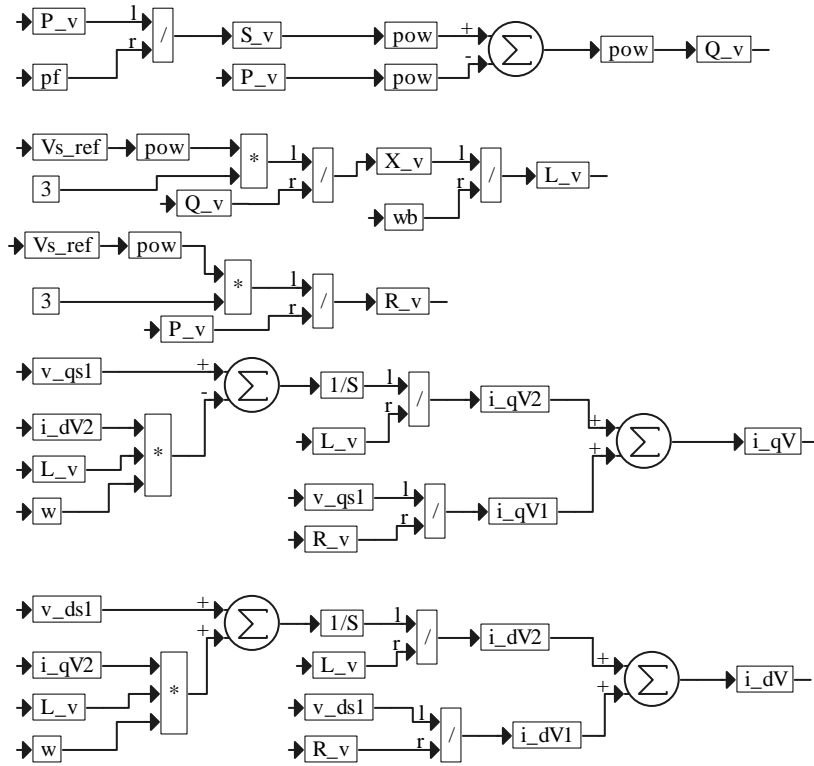
(a)
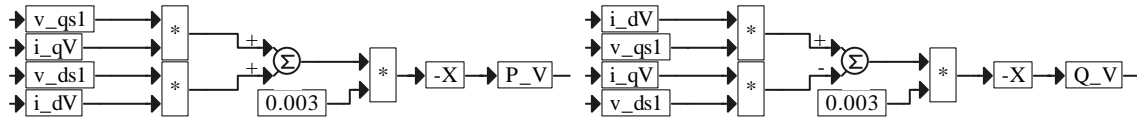
(b)

Figure 6-4. Expansions of the compound blocks shown in Figure 6-2(c): (a) calculations of the q and d components of the village load currents and (b) power calculations

Similarly, for the d-axis component the equations read

$$i_{dv} = i_{dV1} + i_{dV2},$$

$$i_{dV1} = \frac{v_{ds1}}{R_v},$$

$$i_{dV2} = \frac{1}{L_v} \int (v_{ds1} + \omega i_{qv} L_v) dt.$$
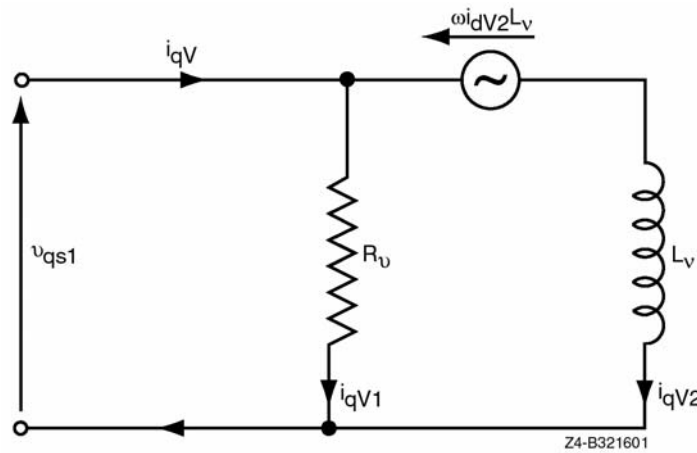
(a)
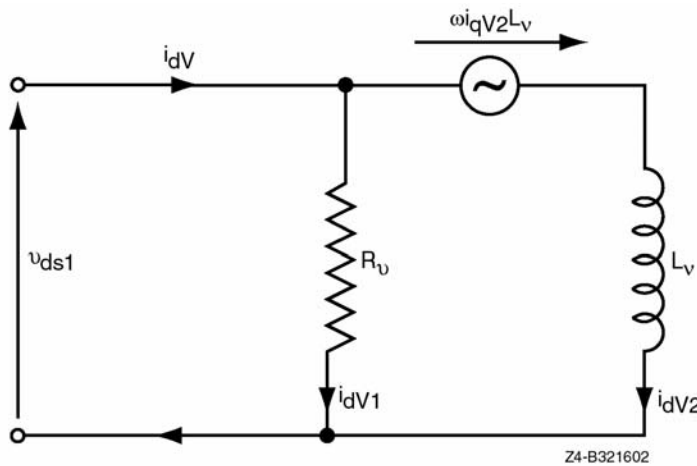
(b)

Figure 6-5. Circuit diagram explaining calculationsof the VL currents:
(a) q-axis and (b) d-axis

Finally, the calculations of the real power P_V and the reactive power Q_V are implemented in Figure 6-4(b), according to the following equations:

$$P_V = -3\times10^{-3}(v_{qs1}i_{qV} + v_{ds1}i_{dV}) \ [\text{kW}],$$

$$Q_V = -3\times10^{-3}(v_{qs1}i_{dV} - v_{ds1}i_{qV}) \ [\text{kVAR}].$$

P_V and Q_V are computed based on the general convention in this program package, meaning that both P_V and Q_V are negative because village load always absorbs the real power and the reactive power (inductive load).

Dump Load

In Figure 7-1, we present a single-line diagram (as in Figure 1-1) of a hybrid power system where we dot-framed the portion of the diagram that represents the dump load. The user brings the dump load to the simulation screen by using the Add command and selecting the file DL.vsm.
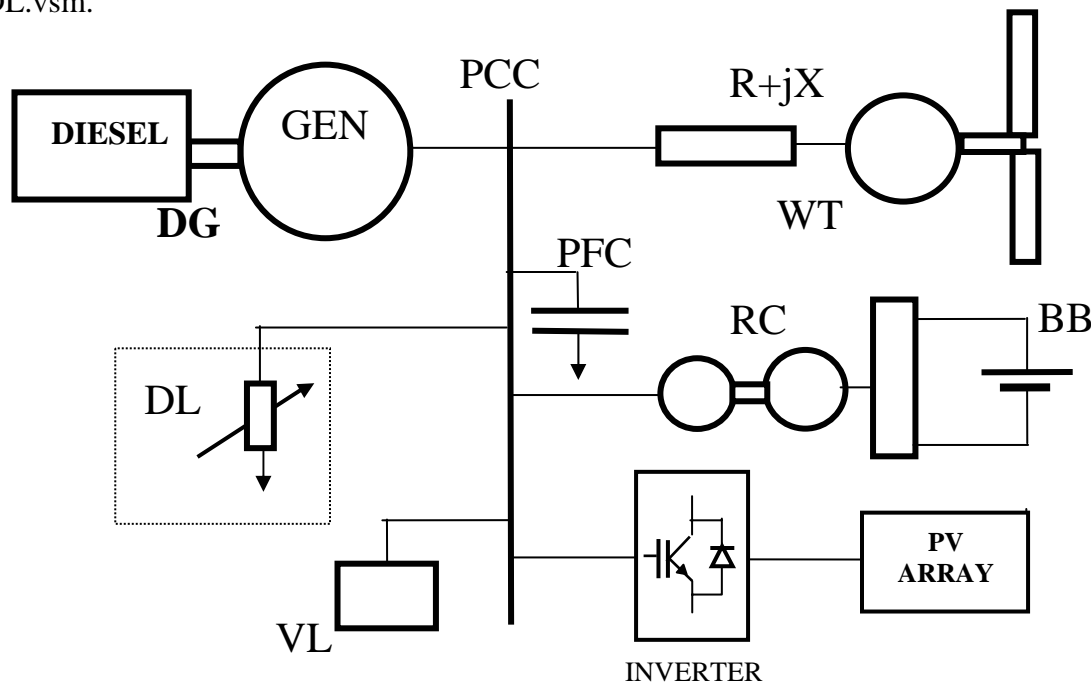
**Figure 7-1. A single-line diagram of a hybrid power system
with the DL module dot-framed**

The dump load is used either to keep the diesel generated power above a user-prescribed fraction of its rated power or to control the line frequency $f = \omega / 2\pi$. The user chooses the control strategy through turning on and off the button by clicking the mouse in the first-level expansion diagram shown in Figure 7-2(b). In this figure, the principal blocks of the DL module are presented, along with their connections. The top-view level representation of the DL module is illustrated in Figure 7-2(a). Each control strategy defines the number of load elements connected in parallel. The control strategy switch passes to its output the number of elements active, generated by the control strategy the user selected. As seen in Figure 7-2, when the button is ON (red) or 1, this output is generated by the minimum diesel power controller. When it is OFF (white) or 0, the output is generated by the frequency-based DL controller. The control strategy

switching is implemented as shown in Figure 7-3. The simulation diagram of the frequency controller is shown in Figure 7-4(a), and its parameter module is expanded in Figure 7-4(b).

(a)   **(b)**
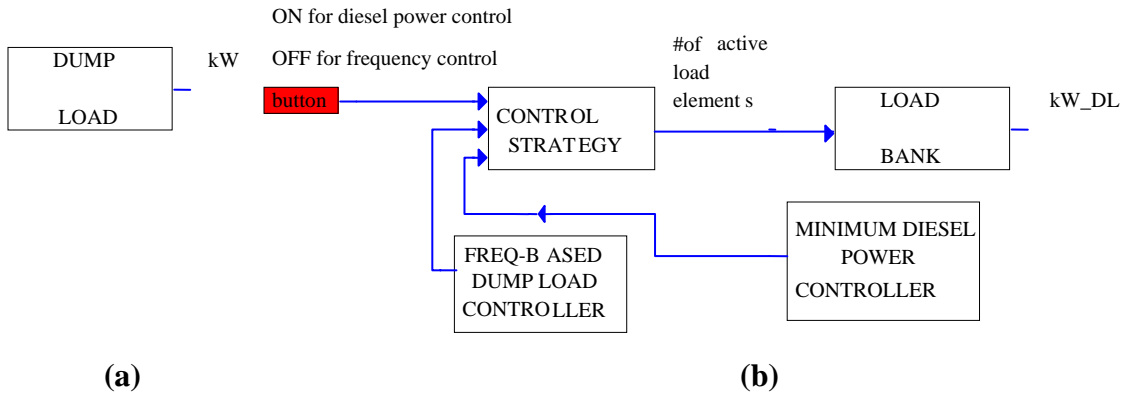
Figure 7-2. Block diagrams of the DL module: (a) representation of the DL module in simulation diagrams and (b) first-level expansion
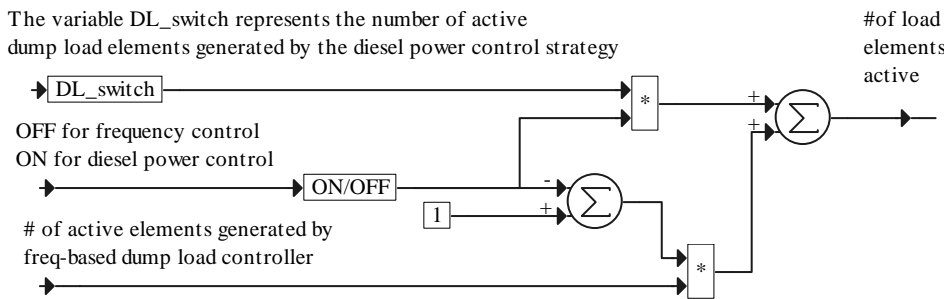
Figure 7-3. Control strategy switch of the DL module

(a)   **(b)**
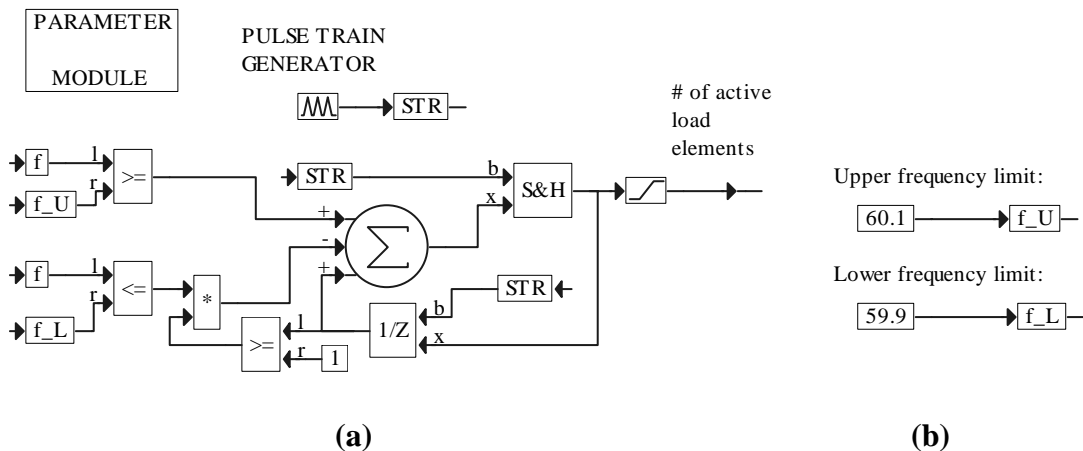
Figure 7-4. Frequency-based DL controller: (a) simulation diagram and (b) expansion of the parameter module
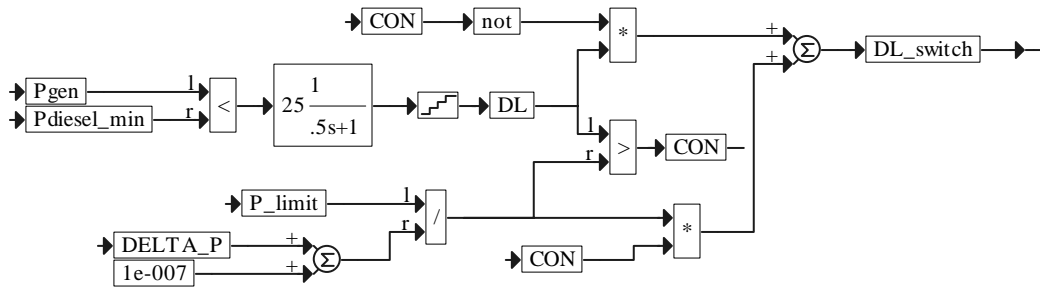
Figure 7-5. Minimum diesel power controller

It contains the upper frequency limit f_U and the lower frequency limit f_L, both of which are chosen by the user. The output of the frequency-based DL controller is updated every sampling period, established by the pulse-train generator. Its value is set to 0.1 sec, but the user can change it easily. Because of the limiter connected at the output, the number of active load elements generated by this controller is never less than one. So the minimum load is represented by one active load element. Because of the unit delay element, activated every sampling period, the unconstrained (meaning taken before the limiter) number of active load elements at the previous sampling instant is obtained. If this number is greater than or equal to 1 and the current line frequency is less than or equal to f_L, the controller decreases the number of active load elements by 1, which results in a decreased load. On the other hand, as long as the current line frequency remains greater than f_U, the number of active load elements will increase by 1 every sampling instant.

Figure 7-5 shows the simulation diagram of the minimum diesel power controller. The system load, represented by the power P_{gen}, is compared with the minimum diesel load $P_{diesel\_minimum}$. The goal is to implement a diesel power control strategy by generating a number of active dump load elements (connected in parallel), which are needed to keep the generated power P_{gen} above a fraction $P_{diesel\_minimum}$ of the diesel rated power that the user prescribed in the diesel generator simulation diagram. In the simulation diagram in Figure 7-5, the variable DL_{switch} represents the number of active load elements. To determine the value of the variable DL_{switch}, we introduce an auxiliary variable DL, which assumes positive integer values whenever the diesel load P_{gen} drops below the minimum diesel load value. The increments of DL correspond to dump load power increments $DELTA\_P$, as can be seen in Figure 7-6. The maximum number of these increments is calculated as

$$n = \frac{P\_limit}{DELTA\_P}.$$

Then, as shown in the simulation diagram in Figure 7-5, we have

$$DL_{switch} = \begin{cases} DL & \text{if } DL \leq n \\ n & \text{otherwise} \end{cases}.$$

The implementation of the load bank block is shown in Figure 7-6(a) and its parameters in Figure 7-6(b). The user declares a value of the variable *P_limit* that is the power limit of the DL
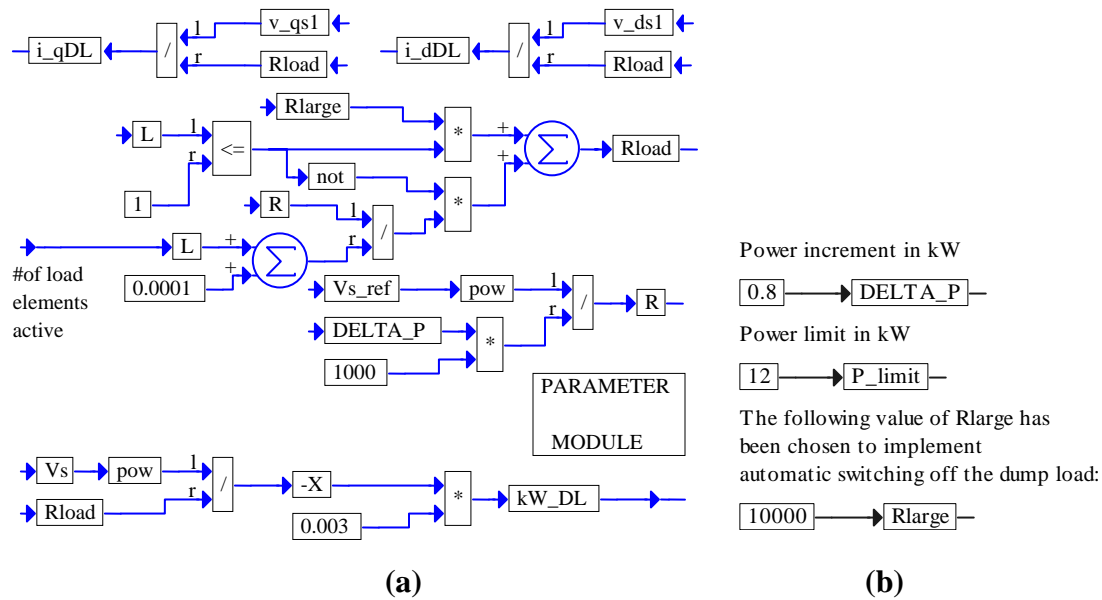
Figure 7-6. Load bank block: (a) simulation diagram with power calculation and (b) expansion of the parameter module

or total DL power that can be consumed in the system. In addition, the user must also define the power increment *DELTA_P* (per phase).

We now explain how the values of these two variables are related to the DL structure of the simulated power system. Consider the values shown in Figure 7-6(b) as an example. We determine that we need 15 increments of 0.8 kW to generate the load of 12 kW. Such load can be implemented with 15 equal load sections or only 4 load sections if the load structure is binary; i.e., the load sections are 0.8 kW, 1.6 kW, 3.2 kW, and 6.4 kW. In general, if we have a binary load with *n* sections and we want to have a power increment of *DELTA_P*, we may have

$$P\_limit = (2^n-1)\ DELTA\_P.$$

The resistance of the dump load R_{load} is calculated, and if the number of load elements active equals 1 (which corresponds to the smallest load), the dump load is practically disconnected by making R_{load} equal R_{large}. In the same simulation diagram, the components of the current contributed to the PCC module are determined; i.e.,

$$i_{qDL} = \frac{v_{qs1}}{R_{load}}, \qquad i_{dDL} = \frac{v_{ds1}}{R_{load}}.$$

In addition, the real power consumed is found as

$$kW_{DL} = -10^{-3}\ \frac{V_s^2}{R_{load}}\ [kW].$$

Inverter

In Figure 8-1, we show a single-line diagram (as in Figure 1-1) of a hybrid power system where we dot-framed the portion of the diagram that represents the inverter. As shown in this figure, the system consists of two machines: (1) a diesel engine and (2) a synchronous generator. The user brings the inverter module to the simulation screen using the Add command and selecting the file INV.vsm. In addition, the user must add the DG/inverter control block to the simulation screen by selecting the file DG_INV_CTRL.vsm. This block is used to program diesel/inverter operation and is required if either the DG or the inverter, or both, are involved in the simulated power system. If the DG is not part of the simulated power system, the user must also add the NO_DIESEL block by selecting the file NO_Diesel.vsm.
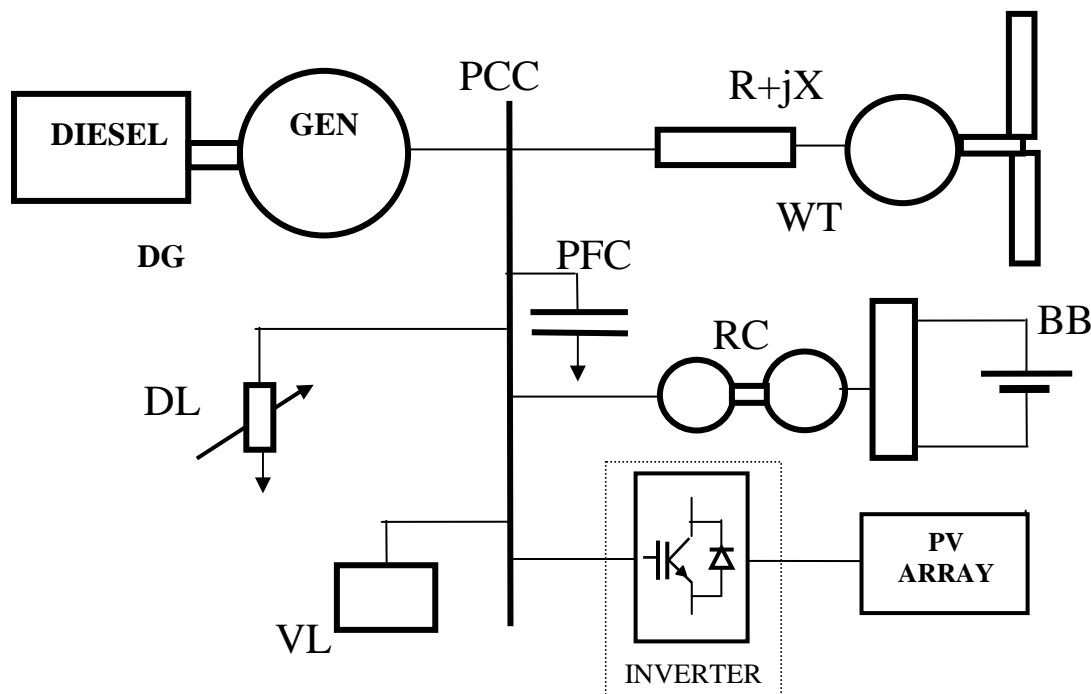
Figure 8-1. A single-line power system diagram with the inverter portion dot-framed

Inverters are power electronics devices that convert DC power to AC power. At this time, most inverters use IGBTs (insulated gate bipolar transistors), which can be turned on and off at a very fast rate. With IGBT switches, the power converter can function as an inverter (power flows from the DC side to the AC side) or as a rectifier (power flows from AC to DC). In daily applications, IGTBs are used as variable frequency drives (VFD) or at constant frequency such as in an uninterruptible power supply (UPS). Many other applications can be found in power systems applications, such as reactive power compensators or active filters. Figure 8-2 shows a

typical inverter. As elements of power systems, they can work in one of two modes—the master mode or the slave mode.

In the master mode, the inverter controls the system's frequency and voltage. We show an example of such a system in Figure 8-3. In this system, the inverter is connected to a battery bank. In such a system, the inverter can provide or absorb both the real and the reactive power. On the other hand, in conjunction with the PV array, the inverter can supply real power and provide or absorb the reactive power. In this case, the power exchange is determined by the system's power balance.

In the slave mode, the user specifies the real and the reactive power required to be generated or absorbed.. Figure 8-4 illustrates an example of such a system. The real and reactive power variables are shown as variables controlled by the inverter or following the reference trajectory the user has determined.
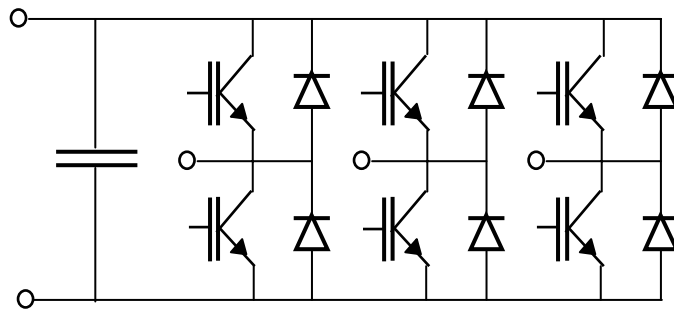
Figure 8-2. A typical inverter
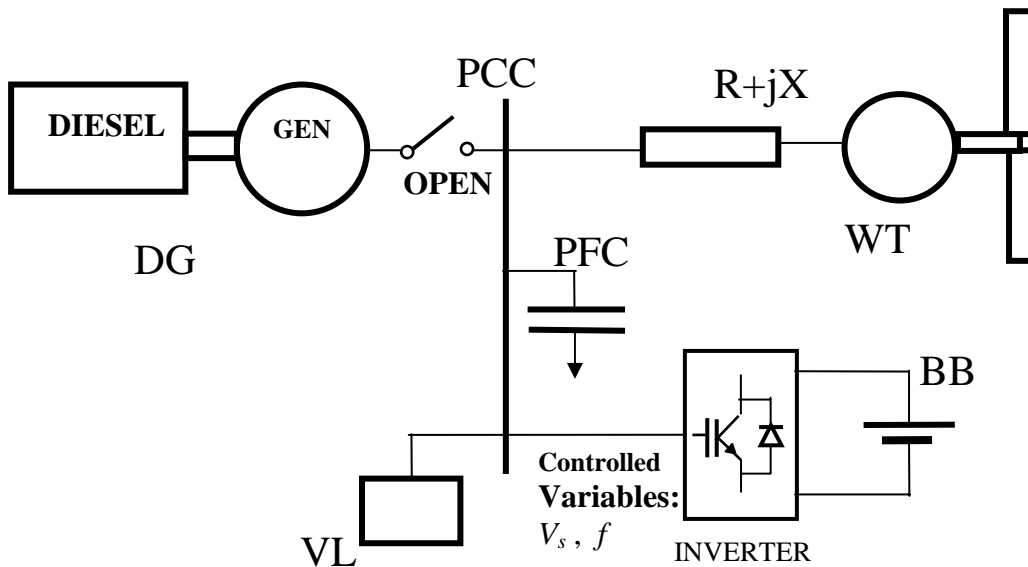
Figure 8-3. An inverter operating in the master mode
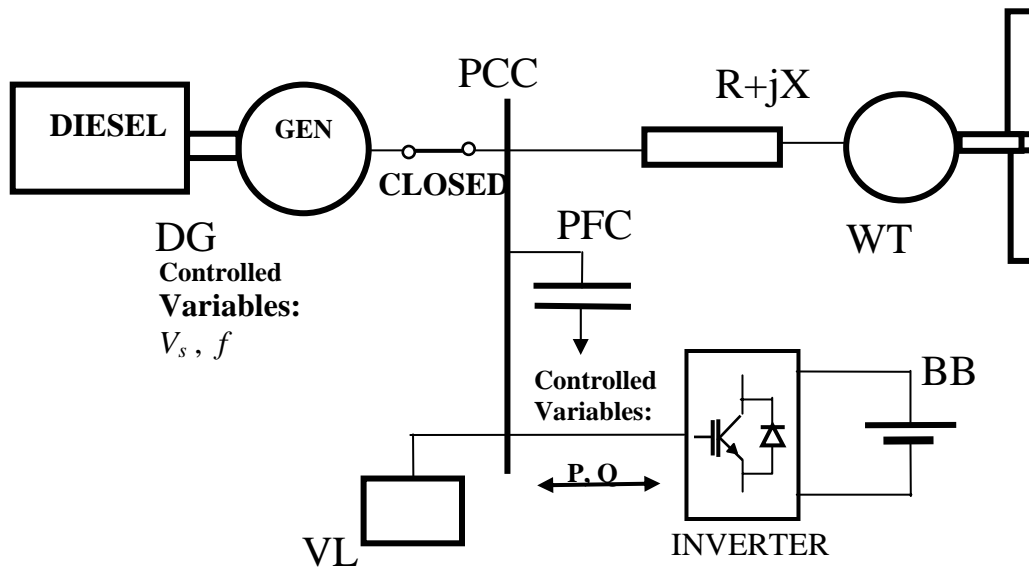
Figure 8-4. An inverter operating in the slave mode

The control strategy developed by the hybrid power plant designer or operator performs the transfer from slave mode to master mode. This is suitable, for example, when the inverter uses a sufficient battery storage site. In this case, during night operation with light load condition, the inverter's battery carries the load and the diesel generator is turned off. Power generated by occasional wind during the night will be stored in the battery. During the day, when the load is close to rated power, the diesel is turned on and the inverter is operated in the slave mode to charge the battery and to support the occasional peak load.

We developed a model of the inverter that makes all specified options of operation possible. We tested this model under variable load conditions and by switching between the slave mode, in which the diesel generator controls the system's voltage and frequency, and the master mode, in which the diesel generator is disconnected and the inverter takes over the voltage and frequency control. In addition, we tested the inverter's operation in conjunction with the battery and the PV array.

Diesel/Inverter Operation Control

The diesel/inverter operation control is a complex task, which involves the following simulation blocks:

- DG/inverter control block, which has to be brought to the simulation screen when either the DG or the inverter or both are involved in the simulated power system.
- DG/inverter switch block, which is part of the DG module.
- NO_DIESEL block, which has to be brought to the simulation screen when the simulated system includes an inverter and does not include a diesel generator.

(a)
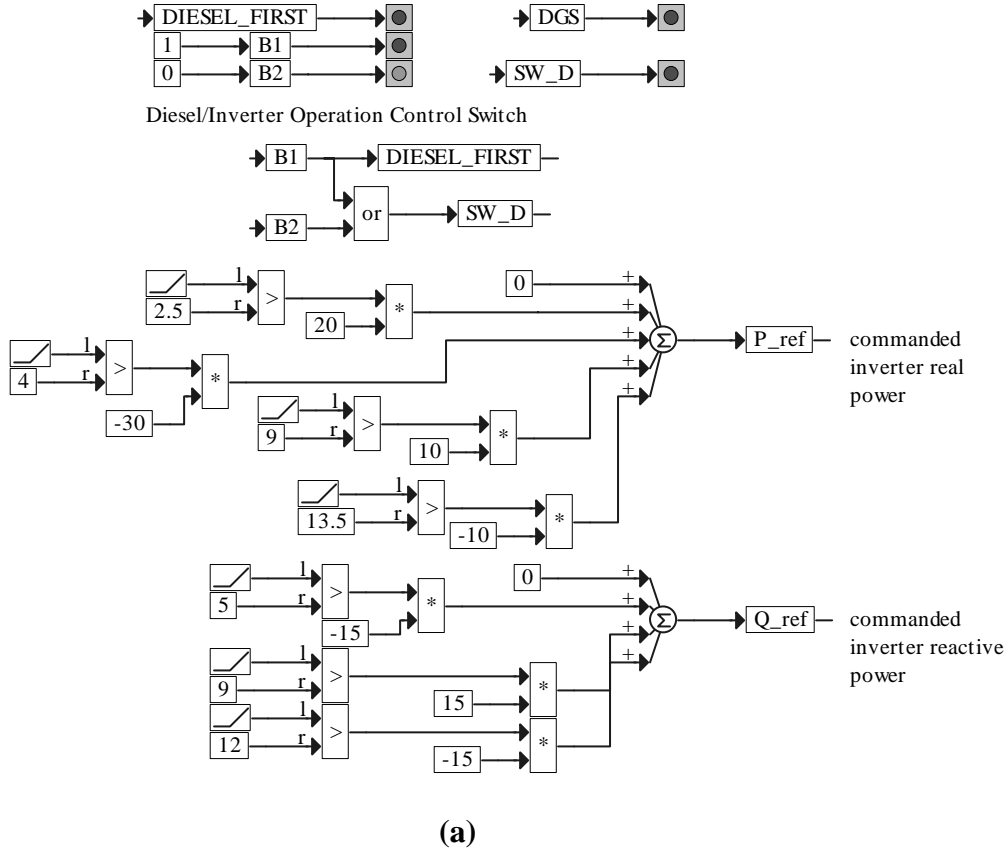
PROGRAMMING/MONITORING GUIDE

B1=1, B2=0 sets DGS=1

       startup of the DG, the inverter operates as a slave

Note 1: DGS=1 indicates that the DG is a master and the inverter is a slave

       DGS=0 indicates that the DG is idling and the inverter is a master

Note 2: SW_D=(B1)or(B2)

B1=0, B2=0 sets DGS=0

       the commanded values P_ref and Q_ref have no effect

B1=0, B2=1 sets SW_D=1

       the process of synchronization starts.

       Its completion results in setting DGS=1

(b)

Figure 8-5. The DG/inverter control block: (a) simulation diagram and (b) programming/monitoring guide

The user must program the sequence of requests for switching the master function between the diesel and the inverter. To facilitate the implementation of this function, we introduced the DG/inverter control block as a separate module. Its simulation diagram is shown in Figure 8-5(a). The binary variables $B1$ and $B2$, shown in this figure, can be used to program any diesel/inverter switching strategy. A combination of their values defines one of the following states of operation:

STATE 1: Inverter as a master (controls voltage and frequency, the DG is disconnected): $B1 = 0$
        and $B2 = 0$
STATE 2: System started with the DG (the inverter operates as slave): $B1 = 1$ and $B2 = 0$
STATE 3: The process of the DG synchronization starts and is followed by switching the master
        function to the DG: $B1 = 0$ and $B2 = 1$.

In particular, if we have only the inverter on the system, the system is in STATE 1 all the time. When starting with the DG and turning it off and on, we have the following sequence of states:

        STATE 2, STATE 1, STATE 3, STATE 1, STATE 3, STATE 1, STATE 3,… .

When we start with the inverter as a master (DG off) and then turn the DG on and off, we have the following sequence of states:

        STATE 1, STATE 3, STATE 1, STATE 3, STATE 1, STATE 3,… .

The user must program the required sequence of state switching (using the simulation time as an auxiliary variable available as the ramp block output). Figure 8-5(b) summarizes the programming/monitoring information. This information pops up along with the simulation diagram of Figure 8-5(a). An example of a state-switching program, which includes several lights that inform the user of the status of the simulation, is shown in Figure 8-6. In both STATE 2 and STATE 3 (and when the DG controls voltage and frequency), the user can additionally program the commanded values of the inverter's real and reactive reference power, denoted by P_{ref} and Q_{ref}, respectively. The power generated is programmed as a positive number and the power absorbed as a negative number. In particular, if the inverter works with a battery bank connected and we want to charge the battery, the sign of the required real power has to be negative. Figure 8-5(a) includes an example of the inverter's commanded power program.

Figure 8-6. An example of a state-switching program

It is important to realize that switching to STATE 3 requires synchronization of the DG to the inverter-controlled grid. It does not happen automatically. To synchronize the DG to the grid

- The voltage magnitudes must be equal
- The frequency must be same as the grid frequency
- The phase angles must be equal.

Consequently, setting $B2 = 1$ results in $SW\_D = 1$ and the synchronization process of the DG is initiated. The DG remains unloaded until the required conditions are met (as shown in Figure 8-7), which results in $DGS = 1$. This, in turn, results in loading or activation of the DG and the inverter is switched to the slave mode. The implementation of the DG activation by $DGS = 1$ is apparent from referring back to Figure 3-5.

Switching to STATE 1 (the inverter in the master mode and the DG disconnected, in which $B1 = 0$ and $B2 = 0$ and causes $SW\_D = 0$ and $DGS = 0$), happens instantly. In the DG simulation (refer to Figure 3-5), $DGS = 0$ cuts off the currents i_qSD and i_dSD. However, we must also make the DG ready to become a master when the next switching is commanded. In other words, we keep the DG idling. This is implemented by freezing certain variables. The freeze is implemented with a special reset integrator provided in VisSim. In Figure 3-5, the binary variable N_DGS (defined in Figure 8-7 as a complement of the variable DGS) is used to freeze the output of the reset integrator. In addition, the binary variable R (defined in Figure 8-7 as a complement of SW_D) is used to implement freezing of integration

- In the engine speed controller (frequency control) as shown in Figure 3-7
- In the voltage controller in Figure 3-8, repeated here for convenience as Figure 8-8
- In the torque equation block (to freeze the speed of the DG) as shown in Figure 3-6(a).
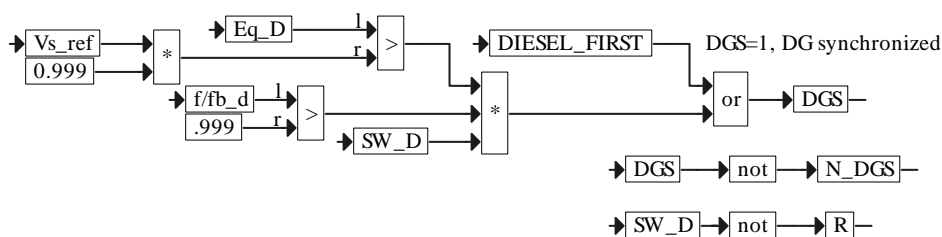
Figure 8-7. Simulation diagram of the DG/inverter switch: the conditions for loading the DG after STATE 2 or STATE 3 is commanded, along with the definitions of auxiliary variables

Consider now simulation diagram in Figure 8-8 for a complete description of the operation of the DG voltage controller. It can operate in two modes:

- Mode 1: The DG is about to synchronize to the grid. The difference Vs_{ref} - Eq_D constitutes the input to the voltage controller. This mode represents transition from STATE 1 to STATE 2.
- Mode 2: *DIESEL_ON* assumes the value of 1. The DG is synchronized and it takes control of the voltage *Vs* and the frequency *fb*. The difference Vs_{ref}-*Vs* becomes the input to the voltage controller. This mode represents STATE 2 or STATE 3.
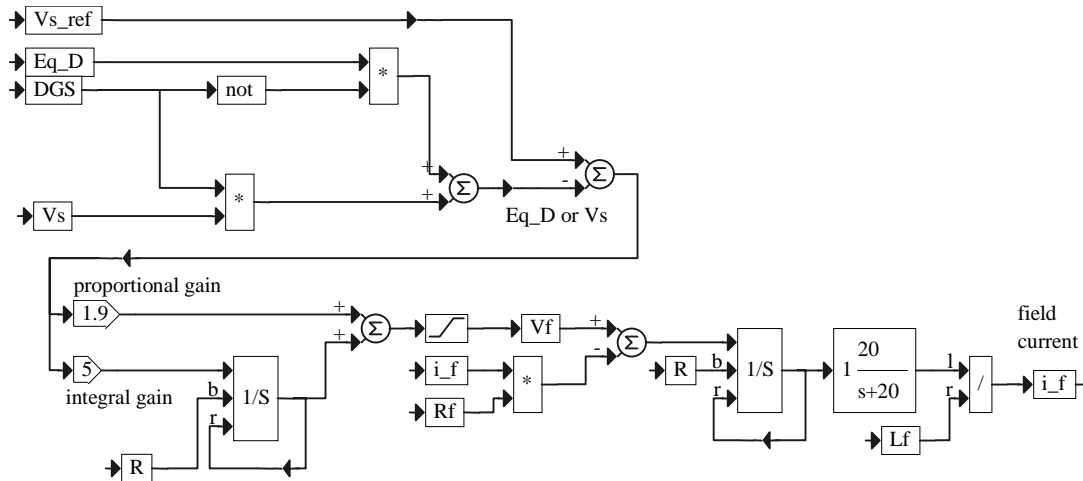
Figure 8-8. Voltage controller of the DG

The simulation of the torque equation, embedded in the synchronous generator block, is enabled only when the DG is in control of the system. Such operation is achieved by freezing the output of the reset integrator at all other times.

As we already mentioned, the NO_DIESEL block is involved in the diesel/inverter operation control. It has to be brought to the simulation screen whenever the simulated system includes an inverter, and it does not include a diesel generator. This block contains two assignments: *DGS* = 0 and *N_DGS* = 1. The system needs this information to properly control the operation of the inverter.

Inverter Module Description

The inverter module has the capability to operate in the slave mode, in the master mode, and by switching between master and slave mode. Figure 8-9(a) shows the top view of its simulation diagram. This is what shows in the simulation screen when the inverter is added to the simulated power system. The variable v_{DC} represents the output voltage of the DC source such as the battery or the PV array. The other two inputs (to be programmed by the user) are only used in the slave mode. These are (1) the commanded real power P_{ref} to be provided (if positive) or to be absorbed (if negative) by the DC source and (2) the commanded reactive power Q_{ref} (generated by the inverter if positive or absorbed by the inverter if negative). In the master mode, the values of P_{ref} and Q_{ref} are irrelevant. For this reason, the user can leave them unchanged when switching to the master mode. The inverter has two outputs: (1) the actual real power provided or absorbed P_{inv} and (2) the actual reactive power provided or absorbed Q_{inv}. In the steady state of the slave mode, the values of these two variables are equal to the commanded values. In the master mode,

these variables assume the values, which are the consequence of the power balance in the simulated system.
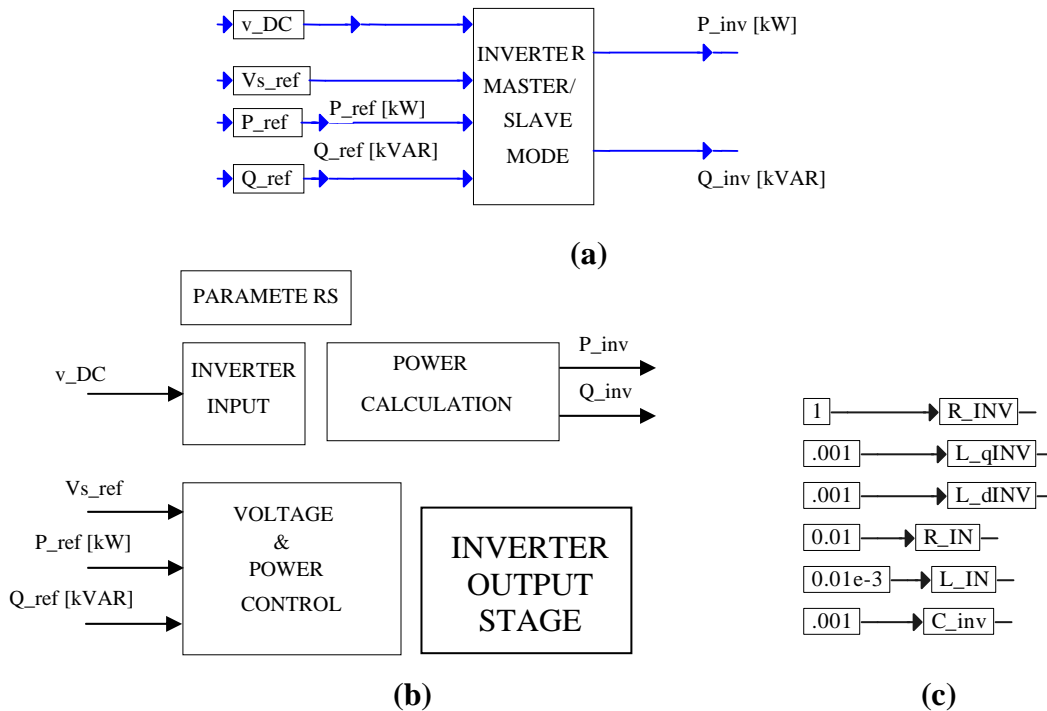
Figure 8-9. Simulation diagram of the inverter with the capability of master/slave switching: (a) top-view diagram, (b) second-level expansion of the main block showing principal functional modules, and (c) expansion of the parameter module

In Figure 8-9(b), we see the second-level expansion of the inverter with all principal modules shown. These are: the parameter module, the inverter input module, the inverter output stage, the power calculation module, and the voltage and power control module. The parameter module is further expanded in Figure 8-9(c). We clarify the role of the parameters shown in this figure below.

In Figure 8-10, we show the inverter input module. The equivalent circuit diagram, shown in Figure 8-10(a), clarifies the simulation diagram presented in Figure 8-10(b). Assuming that the inverter's real power, provided or absorbed, is known, we calculate the DC current I_{DC} drawn from or provided to the DC source. In this module, we use three of the parameters declared in the parameter module.

In Figure 8-11, we show the inverter output stage module, in which the inverter output current q- and d-components, contributed at the PCC, are generated. Each of these components is shown as a sum of a component generated in the slave mode and a component generated in the master mode. However, at a given time only one of them has a non-zero value. In the lower part of this diagram, we calculate the q- and d-component of the inverter current contributed at the PCC in the slave mode. The multipliers K_P and K_Q, which are used in this diagram, are generated in the voltage and power control module by the real and the reactive power controllers. The inverter

current components contributed at the PCC in the master mode are generated in Q- and D-generator, which are presented in Figure 8-12.

(a)

(b)
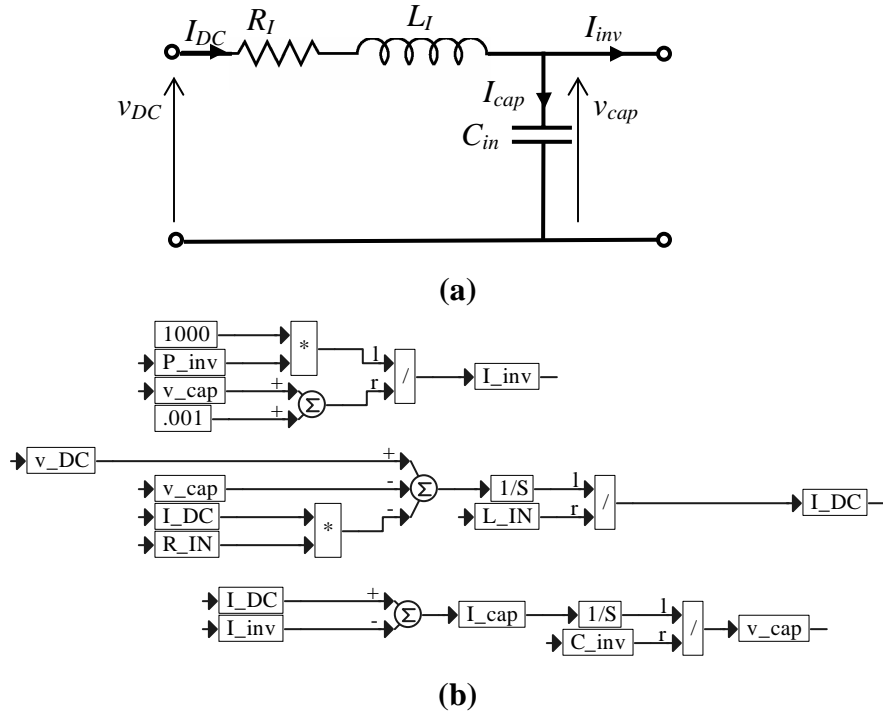
Figure 8-10. Inverter input module: (a) equivalent diagram and (b) simulation diagram
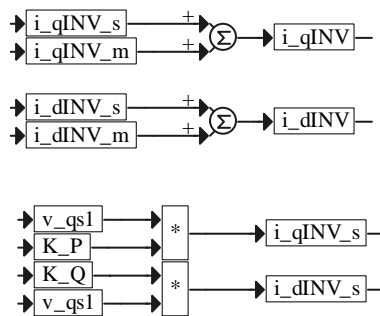
Figure 8-11. Inverter output stage
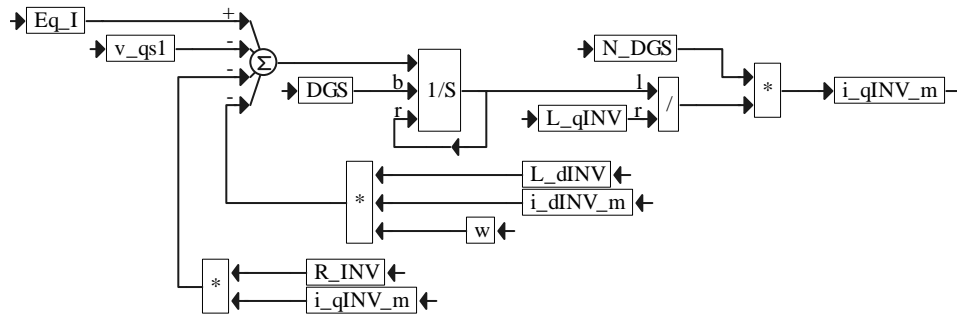
Q-generator
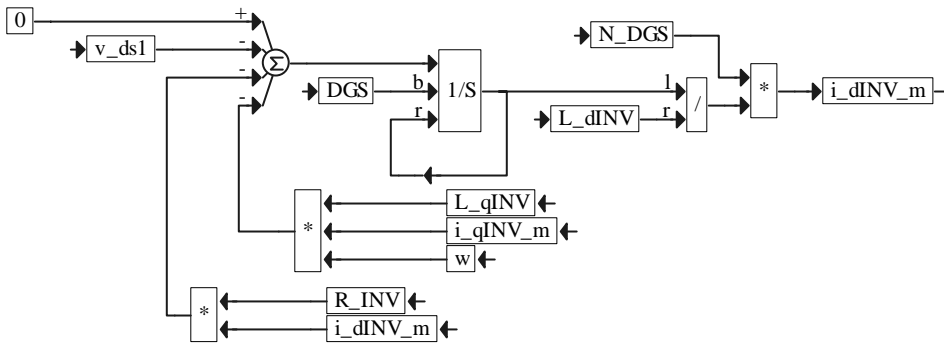
D-generator

Figure 8-12. Simulation diagram of the Q-generator and D-generator of the inverter (operating only in master mode)

In Figure 8-13, we show the simulation diagram of the power calculation module of the inverter. Using current components defined (as described above) in the inverter output stage module, we calculate in this simulation diagram the real power P_{inv} and the reactive power Q_{inv}.

In Figure 8-14(a), we show the simulation diagram of the master mode voltage controller, which generates the electromotive force

$$E_{q\_I} = K_e v_{DC},$$

which is required at the given load to maintain the system's voltage. This value of E_{q_I} is used in the Q-generator (shown in Figure 8-12) to generate the q-component of the current contributed at the PCC by the inverter operating in the master mode. In Figure 8-12, we also have the D-generator, whose input equals zero. This is the consequence of the assumed reference frame. The same convention is used for the DG and, in principle, both inverter generators are identical to those of the DG. Thus, we will not give more explanation of the simulation diagram in Figure 8-

12. In Figure 8-14(b), we have the real and reactive power controllers, which are active only in the slave mode. They generate the multipliers K_P and K_Q. These multipliers are used in the simulation diagram of Figure 8-10 to obtain the values of the q- and the d-component of the inverter's current, which in the slave mode must be contributed at the PCC to maintain a required or programmed power output.
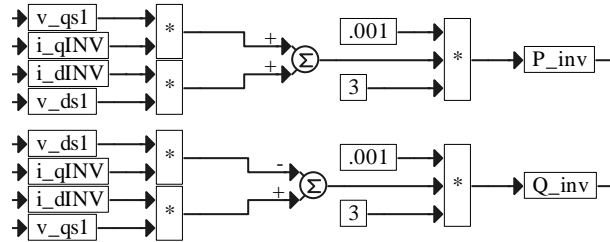
Figure 8-13. Simulation diagram of the power calculation module of the inverter

(a)

(b)
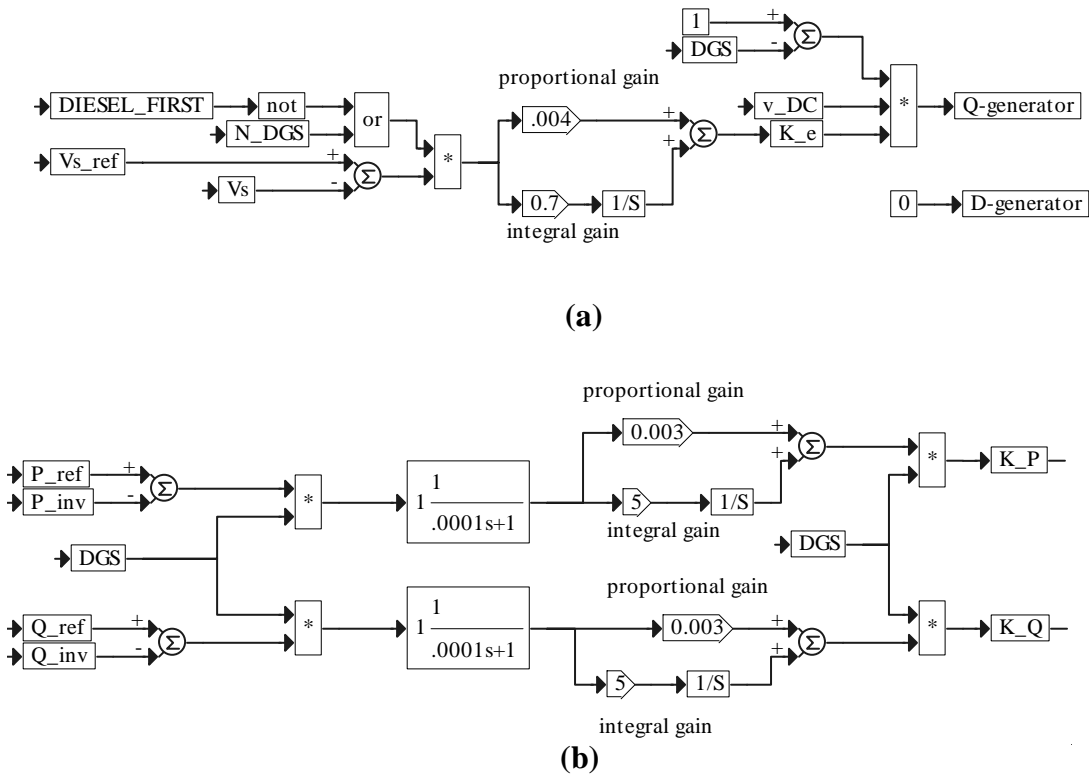
Figure 8-14. Simulation diagram of the voltage and power control module: (a) master mode voltage controller and (b) slave mode power controller

Case Study

Principal modules in this case study include:

- A diesel generator with a rated power of 200 kW

- A village load of 50 kW at the power factor $pf = 0.8$

- An inverter

- A battery bank

The operation of this system is programmed as shown in Figure 8-5, and Figure 8-15 shows the simulation results. The simulation diagram is obtained by adding the following files to the simulation screen: PCC_m.vsm, DG_m.vsm, VL.vsm, INV.vsm, and BAT.vsm. For this system, we obtained traces of power, current, voltage, and frequency as shown in Figure 8-15. Next, we explain the sequence of the simulation events documented in Figure 8-5.

Time/Event Sequence

$t = 0$ $B1 = 1$, $B2 = 0$; the diesel generator starts up.

$DGS = 1$; the diesel generator is loaded and controls voltage and frequency.

The inverter is in the slave mode and has the ability to deliver commanded real power P_{ref} and commanded reactive power Q_{ref}, and

$P_{ref} = 0$ and $Q_{ref} = 0$.

$t = 2.5$ sec $P_{ref} = 20$ kW results in $P_{inv} = 20$ kW (the battery is discharging).

$t = 4$ sec $P_{ref} = $ -10 kW results in $P_{inv} = $ -10 kW (the battery is charging).

$t = 5$ sec $Q_{ref} = $ -15 kW results in $Q_{inv} = $ -15 kW (the inverter is absorbing reactive power).

$t = 7$ sec $B1 = 0$, $B2 = 0$

$DGS = 0$, the DG remains running but is disconnected from the load (idling); the inverter operates as a master, controlling voltage and frequency and supplying necessary real and reactive power.

$t = 9$ sec   In this state, P_{ref} and Q_{ref} have no effect, but their values are set to zero

$t = 10$ sec $B1 = 0$, $B2 = 1$
                $DGS = 1$; the diesel generator, which was idling, becomes a master and the inverter becomes a slave.

$t = 12$ sec $Q_{ref} = -15$ kW results in $Q_{inv} = -15$ kW (the inverter is absorbing reactive power)

$t = 13.5$ sec $P_{ref} = -10$ kW results in $P_{inv} = -10$ kW (the battery is charging)

$t = 16$ sec $B1 = 0$, $B2 = 0$

                $DGS = 0$; the diesel generator remains running but is disconnected from the load (idling); the inverter operates as a master, controlling voltage and frequency and supplying necessary real and reactive power.
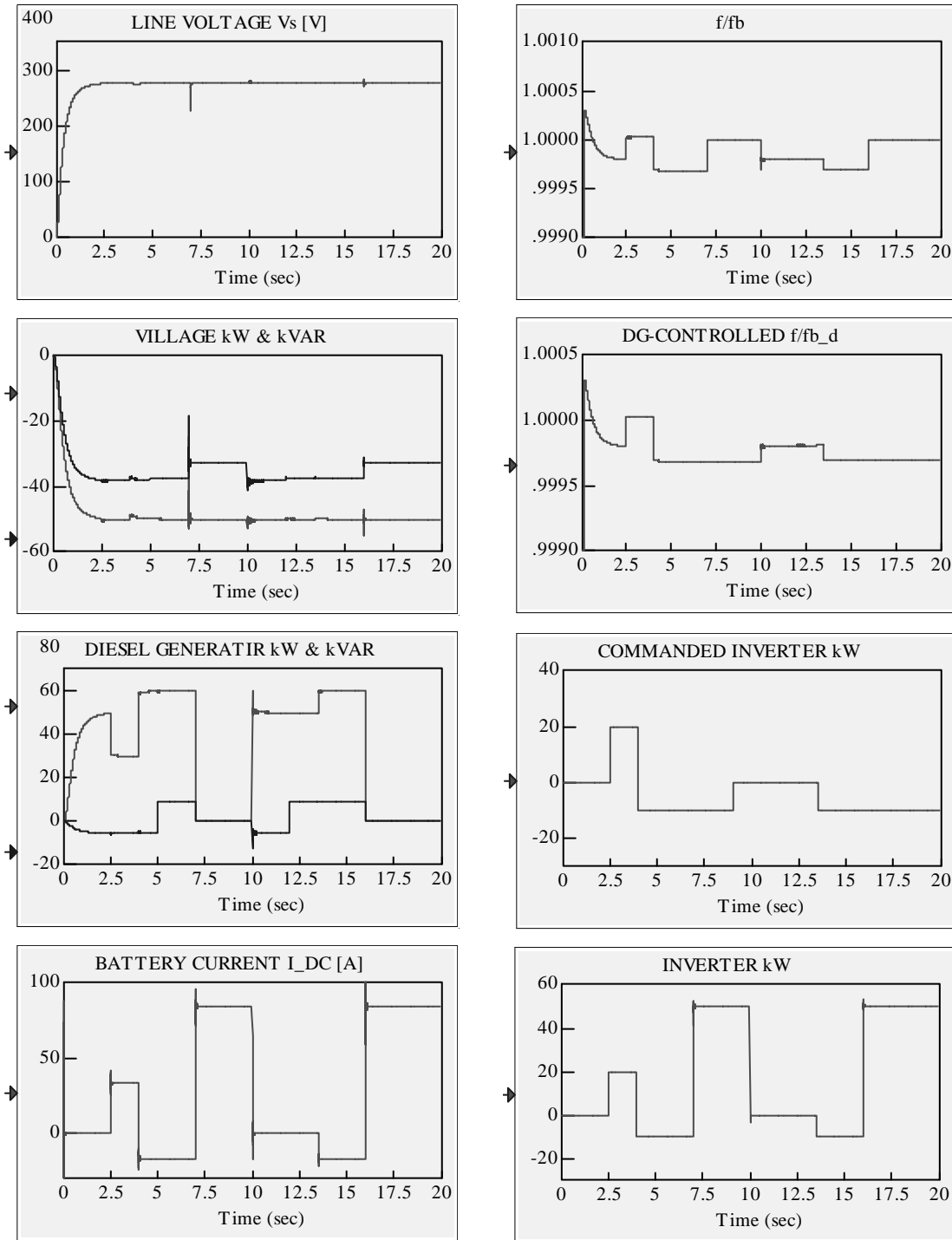
Figure 8-15. Traces of power, current, voltage, and frequency for the system composed of a DG, an inverter, a BB, and a VL
(continued on the next page)
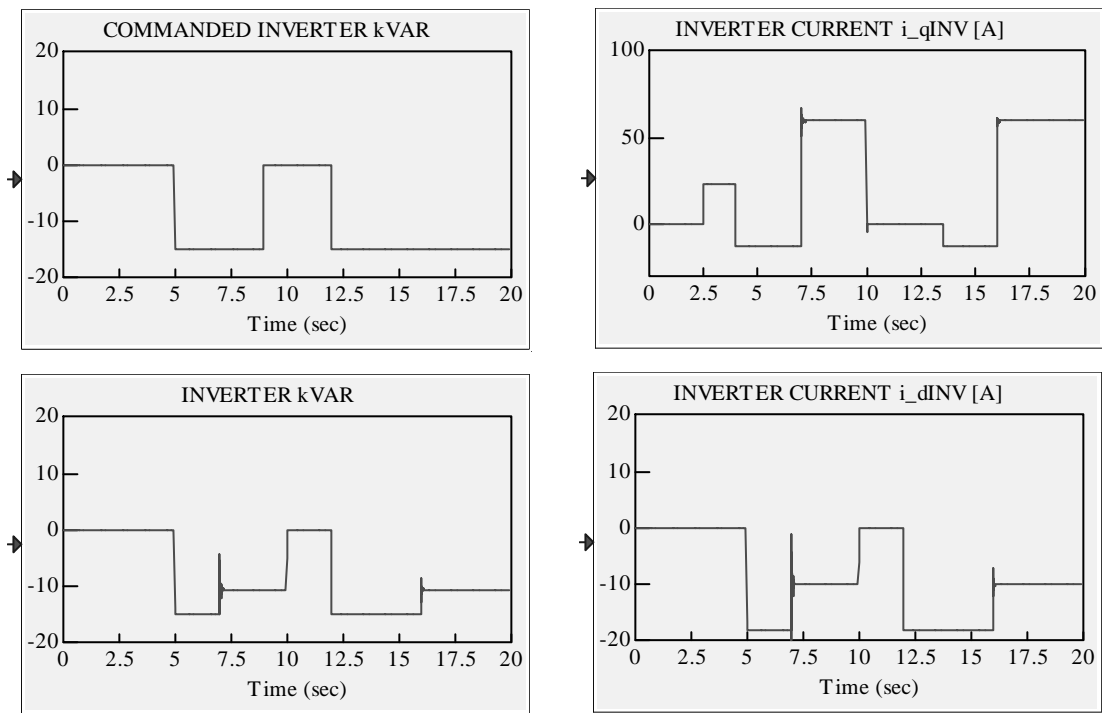
Figure 8-15. Traces of power, current, voltage, and frequency for the system composed of a DG, an inverter, a BB, and a VL (concluded)

Photovoltaic Array

In Figure 9-1, we show a single-line diagram (as in Figure 1-1) of a hybrid power system where we dot-framed the portion of the diagram that represents the PV array. As shown in this figure, this source of energy is connected to the system through the inverter. The user brings the PV array module to the simulation screen using the Add command and selecting the file PV_ARRAY.vsm. It appears on the screen as a block with the load current I_{DC} input set by the inverter (or rotary converter) and the DC bus voltage v_{DC} set as output voltage by the PV array module. Figure 9-2 shows this top view of the PV array module.
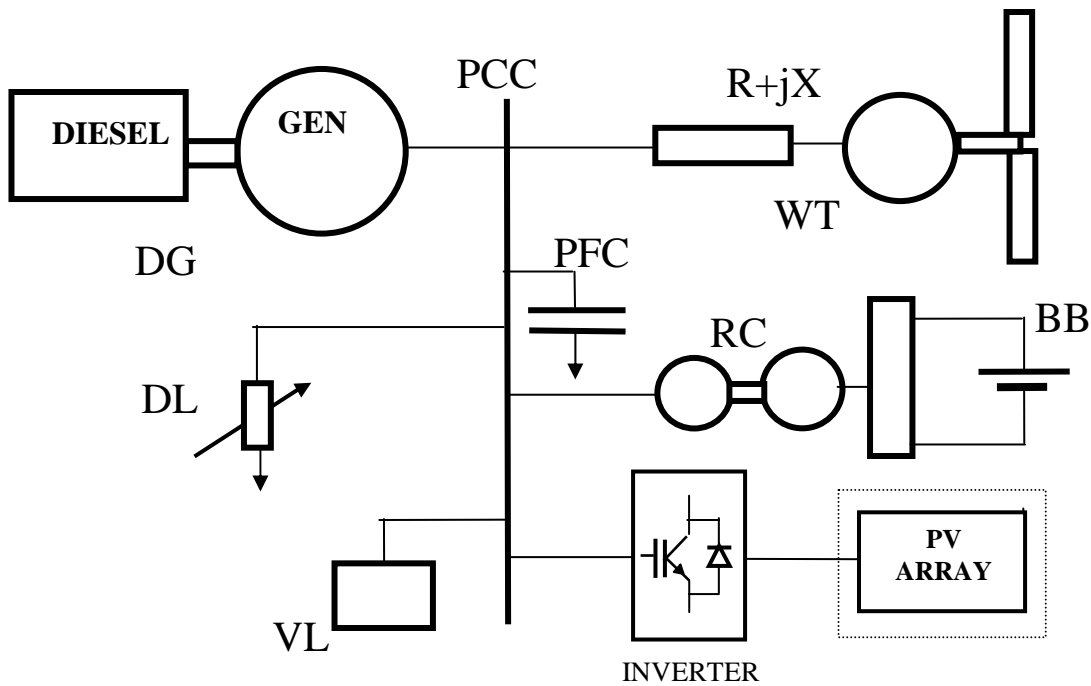
Figure 9-1. A single-line power system diagram with the PV array portion dot-framed

Figure 9-2. Top view of the PV array module

Photovoltaic or solar arrays are composed of a large number of solar cells connected in series and parallel. These cells produce a DC voltage when they are exposed to sunlight. Figure 9-3 shows the *I-V* characteristics of such a cell at a constant temperature and various sun intensity or

Figure 9-3. *I-V* characteristics of a solar cell for various insolation levels at a constant temperature

Figure 9-4. *I-V* characteristics of a solar cell for various temperature levels at a constant insolation level

insolation levels. Figure 9-4 presents the *I-V* characteristics at a constant insolation level and various temperatures. These figures show that the current is limited when the cell is short-circuited.


Figure 9-5. Lower level expansion of the PV_ARRAY block

Figure 9-5 shows the lower level expansion of the PV_ARRAY block introduced in Figure 9-2. In this simulation diagram, we represent a single cell characteristic by a two-column pv.map file. This ASCII file specifies the cell voltage and current under chosen temperature and isolation conditions. The representation of a cell for varying insolation levels and temperatures is accomplished using the scaling coefficients K_v and K_i. The user can set these parameters either as constants or make them functions of time. In addition, they can be applied as inputs to the I-V CHAR CONTROL block, which automatically generates K_v and K_i. This block contains the K_v.map file and K_i.map file, which, respectively, implement K_v and K_i as functions of the insolation and temperature. These functions of two variables are represented at several points in the form of a two-dimensional table. The I-V CHAR CONTROL block uses interpolation and extrapolation to determine the values of K_v and K_i for temperature and isolation values not included in the table. By properly setting the values of these parameters, we obtained the families of the *I-V* characteristics shown in Figures 9-3 and 9-4. The user may choose the array size, as determined by the number of cells connected in series N_{ser} or the number of cells in one row and the number of cell rows connected in parallel N_{par}. The concept of solar array is symbolically illustrated in Figure 9-6 and Figure 9-7 gives the circuit showing its connection to the DC bus.

We can see from Figure 9-5 that the *I-V* characteristic of the PV array under the fixed insolation and temperature conditions depends on these numbers. We show in Figure 9-8 one such characteristic (obtained for $N_{se\ r}$= 100 and N_{par} = 20 at 0°C and an insolation level of 75 mW/cm^2) together with the load characteristic setting the point of operation for maximum power condition, which occurs at the knee of the characteristic. Operating at the maximum power point is desirable. The variables V_{bus} and I_{load}, which are defined in Figure 9-5 and Figure 9-7, correspond to this point.

(a)   (b)   (c)

Figure 9-6. The concept of a solar array: (a) a single solar cell, (b) a series connection of solar cells (N_{ser} = 3 and N_{par}= 1)**, and (c) a solar array** (N_{ser}= 3 and N_{par} = 2)

Figure 9-7. Solar cell connection to the DC bus

In other words, as the load conditions change, the operating point traverses along the *I-V* characteristic of the array. This is illustrated in Figure 9-9, which shows three different load characteristics.
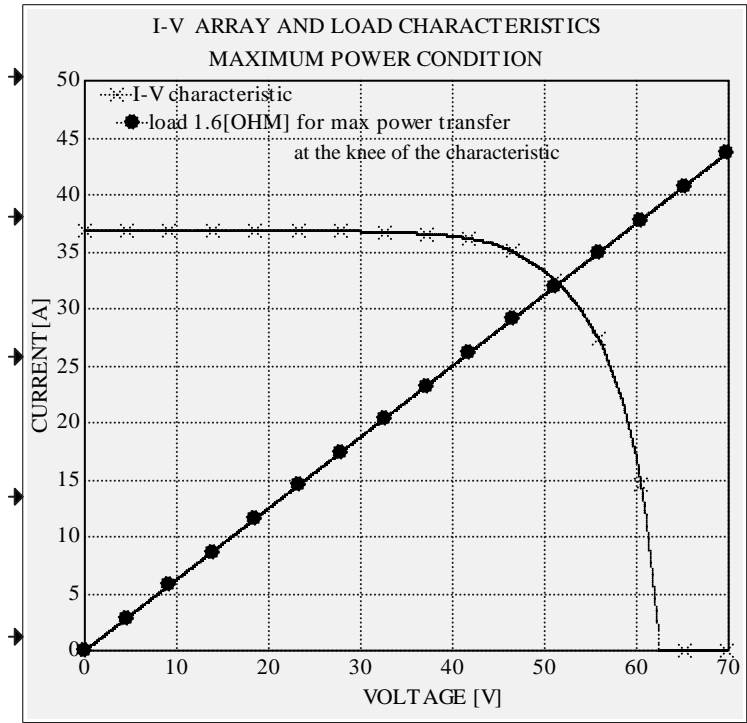
Figure 9-8. Maximum power condition
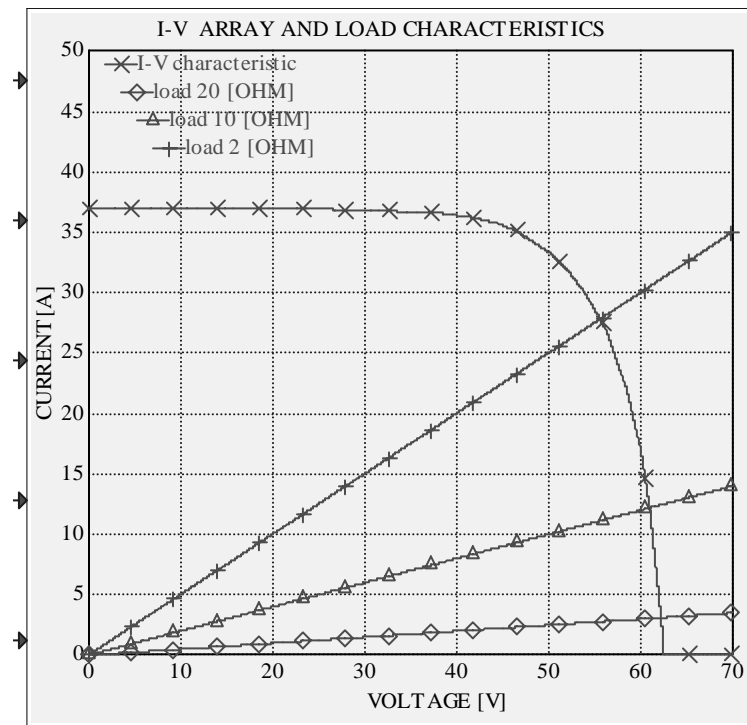
Figure 9-9. Point of operation follows the load along the *I-V* array characteristic

To demonstrate how the voltage V_{bus} and the current I_{load} follow the step changes of the load, we set up the simulation shown in the diagram in Figure 9-10. Figure 9-11 presents the results of this simulation. The consecutive values of the load resistance correspond to the load characteristics found in Figure 9-9.

The PV arrays are commercially available in modules, which consist of a number of cell strings connected in parallel. Each string is a series connection of a number of cells. These numbers depend on the model (or manufacturer, or both) of the module. The PV modules are used to build an array and their *I-V* characteristics are considered as *I-V* characteristics of the elementary PV array unit. Note that we have introduced a single solar cell as this elementary unit. Consequently, when setting up the simulation with commercial PV arrays, the user will need to declare N_{ser} as a number of modules in one raw or connected in series and N_{par} as a number of module rows connected in parallel.
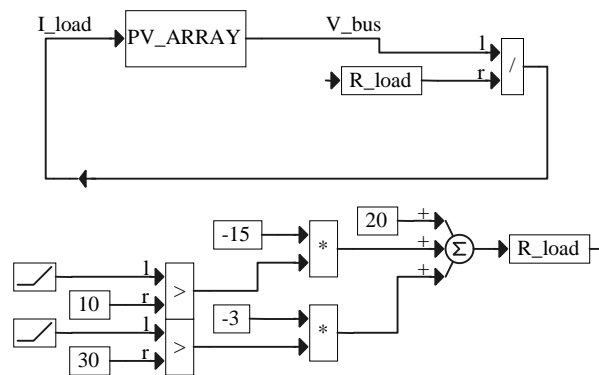
Figure 9-10. Step changes of the load

The I-V characteristics for a number of the commercial PV modules under adjustable environmental parameters such as temperature, beam irradiance, diffuse irradiance, wind speed, site altitude, sun elevation, angle of incidence, and others (along with the manufacturer's module parameters) e can be obtained using the Sandia IVTracer Program. Using these data (for a particular solar module involved in the simulated system), we can generate the files K_v.map and K_i.map as described above, which are required by the I-V CHAR CONTROL block.

Example

Using the Sandia IVTracer Program, we selected a PV module (model ASE-100-ATF/17). Next, we set the following base conditions: ambient temperature at 25°C, total irradiance at 50 mW/cm^2, sun elevation at 90°, angle of incidence at 0°, site altitude at 1,600 m, and wind speed 3 m/sec. The corresponding I-V characteristic is shown in Figure 9-12. For this particular characteristic, the short-circuit current $I_{sc} = 3.17$ A was assumed as a base value and denoted I_{scb} and the open-circuit voltage V_{oc}=19.13 V was assumed as a base value and denoted V_{ocb}. The files K_v.map and K_i.map contain values of K_v and K_i, respectively (as shown in Table 9-1)**.**
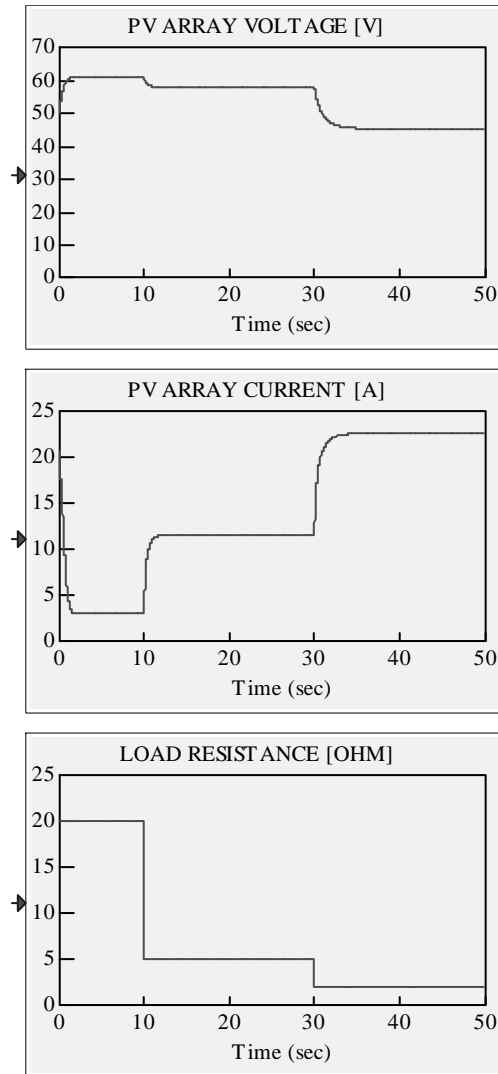
Figure 9-11. PV array voltage and current responses to the step changes of the load

Table 9-1. Scaling coefficients K_v and K_i

	K_v	-10	0	10	15	25	35	50
TO	25	-0.118	-0.084	-0.047	-0.027	0.015	0.062	0.139
TA	50	-0.126	-0.093	-0.058	-0.040	0	0.043	0.115
L	60	-0.125	-0.093	-0.058	-0.039	0	0.043	0.114
IRR	70	-0.123	-0.091	-0.056	-0.038	0.001	0.044	0.114
ADI	80	-0.120	-0.088	-0.053	-0.035	0.004	0.046	0.117
AN	90	-0.117	-0.085	-0.050	-0.032	0.007	0.049	0.120
CE [mW/cm²]	100	-0.114	-0.081	-0.046	-0.027	0.011	0.054	0.125

A M B I E N T TEMPERATURE [°C] (header above K_v table)

	K_i	-10	0	10	15	25	35	50
TO	25	-1.64	-1.62	-1.61	-1.61	-1.58	-1.58	-1.56
TA	50	-0.09	-0.05	-0.04	-0.03	0	0.02	0.06
L	60	0.53	0.57	0.59	0.61	0.63	0.66	0.71
IRR	70	1.16	1.19	1.23	1.24	1.29	1.31	1.36
ADI	80	1.76	1.83	1.87	1.89	1.93	1.97	2.03
AN	90	2.42	2.47	2.51	2.53	2.58	2.62	2.69
CE [mW/cm²]	100	3.06	3.1	3.15	3.18	3.23	3.27	3.35

A M B I E N T TEMPERATURE [°C] (header above K_i table)
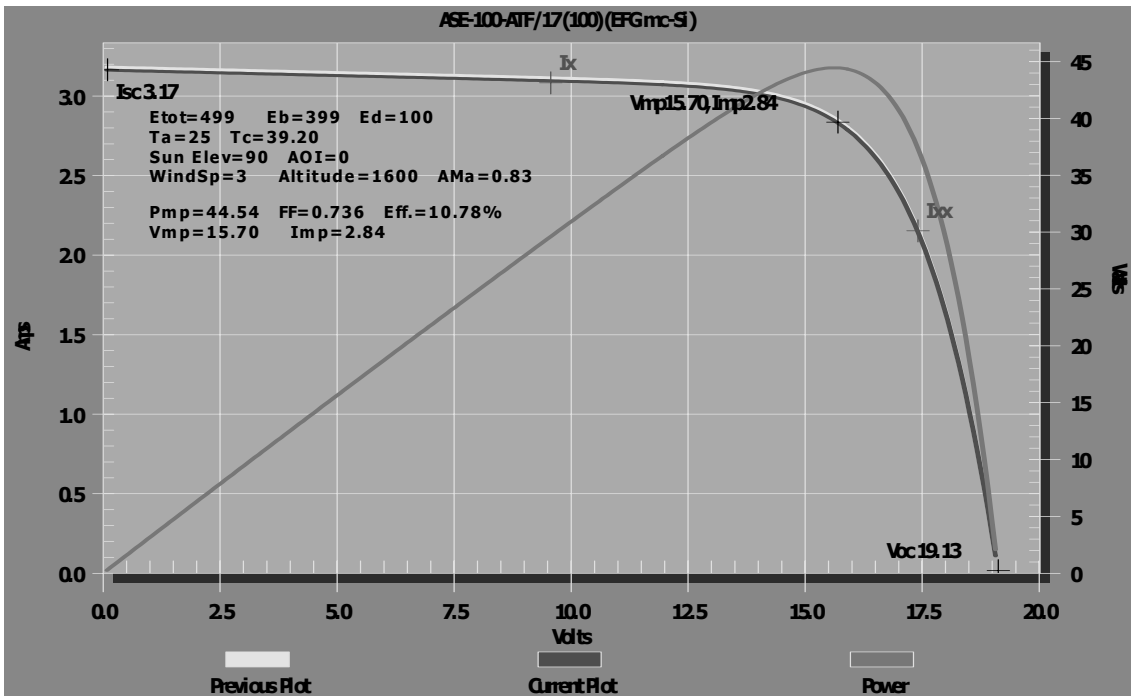
Figure 9-12. I-V characteristics for the base conditions

ASE-100-ATF/17(100)(EFGmc-Si)
Isc 3.17
Etot=499 Eb=399 Ed=100
Ta=25 Tc=39.20
Sun Elev=90 AOI=0
WindSp=3 Altitude=1600 AMa=0.83
Pmp=44.54 FF=0.736 Eff.=10.78%
Vmp=15.70 Imp=2.84
Vmp 15.70, Imp 2.84
Voc 19.13
Previous Plot Current Plot Power

These values were determined for several ambient temperature values and several total irradiance values. The required values of I_{sc} and V_{oc} were determined by generating the I-V characteristics (for all temperature-irradiance pairs shown in the above tables) using the Sandia IVTracer Program. To determine elements of the files K_v.map and K_i.map, we use the following equations:

$$K_v = \frac{V_{ocb}}{V_{oc}} - 1,$$

$$K_i = I_{sc} - I_{scb} \ .$$

To represent K_v and K_i as functions of two variables—the temperature and the irradiance—we use VisSim's map block. It is important that the Interpolate action and the Extrapolate action are both checked in the dialog box for this block (entitled Map Properties). Note that this is only an example; the user must follow this example and set up the files K_v.map and K_i.map for the PV module involved in a simulated system.

To use the DC power generated by the PV array in an AC power system, we need to convert it to AC power. One way to do this is by using the rotary converter. In this case, we connect the V_{bus} voltage to the rotary converter and use the armature current of the DC machine of the rotary converter as the I_{load} current of the PV array. Next, the variable P_BAT_set in the battery power control block of the rotary converter is used to set the commanded power of the PV array. To demonstrate how this PV Array–RC assembly operates, we added this assembly to the simulation diagram of Case Study 1 described in Chapter 10. The simulation results for this modified Case Study 1 are self-explanatory and are shown in Figure 9-13.

Another, more typical way to handle the same problem of converting the DC power generated by the PV array to the AC power is to use the inverter. To illustrate how the system with such conversion operates, we again used Case Study 1 with the addition of the PV Array-Inverter assembly available as PV_INV.vsm. The simulation results, shown in Figure 9-14, are similar to those presented in Figure 9-13. However, note that because of the elimination of the mechanical time constant of the RC, there is no visible inertia in this conversion process. The only visible inertia is that involved in the frequency and voltage control, which results from the mechanical time constant of the diesel generator.

The simulation results in Figure 9-15 illustrate the operation of the power system composed of a variable village load and a PV Array-Inverter assembly with the temperature and insolation levels given as functions of time. These functions of time represent the real data recorded on July 10, 1999, in Golden, Colorado. However, the time scale was changed by a proper declaration in the VisSim's import block. Because of time scaling, the simulation period of 30 sec actually corresponds to the real period from 4:00 A.M. to 8:40 P.M. The PV array is the only power source in this system. Therefore, to avoid meaningless transients, the village power is set to zero during the early morning and evening hours when the insolation is very low. The simulation diagram for this case study is available as a file named CS_PVm_INV.vsm in the C_STDS subdirectory. The same case study was repeated for a real PV array, which was the 20×20 array model ASE-100-ATF/17. The simulation diagram is available as a file named CS_PVm_INV_RE.vsm in the C_STDS subdirectory.

To download the PV insolation and temperature data from the Internet, follow these 10 steps:

1. Open http://srrl.nrel.gov/bms/
2. Go to DAILY PLOTS and RAW DATA FILES
3. Choose the date you want (example: Jan 1, 99 to Jan 31, 2000)
4. Select the start and the end date of the data you want
5. Choose 24 hour or 1 day time only
6. Choose global normal (the sun light is normal to the PV panel)
7. Choose the roof temperature
8. Choose selected data
9. Submit
10. Save the file as a plain text file.
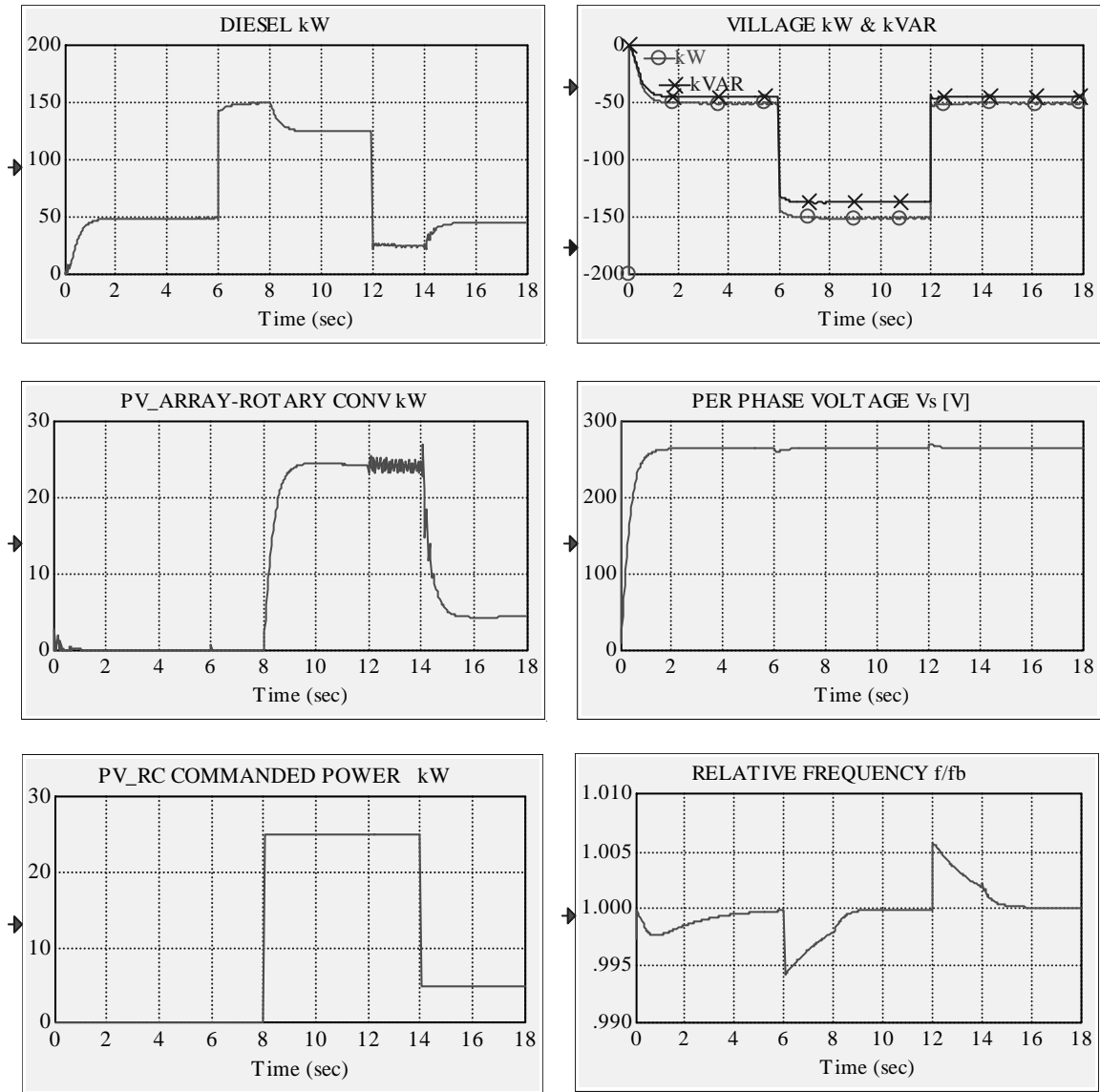
Figure 9-13. Simulation results illustrating the operation of the power system composed of a DG, a variable VL, and a PV array–RC assembly
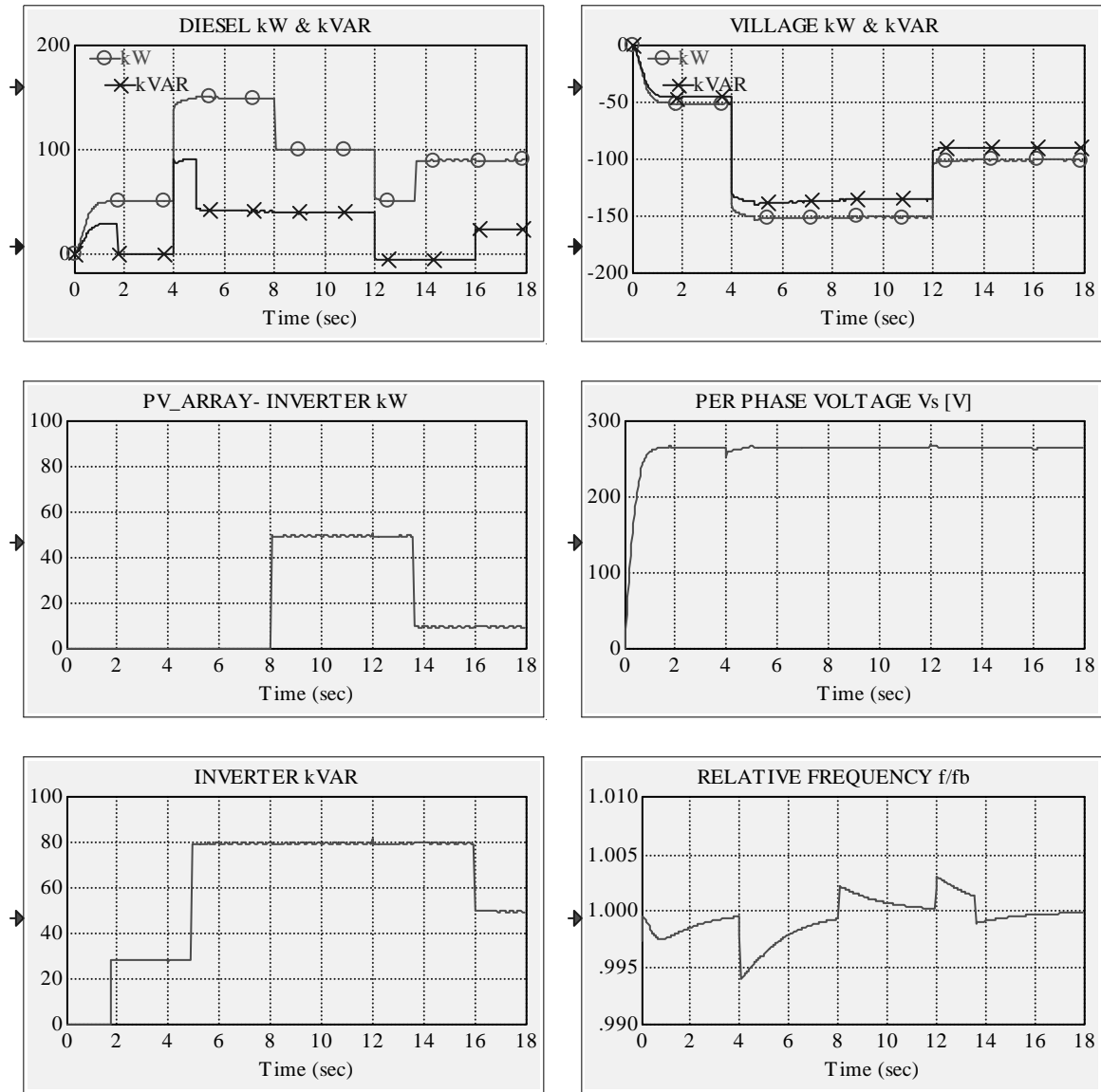
Figure 9-14. Simulation results illustrating the operation of the power system composed of a DG, a variable VL, and a PV array–inverter assembly
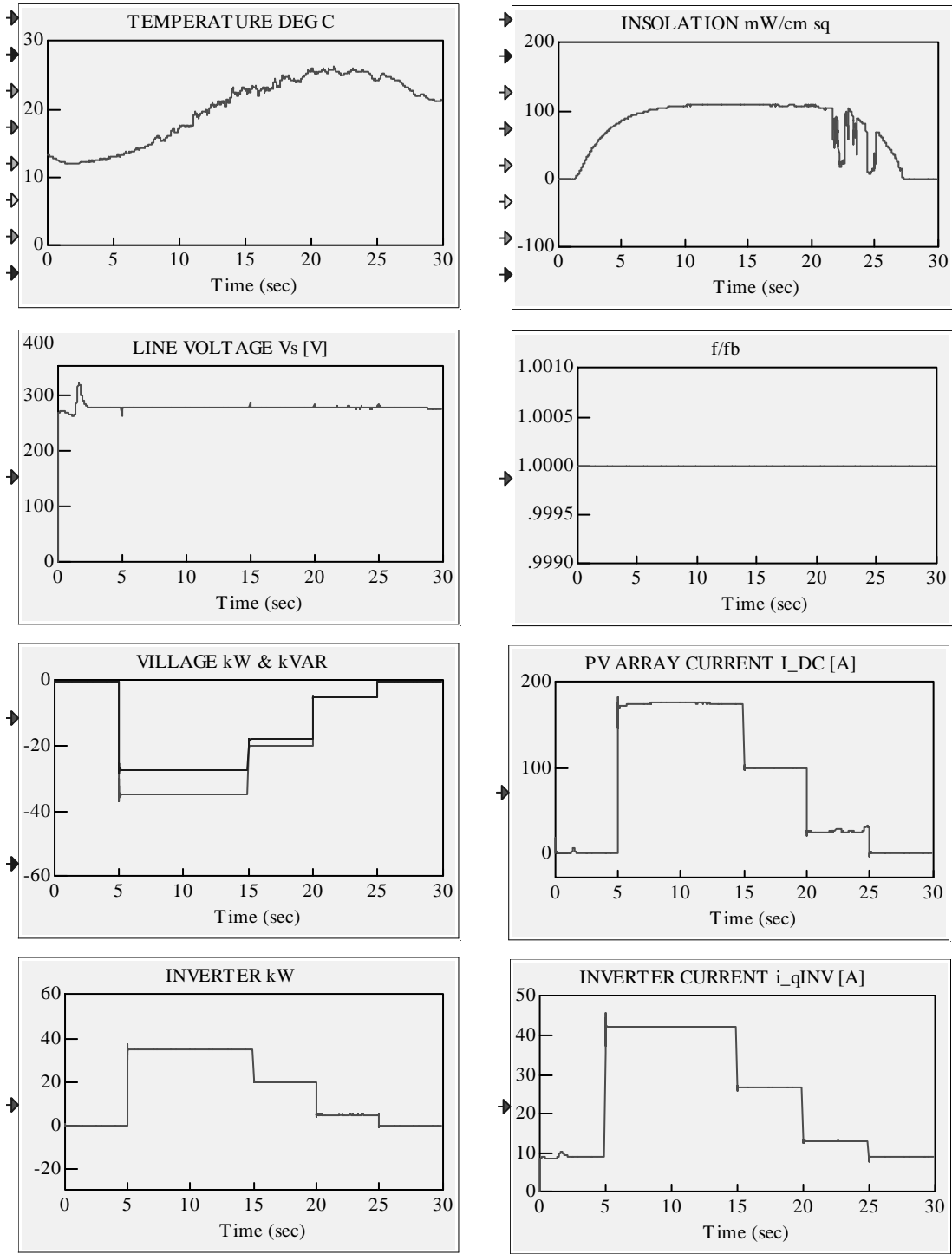
Figure 9-15. Simulation results illustrating the operation of the power system composed of a variable VL and a PV array–inverter assembly with the temperature and insolation given as functions of time

Case Studies

The modular simulation system RPM-S_{IM} has been developed to:

- Facilitate an application-specific and low-cost performance study of wind-diesel hybrid power systems (both mechanical and electrical components are simulated)

- Analyze both static and dynamic performance

- Help in the development of control strategies

- Simulate different wind speed profiles and different village load profiles.

The system has the following capabilities and characteristics:

- Modular and multilevel structure provided by the VisSim visual environment

- Clear and easy-to-understand system presentation

- Customized configuration setup is within a click of the mouse

- Modifications are easy to make

- Effects of system modifications can be immediately examined.

How Can This Simulation Tool Be Used?

- **Simulating control strategies**

  A proper control strategy must be developed to take full advantage of the wind energy when it is available and to minimize diesel fuel consumption, while maintaining desired system performance.

- **Including constraints**

  To implement this control strategy, a control system must be designed subject to the constraints specific to a particular application. These include the power generation limitations of the diesel generator, wind turbine generator, and battery bank/rotary converter assembly; excitation time constants; and dump load parameters.

- **Checking stability of the power system under time-varying conditions**

  To properly control the system's voltage and frequency, the time-varying power generation/consumption conditions of the system must be considered. The levels of changes that drive the system into instability should be determined. The factors to be considered are:

  - Wind speed: high winds may try to drive the diesel engine resulting in the loss of frequency control and instability
  - Village load (represented by the real power and the power factor) including events such as start-up of induction motor load, start-up of large heating load, loss of load, and sudden change of power factor.

  To maintain the system stability by keeping the diesel generation at a required minimum level, a proper dump load control strategy must be developed.

In this chapter, we use case studies of a hybrid system to demonstrate some of the benefits that result from the ease of understanding the effects of the modifications that the designed introduced in these complex and dynamic systems. In all the case studies that follow, we assumed the following power sign convention:

- Power generated is positive.

- Power consumed is negative.

Using Case Study 3 as an example, Appendix A contains a step-by-step procedure for how to set up the simulation diagram and run the simulation.

Case Study 1: PCC+DG+VL

Principal modules in this case study include:

- A diesel generator with a rated power of 200 kW

- A village load of 50 kW at the power factor $pf = 0.75$, switched to 150 kW at $t = 6$ sec, and switched again to 75 kW at $t = 12$ sec.

A power system with this configuration is presented in Figure 10-1, where we show both the single-line diagram and the top-view RPM-Sɪᴍ simulation diagram. This simulation diagram is obtained by adding the following files to the simulation screen: PCC_m.vsm, DG_m.vsm, DG_INV_CTRL.vsm, and VL.vsm. For this system, we obtained traces of power, voltage, and frequency as shown in Figure 10-2. Next, we explain the sequence of simulation events documented in Figure 10-2.

Time/Event Sequence

$t = 0$	The diesel generator starts up.
$t = 4$ sec	Line voltage V_s reaches the reference value of 266 V; the relative frequency is close to 1.
	Power generated by the diesel generator is at the level of 50 kW; the same power is consumed by the village load.
$t = 6$ sec	The village load is increased to 150 kW.
	This increment is followed by the sharp increase to the value of 150 kW of the power that the diesel generator provides to the system. Transient small dips of frequency and line voltage can be seen.
$t = 12$ sec	The village load is reduced to 75 kW.
	Power generated by the diesel generator decreases sharply to this value.
	Transient small jumps of frequency and line voltage can be seen.
$t > 16$ sec	Steady state is reached with all variables constant.
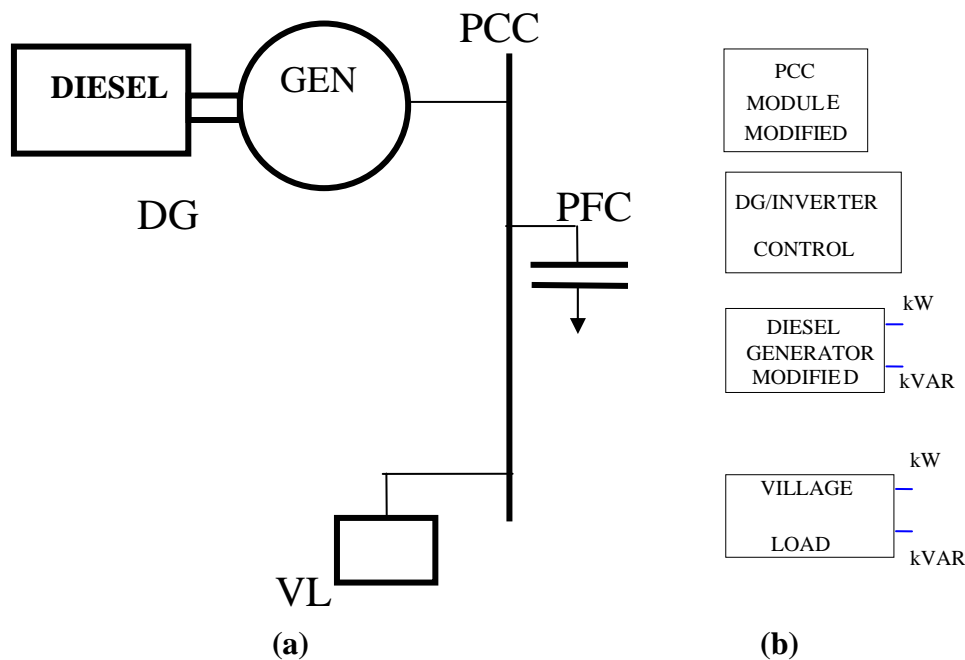
Figure 10-1. Power system composed of a DG and a VL: (a) single-line diagram and (b) top view of the RPM-S_{IM} simulation
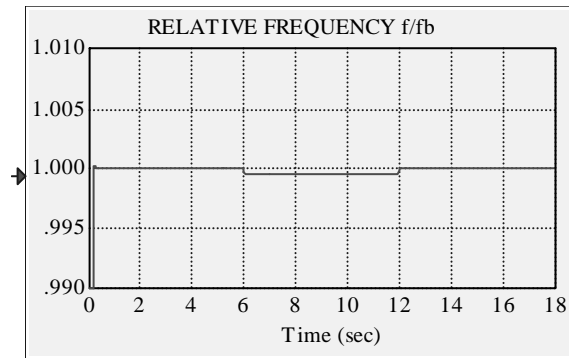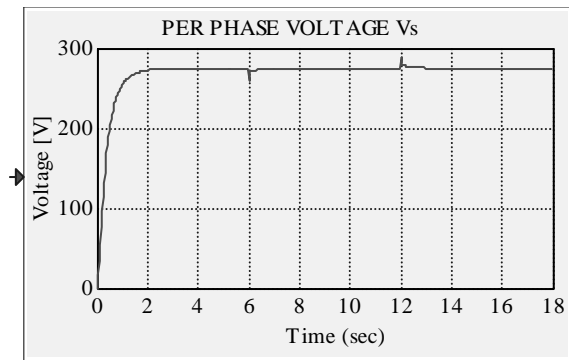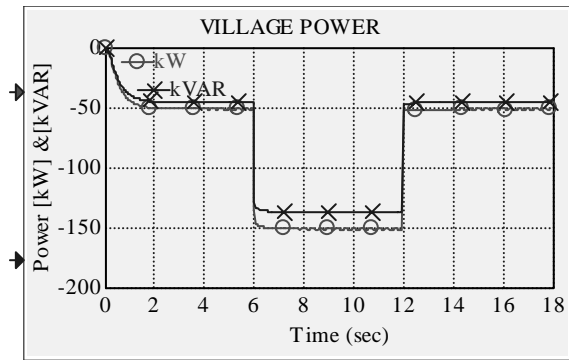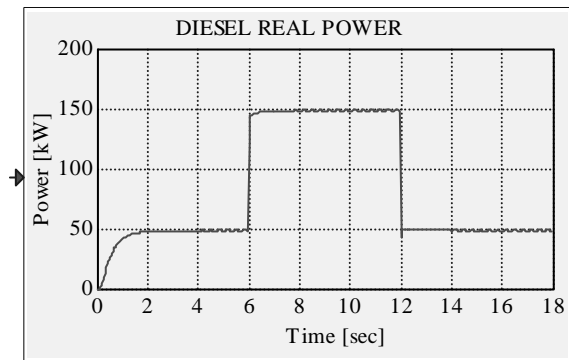
Figure 10-2. Traces of power, voltage, and frequency for the system composed of a DG and a variable VL

Case Study 2: PCC+DG+WT+VL

Principal modules in this case study include:

- A diesel generator with a rated power of 200 kW

- An AC WT driven by the wind, given by a file of the wind speed time series

- A village load of 30 kW at the power factor $pf = 0.75$.

A power system with this configuration is presented in Figure 10-3, where we show both the single-line diagram and the top-view RPM-S$_{IM}$ simulation diagram. The simulation diagram is obtained by adding the following files to the simulation screen: PCC_m.vsm, DG_m.vsm, DG_INV_CTRL.vsm, VL.vsm, and wtg_base_m.vsm. For this system, we obtained traces of power, voltage, and frequency as shown in Figure 10-4. Next, we explain the sequence of simulation events documented in Figure 10-4.

Time/Event Sequence

$t = 0$ The diesel generator starts up.

$t = 2.5$ sec   Line voltage V_s reaches the reference value of 266 V; the relative frequency is 1.

                    Power generated by the diesel generator is at the value of 30 kW (without the dump load no minimum value can be imposed); the same power is consumed by the village load.

$t = 6$ sec   The induction machine starts to motor the wind turbine and creates a large load.

                    Power generated by the diesel generator increases sharply.

                    Transient small frequency and line voltage dips are observed.

$t = 7$ sec   Power consumption of the induction machine, reaching the synchronism, rapidly drops.

$t = 7.25$ sec   The wind turbine generator starts to generate.

                    Power generated by the diesel generator decreases below 30 kW, which is the consumption level of the village.

$t > 12.5$ sec   Power generated by the wind turbine generator increases because of a wind gust.

(a)

(b)

Figure 10-3. Power system composed of a DG, an AC WT, and a VL: (a) single-line diagram and (b) top view of the RPM-SIM simulation
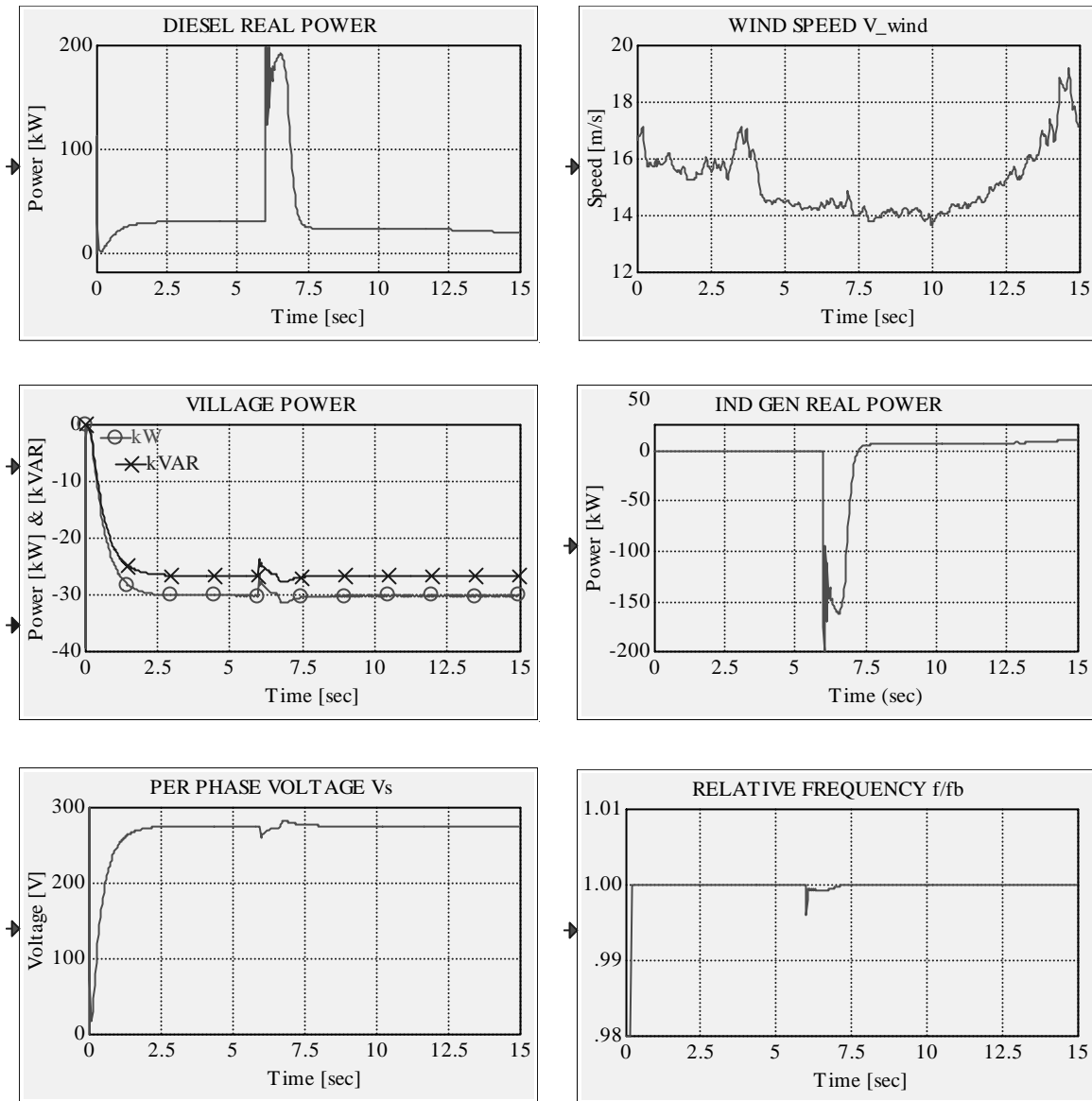
Figure 10-4. Traces of power, voltage, and frequency for the system composed of a DG, an AC WT, and the constant VL

Case Study 3: PCC+DG+WT+VL+DL

Principal modules in this case study include:

- A diesel generator with a rated power of 200 kW and a minimum load of 50 kW

- An AC WT driven by the wind determined by a file of the wind speed time series

- A village load of 30 kW at the power factor $pf = 0.75$

- A dump load incremented by the diesel power control strategy.

A power system with this configuration is presented in Figure 10-5, where we show both the single-line diagram and the top-view RPM-S$_{IM}$ simulation diagram. The simulation diagram is obtained by adding the following files to the simulation screen: PCC_m.vsm, DG_m.vsm, DG_INV_CTRL.vsm, VL.vsm, DL.vsm and wtg_base_m.vsm. For this system, we obtained traces of power, voltage, and frequency as shown in Figure 10-6. Next, we explain the sequence of simulation events documented in Figure 10-6.

Time/Event Sequence

$t = 0$	The diesel generator starts up.
	Power generated by the diesel generator increases to its specified minimum value of 50 kW, and the power consumed by the village load increases to its specified required value of 30 kW; the steady-state power difference of 20 kW is consumed by the dump load controlled by the diesel power control strategy.
$t = 2.5$ sec	Line voltage V_s reaches the reference value of 266 V; the relative frequency equals 1.
	Power generated by the diesel generator is at its specified minimum value of 50 kW.
$t = 4$ sec	The induction machine starts to motor the wind turbine and creates a large load.
	Power generated by the diesel generator increases sharply.
	The dump load is gradually reduced to zero.
	Transient small dips of frequency and line voltage are observed.
$t = 5$ sec	Power consumption of the induction machine, reaching the synchronism, rapidly drops.
$t = 5.5$ sec	Power generated by the diesel drops to its minimum level of 50 kW.
	The diesel power control strategy compensates for the power surplus by incrementing the dump load.
$t > 6$ sec	Steady state is reached and all system variables remain constant.

t > 12.5 sec   A wind gust results in an increase of the wind turbine generator power, compensated by the dump load power consumption.
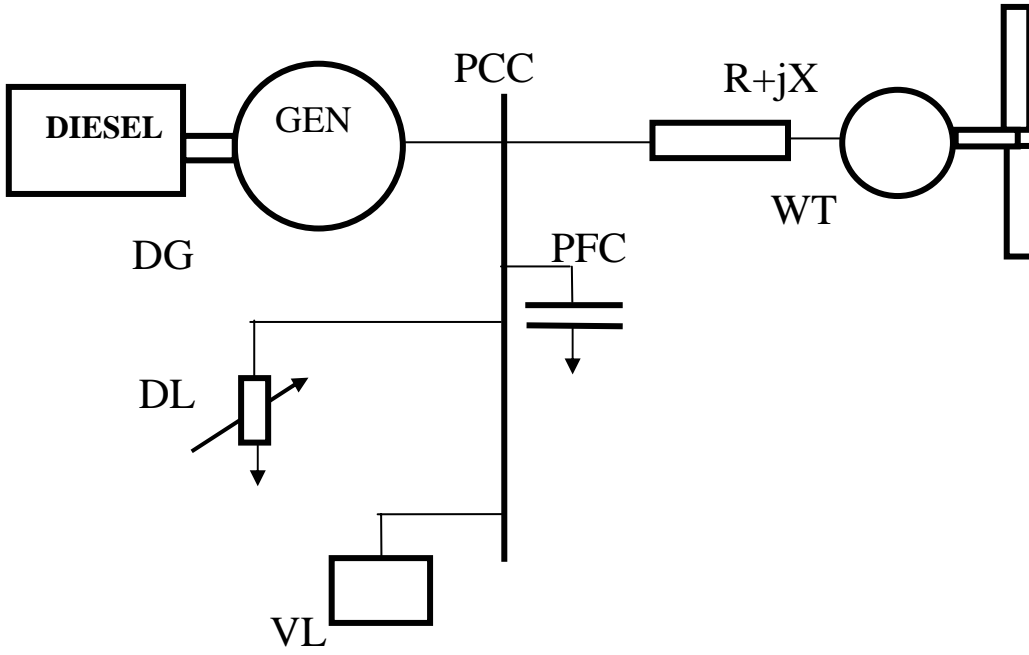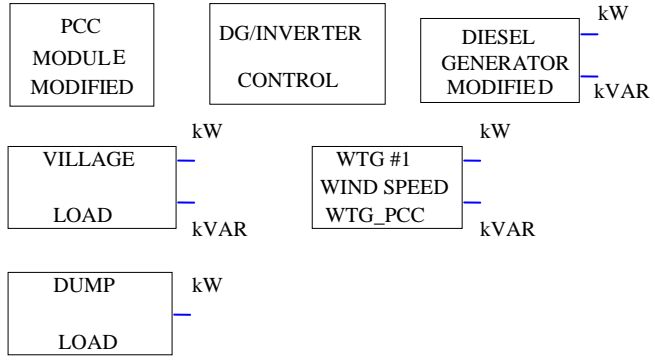
(a)

(b)

Figure 10-5. Power system composed of a DG, an AC WT, a DL, and a VL: (a) single-line diagram and (b) top view of the RPM-SᵢM simulation
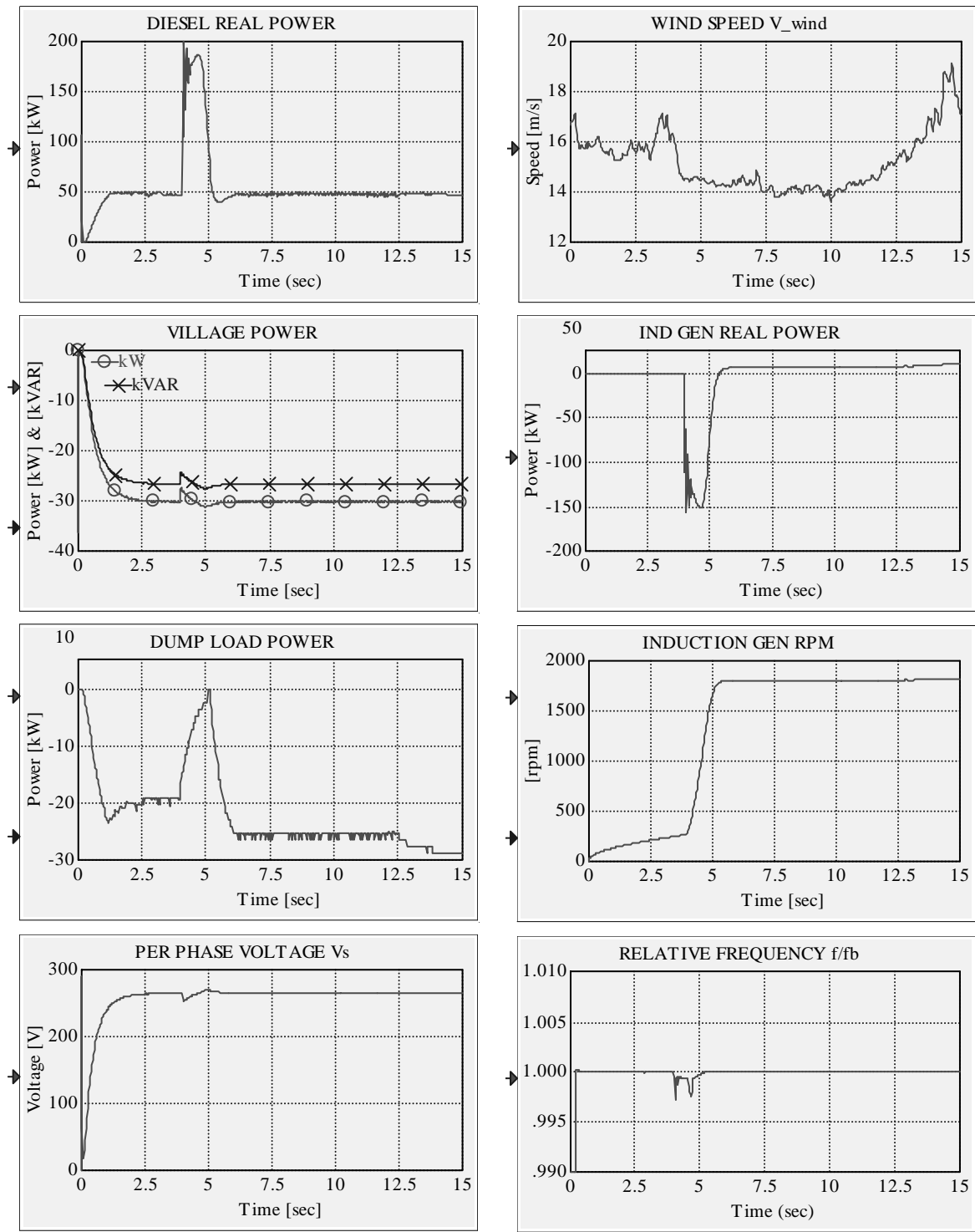
Figure 10-6. Traces of power, rpm, voltage, and frequency for the system composed of a DG, an AC WT, the constant VL, and a DL

Case Study 4: PCC+DG+RC+VL

Principal modules in this case study include:

- A diesel generator with a rated power of 200 kW and a minimum load of 50 kW

- A village load of 100 kW at the power factor $pf = 0.75$

- A rotary converter with a preprogrammed battery reference power.

A power system with this configuration is presented in Figure 10-7, where we show both the single line diagram and the top-view RPM-SIM simulation diagram. The simulation diagram is obtained by adding the following files to the simulation screen: PCC_m.vsm, DG_m.vsm, VL.vsm and BB_RC.vsm. For this system, we obtained traces of power, voltage, and frequency as shown in Figure 10-8. Next, we explain the sequence of simulation events documented in Figure 10-8.

Time/Event Sequence

$t = 0$ The diesel generator starts up.

$t = 5$ sec Line voltage V_s reaches the reference value of 266 V; the relative frequency is close to 1.

The power generated by the diesel generator is at 100 kW; the same power is consumed by the village load.

The battery reference power $P_{BAT\_ref} = 0$.

$t = 6$ sec The battery reference power is switched to -20 kW (which, according to our convention, is a request for charging the battery).

This increment is followed by the power consumed and transmitted to the battery by the rotary converter (the response is slow because of a large time constant of the field-controlled DC motor of the rotary converter).

The power generated by the diesel generator reaches a level of approximately 120 kW to cover the demand of 100 kW from the village and 20 kW from the battery.

The line voltage remains constant.

The frequency recovers to its reference value after a slight dip.

$t = 21.5$ sec The battery reference power is switched to 20 kW (which, according to our convention, is a request for discharging the battery).

This increment is followed by the power generated by the rotary converter; i.e., this corresponds to the increment of 40 kW.

The power generated by the diesel generator decreases from the level of 120 kW with the same time constant and reaches the value of 80 kW at the new steady state.

The transient power changes result in a small transient increase of the frequency.

The line voltage remains constant.

The power consumed by the village remains constant and is provided partially by the diesel generator and partially by the battery.
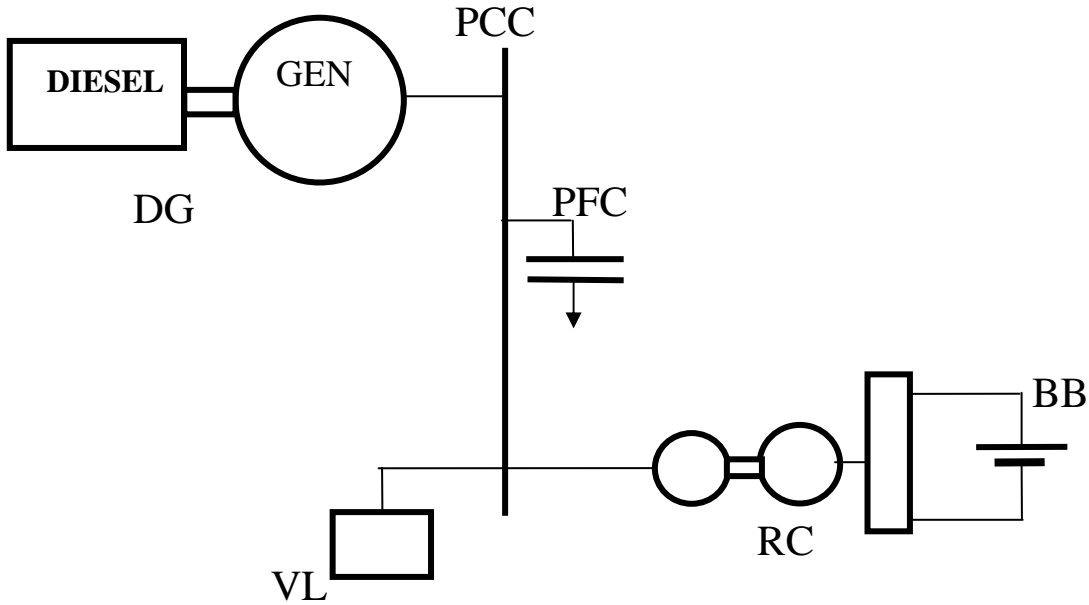

(a)
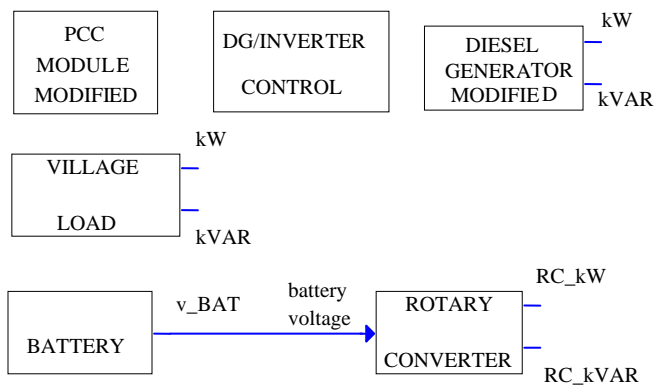
(b)

Figure 10-7. A power system composed of a DG, a VL, and an RC/BB assembly: (a) single-line diagram and (b) top view of the RPM-SIM simulation
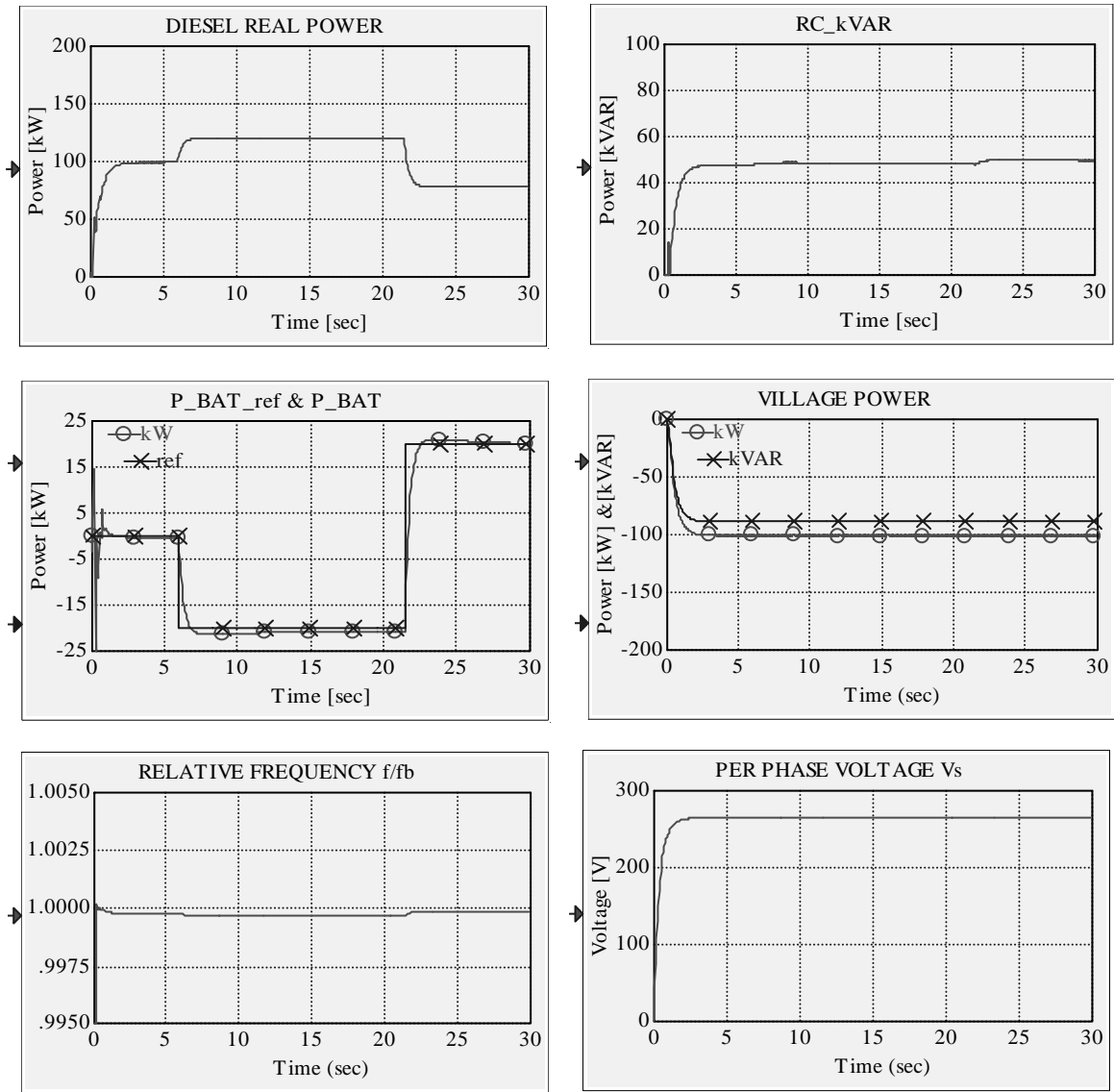
Figure 10-8. Traces of power, voltage, and frequency for the system composed of a DG, an RC, and the constant VL

Case Study 5: PCC+DG+WT+RC+VL+DL

Principal modules in this case study include:

- A diesel generator with a rated power of 200 kW and a minimum load of 50 kW

- An AC WT driven by the wind given by a file of the wind speed time series

- A village load of 50 kW at the power factor pf=0.75, switched to 80 kW at t= 10.5 sec

- A rotary converter with a preprogrammed battery reference power

- A dump load incremented by the diesel power control strategy.

A power system with this configuration is presented in Figure 10-9, where we show both the single-line diagram and the top-view RPM-S$_{IM}$ simulation diagram. The simulation diagram is obtained by adding the following files to the simulation screen: PCC_m.vsm, DG_m.vsm, DG_INV_CTRL.vsm, VL.vsm, DL.vsm, wtg_base_m.vsm and BB_RC.vsm. For this system, we obtained traces of power, voltage, and frequency as shown in Figure 10-10. Next, we explain the sequence of simulation events documented in this figure.

Time/Event Sequence

$t = 0$ The diesel generator starts up.

$t = 2.5$ sec   The line voltage V_s reaches the reference value of 266 V; the relative frequency is approximately 1.

                      The power generated by the diesel generator is at its specified minimum value of 50 kW; the same power is consumed by the village load

                      The battery reference power $P_{BAT\_ref} = 0$.

$t = 4.5$ sec   The battery reference power is switched to 20 kW.

                      This increment is followed by the power provided to the system by the rotary converter (the response is slow because of a large time constant of the field-controlled DC motor of the rotary converter).

                      The dump load is gradually incremented by the diesel power control strategy to keep the diesel generator load at its minimum of 50 kW.

                      The line voltage and frequency remain constant.

$t = 7.5$ sec   The induction machine starts to motor the wind turbine and creates a large load.

                      The power generated by the diesel generator increases sharply.

The dump load tends gradually to 0.

The transient small dips of frequency and line voltage are observed.

$t = 8.2$ sec   The power consumption of the induction machine, reaching the synchronism, rapidly drops.

$t = 9$ sec   The wind turbine generator starts to generate.

The diesel power control strategy tries to compensate for the transient power surplus by incrementing the dump load.

$t = 10.5$ sec   The village load is increased to 80 kW.

$t = 12$ sec   The reference battery power is set at -10 kW; i.e., the battery is being charged (consuming the power surplus).

The dump load is now set at 0.

The diesel generated power increases to approximately 80 kW to balance the power requirements.

The line voltage and frequency remain constant.

(a)

(b)
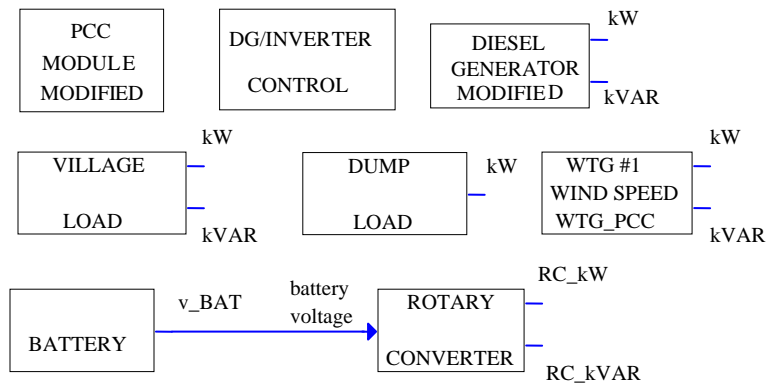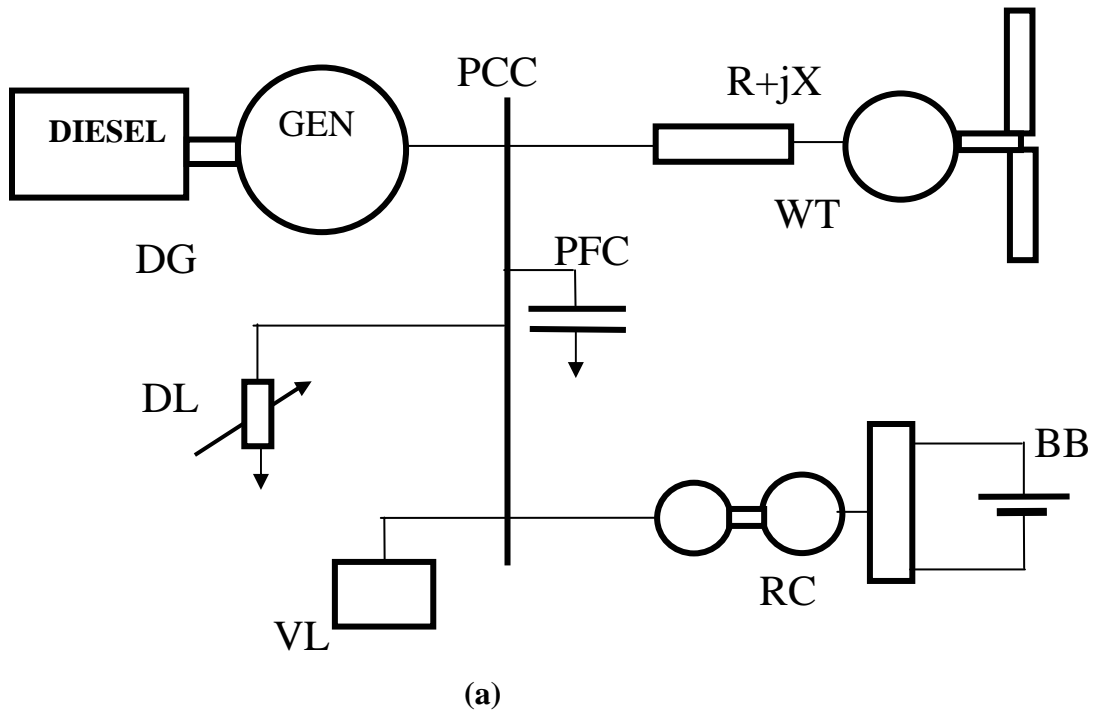
Figure 10-9. A power system composed of a DG, an AC WT, an RC/BB assembly, a VL, and a DL: (a) single-line diagram and (b) top view of the RPM-Sɪᴍ simulation
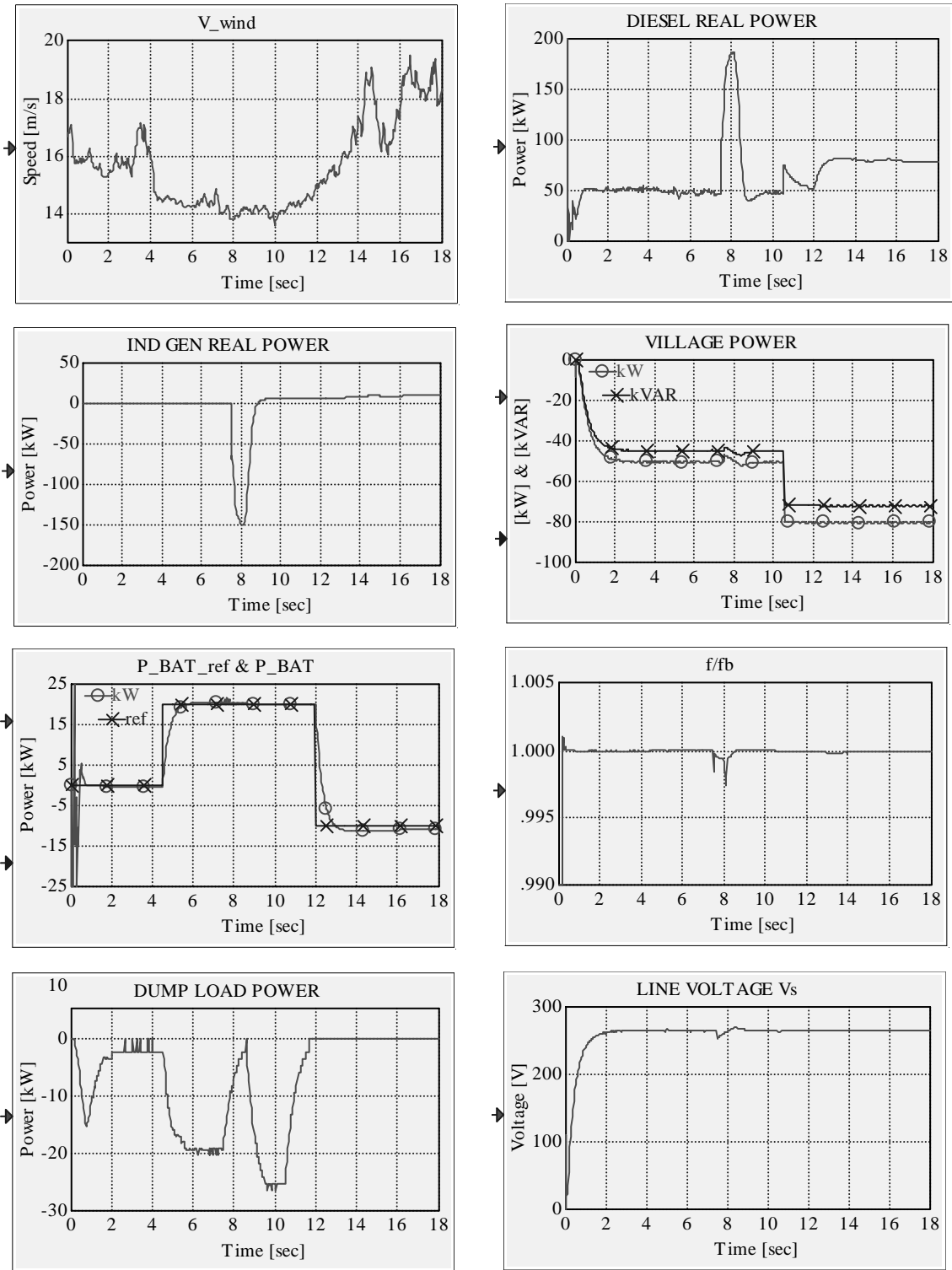
Figure 10-10. Traces of power, voltage, and frequency for the system composed of a DG, an RC, an AC WT, a variable VL, and a DL

Case Study 6: PCC+DG+WT+RC+VL+DL with RC in Synchronous Condenser Mode

Principal modules in this case study include:

- A diesel generator with a rated power of 200 kW and a minimum load of 50 kW

- An AC WT driven by the wind given by a file of the wind speed time series with induction machine motoring preprogrammed to start at $t = 4$ sec

- A village load of 30 kW at the power factor $pf = 0.98$, switched to $pf = 0.75$ at $t = 1.5$ sec, switched to 100 kW at $t = 9$ sec, switched to $pf = 0.98$ at $t = 13$ sec, and switched to 20 kW at $t = 15.5$ sec

- A rotary converter in synchronous condenser mode ($P\_BAT\_ref = 0$) started at $t = 2$ sec with a preprogrammed reference value of the reactive power of 20 kVAR, switched to 50 kVAR at $t = 5$ sec, switched to -10 kVAR at $t = 10.5$ sec, and switched to 20 kVAR at $t = 14$ sec

- A dump load incremented by the diesel power control strategy.

The power system configuration remains the same as the one presented in Figure 10-9, where we show both the single-line diagram and the top-view RPM-S$_{IM}$ simulation diagram. The simulation diagram is obtained by adding the following files to the simulation screen: PCC_m.vsm, DG_m.vsm, DG_INV_CTRL, VL.vsm, DL.vsm, wtg_base_m.vsm, and BB_RC.vsm. For this system, we obtained traces of power, voltage, and frequency as shown in Figure 10-11. Next, we explain the sequence of simulation events documented in Figure 10-11.

Time/Event Sequence

$t = 0$ The diesel generator starts up.

$t = 1.5$ sec   The power factor of the village load is switched from $pf = 0.98$ to $pf = 0.75$.

$t = 2$ sec   The rotary converter is started in synchronous condenser mode ($P\_BAT\_ref = 0$) with a preprogrammed reference value of the reactive power equaling 20 kVAR.

$t = 2.5$ sec   The line voltage V_s reaches the reference value of 266 V; the relative frequency is close to 1.

                  The power generated by the diesel generator is at its specified minimum value of 50 kW and is consumed by the village load and the dump load.

The reactive power generated by the rotary converter reaches the value of $Q\_SR = 20$ kVAR (equal to the current reference value) and is absorbed by the village load and by the diesel generator.

$t = 4$ sec   The induction machine starts to motor the wind turbine and creates a large load in both the real power and the reactive power.

The real and reactive power generated by the diesel generator increases sharply.

The dump load is immediately reduced to 0.

Transient small dips of frequency and line voltage are observed.

$t = 5$ sec   The preprogrammed reference value of the reactive power generated by the synchronous condenser of 20 kVAR is switched to 50 kVAR.

This increment is followed by the gradual increase of Q_SR because, at the same time, the reactive power absorbed by the induction generator sharply decreases, the reactive power generated by the diesel generator must decrease, and even sign is reversed (becoming absorbed).

The real power consumption of the induction machine, reaching the synchronism, rapidly drops.

$t = 5.5$ sec   The wind turbine generator starts to generate power.

The dump load is gradually incremented by the diesel power control strategy to keep the diesel generator load at its minimum of 50 kW.

$t = 6.5$ sec   The reactive power generated by the rotary converter reaches the value of $Q\_SR = 50$ kVAR (equal to the current reference value) and is absorbed by the village load and by the diesel generator.

Small transient changes in the line voltage and frequency can be observed.

$t = 9$ sec   The village load is increased to 100kW and its power factor remains unchanged; i.e., the demand for real power and reactive power in the system increases sharply.

The diesel generator starts to generate the reactive power and sharply increases the level of generated real power.

The dump load decreases to zero.

$t = 10.5$ sec   The preprogrammed reference value of the reactive power generated by the synchronous condenser of 50 kVAR is switched to -10 kVAR; with the village load unchanged, this results in an additional demand for reactive power of 60 kVAR.

The diesel generator provides the required reactive power.

$t = 13$ sec	The village load of 100 kW at the power factor $pf = 0.75$ is switched to $pf = 0.98$; i.e., the demand for reactive power drops sharply.
	The reactive power generated by the diesel generator decreases accordingly.
$t = 14$ sec	The preprogrammed reference value of the reactive power absorbed by the synchronous condenser of -10 kVAR is switched to 20 kVAR; during steady –state, this means that an additional 30 kVAR of reactive power can be absorbed in the system.
	The diesel generator reduces the generated reactive power and finally starts to absorb the reactive power.
$t = 15.5$ sec	The village load of 100 kW at the power factor $pf = 0.98$ is switched to 20 kW at the same power factor
	The wind turbine tries to overpower the diesel generator; for a short time, the diesel real power drops below 0.
	The diesel power control strategy is fast enough to compensate for this power surplus, as the dump load is incremented to save the synchronism.
	The real power provided to the system by the diesel generator returns to its minimum value of 50 kW.
$t > 17$ sec	Wind gusts occur.
	The power generated by the wind turbine increases.
	The real power generated by the diesel generator and the wind turbine generator is absorbed by the village load and the dump load.
	The reactive power provided by the synchronous condenser is absorbed by the village load, the diesel generator, and the induction generator.
	Dump load increments occur to keep the diesel generated power at its required minimum.
	Line voltage and frequency remain constant.
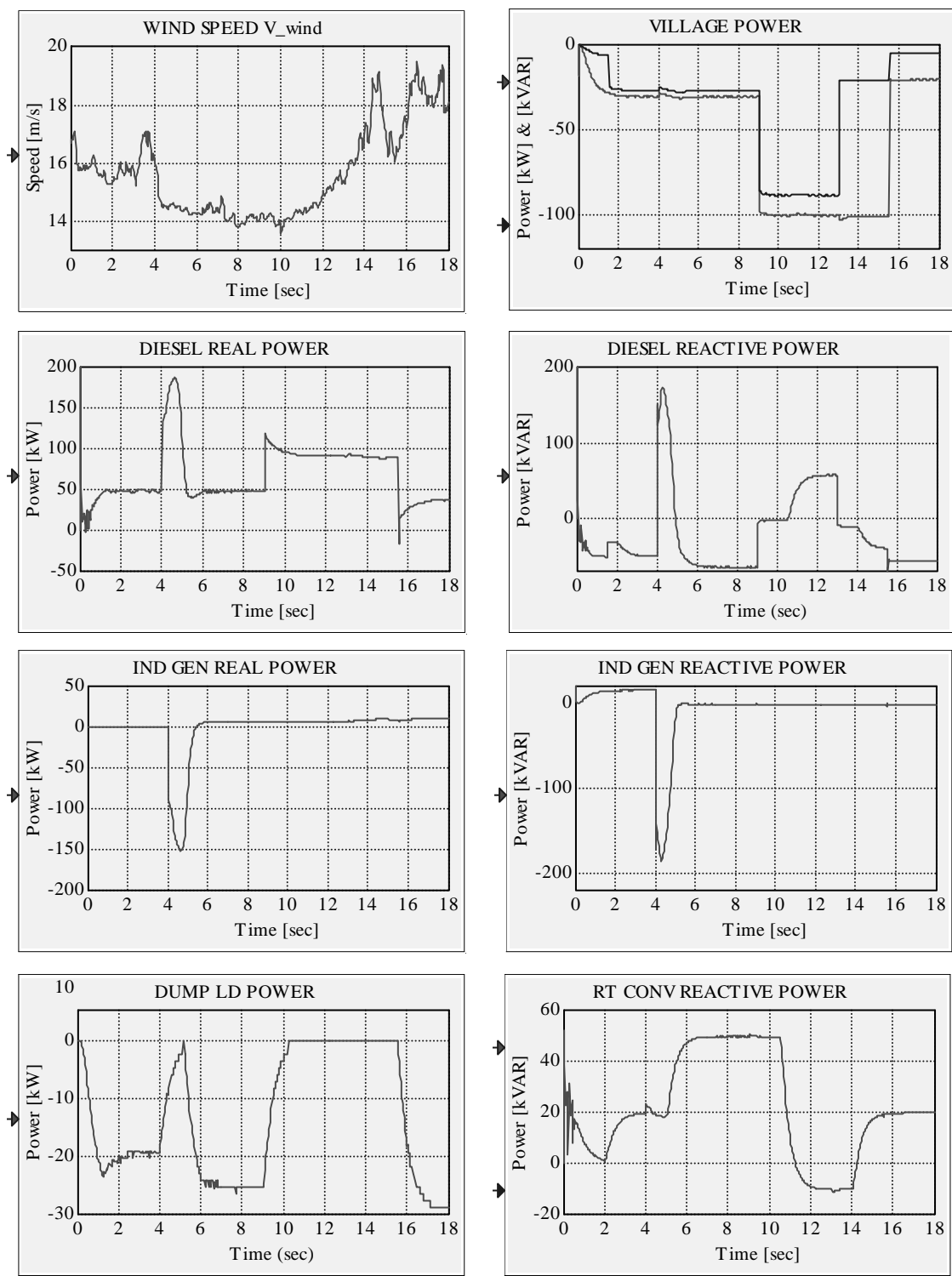
Figure 10-11. Traces of power, voltage, and frequency for the system composed of a DG, an RC, an AC WT, a variable VL, and a DL (continued on the next page)
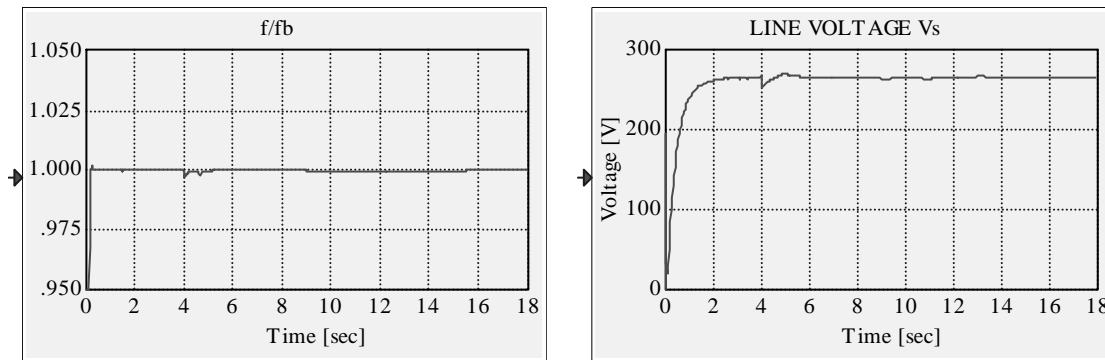
Figure 10-11. **Traces of power, voltage, and frequency for the system composed of a DG, an RC, an AC WT, a variable VL, and a DL** (concluded)

Case Study 7: PCC+DG+WT1+WT2+VL+DL

Principal modules in this case study include:

- A diesel generator with a rated power of 200 kW and a minimum load of 50 kW

- An AC WT (WT1) driven by the wind determined by a file of the wind speed time series with induction machine motoring preprogrammed to start at $t = 4.5$ sec

- An AC WT (WT2) driven by the wind given by a file of the wind speed time series with induction machine motoring preprogrammed to start at $t = 9$ sec

- A village load of 30 kW at the power factor $pf = 0.75$, switched to 150 kW at $t = 12.5$ sec to provide adequate load for both wind turbines

- A dump load incremented by the diesel power control strategy.

The power system configuration is presented in Figure 10-12, where we show both the single-line diagram and the top-view RPM-SIM simulation diagram. The simulation diagram is obtained by adding the following files to the simulation screen: PCC_m.vsm, DG_m.vsm, DG_INV_CTRL, VL.vsm, DL.vsm, wtg_base_m.vsm (adds WT1), and WTG_m.vsm (adds WT2)**.** Then the variable *V_wind* must be added and connected to the input of the AC WT block representing WT2. Moreover, WT2 must be connected to the system through PCC_WT by adding d- and q-components of its transmission line current. It is assumed that both turbines have the same wind profile shown in Figure 1-3. For more details on the simulation of a multiple wind turbine system, refer to Chapters 1 and 4. For the system in this case study, we obtained traces of power, voltage, and frequency as shown in Figure 10-13. Next, we explain the sequence of simulation events documented in this figure.
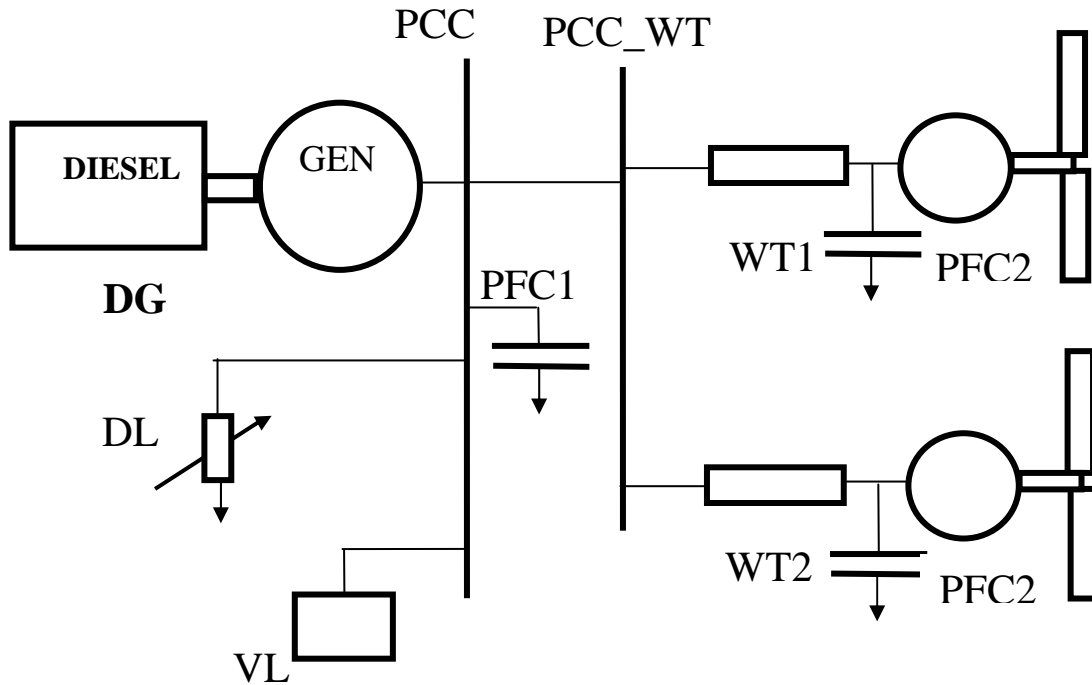
(a)
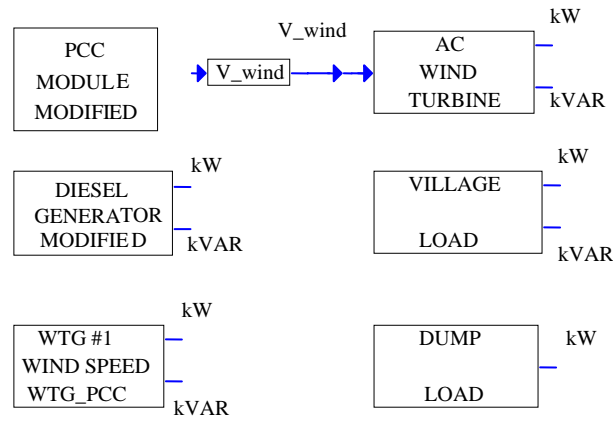
(b)

Figure 10-12. A power system composed of a DG, an AC WT (WT1), an AC WT (WT2), a VL, and a DL: (a) single-line diagram, and (b) top view of the RPM-SIM simulation
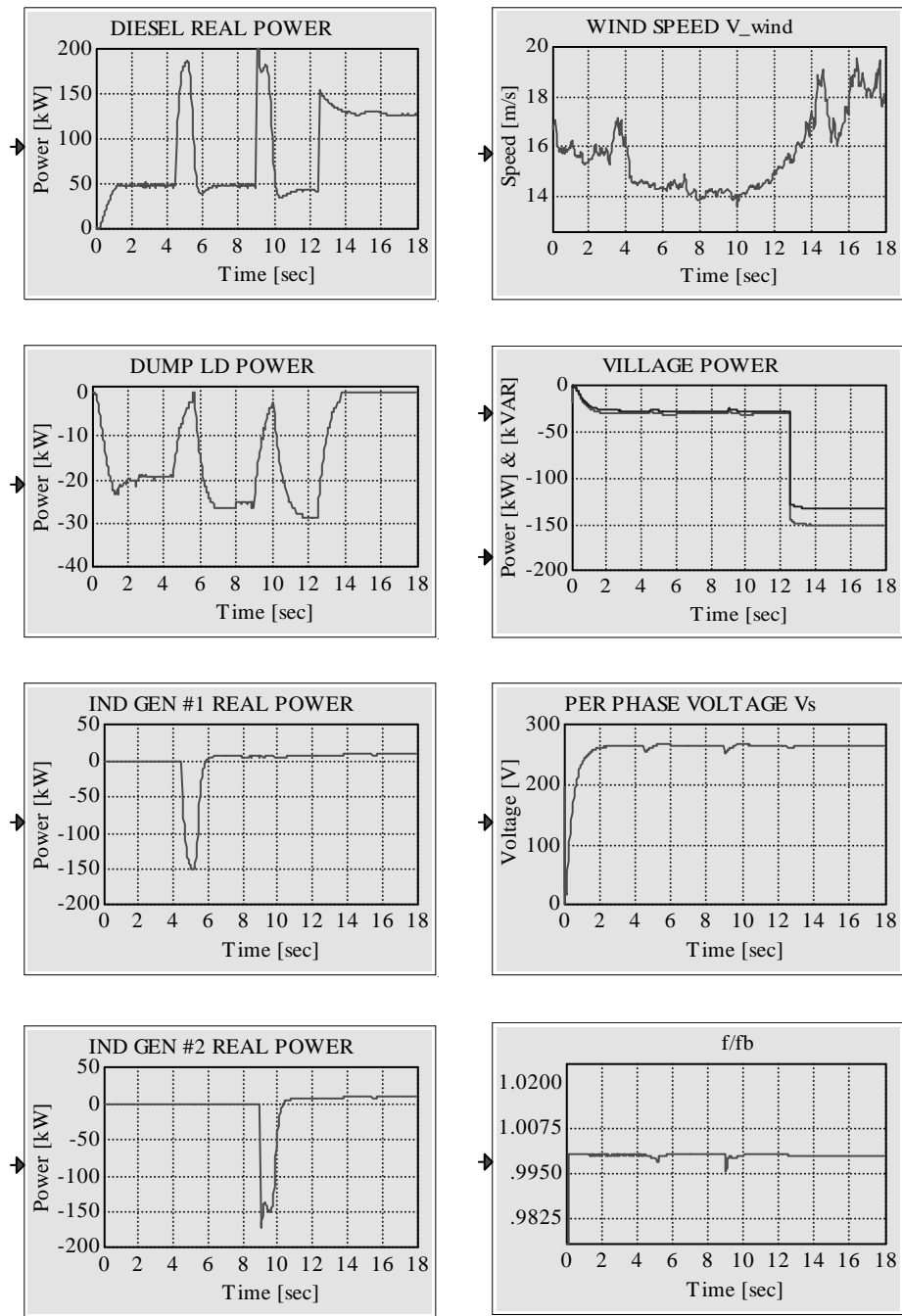
Figure 10-13. Traces of power, voltage, and frequency for the system composed of a DG, an AC WT (WT1), an AC WT (WT2), a variable VL, and a DL

Time/Event Sequence

$t = 0$ The diesel generator starts up.

The dump load is incremented to bring the power generated by the diesel generator to a minimum value of 50 kW.

$t = 3$ sec   The line voltage V_s reaches the reference value of 266 V; the relative frequency is close to 1.

The power generated by the diesel generator is at its specified minimum value of 50 kW and is consumed by the village load and the dump load.

$t = 4.5$ sec   The induction machine starts to motor WT1 and creates a large load.

The power generated by the diesel generator increases sharply.

The dump load is gradually reduced to 0.

Transient small frequency and line voltage dips are observed.

$t = 5.5$ sec   Real power consumption of induction machine #1, reaching the synchronism, rapidly drops, and so does the power generated by the diesel generator.

$t = 6$ sec   The dump load is incremented by the diesel power control strategy to keep the diesel generator load at its minimum of 50 kW.

WT1 starts to generate power.

$t = 9$ sec   The induction machine starts to motor WT2 and creates a large load.

The dump load is gradually reduced to 0.

The power generated by the diesel generator increases sharply.

$t = 10$ sec   Real power consumption of induction machine #2, reaching the synchronism, rapidly drops, and so does the power generated by the diesel generator.

$t = 10.5$ sec   WT2 starts to generate power.

$t = 12.5$ sec   The village load is increased to 100 kW.

The power generated by the diesel generator sharply increases.

Transient small frequency and line voltage changes are observed.

$t > 13$ sec   Both WT1 and WT2 are generating power.

Transient changes of the diesel power correlate well with the wind gusts influencing the power generated by the wind turbine generators.

Both frequency and line voltage stabilize at their reference values.

Case Study 8: PCC+RC (125-hp Reliance Electric DC Machine and 125-kW KATO AC Machine)+WT (AOC 15/50)+VL+DL

In this case study, we report the simulation study of the above listed configuration of the Hybrid Power Test Bed (HPTB) system at the National Renewable Energy Laboratory's National Wind Technology Center. Note that the diesel generator is not included in this configuration. The simulation study was performed for the following modes of operation:

1. Mode 1 operation, frequency control by the DC machine

   Wind turbine on line
   RC AC machine on line
   RC DC machine doing frequency control
   No dump load.

2. Mode 2 operation, frequency control by the DL, battery disconnected

   Wind turbine on line
   RC AC machine on line
   RC DC machine off line.

3. Mode 3 operation, frequency control by the DL, battery connected

   Same as Mode 2 except the DC machine is on line in zero current-control mode.

All three modes were tested using the system configuration shown in Figure 10.14, with each of the components either on or off line as specified above for each mode of operation.

The RPM-S$_{IM}$ models of the following machines are used in this study:

- AOC 15/50 WT generator
- 125-kW KATO synchronous machine (RC AC machine)
- 125-hp Reliance Electric DC motor (RC DC machine). The field saturation effect is included in the DC machine model.
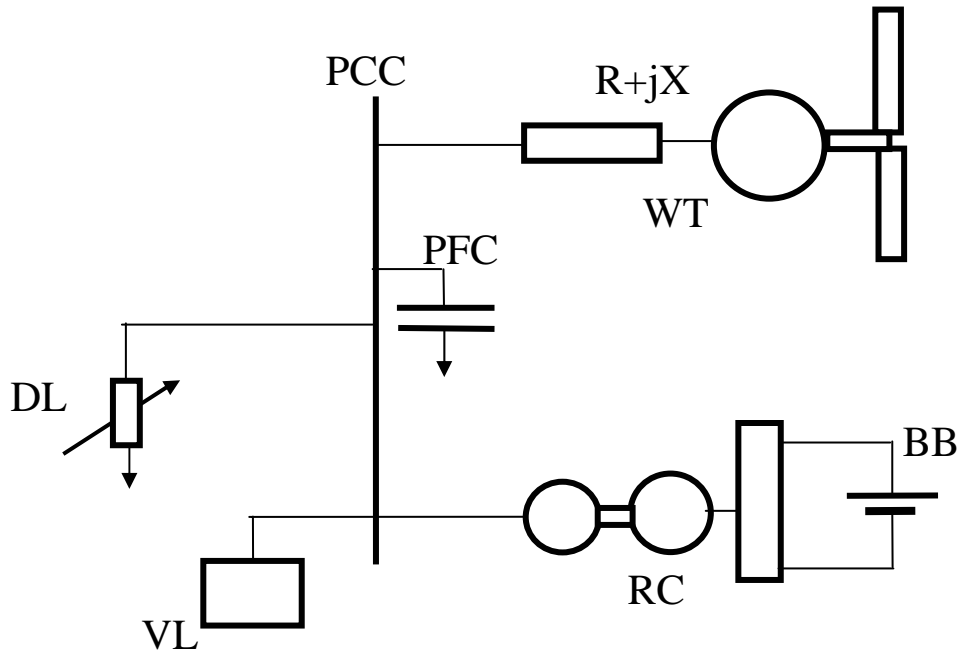
Figure 10-14. Single-line diagram of the system configuration used in the simulation study

In addition, to be able to start the system, we included the RPM-SIM VL model. Because the VL is not included in any of the operation modes to be investigated, it is then set to zero.

The compound block named sequence of events is added to the simulation screen. This block is shown in an expanded form in Figure 10-15 for the mode 1 operation and in Figure 10-16 for the mode 2 and mode 3 operation. Note that the light indicators connected at several locations in this simulation diagram turn red when an associated signal switches from 0 to 1, indicating that a particular event took place. Consequently, the user can easily identify the current state of the simulation. To reach mode 1 operation, we start with the configuration in which the RC discharges the battery and transfers the energy to the VL, controlling both the voltage and frequency. In the mean time, the wind drives the wind turbine generator (WTG). The WTG start-up takes place at 1,700 rpm and the wind energy is now being transferred to the battery and to the village load. Then, 1.5 sec later, the village load is reduced to zero over a period of 200 msec. The wind energy is now being entirely transferred to the battery; i.e., the system operates in mode 1. The traces of the system variables of interest are shown in Figure 10-17. Comparing the real power traces of the RC (negative, indicating energy consumption) and the WTG (positive, indicating energy generation), we can see that at any time when $t > 6.5$ sec, their absolute values are equal.

SEQUENCE OF EVENTS

The RC controls the voltage and frequency and transfers energy from the battery to the VL

WTG startup at 1700 RPM

WIND ENERGY TRANSFERRED TO THE BATTERY AND TO THE VILLAGE LOAD

VL SET TO 0
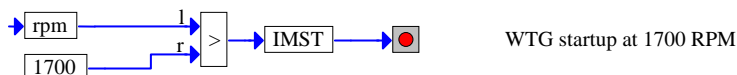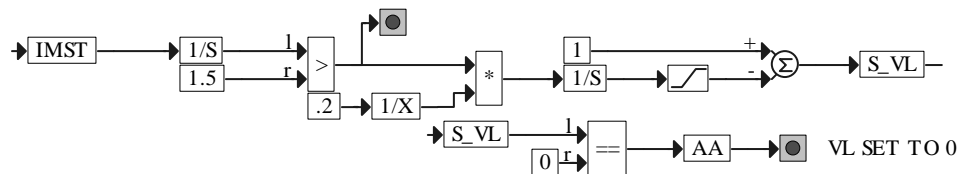
1.5 s later the VL is reduced to 1W (zero) over a period of 200ms
to simulate a smooth transition

ALL WIND ENERGY CAPTURED IS TRANSFERRED TO THE BATTERY

Figure 10-15. Sequence-of-events compound block for mode 1 operation (charging the battery): the RC DC machine controls the system frequency and the RC AC machine controls the system voltage

To reach mode 2 or mode 3 operation, we pass through mode 1 operation. This is documented by the sequence of events shown in Figure 10-16. To make the initial phase of the simulation shorter and to better model the real system, we added the pony motor to drive the RC. This motor is disconnected when the angular frequency reaches 355 rad/sec. Two seconds after reaching mode 1 operation, indicated by the binary variable AA switching from 0 to 1, the dump load is connected and takes over the frequency control. Simultaneously, setting the frequency error (in the field-current controller) to zero disables the frequency control by the DC machine. To reach

- Mode 2 operation, the DC machine and the battery are disconnected by opening the armature circuit of the DC machine, which is simulated by the ramp increase of the armature impedance. As a consequence of setting the frequency error to 0, the field voltage V_{f_DC} is frozen and the field current assumes some steady-state value, which is irrelevant for system operation.

- Mode 3 operation, the DC machine field current is adjusted so that its armature current assumes the value of 0, which results in a 0 torque. This is accomplished by feeding the armature current I_{DC} (treated as the error to be driven to 0) as the input to the PI controller whose output is then fed to the PID controller formerly used to control frequency through the proper adjustment of the DC machine field current. Figure 10-18 shows the field-current control for this mode.

SEQUENCE OF EVENTS

The RC controls the voltage and frequency and transfers energy from the battery to the VL

WTG startup at 1700 RPM

WIND ENERGY TRANSFERRED TO THE BATTERY AND TO THE VILLAGE LOAD

VL SET TO 0
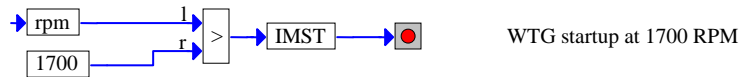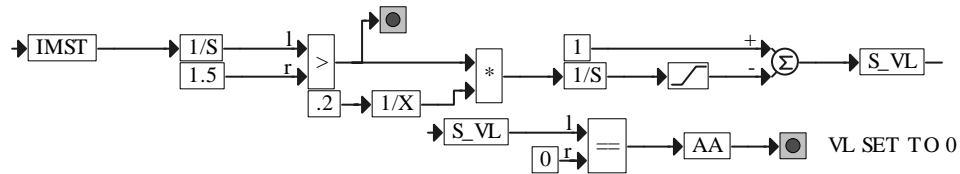
1.5 s later the VL is reduced to 1W (zero) over a period
of 200ms
to simulate a smooth transition

ALL WIND ENERGY CAPTURED IS TRANSFERRED TO THE BATTERY
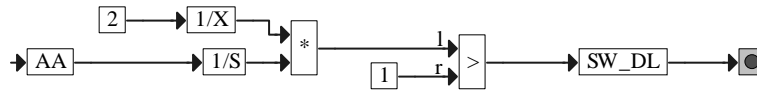
2 s later the DL is connected and the DC machine is disconnected

(rotary converter turned into synchronous condenser)

FREQUENCY CONTROL IS TAKEN OVER BY THE DL.
THE SYNCHRONOUS CONDENSER CONTROLS THE VOLTAGE.

THE WIND ENERGY IS TRANSFERRED TO THE DL AND
TO THE SYNCHRONOUS CONDENSER
(OPERATING AS THE SYNCHRONOUS MOTOR)

**Figure 10-16. Sequence-of-events compound block for mode 2 and 3 operation
(wind energy transferred to the DL and to the synchronous condenser): the
system frequency control is taken over by the DL and the RC AC machine controls
the system voltage**
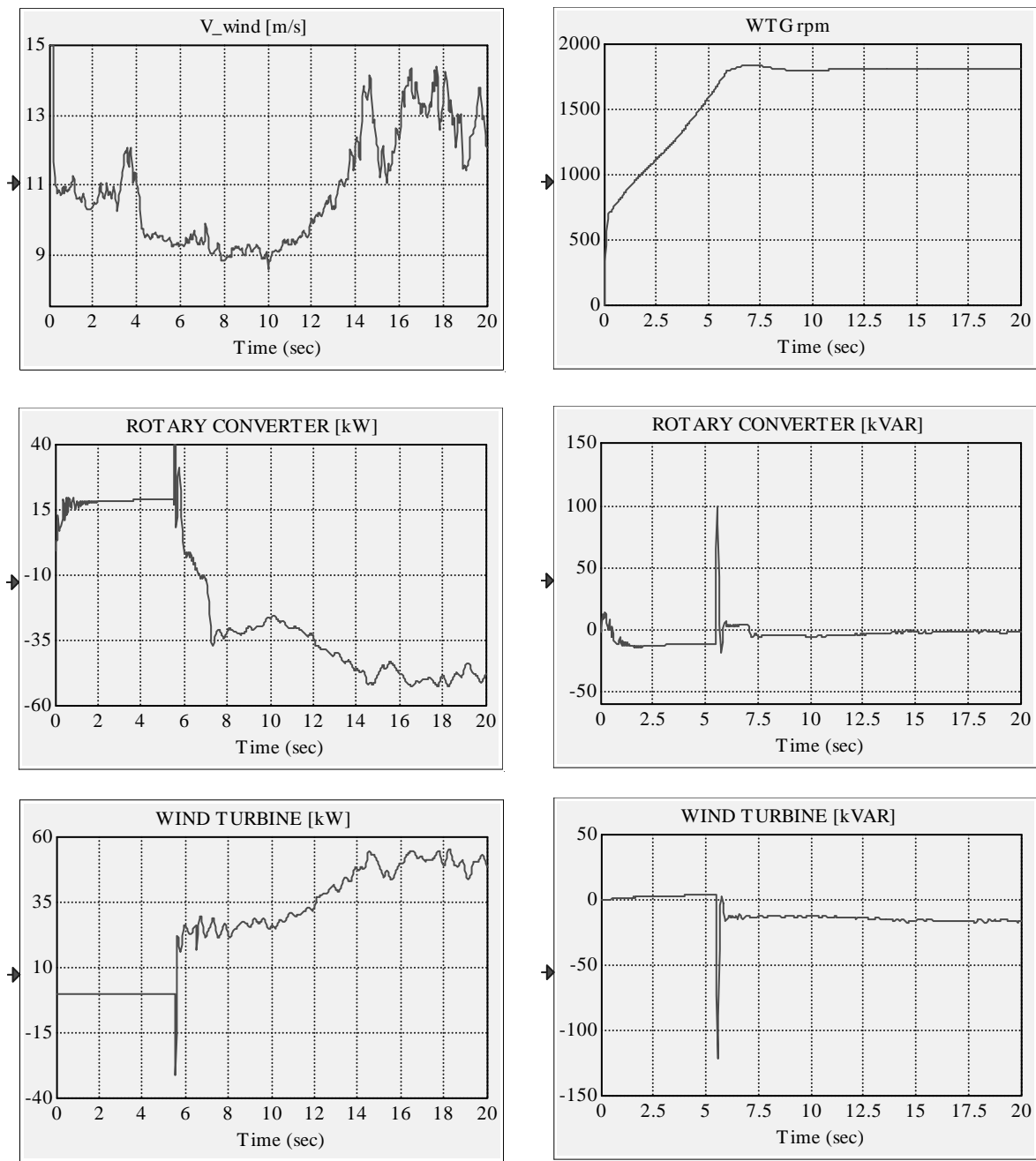
Figure 10-17. Traces of system variables for the mode 1 operation, which starts at approximately t = 6.5 sec when the VL is disconnected and the wind energy is transferred entirely to the battery (visible sudden increment of the real power consumed by the RC) (continued on the next page)
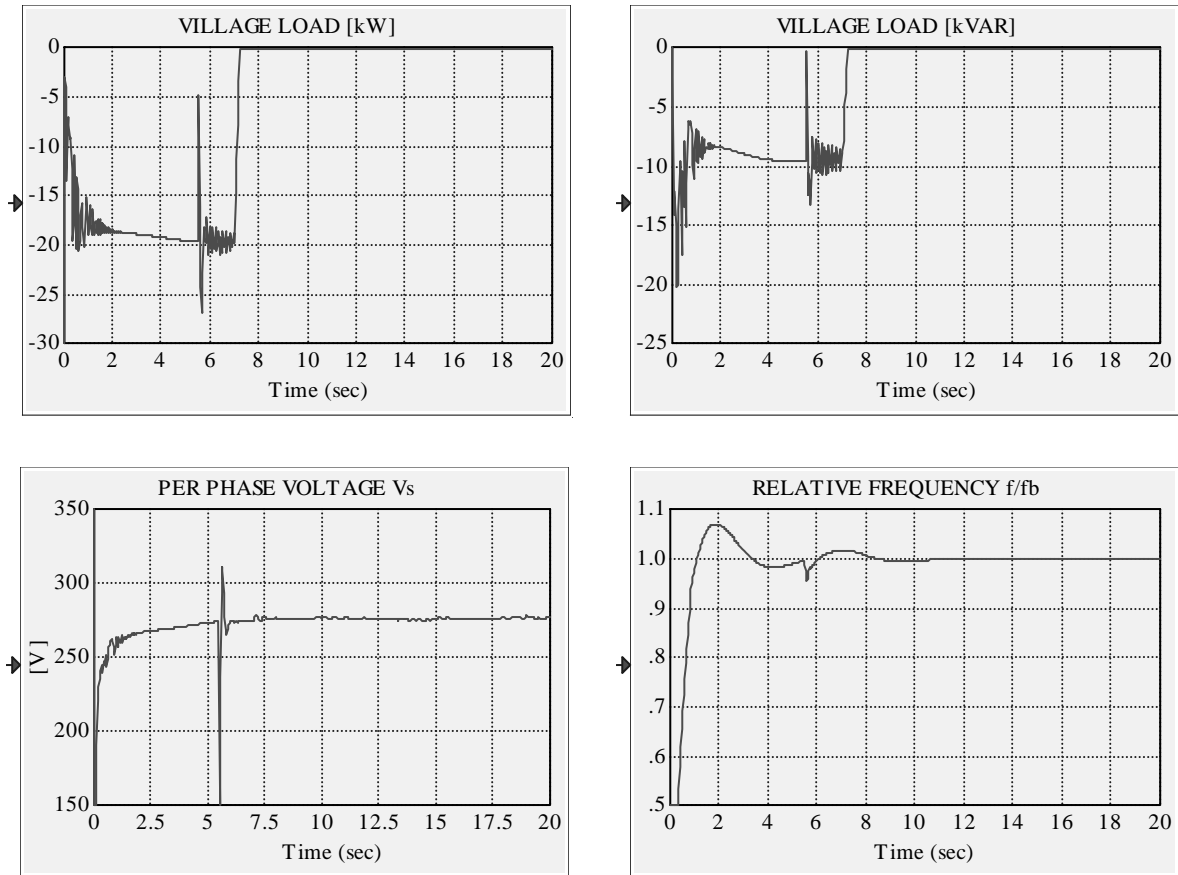
Figure 10-17. Traces of system variables for mode 1 operation, which starts at approximately t = 6.5 sec when the VL is disconnected and the wind energy is transferred entirely to the battery (visible sudden increment of the real power consumed by the RC) (concluded)

NOTE: It is important for all three modes to properly set the low limit $THETA_{Llimit}$ for the angle $THETA$ of the DC machine field power supply. To find this limit, we determine the approximate value of the field current, at which the no-load characteristic or field saturation curve $E_{a\_nl}(i_{f\_DC})$ enters the saturation region. For the DC machine involved in this simulation, this is the approximate value of 2 A, as shown in Figure 10-19. Then, we take 25% of this value (which is 0.5 A), and we request $THETA_{Llimit}$ to be the value, which results in the steady-state field current of 0.5 A. For the field power supply shown in Figure 10-18, then, we have the following equation:

$$\frac{650(1 - \cos THETA_{L\lim it})}{R\_f} = 0.5, \quad R\_f = 70,$$

from which we find $THETA_{Llimi\,t} = 0.33$ rad.

As a result of the sequence of events shown in Figure 10-16, for both mode 2 and mode 3 operation, the synchronous generator functions as a synchronous condenser. The field current of the synchronous condenser controls the system voltage. Ensuring that the rotor speed of the synchronous condenser is constant controls the system frequency.
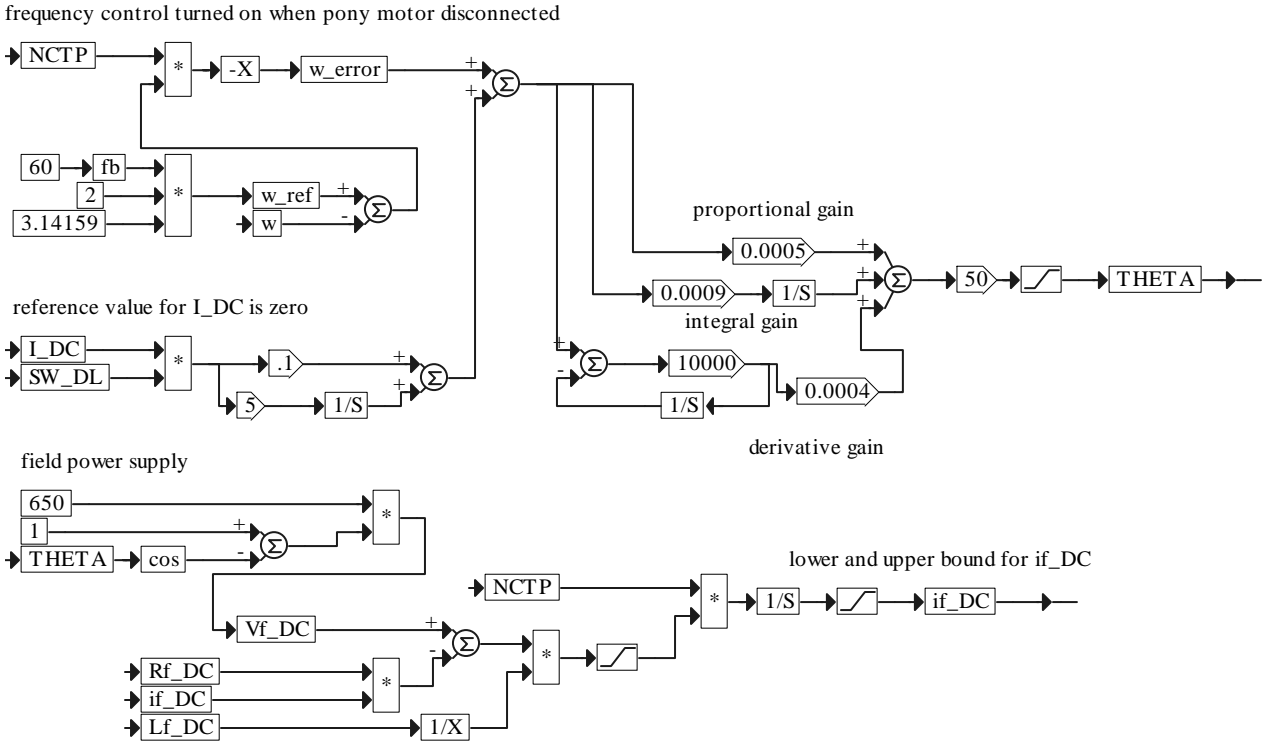
**Figure 10-18. Field-current controller and circuit**

This is accomplished by controlling the dump load so that it almost totally consumes the power generated by the WTG. The small amount of the real power enters the synchronous condenser to cover the losses. Consequently, for both modes of operation, the traces of the system variables (shown in Figure 10-20) are identical. The dump load takes over the frequency control at $t = 8.5$ sec.
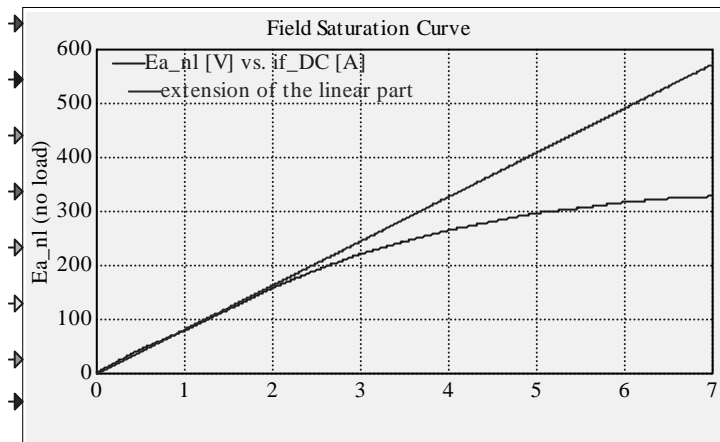
Figure 10-19. The field saturation effect:
the characteristic remains linear for $i_{f\_DC} < 2A$
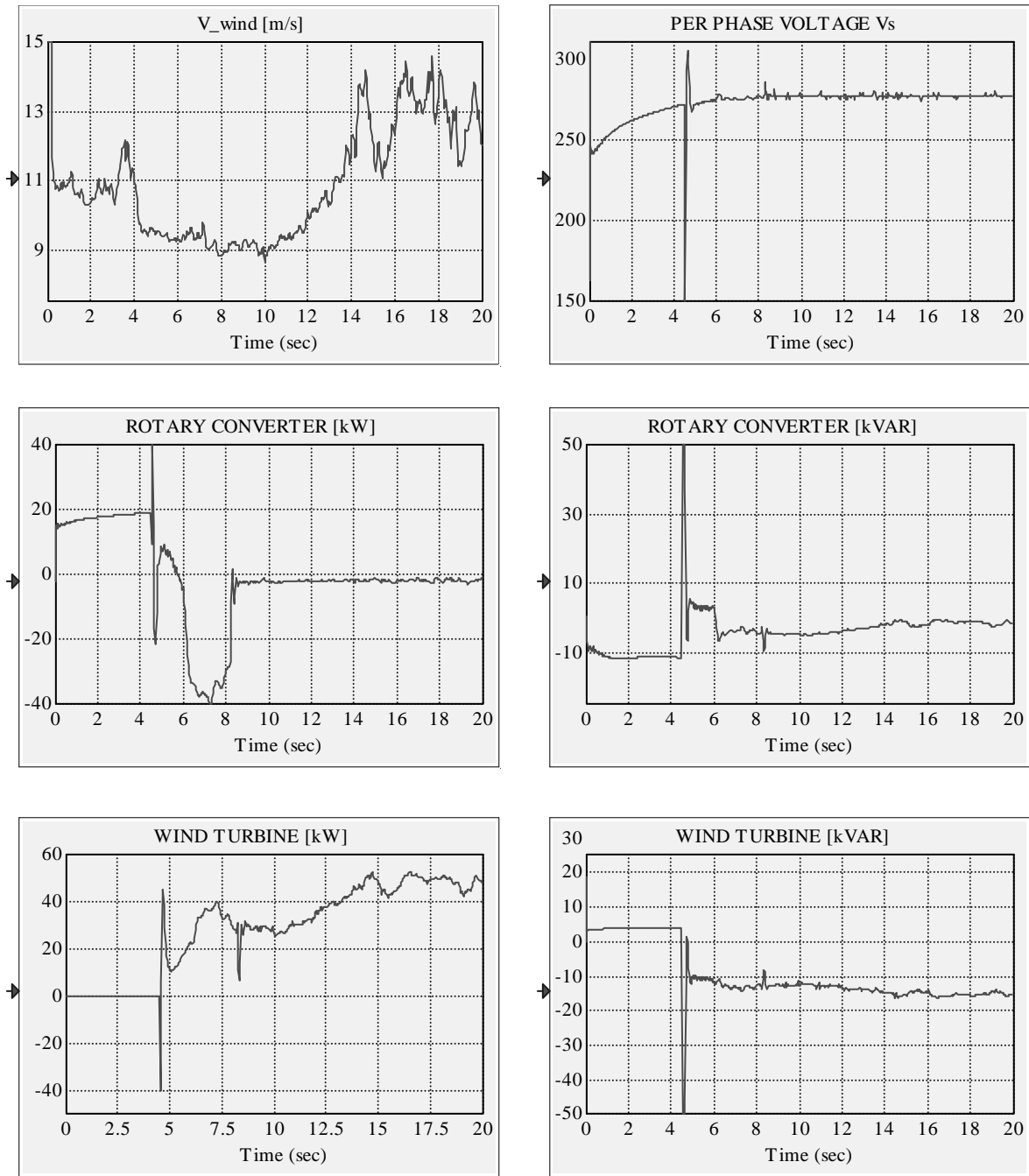
Figure 10-20. Traces of the system variables for mode 2 and mode 3 operation, which starts at approximately *t* = 8.5 sec when the DL takes over the frequency control and consumes almost all of the wind energy
(with the exception of the RC AC machine losses)
(continued on the next page)
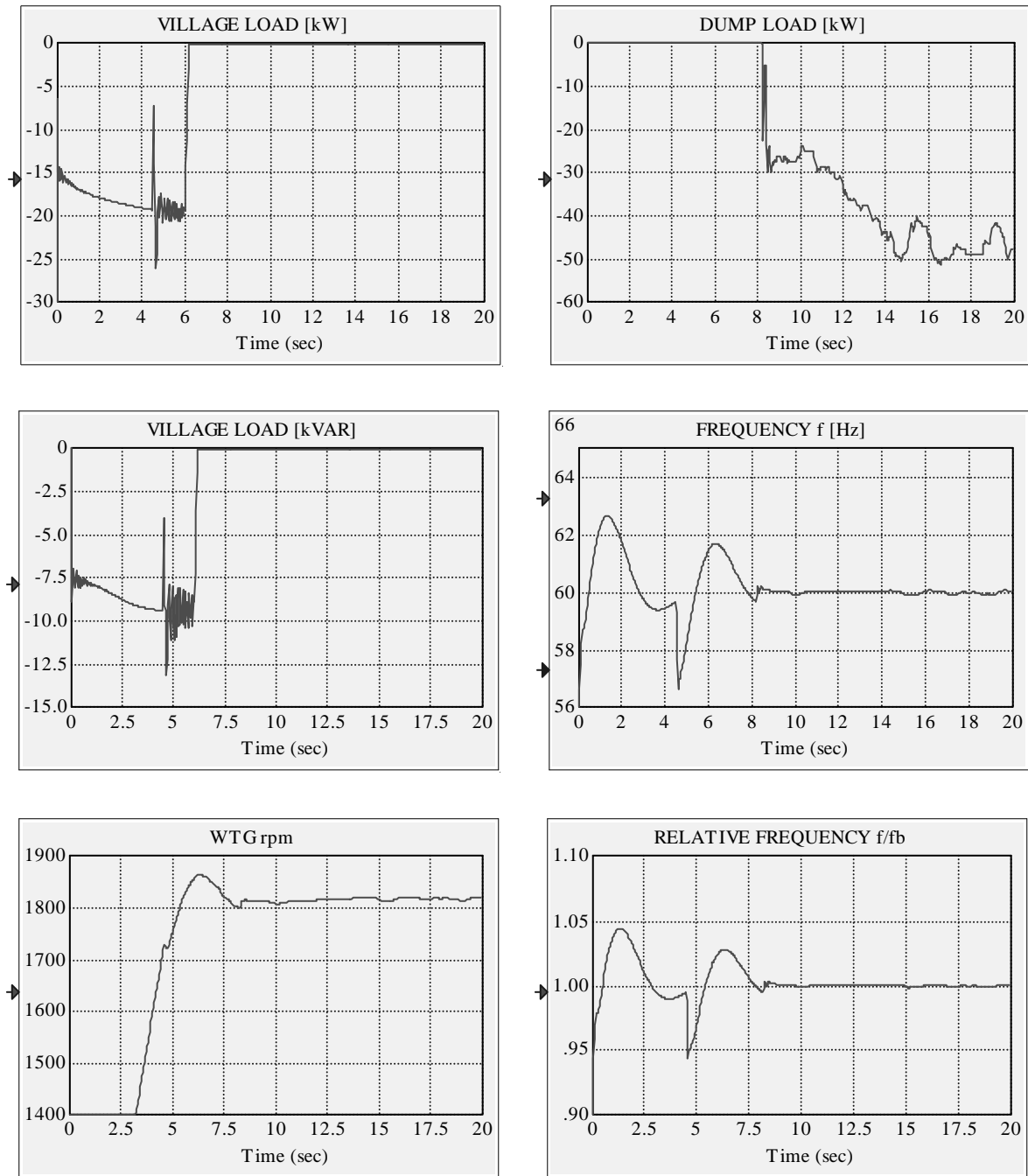
Figure 10-20. Traces of the system variables for mode 2 and mode 3 operation, which starts at approximately *t* = 8.5 sec when the DL takes over the frequency control and consumes almost all of the wind energy
(with the exception of the RC AC machine losses) (concluded)

The difference between mode 2 and mode 3 operation can be seen by comparing the traces of the RC DC machine field current and armature current shown in Figure 10-21

for mode 2 operation and in Figure 10-22 for mode 3 operation. In the former case and starting at $t = 8.5$ sec (Figure 10-21), the RC DC machine is off line, which is equivalent to zero shaft torque or zero armature current obtained by opening the armature circuit. At the same time, the field voltage remains frozen and the field current reaches a certain (and irrelevant) steady-state value. In the latter case and starting at $t = 8.5$ sec (Figure 10-22), the battery remains connected and the field current is adjusted (at approximately 1.5 A) so that the armature current assumes the value of 0; i.e., the RC DC machine remains on line in the zero current-control mode. All the actions described, associated with switching from mode 1 to mode 2 or to mode 3, are initiated by changing the value of the binary variable SW_DL from 0 to 1. However, the control mechanisms are, of course, different for each of the two cases.
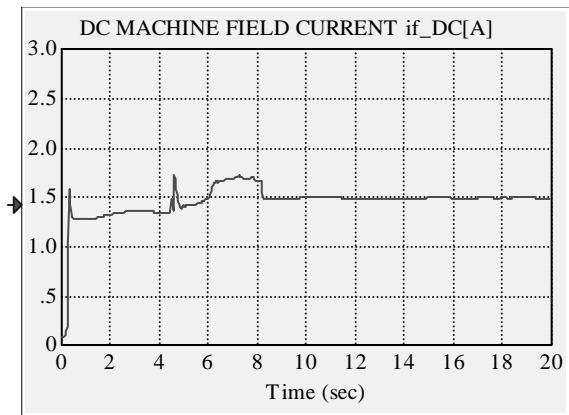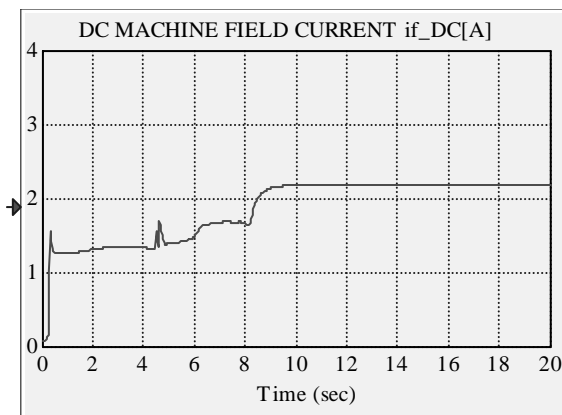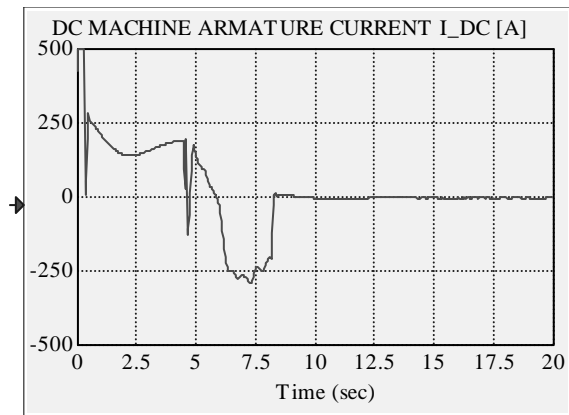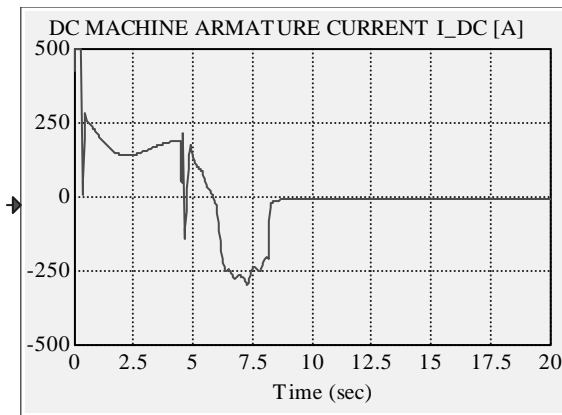
Figure 10-21. Switching from mode 1 to mode 2 operation at *t* = 8.5 sec: battery disconnected and RC DC machine off line
($I_{DC} = 0$, I_{fDC} is no longer controlled and reaches a steady-state value)

Figure 10-22. Switching from mode 1 to mode 3 operation at *t* = 8.5 sec: battery connected and RC DC machine on line in zero current-control mode
($I_{DC} = 0$ due to I_{fDC} 1.5 A)

Frequency Control by the Dump Load

The DL frequency controller, used in mode 2 and mode 3 operation, is shown in Figure 10-23. It starts to operate when the value of the variable SW_DL, which was defined in Figure 10-17, switches from 0 to 1. The PI controller determines the number of active dump load elements. The round block converts this number to an integer. The power increment, set by the user, relates this number to the dump load power.
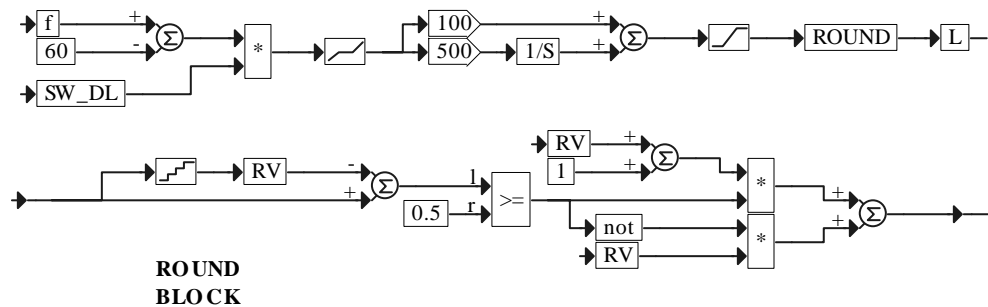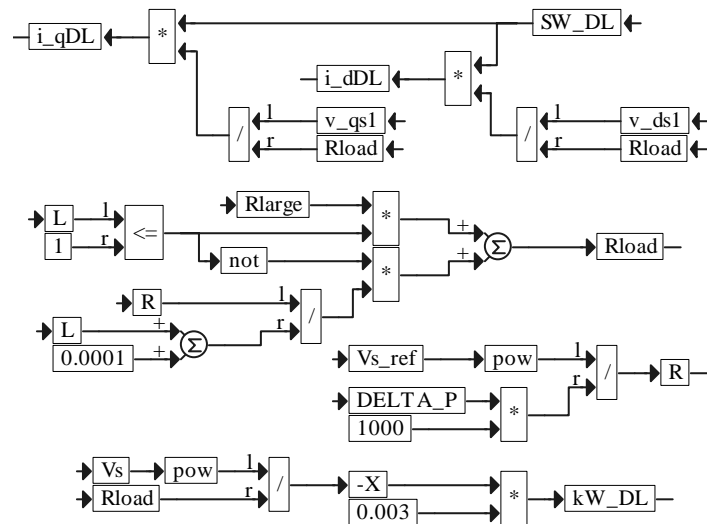
Figure 10-23. The DL frequency controller

Case Study 9: Furling Control for Small Wind Turbine Power Regulation

Performance Analysis Using an Example of Battery Charging System

Many small wind turbines use an upwind rotor configuration with a tail vane for passive yaw control. It allows the rotor to furl (turn away from the wind direction) in high winds, providing both power regulation and overspeed protection. In our model, we are not simulating the furling dynamics but rather their impact on the power system. We analyze steady-state performance and dynamics of such systems using an example of a battery-charging wind turbine system. This system, shown in Figure 10-24, consists of a permanent magnet synchronous generator and a three-phase diode rectifier that charges a battery.
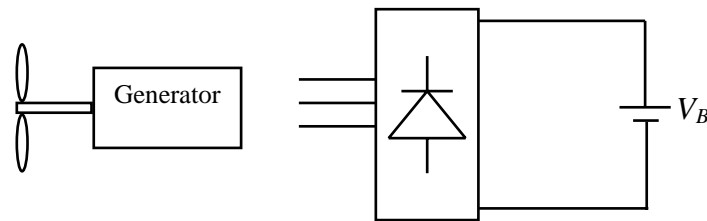
Figure 10-24. A battery-charging system
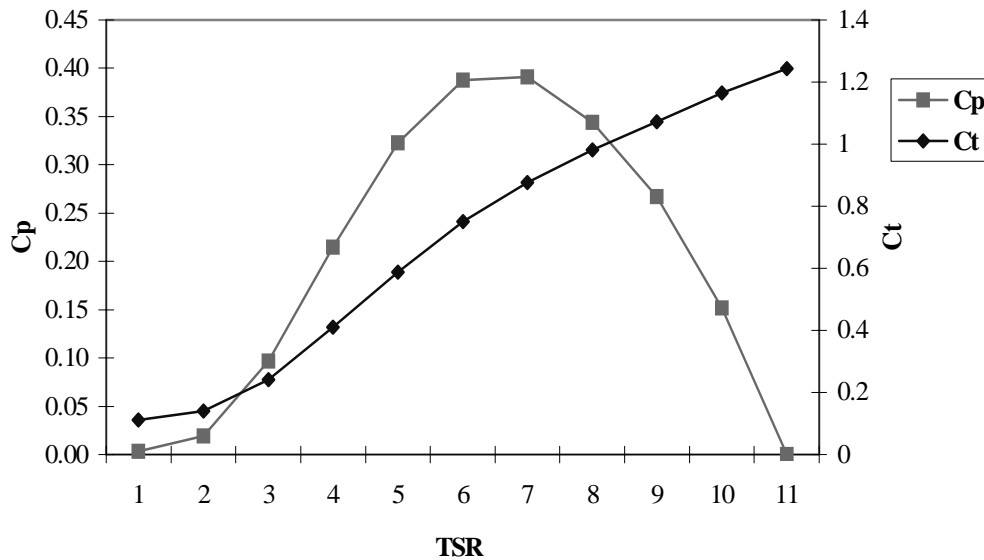
Figure 10-25. Power coefficient and coefficient of thrust as function of TSR

The wind turbine aerodynamic power is given by the following equation:

$$P_{aero} = 0.5\rho A C_p(TSR)V^3 \qquad\qquad (10\text{-}1)$$

where ρ is the air density (kg/m³), A is the swept area of the blades, the power coefficient C_p is shown in Figure 10-25 to be a function of TSR, and V is the wind speed (m/sec).

The tip speed ratio

$$TSR = \frac{\omega R}{V}, \qquad\qquad (10\text{-}2)$$

where ω is the rotor angular velocity (rad/sec) and R is the rotor radius (m). Thus, the power delivered by the wind turbine depends on the wind speed and the rotor angular velocity or its equivalent inrpm. This angular velocity is directly related (through the system's equations) to the rpm of the generator. Substituting V from (10-3) into (10-2) we obtain:

$$P_{aero} = 0.5\rho A C_p(TSR)(R/TSR)^3\omega^3. \qquad\qquad (10\text{-}3)$$

This equation shows that when the *TSR* is constant, the wind power generated by the wind turbine rotor is proportional to the angular velocity or to the equivalent rpm cubed.

So far, we have assumed that the wind direction is normal to the rotor plane, or we can say that the wind speed V has only the normal component ($V_n = V$). When the wind is strong, the furling mechanism comes into play and [as illustrated in Figure 10-26(b)] turns the rotor by the angle θ. Then, the effective wind speed component becomes

$$V_n = V\cos\theta. \qquad\qquad (10\text{-}4)$$

This is the wind component replacing V (under furling condition) in equation (10-2), **which results in aerodynamic power reduction.** Considering this condition, the following equation represents mechanical power P_{mech} delivered by the wind turbine:

$$P_{mech} = 0.5\rho A C_p(TSR)V_n^3, \qquad\qquad (10\text{-}1)$$

in which $C_p(TSR)$ is the power coefficient shown in Figure 10-25.

Figure 10-26 shows the free-body diagram of the system under normal and under furling conditions. Under a furling condition, besides the force perpendicular to the plane of rotation, called thrust (T_h) and proportional to the square of the effective component of the wind, the in-plane force P_{force} appears. These are the forces contributing to the moment around the pivot point and are given by the following equations:

$$T_h = 0.5\rho C_t A V_n^2,$$

$$P_{force} = T_h \sin\theta .$$

The furling moment caused by the wind

$$M_W = T_h d_1 + P_{force} d_2 .$$

The restraining moment from the tail vane (with some damping added) can be approximately represented by

$$M_S = K_1 + K_2\theta + K_3\dot{\theta} .$$

The damping component is not used in the current wind turbine designs and can be easily removed in the simulations by setting $K_3 = 0$. It was introduced to investigate its merit through the simulation.

The equilibrium equation is
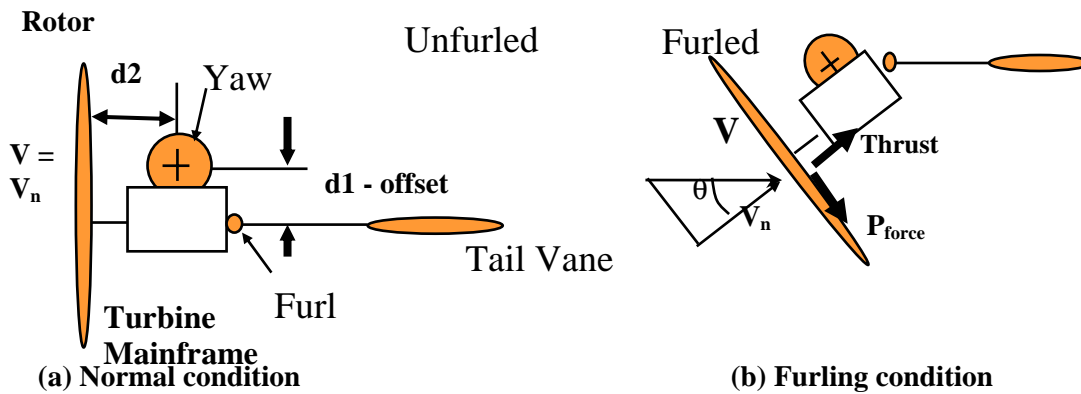
Figure 10-26. Free-body diagram of the furling mechanism

$$J_F\ddot{\theta} = M_W - M_S , \ \theta \le \theta_{LIM} ,$$

where J_F is the moment of inertia of the wind turbine with respect to the yaw axis and the furl angle θ is constrained by θ_{LIM} .

Figure 10-27 represents the drive train, for which the following parameters are known:

J_M = motor inertia, J_R = rotor inertia, C_L = low-speed shaft viscous damping, K_L = low speed shaft stiffness, and N = transmission ratio. As denoted in Figure 10-27, ω_m = mechanical speed at the generator side and the mechanical speed at the low-speed shaft side $\omega_r = \omega_m / N$. In the same figure, we have θ_1 = a angle of rotation of the high-speed

shaft, θ_2 = angle of rotation of the low-speed shaft at the transmission side, and θ_3 = angle of rotation of the low-speed shaft at the rotor side. Consequently, we have the following relations:

$$\omega_m = \dot{\theta}_1 \ , \ \theta_2 = \theta_1 / N \ .$$

The torque transmitted through the low speed shaft

$$T_S = K_L (\theta_2 - \theta_3) + C_L (\dot{\theta}_2 - \dot{\theta}_3) \ .$$

We can write the following engagement equations:

$$J_M \ddot{\theta}_1 = T_{GEN} - T_S / N$$

$$J_R \ddot{\theta}_3 = T_{ROT} + T_S$$

with

$$T_{GEN} = -\frac{P_{SHAFT}}{\omega_m} \ , \qquad T_{ROT} = \frac{P_{mech}}{\omega_r} \ ,$$

where P_{SHAFT}, the generator total power, includes power lost and power delivered.
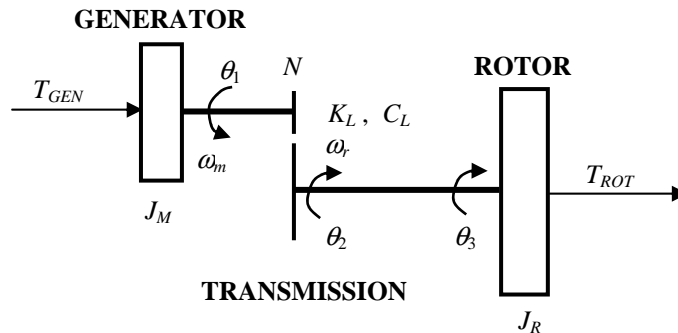
Figure 10-27. Schematic representation of the drivetrain

The generator total power P_{SHAFT} is given by the following equation:

$$P_{SHAFT} = 3V_{ph} I_S + 3R_S I_S^2 + P_{Fe} \ ,$$

where V_{ph} is the per-phase AC voltage at the terminal output of the generator. It is calculated from the following rectifier equation:

$$V_{ph} = \frac{\pi V_B}{3\sqrt{6}} \ ,$$

in which V_B is the battery voltage, and P_{Fe} represents iron losses and is given by

$$P_{Fe} = P_{Fe\_rated}\left(\frac{\omega_e}{\omega_{e\_rated}}\right)^2, \quad \omega_e = \frac{2\omega_m}{\#\,of\,poles}.$$

The relationship between the stator parameters R_S, X_S and variables V_{ph}, I_S explains the equivalent circuit and phasor diagram in Figure 10-28. Using this phasor diagram we derive the equation for I_S.

$$E_S = K_{flux} \times RPM, \quad K_{flux} = V_{ph}/RPM_{cut-in}$$

$$E_S^2 = (V_{ph} + I_S R_S)^2 + (X_S I_S)^2$$

$$I_S = \frac{-2R_S V_{ph} \pm \sqrt{(2V_{ph})^2 - 4(R_S^2 + X_S^2)(V_{ph}^2 - E_S^2)}}{2(R_S^2 + X_S^2)}$$

$$X_S = \omega_e L_S$$
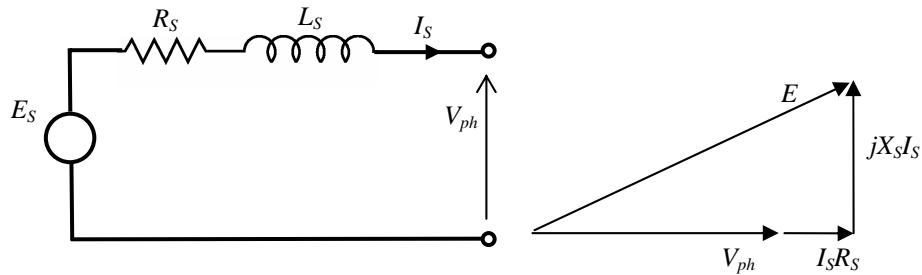
Figure 10-28. Equivalent and phasor diagram of the generator stator

### *Experimental Study of the Furling Mechanism Dynamics*

In Figure 10-29, we present the responses of the system to a simulated ramp wind speed. It can be seen that the furling operation starts when the wind speed reaches 15 m/sec. At this time instant, the rotor has a speed of 250 rpm, the thrust equals 4 kN, and the power has the peak of 28 kW. As a result of this operation, the furling angle θ changes from 0 to its bound of 1.22 rad or $70°$, which can be changed for different wind turbines. This results in a drop of the effective wind speed, the rotor rpm, the thrust, and the wind power captured by the wind turbine generator.

It can be noticed that the operation of the furling mechanism is of the "bang-bang" type. This may have many undesirable effects. We want to capture as much wind power as possible but we do not want this response, represented by the furl angle, to be too fast. This undesirable transient can be seen even better in the responses to a ramp-up-ramp-down wind as shown in Figure 10-30, in which the rotor rpm, the thrust, and the wind

power captured are shown as functions of time. We can see a very short rise time of the furling angle. The increase of this rise time should result in smoothing the furling operation. The increase of the rise time can be achieved by additional damping reflected in equation (10-7) by setting K_3 to some nonzero value. To see how this works, the responses of the furl angle to a step change of the wind speed were recorded for no additional damping, and for two values of the additional damping. The effect, shown in Figure 10-31, is as predicted—additional damping results in an increase of the rise time.
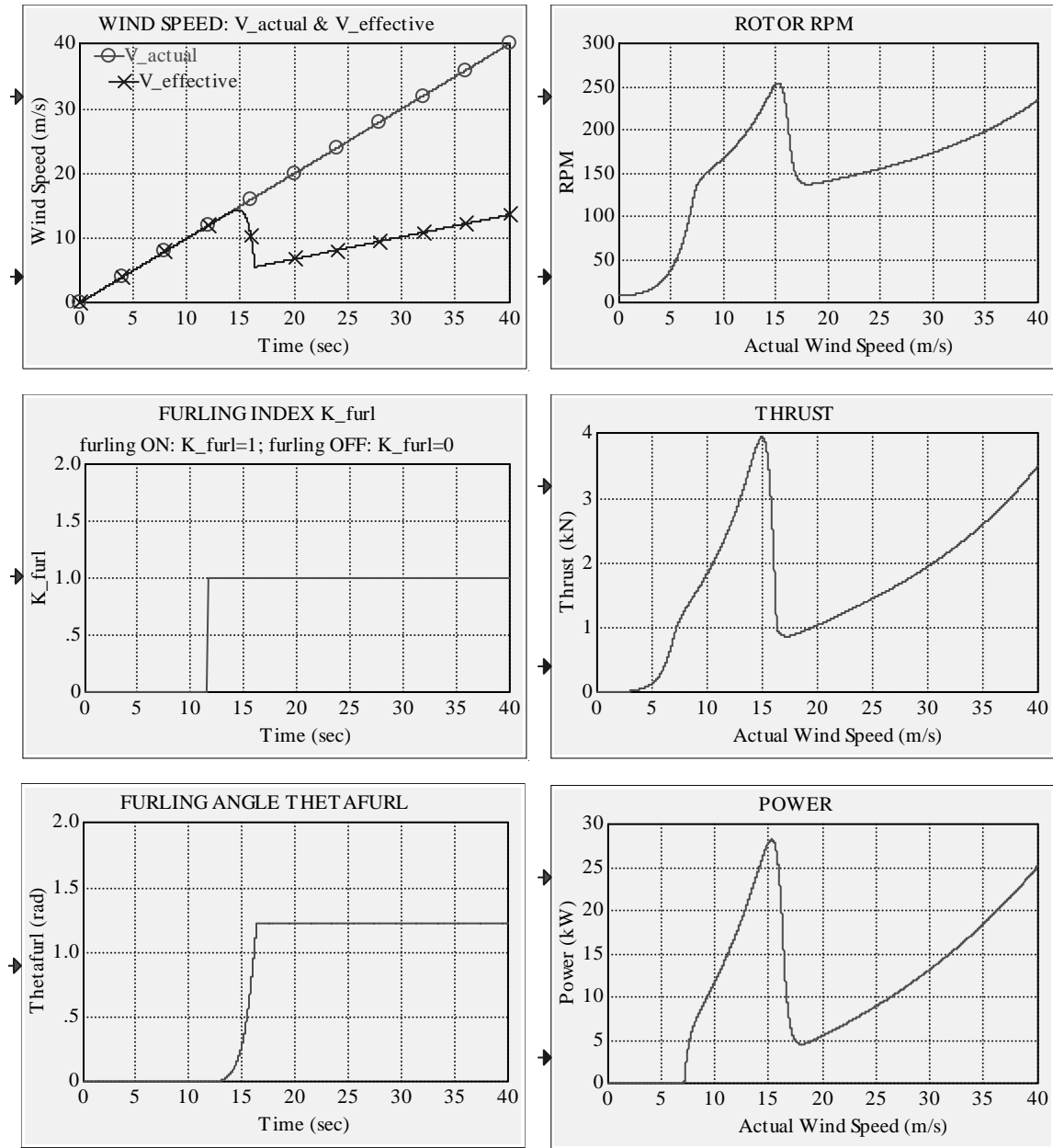
Figure 10.29. Response of the wind generator to a ramp wind caused by furling
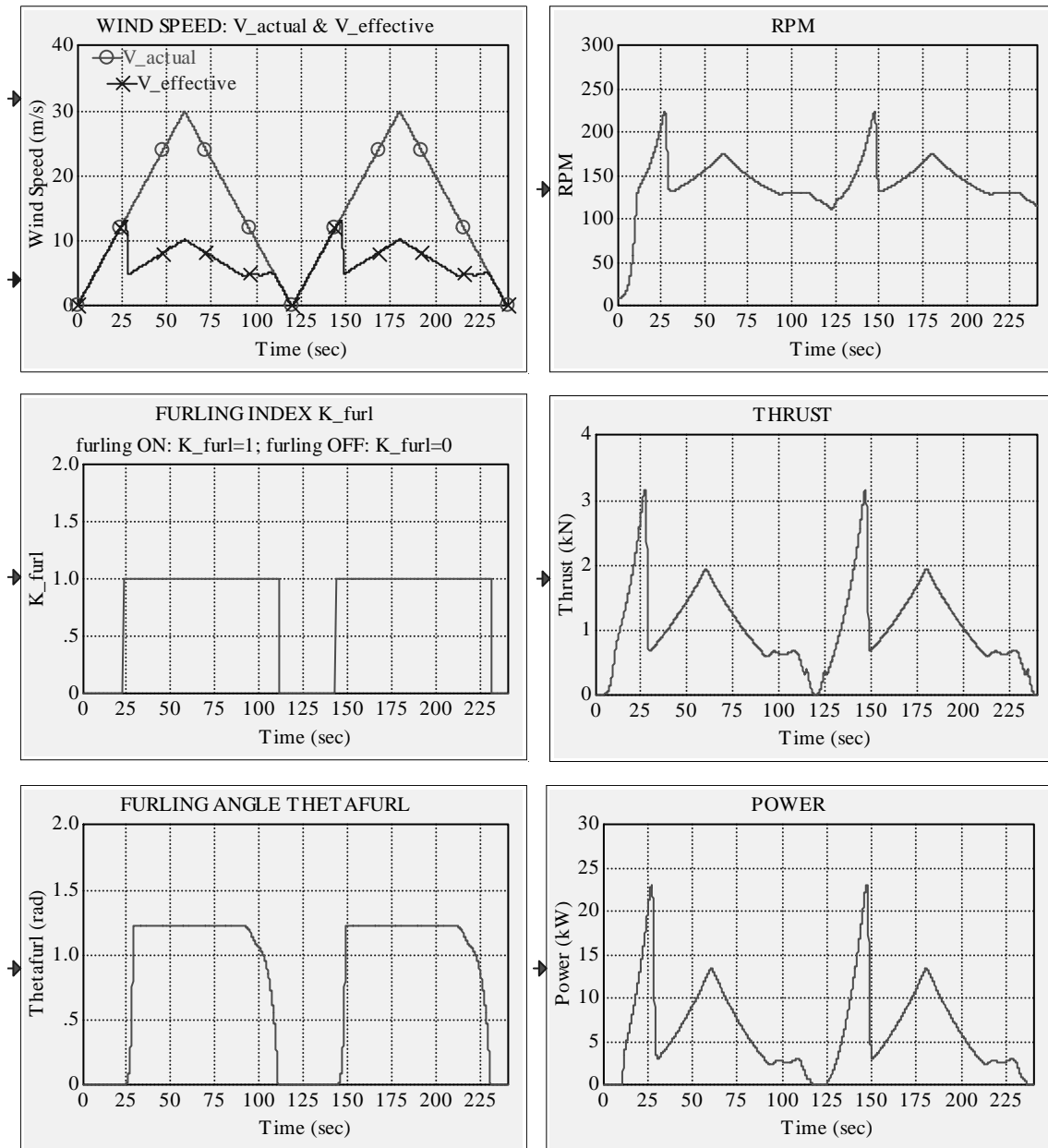
**Figure 10-30. Furling operation in response to a simulated
ramp-up-ramp-down wind**

However, we do not want this effect to be too strong, which may lead to a decrease in the
power captured. Adding the damping to the furling system dynamics, we should consider
a trade-off between maximizing the wind power capture and minimizing the fatigue
damage effects that result from the bang-bang operation.

We simulated the operation of the system in a turbulent wind with no damping added. We
show in Figure 10-32 the performance that results from a furling mechanism. A strong

bang-bang operation can be noticed. This performance, as illustrated in Figures 10-33 and 10-34, can be significantly improved by the addition of damping.
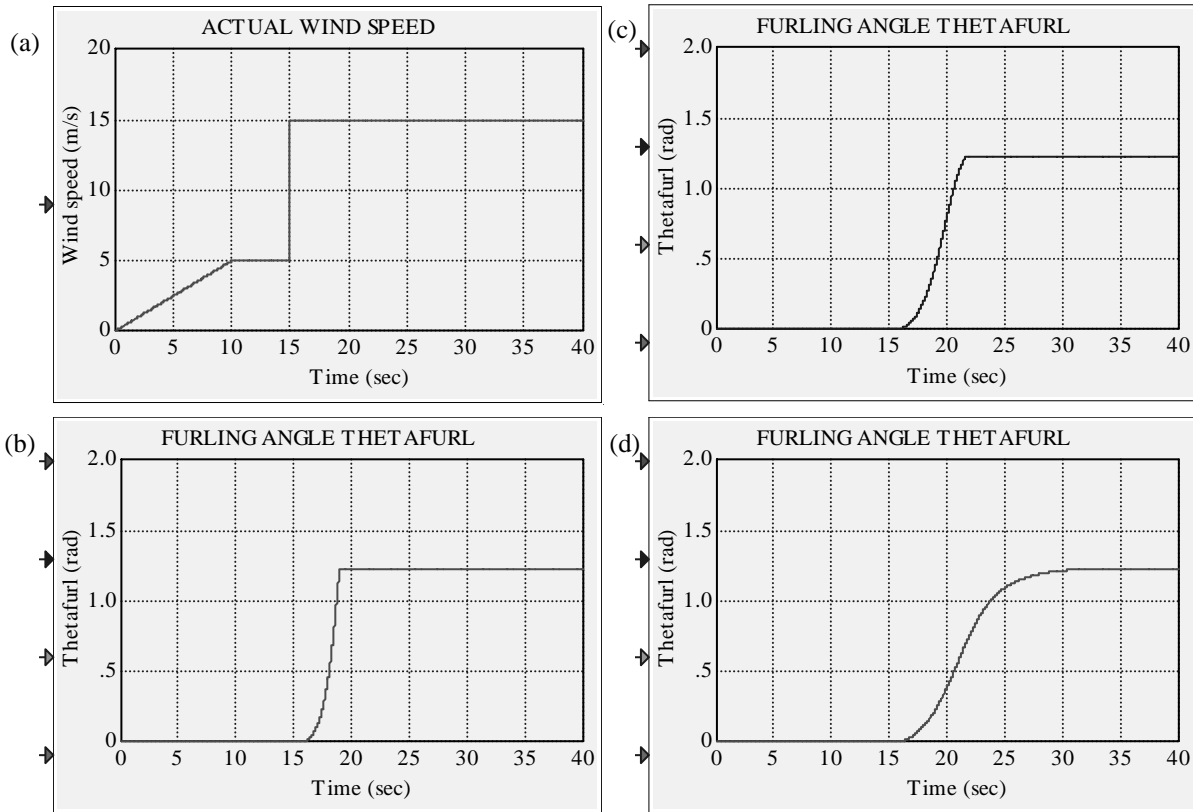
Figure 10-31. Responses of the furl angle to a step change of the wind speed: (a) simulated wind speed, (b) no additional damping, (c) some additional damping, and (d) significanta dditional damping

Battery Charging System with Peak Power Tracker

In the normal wind speed region, the wind turbine is controlled to produce maximum power P_{max}, which is achieved for $C_{p\,max}$ at TSR_{max}. Substituting V from equation (10-2) into equation (10-1), we obtain:

$$P_{max} = 0.5\rho A C_{p\,max}(R/TSR_{max})^3 \omega^3 .$$

The rotor angular velocity ω (equivalent to the rpm of the rotor) is the only variable in this equation. Thus, the generated power is proportional to the rpm cubed.

Such operation takes place as long as the wind direction is normal to the rotor plane, or we can say that the wind speed V has only the normal component ($V_n = V$).

The Peak Power Tracker (PPT) uses the current value of P_{max} (corresponding to the current value of rpm) as a reference and compares this value to the AC power provided

by the wind turbine generator. The power error is driven to zero by a PI controller, which at its output generates the required gain K_{DC} of the voltage rectifier. Because the DC bus voltage V_B is constant, the gain K_{DC} controls the phase voltage of the synchronous generator V_{ph}. This relationship is given by the following equation:

$$V_{ph} = \frac{\pi V_B}{3\sqrt{6}} K_{DC}$$
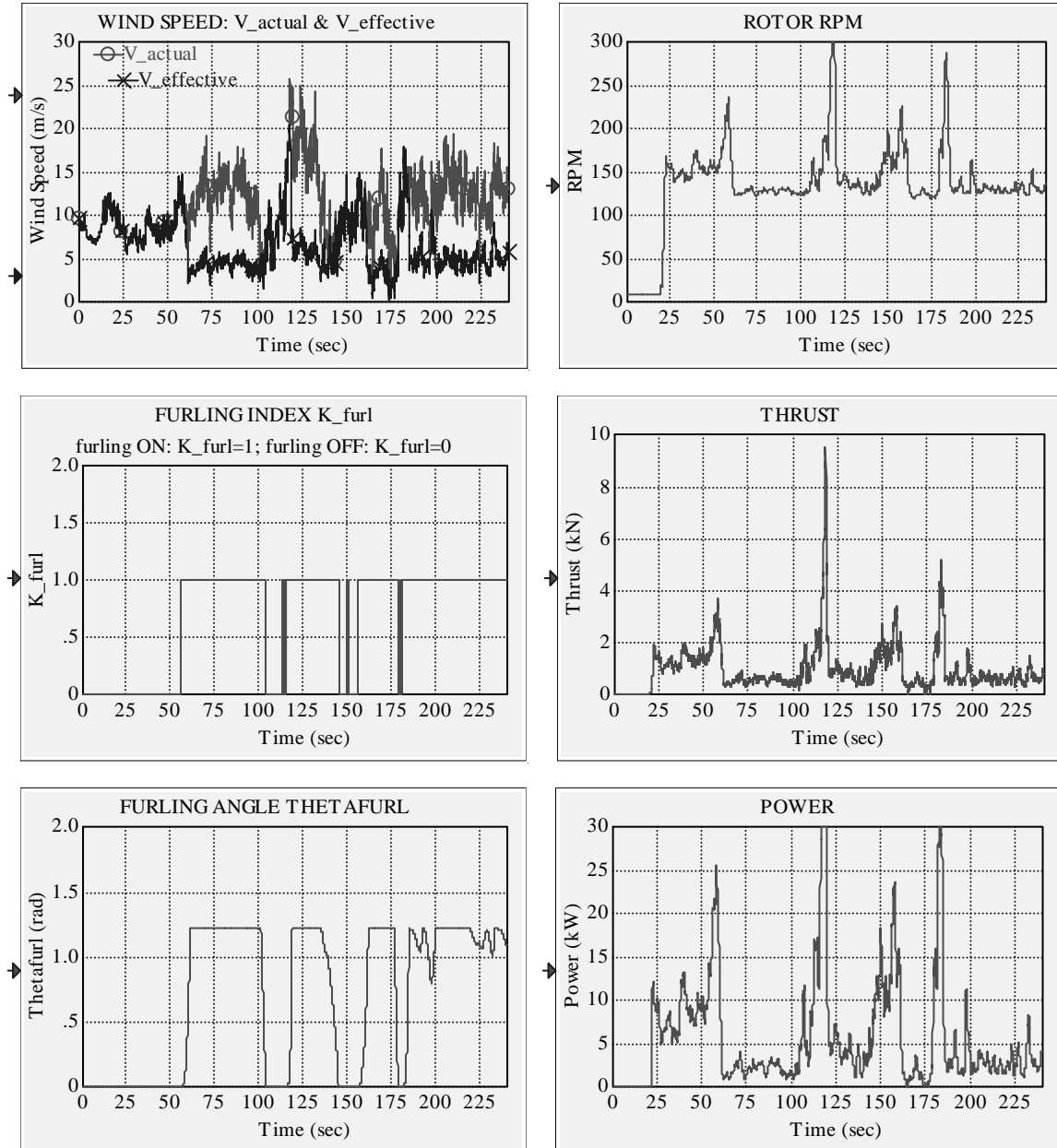
Figure 10-32. Effects of furling control in turbulent wind and with no additional damping

To turn the PPT off, we set $K_{DC} = 1$. Figure 10-35 illustrates the operation of the battery charging system with the PPT off and Figure 10-36 shows the transients of the same system variables when the PPT is operating. For both experiments we used the same simulated linear wind speed profile. We can easily see that the results are as expected.
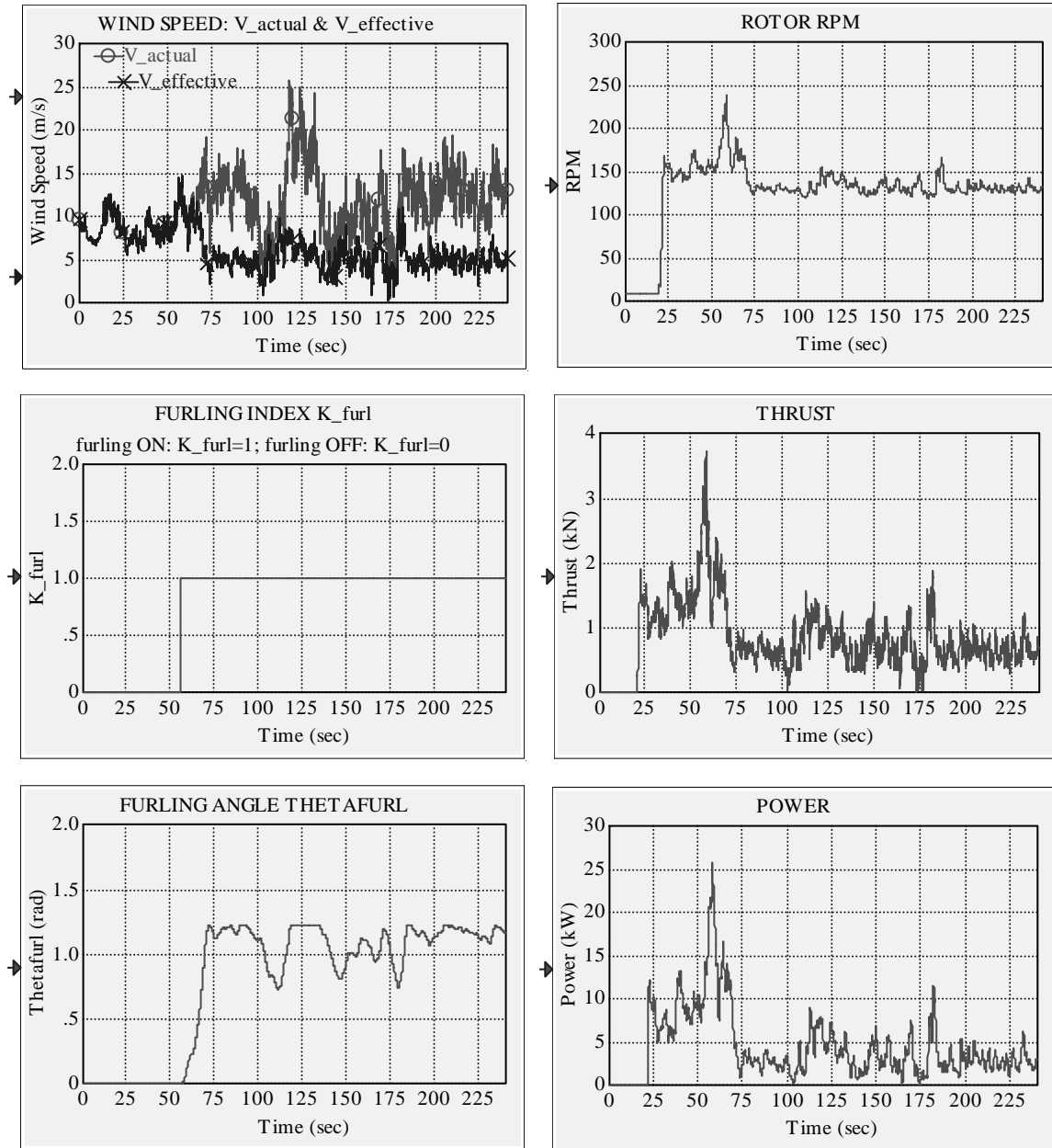

Figure 10-33. Effects of furling control in turbulent wind and with some additional damping
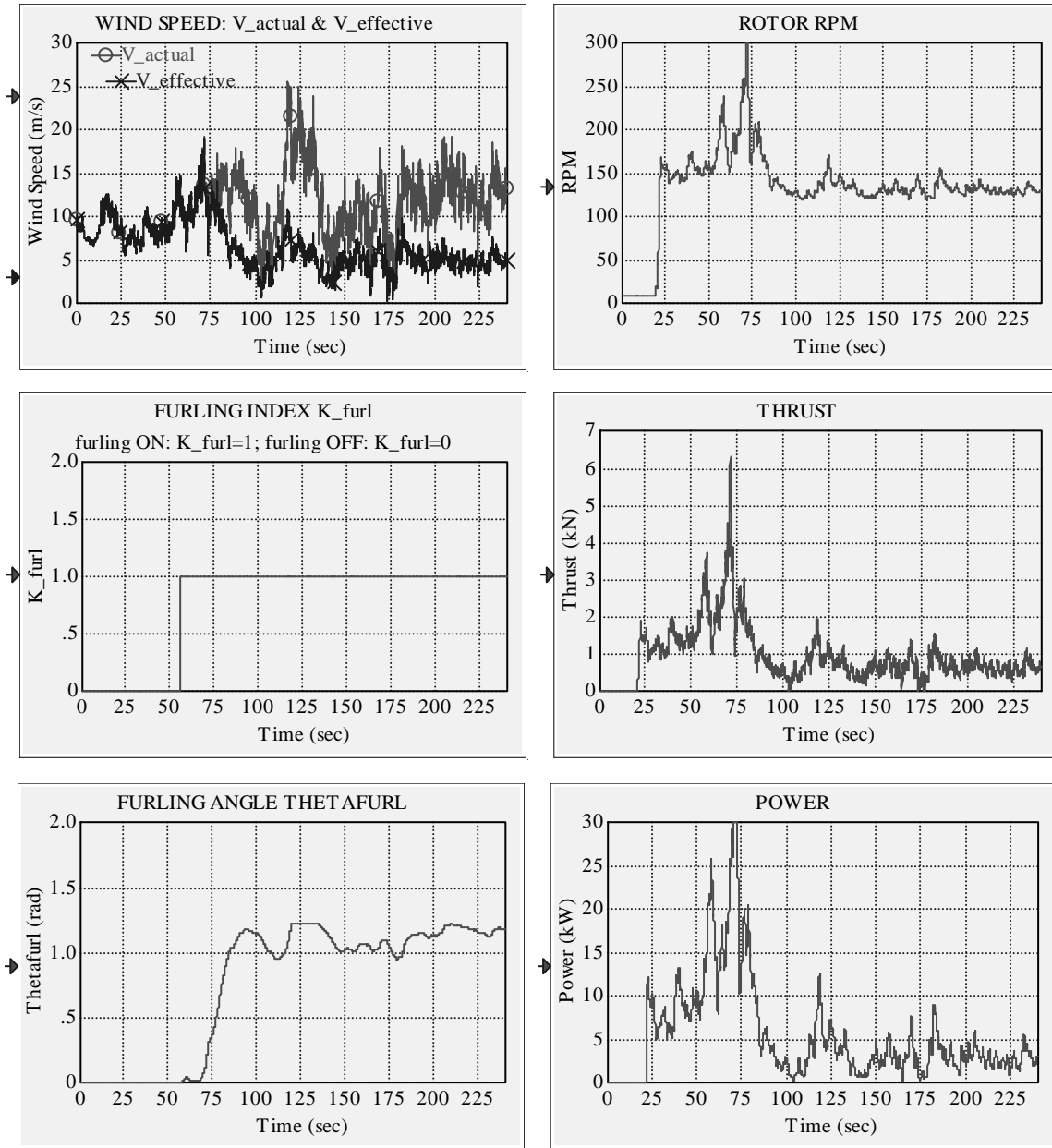
Figure 10-34. Effects of furling control in turbulent wind and with significant additional damping
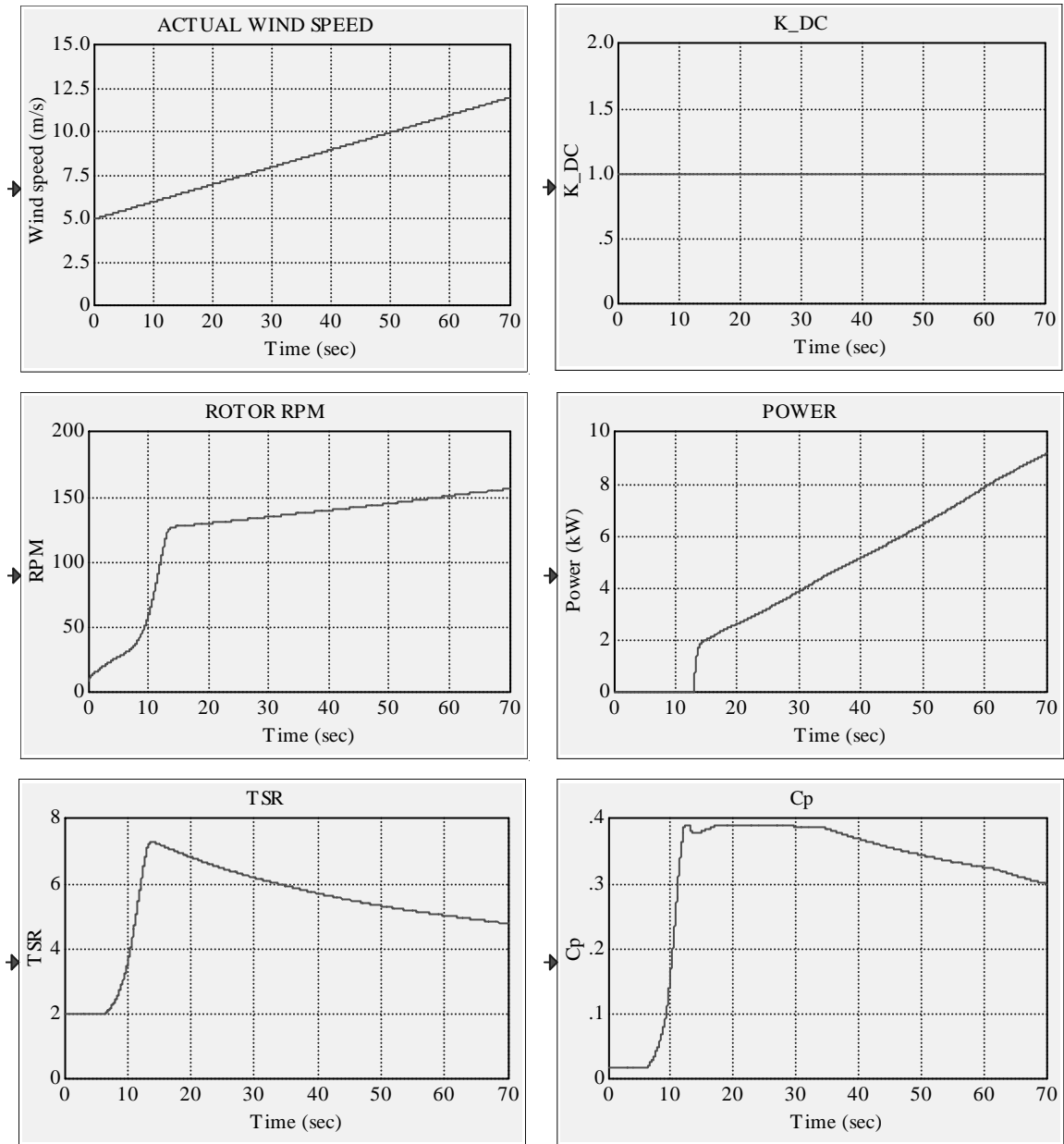
Figure 10-35. Transients of system variables illustrating operation of a battery-charging system without the PPT
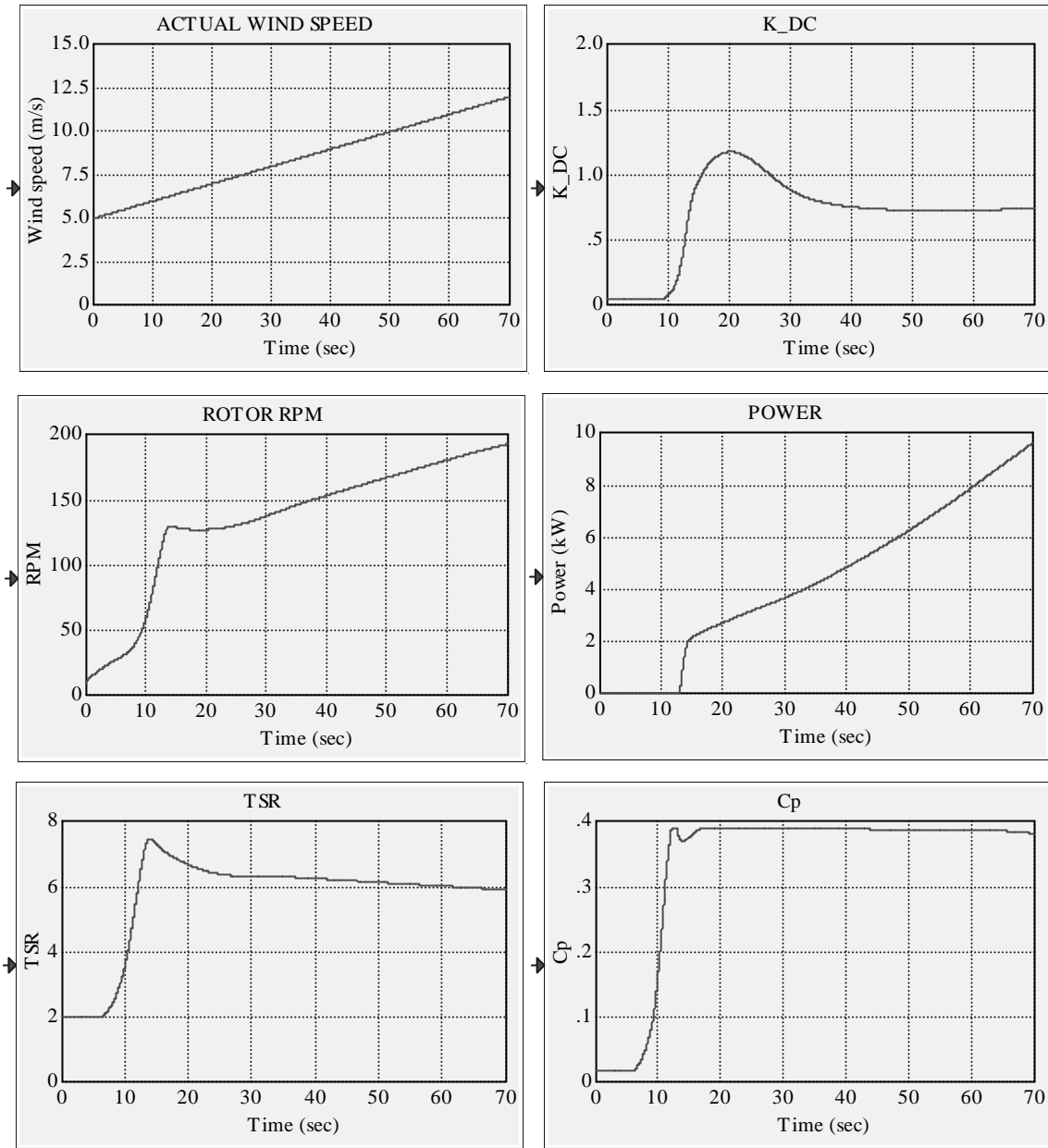
Figure 10-36. Transients of system variables illustrating operation of a battery-charging system with the PPT

Case Study 9.1: Wind Turbine with Furling Control Connected to the Utility through Rectifier, DC/DC Converter, and Inverter

In this case study, we use our standard model of a small wind turbine with a synchronous generator and with furling control. It is connected to the utility through an inverter, which operates in a slave mode. A diesel generator controls the frequency and voltage of the utility. The utility load (village load) is set to be constant. The system considered, shown in Figure 10-37, is modeled using standard RPM-SIM blocks. The inverter is programmed to operate in the slave mode. In this system, we want to maximize the real

power P_{inv} provided by the wind turbine generator to the utility. Therefore, we set reference reactive power Q_{ref} to zero and we replace the reference real power of the inverter P_{ref} by choosing a proper set point V_{DCref}. We compare this value with v_{DC}, the input voltage to the inverter. As shown in Figure 10-38, the difference $v_{DC} - V_{DCref}$ controls the q-component i_{qINVs} of the current contributed to the utility by the inverter. This is the only modification of the standard RPM-SIM inverter model.
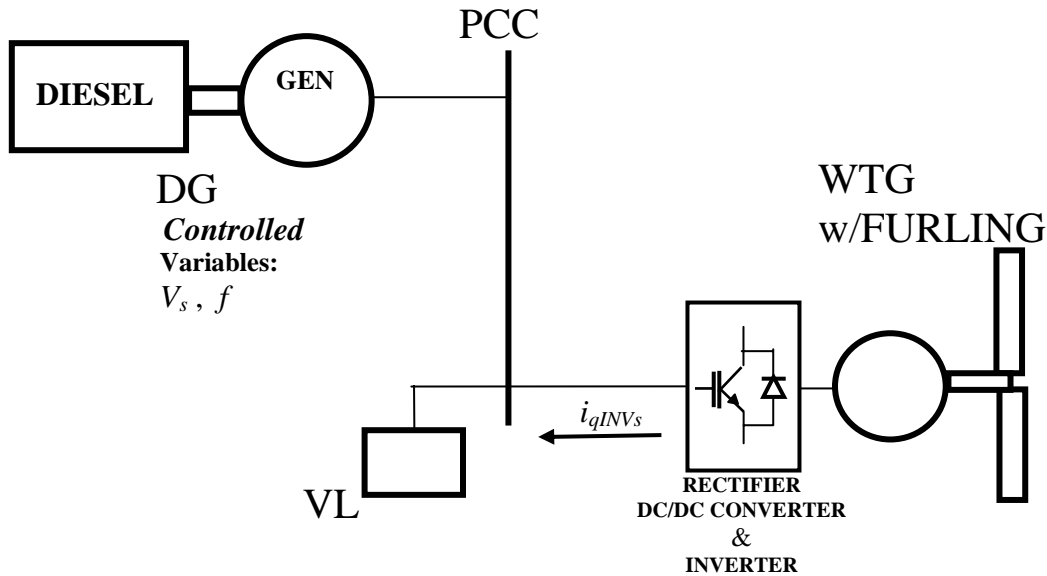

Figure 10-37. The wind turbine generator with furling connected to the utility
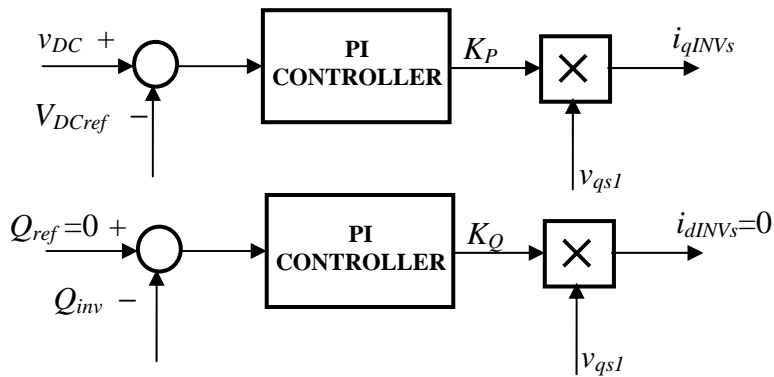

Figure 10-38. Inverter power control

As a guideline, we can choose V_{DCref} to be approximately 30% lower than the output no-load rectifier voltage E_{DC}, calculated as follows:

$$E_{DC} = 1.35\sqrt{3}E_S ,$$

where E_S is the no-load AC output voltage of the synchronous generator. Such a choice is made to ensure maximum power transfer from the wind turbine generator to the utility to minimize the power, which under given load conditions must be provided by the diesel generator.

The circuit diagram, which explains the connection between the rectifier and the inverter, is shown in Figure 10-39. In this circuit, we included a DC/DC converter represented by the gain K_{DC} related directly to the duty ratio D. The DC/DC converter enables peak power tracking. This DC/DC power converter may be

- A buck or step-down converter with $K_{DC} > 1$ and $D = 1/K_{DC}$
- A boost or step-up converter with $0 < K_{DC} < 1$ and $D = 1 - K_{DC}$
- A buck-boost converter with $0 < K_{DC} < 5$ and $D = 1/(K_{DC} + 1)$.

In the system modeled and simulated, we used a buck-boost converter.
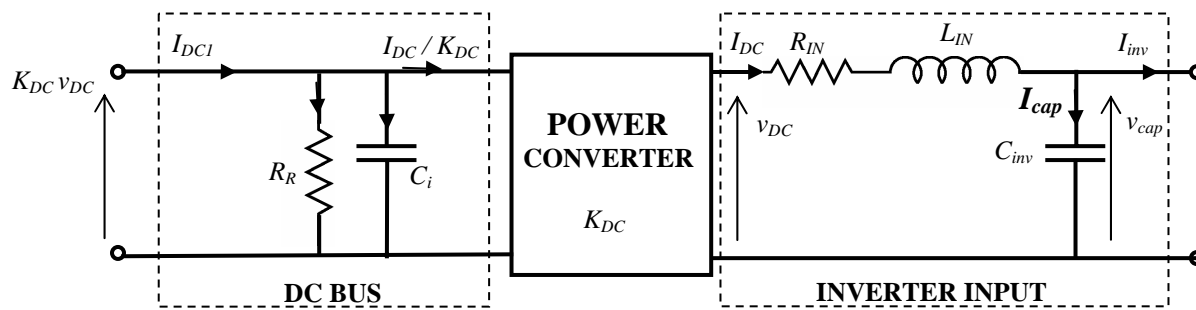
Figure 10-39. Circuit diagram of the connection between the rectifier and the inverter

The output AC power of the wind turbine generator is expressed as

$$P_{AC} = 3V_{ph}I_S$$

with

$$V_{ph} = \frac{\pi}{3\sqrt{6}} K_{DC} v_{DCref}.$$

Then, using the notation introduced in Figure 10-39, the following equations lead to the determination of the inverter current I_{inv}:

$$I_{DC1} = \frac{P_{AC}}{K_{DC} v_{DC}}$$

$$v_{DC} K_{DC} = \frac{1}{C_i} \int \left(I_{DC1} - \frac{K_{DC} v_{DC}}{R_R} - \frac{I_{DC}}{K_{DC}} \right) dt$$

$$v_{cap} = \int (I_{DC} - I_{inv}) dt$$

$$I_{inv} = \frac{P_{inv}}{v_{cap}}$$

Requesting the equality of the inverter's input power and the power provided to the utility, we keep the v_{DC} voltage constant. In Figure 10-39, the capacitor C_i is used to define the voltage $K_{DC} v_{DC}$ and the resistor R_R represents power electronics losses. The PPT operates as described above. We set $K_{DC} = 1$ if operation without the PPT is required.

We considered the operation of the system in a turbulent wind without additional furling damping and without the PPT. Figures 10-40 and 10-41 illustrate the results of the simulation. Figure 10-40 shows the transients for the wind turbine generator side. Figure 10-41 shows the line voltage and the relative frequency controlled by the diesel generator, illustrates the real power balance, and shows the transients for the inverter input (v_{DC} and I_{DC}) and output (i_{qINVs} and P_{inv}). We can clearly see that when the furling mechanism is activated, the diesel generator makes up for the power deficiency.

To see the difference between the operation without and with the PPT, we ran two simulations for the same linearly increasing wind speed but not reaching the value, at which the furling takes place. The results are shown in Figures 10-42 and 10.43. We can see that the results are as expected.

Case Study 9.2: Wind Turbine with Furling Control Connected to the Utility through Rectifier and Inverter

This case study is a modification of the Case Study 9.1, in which we eliminated the DC/DC converter and with this exception it is represented by Figures 10-37 and 10-38. For the purpose of this study, we assume that at all times the wind turbine is capable of delivering the peak power $P_{ref} = P_{max}$, where

$$P_{max} = 0.5 \rho A C_{p\,max} (R/TSR_{max})^3 \omega^3 .$$

The rotor angular velocity ω (or equivalently the rpm of the rotor) is the only variable in this equation. Thus, the generated power is proportional to the rpm cubed.

In addition, we neglect the synchronous generator losses and dynamics, and we assume ideal AC to DC conversion; i.e.,

$$P_{AC} = P_{SHAFT} = P_{ref} ,$$

where P_{AC} is electrical power and P_{SHAFT} is mechanical power.

As a guideline, we can choose V_{DCref} to be equivalent to the rectified line voltage, calculated as follows:

$$V_{DCref} = 1.35\sqrt{3}E_S ,$$

where E_S is the no-load per-phase root mean square AC output voltage of the synchronous generator. Thus, for example, if the line-to-line voltage at the utility grid is 220 V, $V_{DCref} = 1.35 \times 220$ V $= 297$ V.

The line-side (utility) Power Converter is controlled as such to give a unity power factor and to keep the balance of power at the DC bus (i.e., input power = output power). To give a unity power factor, the current is controlled to be in phase with the voltage by forcing the reactive power to be zero. To keep the power at the DC bus balanced, the dc bus voltage is a good variable to use because a rise in DC voltage shows that there is a net positive power accumulated in the DC capacitor. Likewise a fall in DC voltage shows a net negative power accumulation in the capacitor.

The circuit diagram, which explains the connection between the rectifier and the inverter, is shown in Figure 10-44. Using the notation introduced in Figure 10-44, the following equations lead to the determination of the inverter current I_{inv}:

$$I_{DC1} = \frac{P_{AC}}{v_{DC}}$$

$$v_{DC} = \frac{1}{C_i} \int \left(I_{DC1} - \frac{v_{DC}}{R_R} - I_{DC} \right) dt$$

$$v_{cap} = \int (I_{DC} - I_{inv}) dt$$

$$I_{inv} = \frac{P_{inv}}{v_{cap}}$$

Requesting the equality of the inverter's input power and the power provided to the utility, we keep the v_{DC} voltage constant. In Figure 10-44, the capacitor C_i is used to define the voltage v_{DC} and the resistor R_R represents power electronics losses.

The wind turbine generator model includes the furling and the drivetrain dynamics.

The results of simulation are shown in Figures 10-45, 10-46, and 10-47. Figure 10-45 shows the transients for the wind turbine generator side. Figure 10-46 illustrates the effect of peak power tracking. Finally, Figure 10-47 shows the line voltage and the relative frequency controlled by the diesel generator, gives the illustration of the real power balance, and shows the transients for the inverter input (v_{DC} and I_{DC}) and output (i_{qINVs}

and P_{inv}). We can clearly see that when the furling mechanism is activated the diesel generator provides for the power deficiency.

Programs Available

- The results shown in Figures 10-29 to 10-36 have been obtained using the simulation program C_S9_BAT_PPT.vsm available in the subdirectory C_STDS.

- The results shown in Figures 10-40 to10-43 have been obtained using the simulation program C_S9_INV_PPT.vsm available in the subdirectory C_STDS.

- The results shown in Figures 10-45 to 10-47 have been obtained using the simulation program C_S9_INV_PPTm.vsm available in the subdirectory C_STDS.
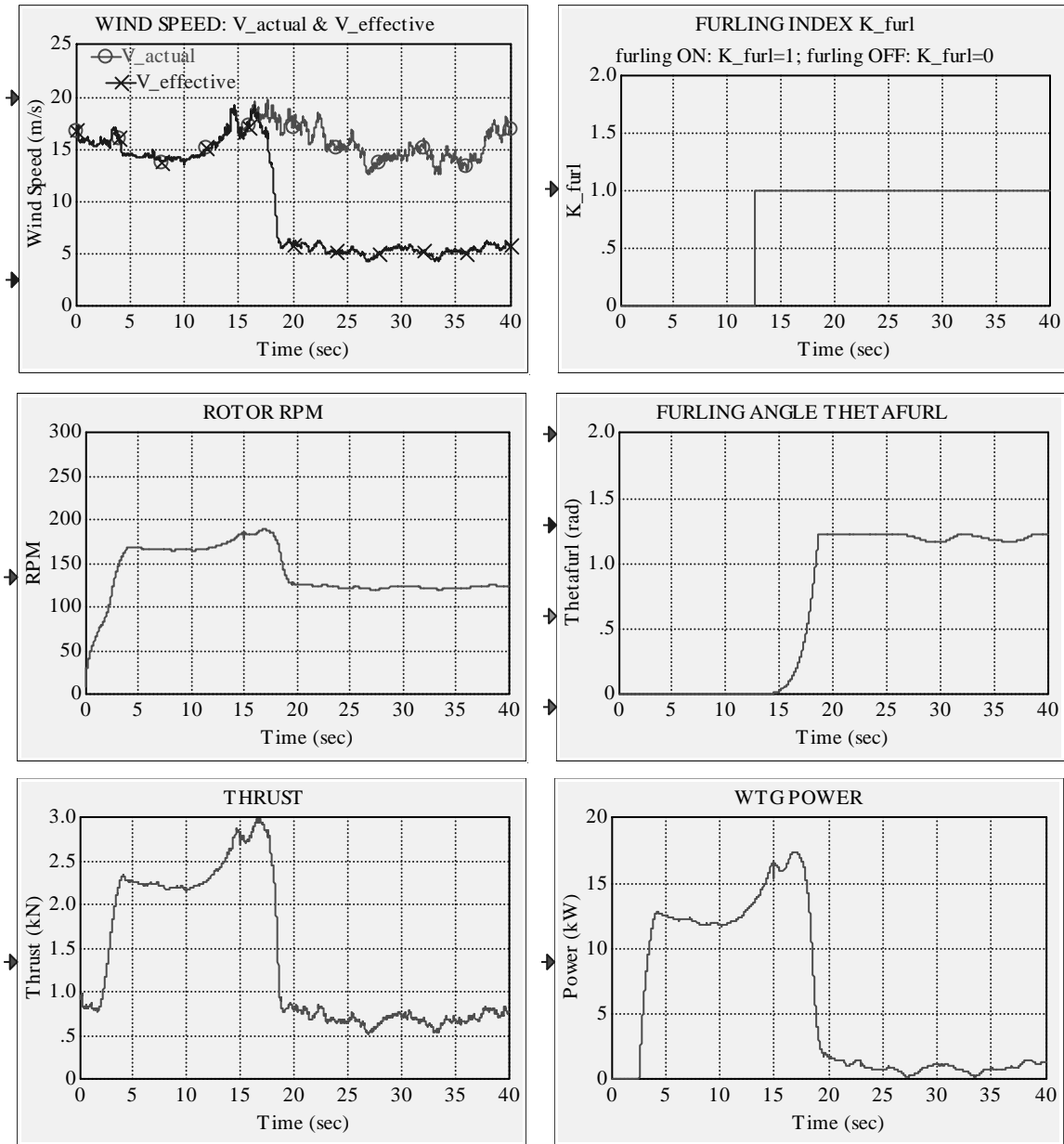
Figure 10-40. Furling effect on the wind turbine generator connected to the utility
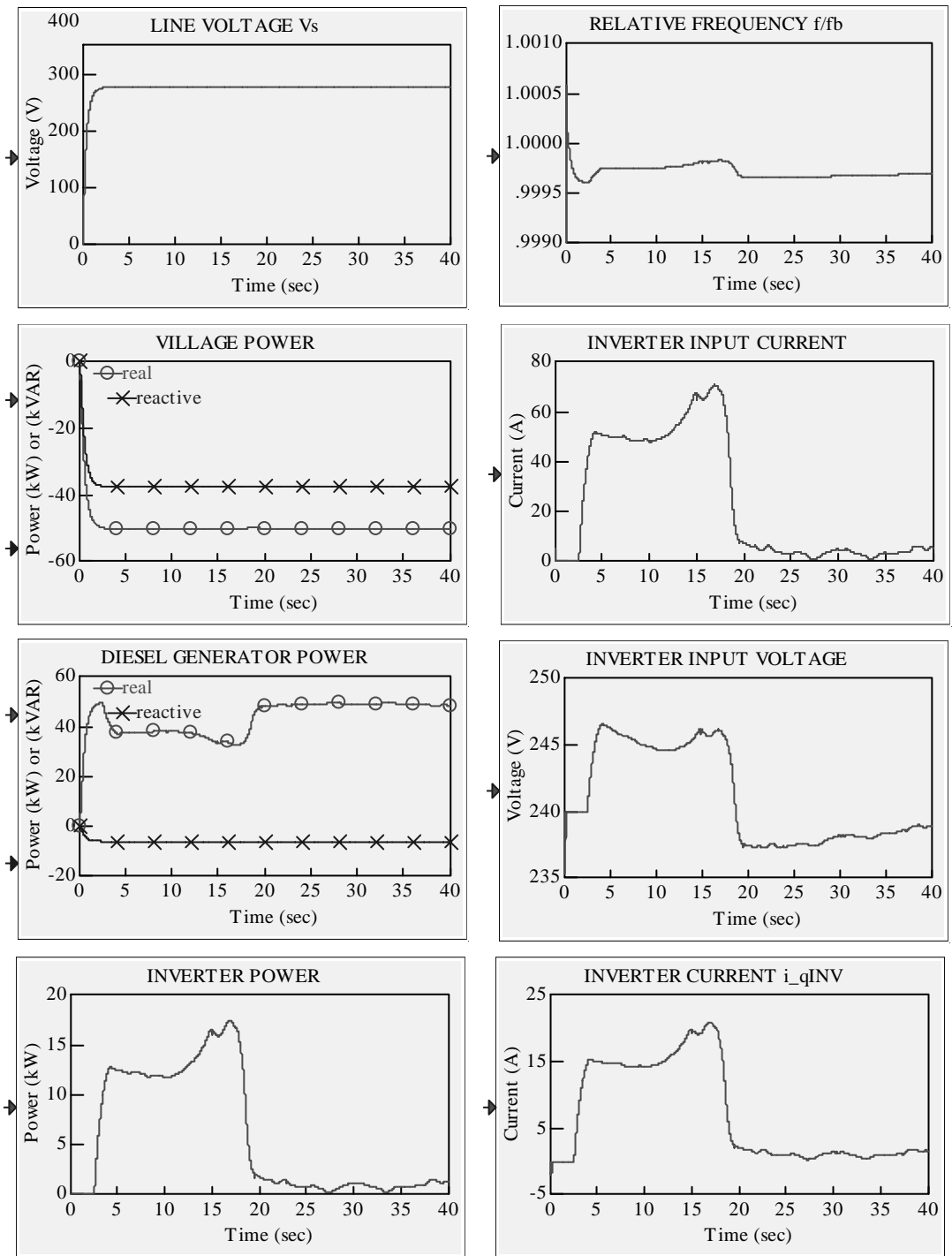
Figure 10-41. Furling effect on the energy system with two power sources: the DG and the WT generator connected to the utility through the inverter
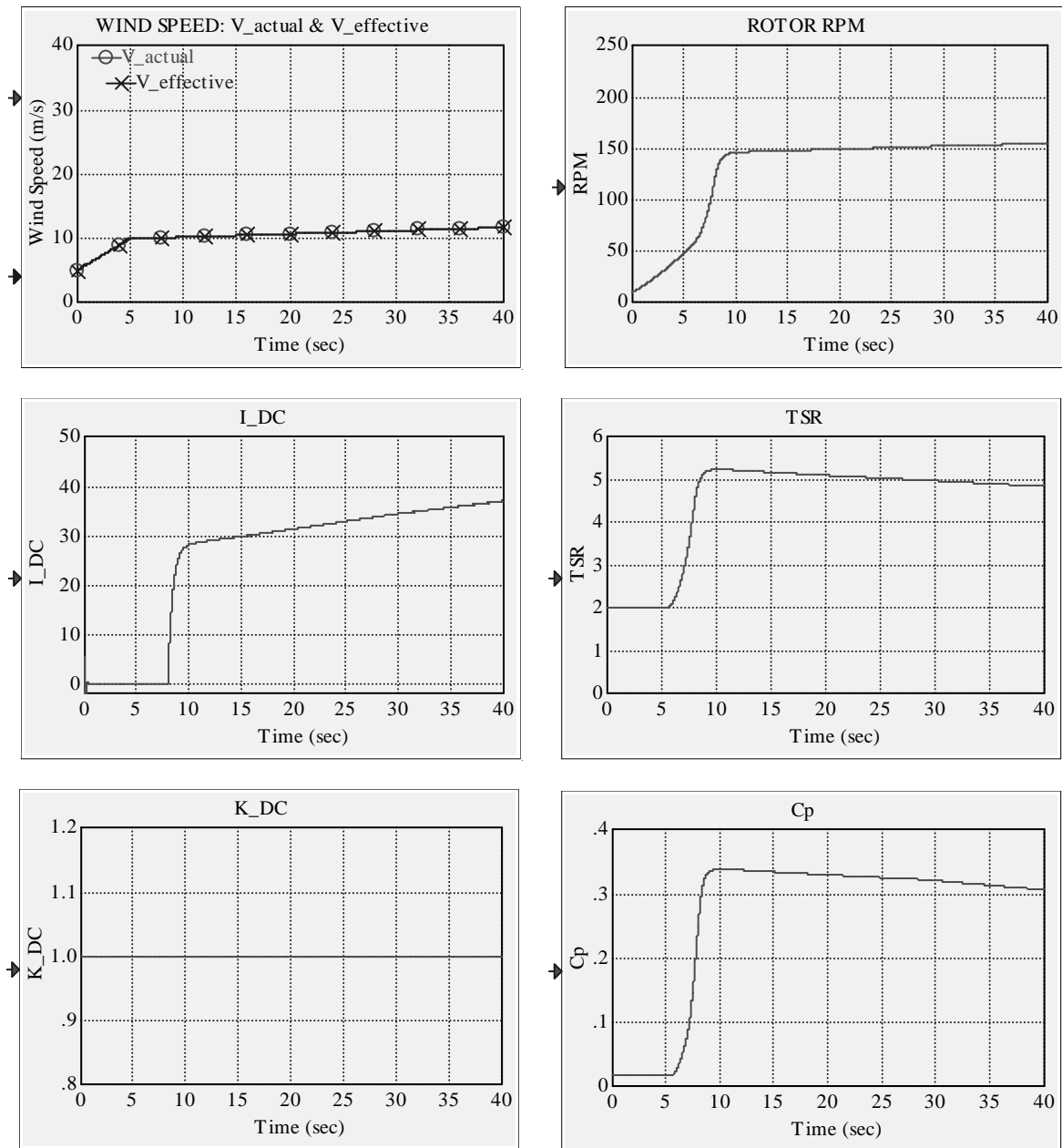
Figure 10-42. Transients of system variables illustrating operation of a utility-connected wind turbine without the PPT
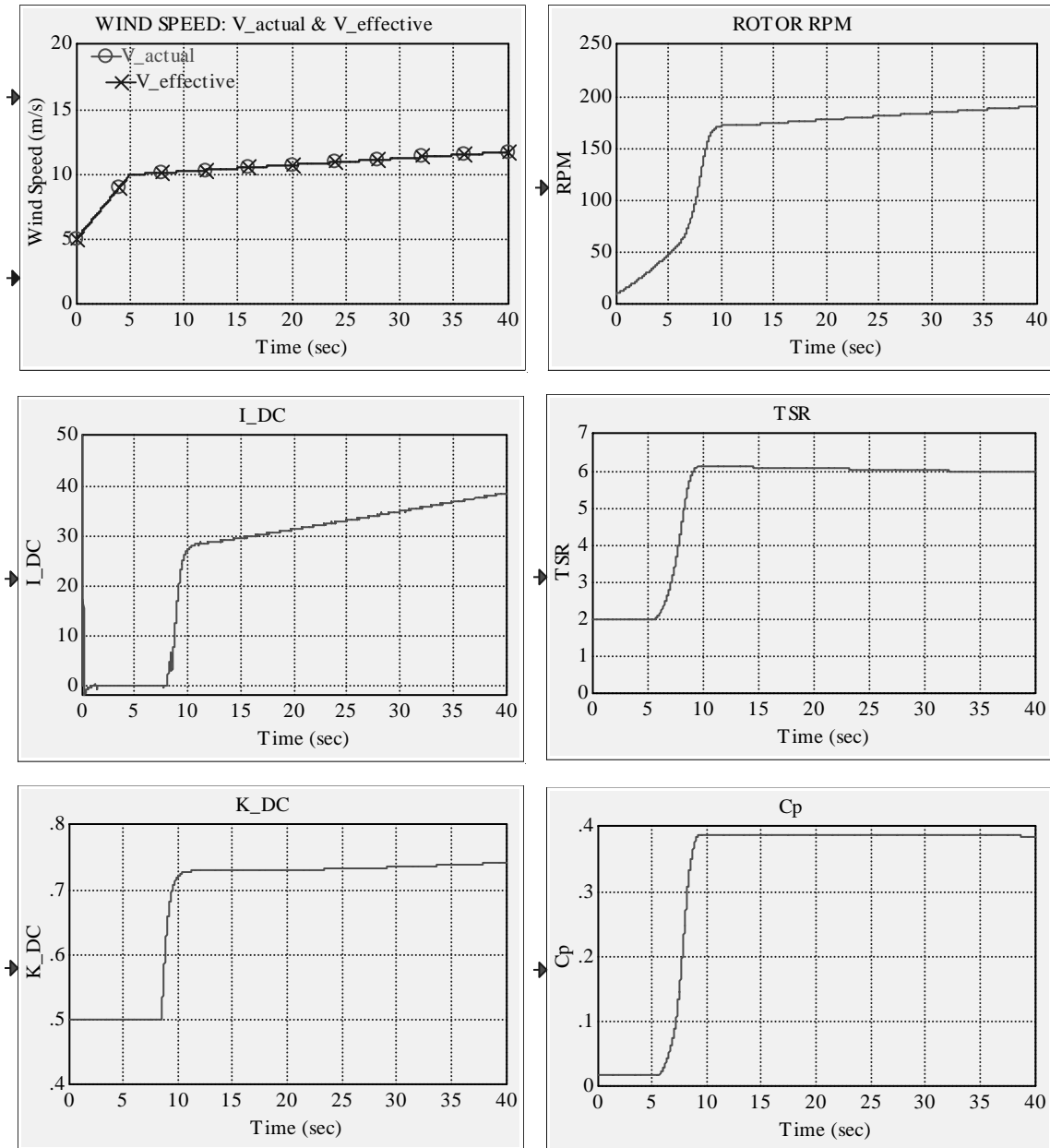
Figure 10-43. Transients of system variables illustrating operation of a utility-connected wind turbine with the PPT
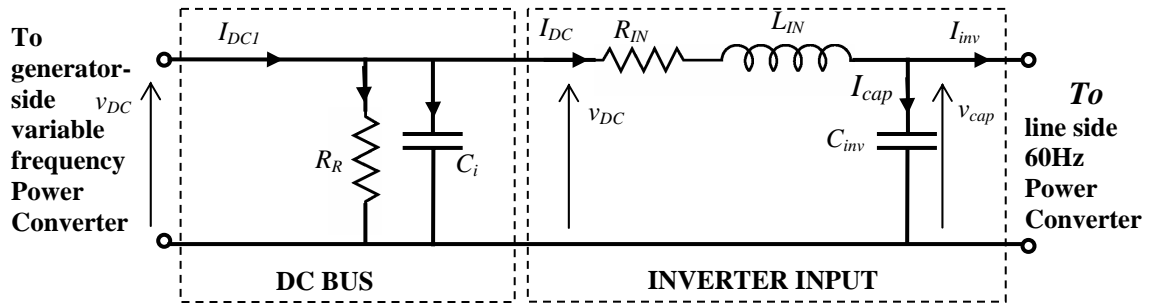
Figure 10-44. Circuit diagram of the connection between the rectifier and the inverter
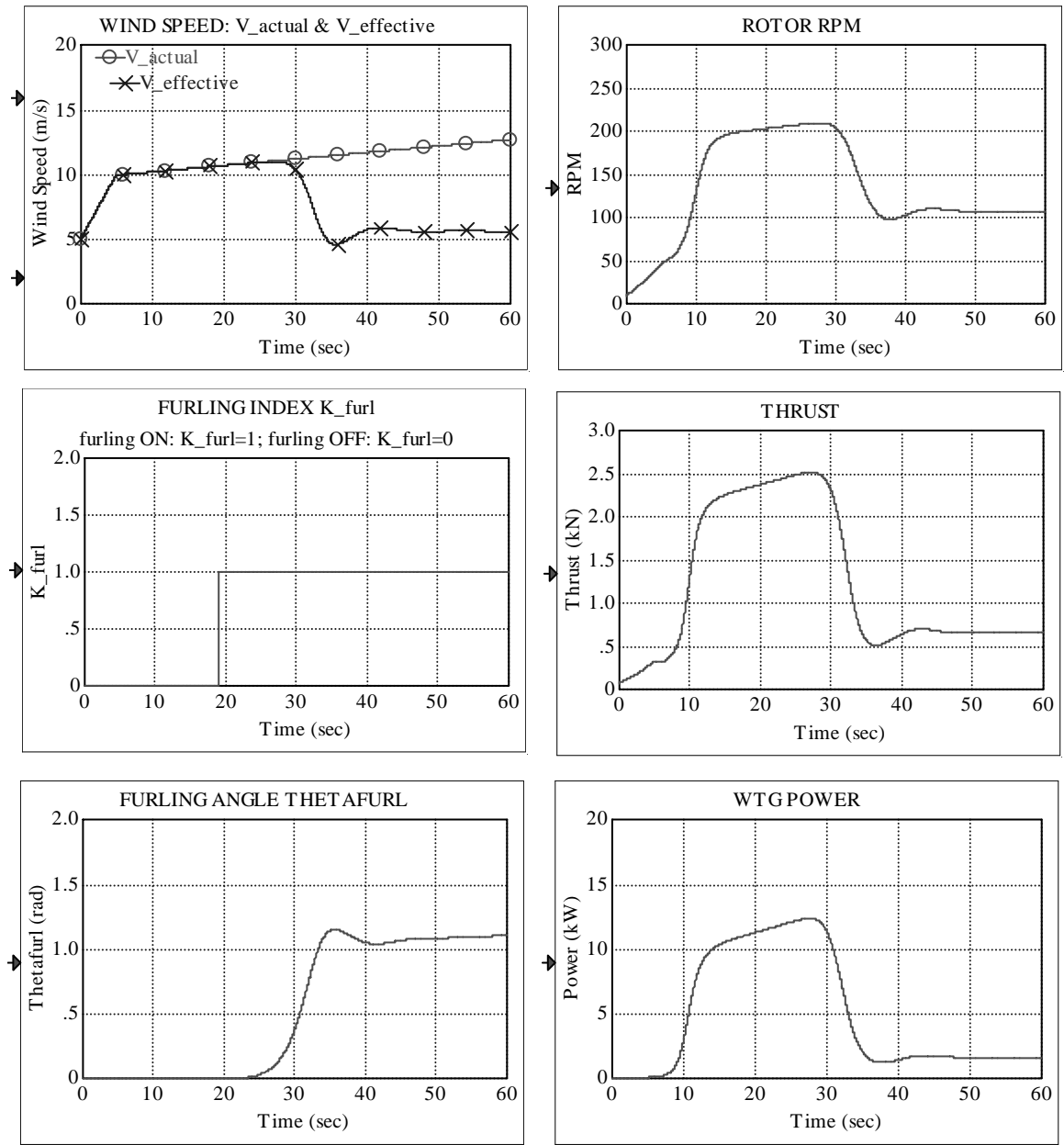
Figure 10-45. Furling effect on the WT generator
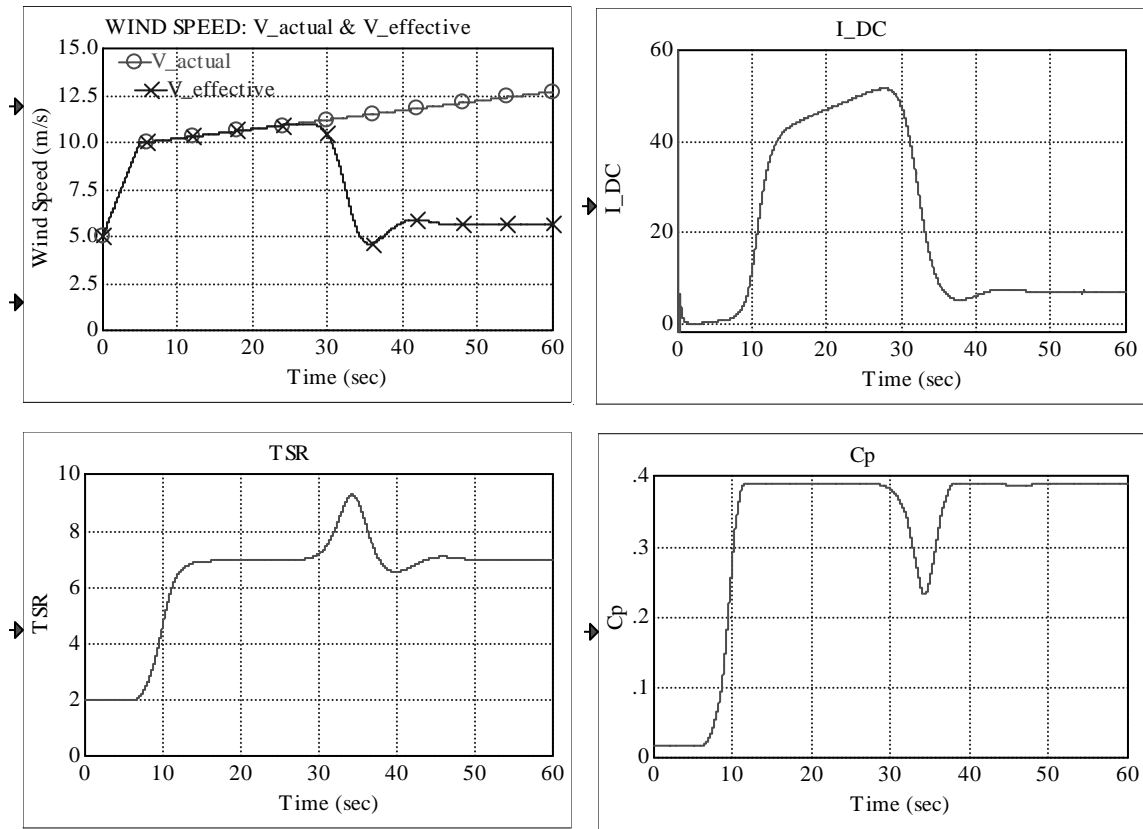
Figure 10-46. Illustration of peak power tracking
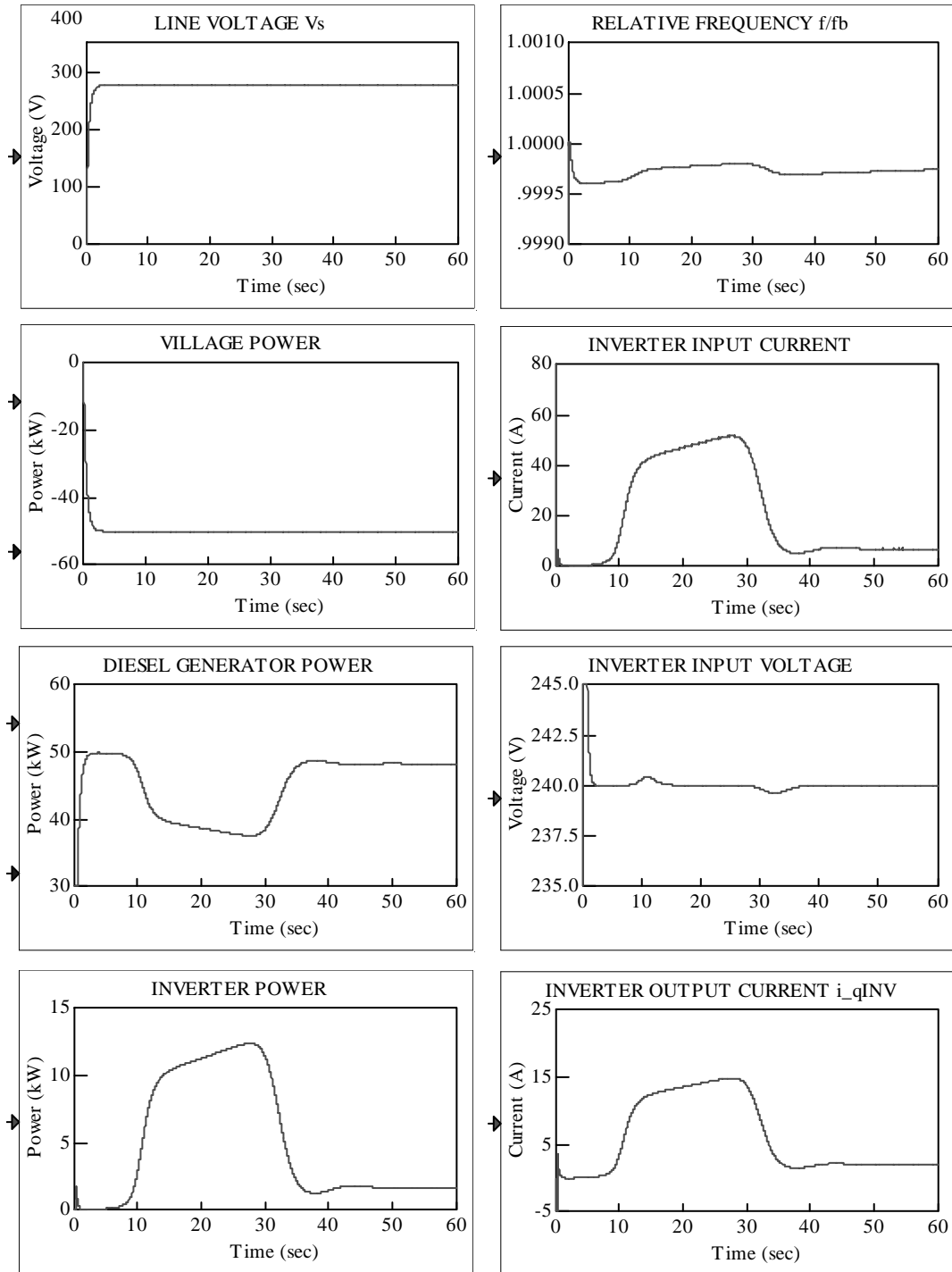
Figure 10-47. Furling effect on the energy system with two power sources: the DG and the WT generator connected to the utility

Validation Tests at the Systems Level

In this chapter, we report the results of the validation tests performed at the systems level using the data recorded from the HPTB at the National Renewable Energy Laboratory. The power system included: a DG, an AOC wind turbine (WT), a DL, and aVL. A power system with this configuration is presented in Figure 11-1, where we show both the single-line diagram and the top-view RPM-SIM simulation diagram. We were provided with data sets for five runs with the following names assigned: case A, case B, AOC start-up, step-in load, and AOC shutdown. To determine the parameters of the DG model, we used the synchronous generator Model E7201L1 data sheet found in Appendix B. These parameters (as they appear in the parameter block of the simulated model) are shown in Figure 11-2.

The data recorded over the interval of 10 sec with a sampling period of 0.01 sec included real and reactive power files for all these modules as well as the line-to-line voltage file and the frequency file. The wind speed was not measured. To use these sets of data for partial validation of the simulator, we could use only the DG block and the PCC block in the original RPM-SIM format. We had to modify the other blocks involved so that they could work with power files as their inputs. These modified blocks also have real and reactive power as their outputs, which are calculated using the voltage generated in the simulated system. Consequently, the simulated power traces closely follow the traces recorded after approximately 2 sec, which is the start-up time for the diesel generator. The traces involved are shown in the following figures:

- Figure 11-3. Simulation results for the case A data

- Figure 11-4. Simulation results for the case B data

- Figure 11-5. Simulation results for the AOC start-up data

- Figure 11-6. Simulation results for the step-in load data

- Figure 11-7. Simulation results for the AOC shutdown data.

Considering a slight oscillatory power imbalance of the recorded data (shown in each figure) and the smoothing involved in the measuring system, there is a very good agreement of the traces recorded with those obtained from the simulation.

We also validated the RPM-SIM simulator using the same data and, in addition to the real DG model, we included the model of the real DL block with the Wales Control System Dump Load Dispatch used at the HPTB. It was implemented according to the description given in Appendix C and is shown in Figure 11-8. In addition, its parameters are shown in Figure 11-9. The traces involved appear in the following figures:

- Figure 11-10. Simulation results for the case A data

- Figure 11-11. Simulation results for the AOC start-up data

- Figure 11-12. Simulation results for the step-in load data

- Figure 11-13. Simulation results for the AOC shutdown data.

We observed a good agreement of the traces recorded with those obtained from the simulation.
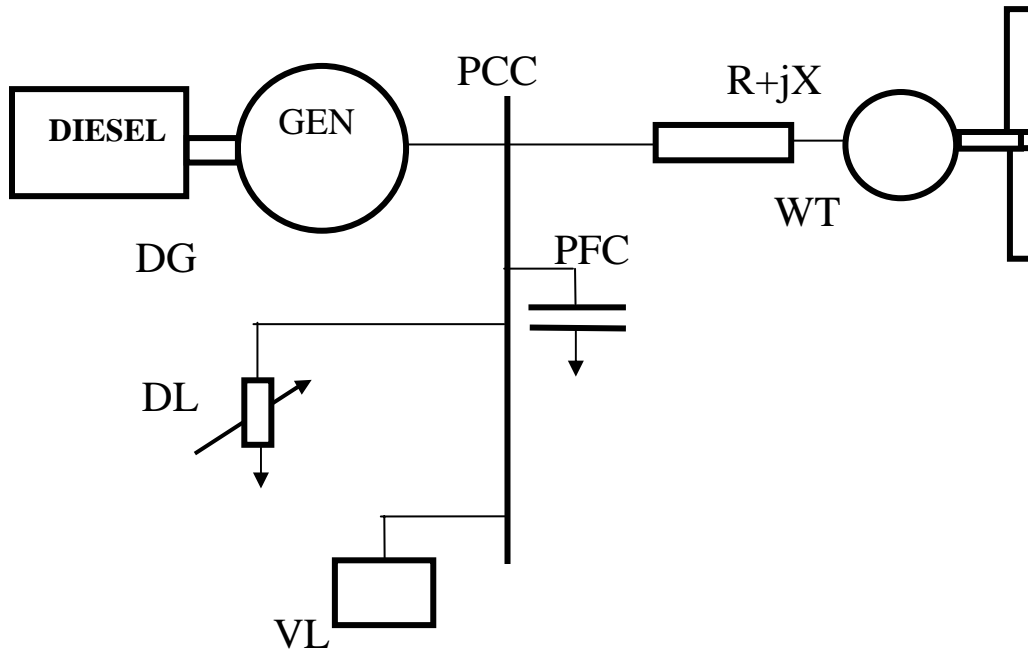
(a)
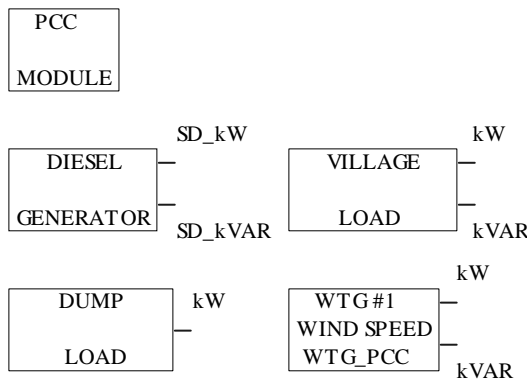
(b)

Figure 11-1. Power system composed of a DG, an AC WT, a DL, and a VL: (a) single-line diagram and (b) top view of the RPM-S<small>IM</small> simulation
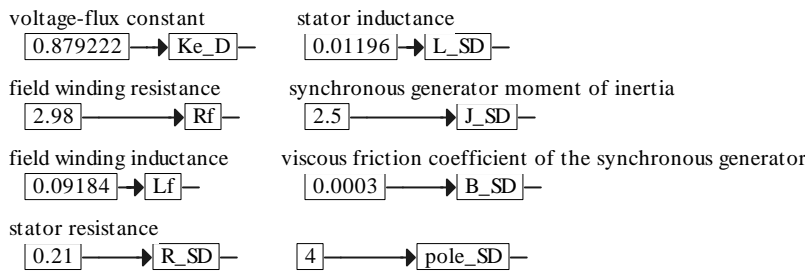
Figure 11-2. Parameters of the diesel generator
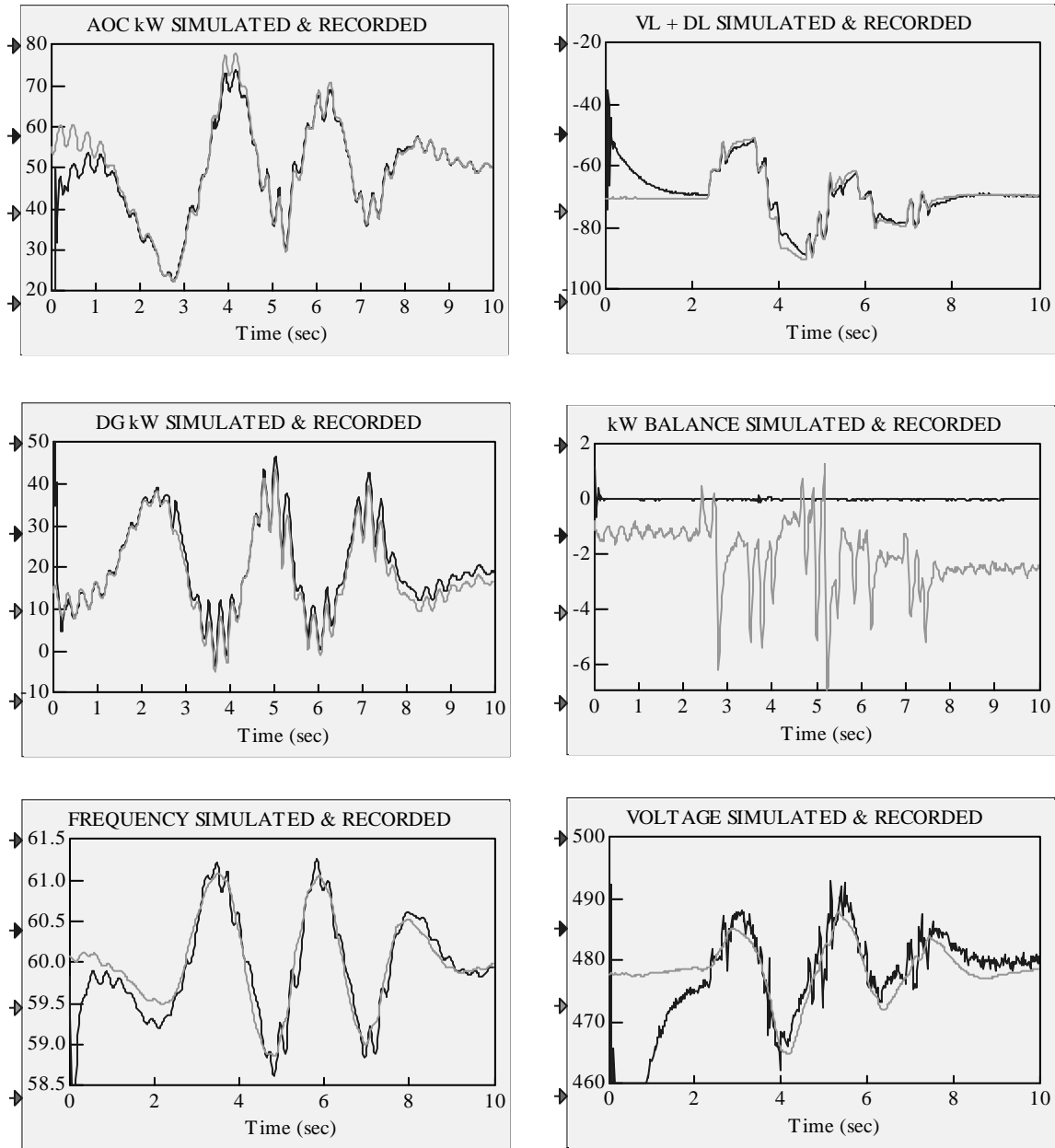
Figure 11-3. Simulation results for the case A data: the dark line is used for traces simulated and the light line is used for traces recorded
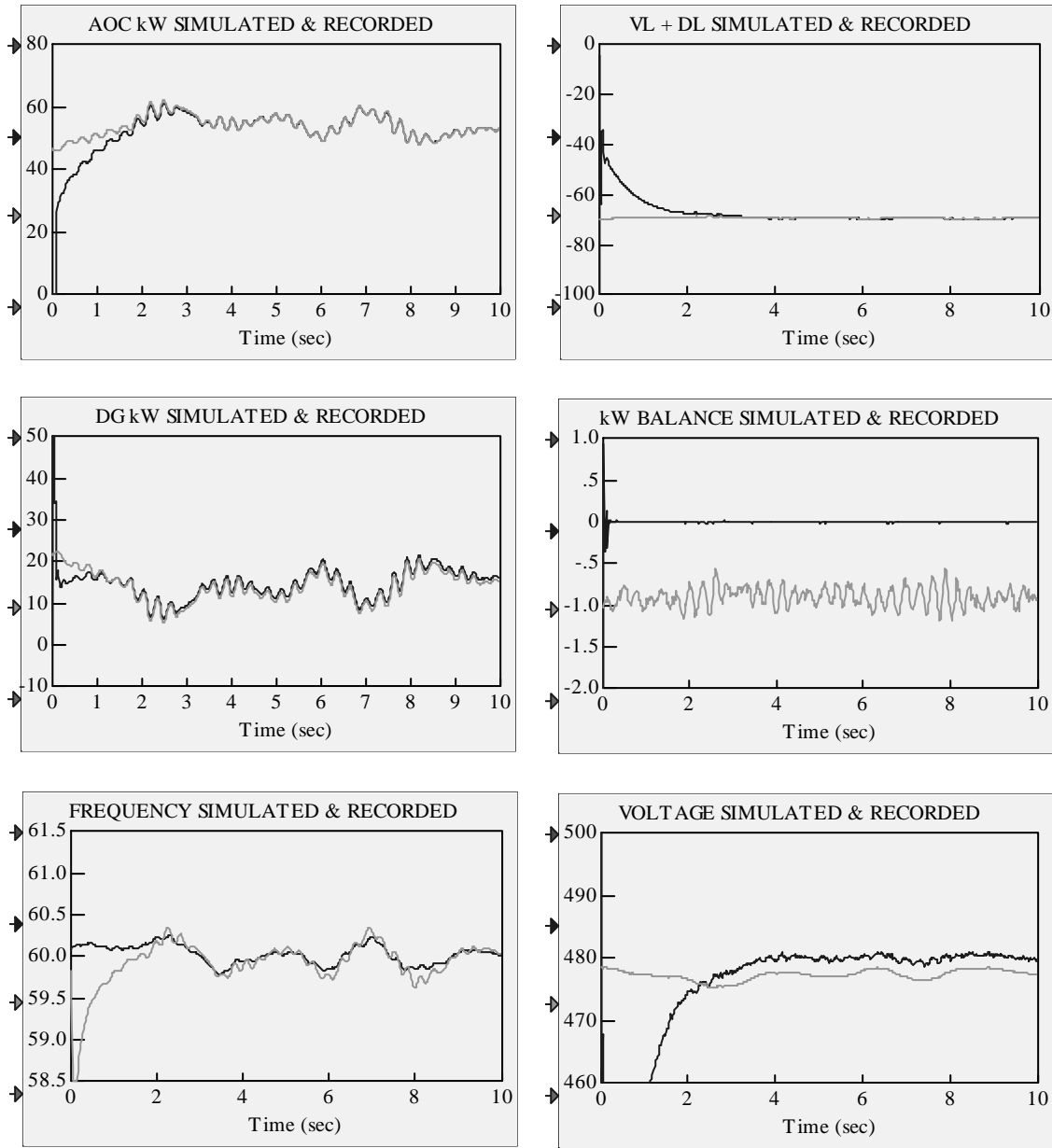
Figure 11-4. Simulation results for the case B data: the dark line is used for traces simulated and the light line is used for traces recorded
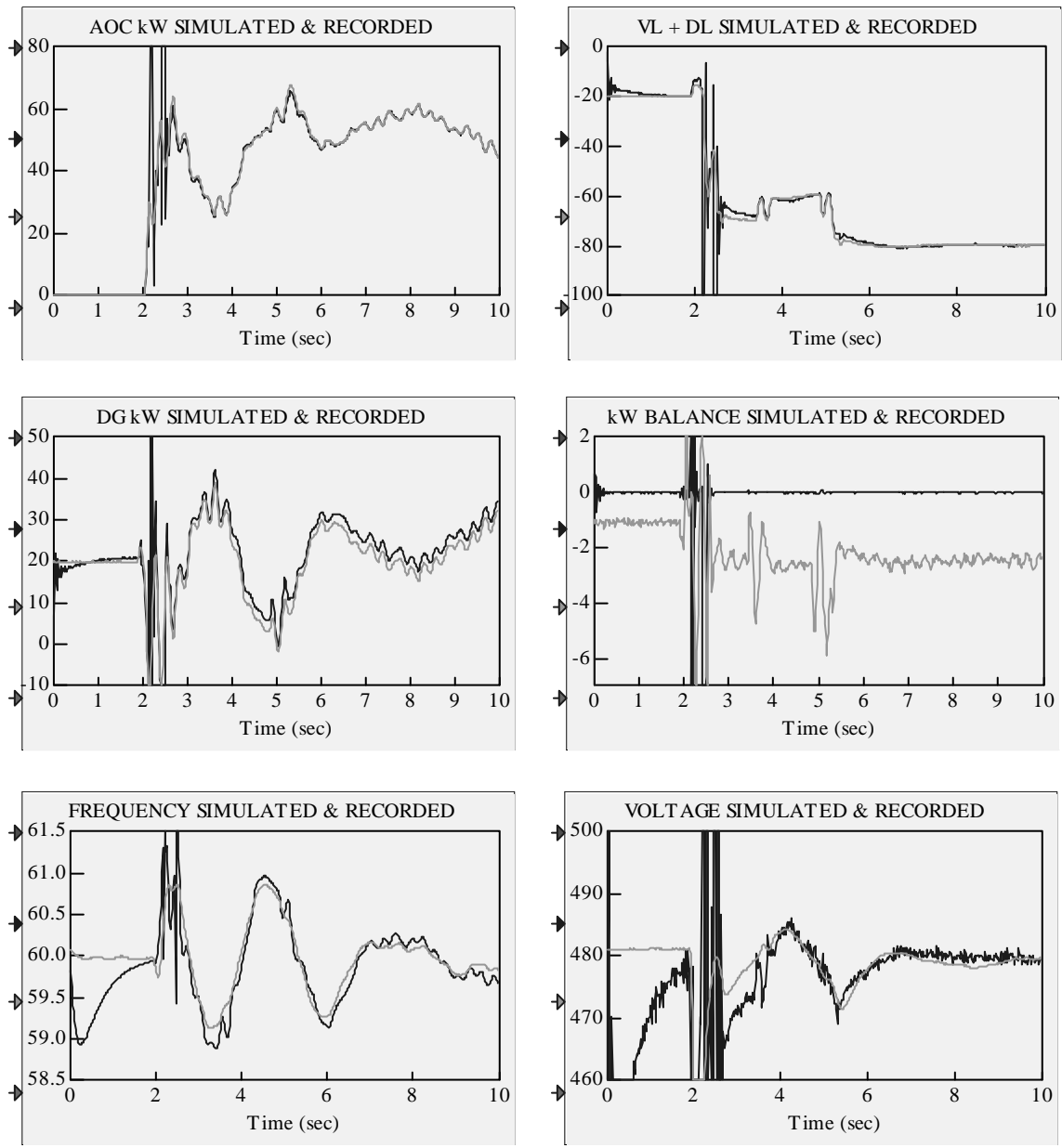
Figure 11-5. Simulation results for the AOC start-up data: the dark line is used for traces simulated and the light line is used for traces recorded
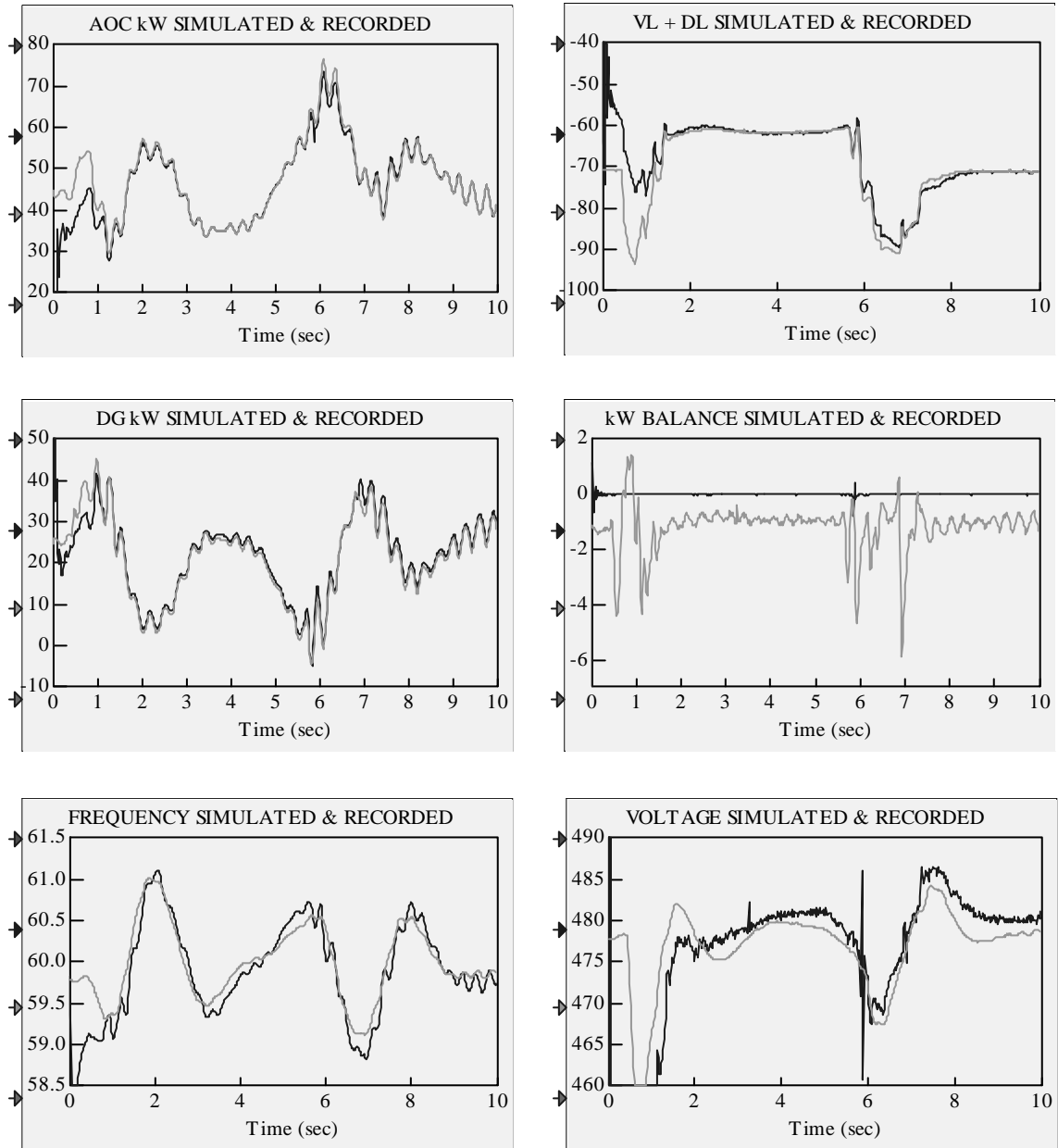
Figure 11-6. Simulation results for the step-in load data: the dark line is used for traces simulated and the light line is used for traces recorded
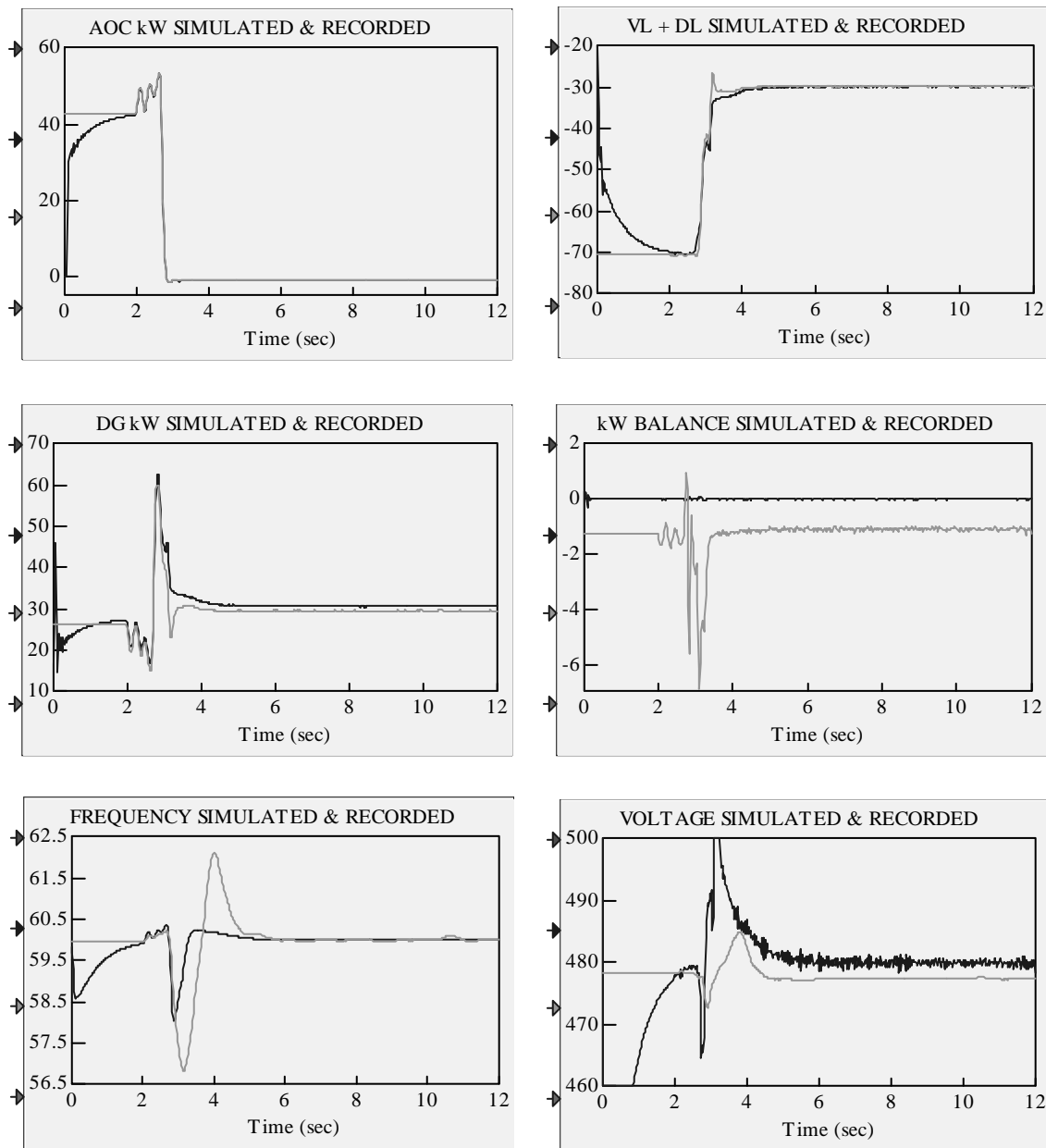
Figure 11-7. Simulation results for the AOC shutdown data: the dark line is used for traces simulated and the light line is used for traces recorded
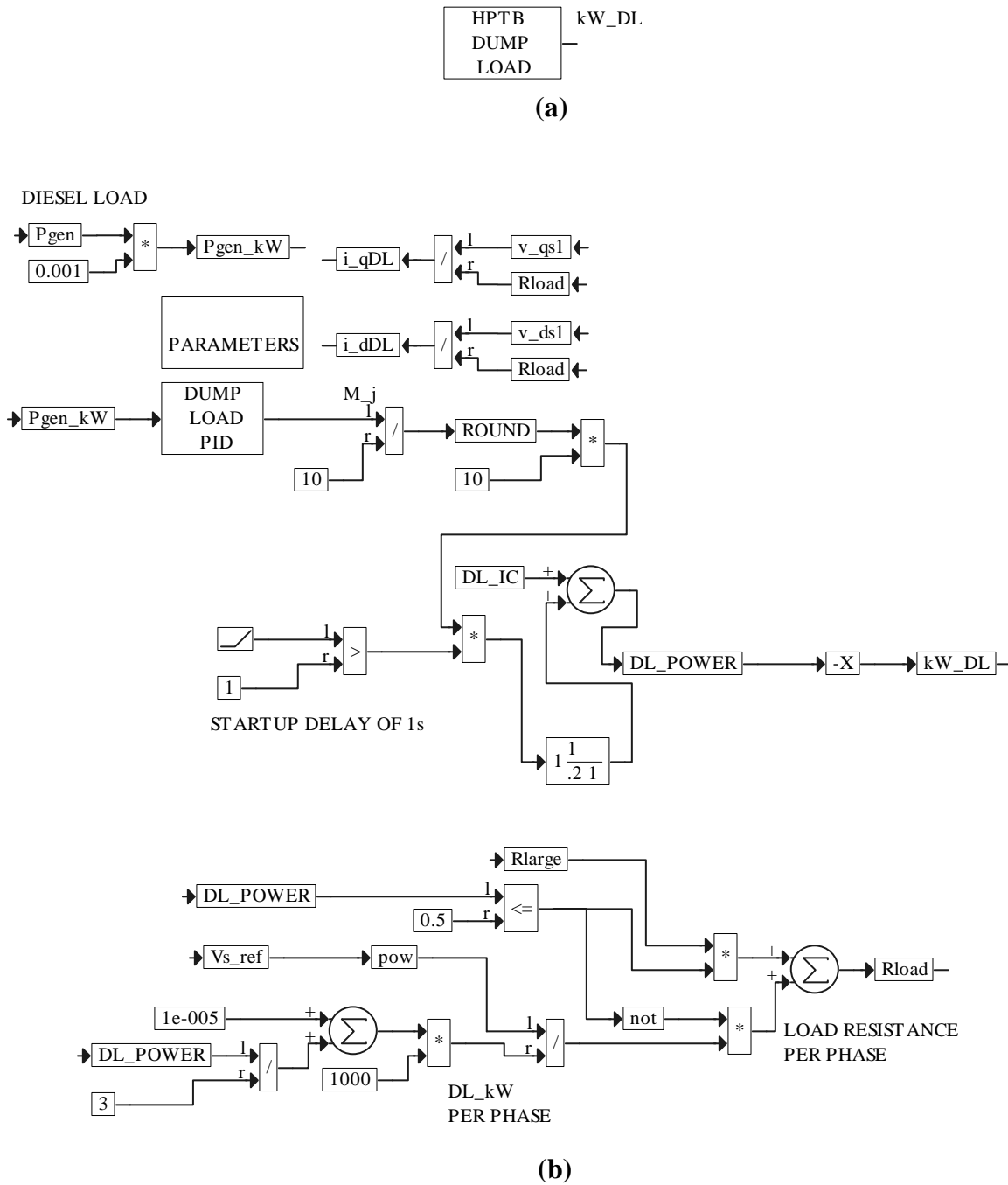
Figure 11-8. DL block with the Wales Control System Dump Load Dispatch used at the HPTB: (a) top-level view and (b) first-level expansion

| 10000 → Rlarge — | resistance representing no dump load |
0.08 → T_i —	integral time
0.31 → T_d —	derivative period
0.04 → T_s —	sampling interval (if changed, should also be changed in pulse train generator in the sampler of diesel load)
200 → M_max —	maximum dump load [kW]
2 → K_r —	derivative gain
1.5 → K_c —	proportional gain
60 → P_DIES —	diesel capacity [kW]
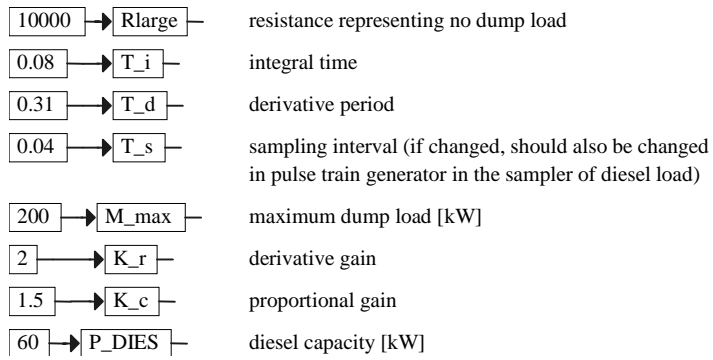
Figure 11-9. Expansion of the PARAMETERS block
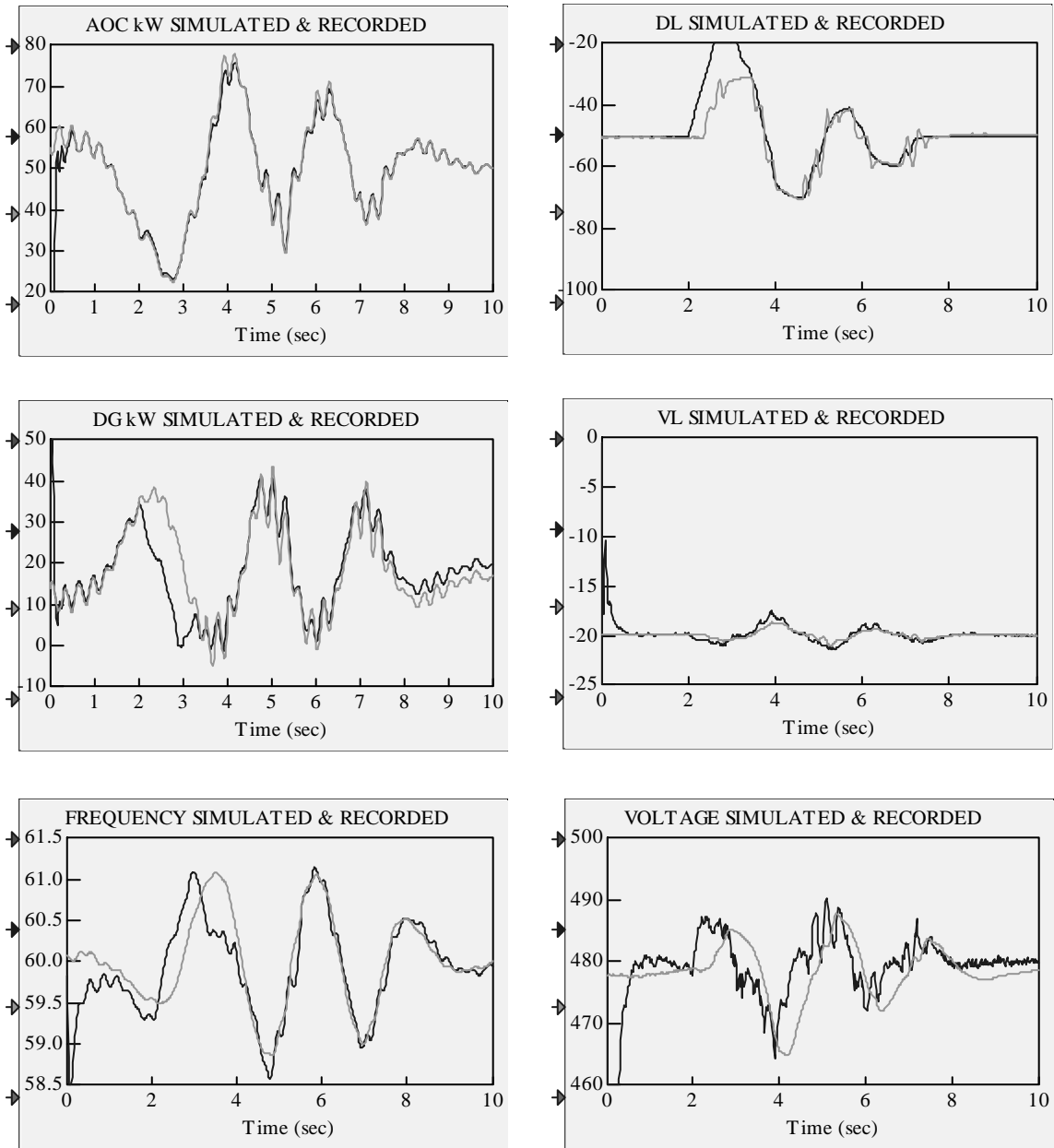
Figure 11-10. Simulation results for the case A data with a real DL model included: the dark line is used for traces simulated and the light line is used for traces recorded
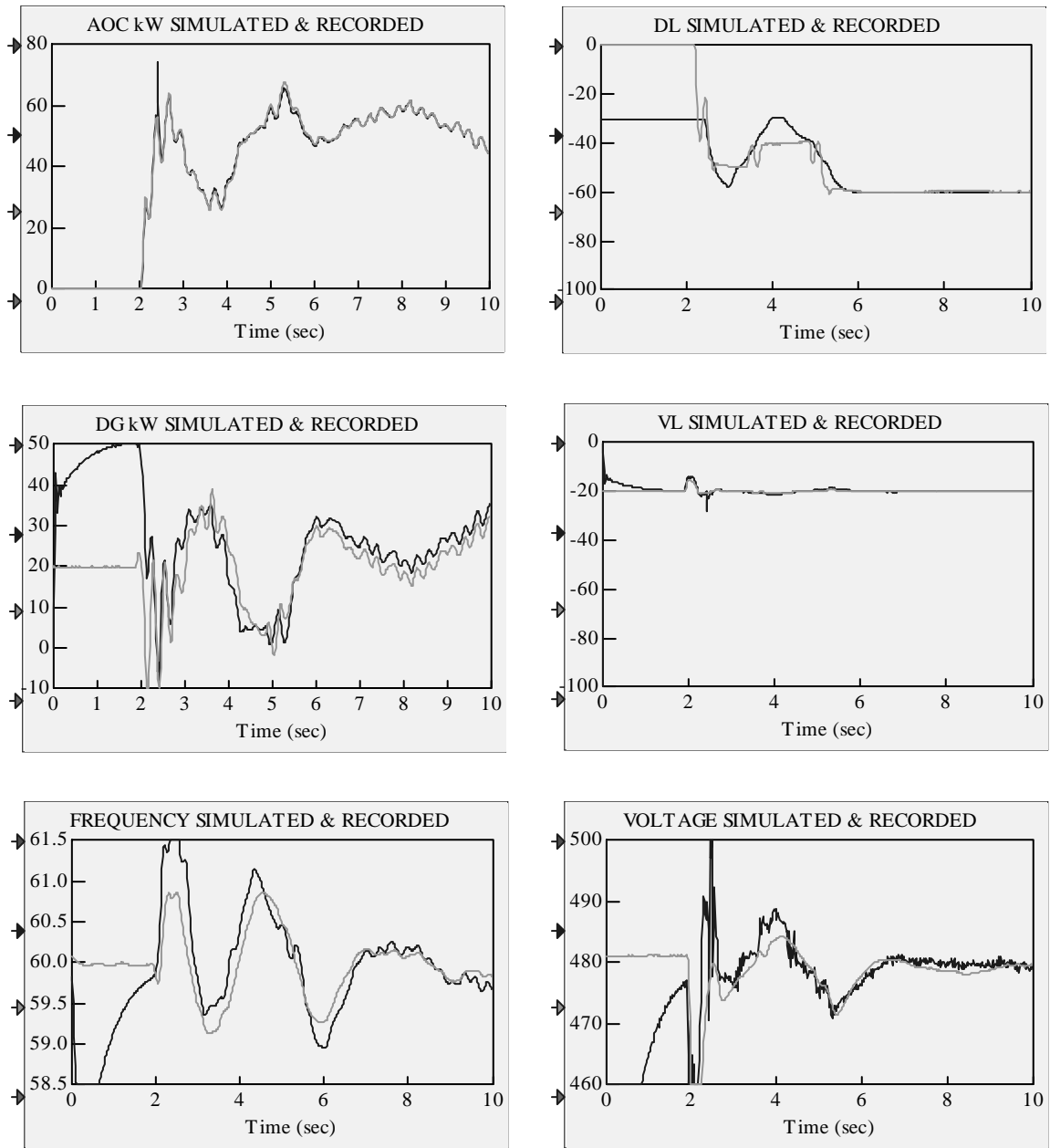
Figure 11-11. Simulation results for the AOC start-up data with a real DL model included: the dark line is used for traces simulated and the light line is used for traces recorded
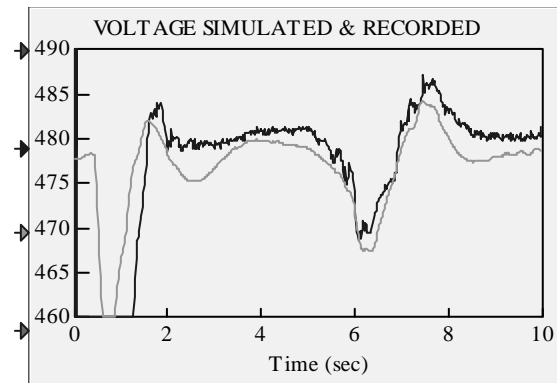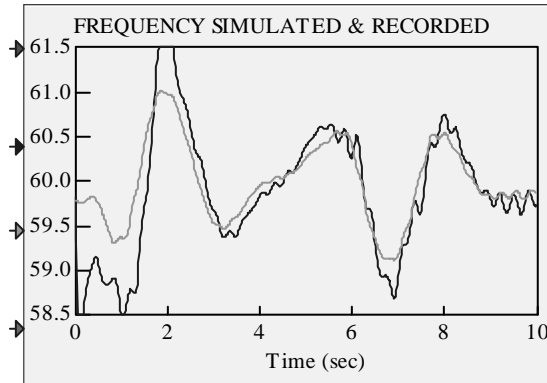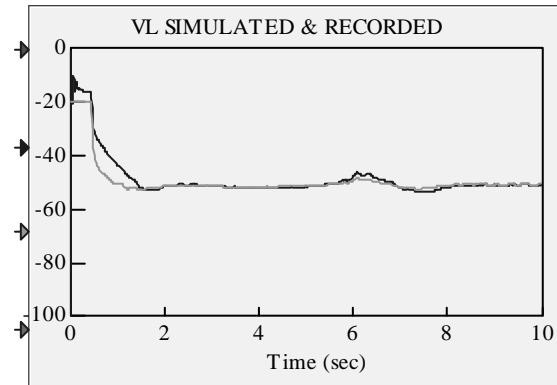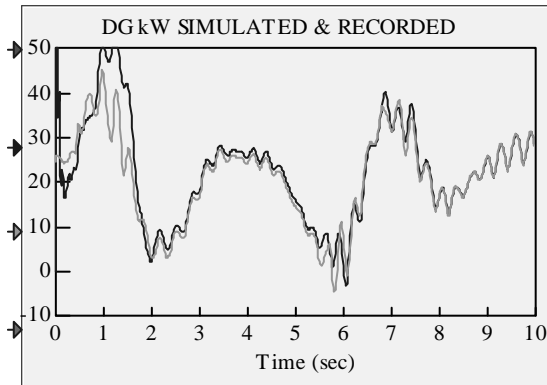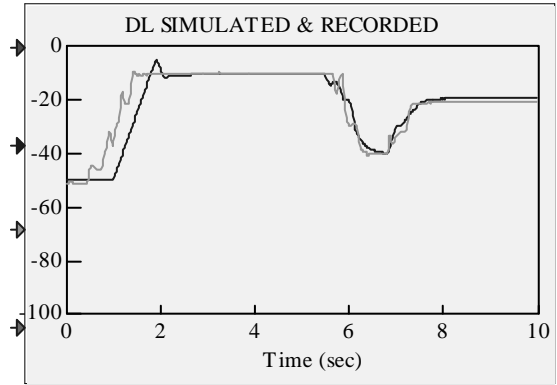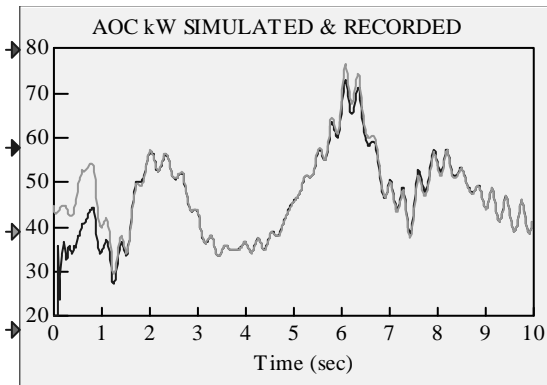
Figure 11-12. Simulation results for the step-in load data with a real DL model included: the dark line is used for traces simulated and the light line is used for traces recorded
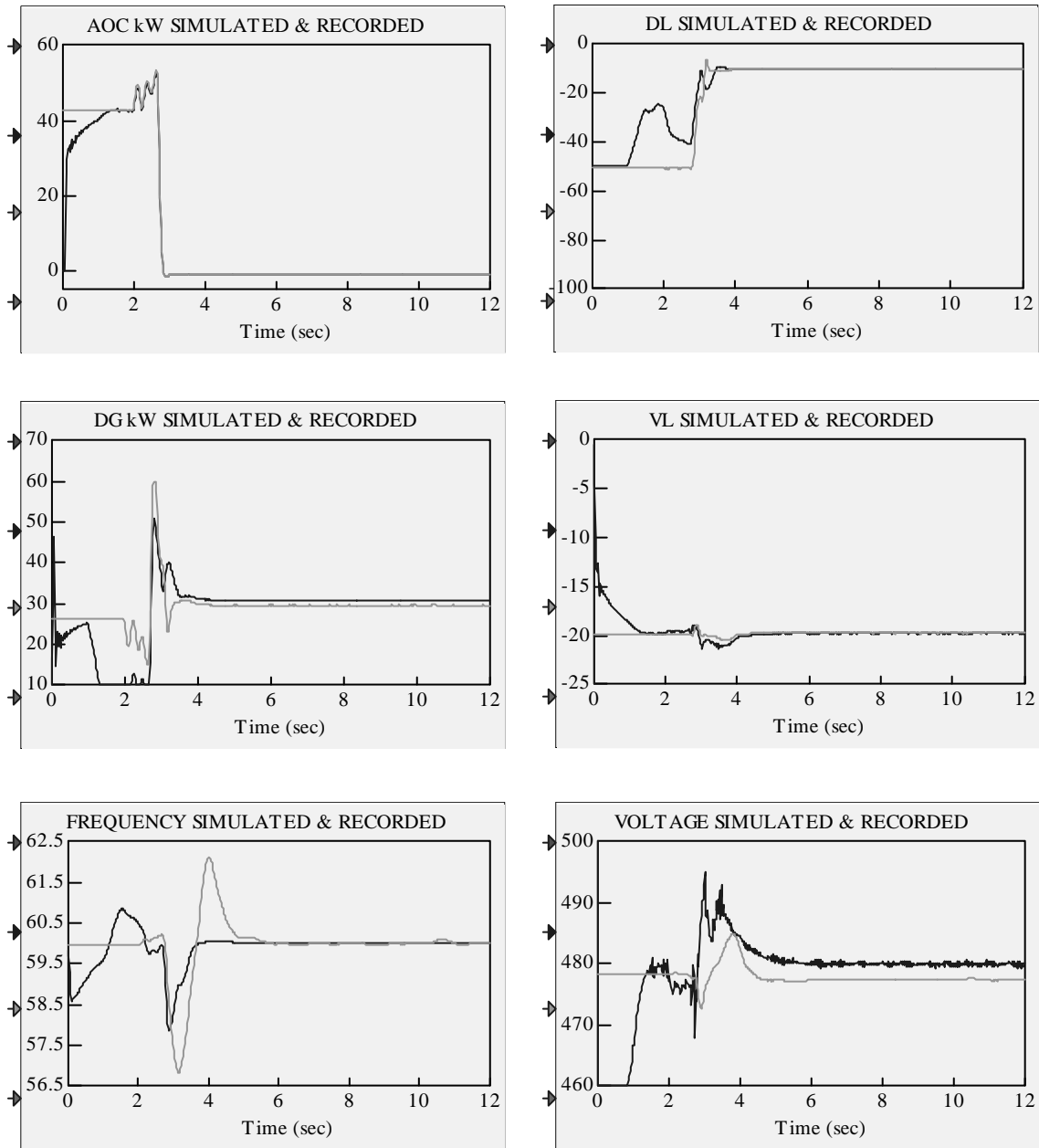
Figure 11-13. Simulation results for the AOC shutdown data with a real DL model included: the dark line is used for traces simulated and the light line is used for traces recorded

How to Set up and Run the Simulation

To demonstrate a step-by-step procedure on how to set up and run the simulation, we use the Case Study 3 presented in Chapter 10. For the user's convenience of the user, we repeat Figure 10-5 here, to show the configuration of the power system considered in a form of single-line diagram and top-view of the RPM-S$_{IM}$ simulation.
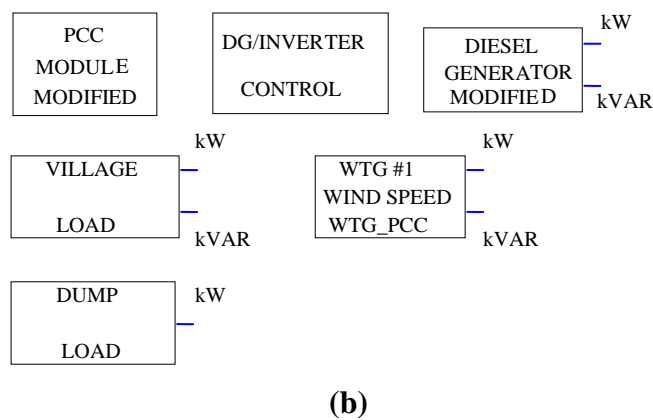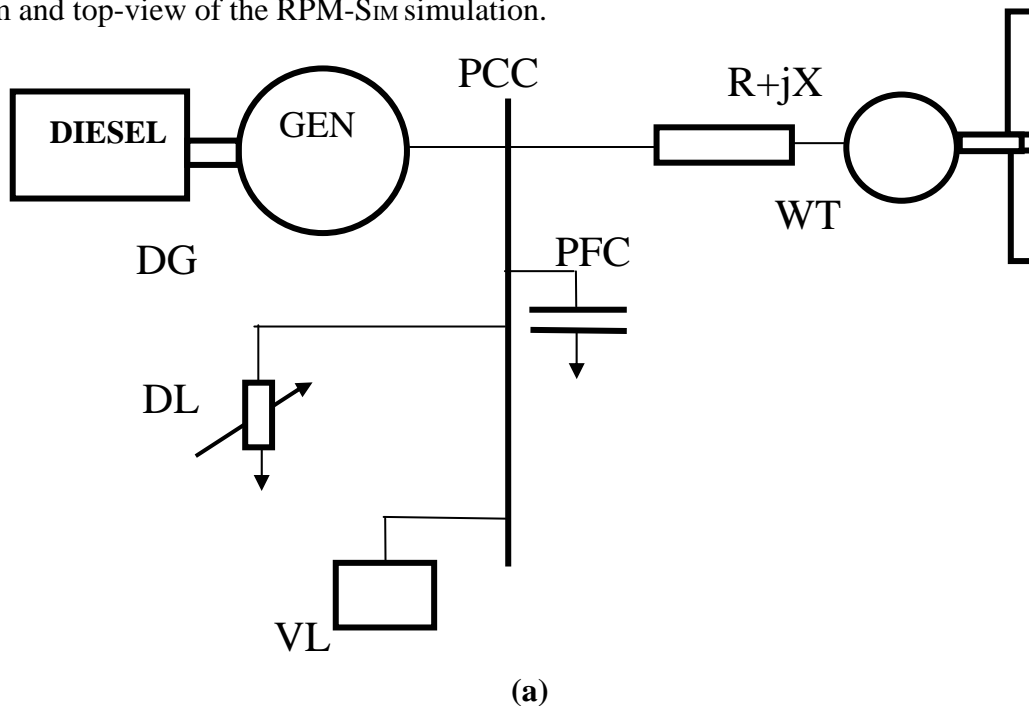
(a)

(b)

Figure 10-5. Power system composed of a DG, an AC WT, a DL, and a VL: (a) single-line diagram and (b) top view of the RPM-S$_{IM}$ simulation

First, copy the directory RPMSim_DST from the CD-ROM and paste it as a subdirectory of Vissim directory.

To set up the simulation:

1. Click on the VisSim icon to obtain the simulation screen.

2. Use the Save As command from the File menu to assign the file name and directory for your simulation.

3. Add RPM-S$_{\text{IM}}$ modules involved in the power system you would like to simulate. Recall that the PCC module must be included in every simulation diagram, and add this module first performing the following steps:

    *   Click on the Add command in the File menu to obtain the Add File dialog box; select directory c:\Vissim4\RPMSim_DST, and the list of RPM-S$_{\text{IM}}$ files will appear. Find the PCC_m.vsm file and double click on it.
    *   You will see a rectangle (with the cursor of the mouse attached) in the simulation screen. Click the mouse and the rectangle will turn into a RPM-S$_{\text{IM}}$ block named PCC MODULE MODIFIED.
    *   Recall the multilevel/compound block simulation concept of VisSim and explore the contents of this module. Click on the block with the right button of the mouse to see the top-view diagram of the PCC as shown in Figure 2-2. For the description and exploration of the compound blocks shown in this diagram, refer to Chapter 2.
    *   The values of the parameters included in the PARAMETER MODULE block can be changed by opening this block (clicking the right button of the mouse on it) and clicking the right button on the parameter value. This opens the Setup Block dialog box and makes the change possible.
    *   To move up one simulation level, point the mouse cursor to empty space in the simulation screen and click the right button.

    Repeat the same steps for each module involved when you are adding their files to the simulation screen. For Case Study 3 you must add DG_m.vsm, DG_INV_CTRL.vsm, VL.vsm, DL.vsm, and wtg_base_m.vsm. As you move up and down the simulation hierarchy of a particular module, refer to the associated chapter in this manual. This will help you to understand what you see, and you will find out which parameters can be changed to represent your system.

    This step will bring you to the simulation diagram shown in Figure 10-5(b). You can move any element of the simulation diagram (or a selected group of elements) by dragging it with the mouse.

4. To monitor your system variables of interest, you will use a VisSim display block (for numerical value) or plot block (to plot your variable as a function of time). Both are available with a click of the mouse in the VisSim menu Blocks\Signal Consumers. These monitor blocks can be directly connected with mouse to a particular variable on the simulation diagram. Alternatively, the variable to be monitored can be replicated (using the Variable block available in the VisSim menu Blocks\Annotation, and setting its name as desired in the associated dialog box) and connected to the display or plot block. You can connect up to eight variables (VisSim 4.0) to a single plot block. The unused connectors of the plot block can be removed with the Remove Connector command in the Edit menu. Double clicking (on the plot block) with the left mouse button opens the Plot Setup dialog box. The options available are self-explanatory. Consult the VisSim manual if necessary.

    Both the display block and the plot block can be added to any simulation level.

5. Open the Simulate menu and click on the Simulation Setup command. The dialog box appears. Choose the adaptive Bulirsh-Stoer integration algorithm to maintain stability. To specify a step size, follow these steps:

    (a) In the Step Size box under Range Control, enter the size that represents the maximum length of the interval. The practical value is 0.0001. If you make this value larger, the algorithm will attempt to use it. This will result in oscillations of your variables, which do not reflect the behavior of the real system. It may even result in simulation instability leading to the overflow error, and may stop the simulation right after it starts.
    (b) In the Min Step Size box under the Integration Algorithm menu, enter a size that represents the minimum length of the interval. The default value of 1e-006 is a good choice.

    Set up the simulation range by choosing the Range Start and Range End parameters.

To control the simulation—to start, stop, and continue—you can use the commands from the Simulate menu or from the simulation Control Panel, or the pushbuttons from the toolbar. Consult the VisSim manual for more details.

GENERATOR DATA SHEET

E7201L1

60 KW 208-240/416-480   Voltage 1800 RPM. 60 Hz, 0.8 P.F.
Amps 208-180/104-90   Weight 825
40 °C Ambient, Dim Code   Engine 4-53
12 Leads

| | | HZ | KW | Voltage | NOMINAL EFFICIENCY | | | .8 P.F. FULL LOAD ON* |
	Duty				Full Load	3/4 Load	1/2 Load	Voltage DIP
NAME PLATE RATING	CONT	60	50	208/416	85.2	84.9	82.9	11.2
			50	240/480	85.7	85.0	82.4	8.4
	STAND BY		60	208/416	84.5	84.7	83.3	13.5
			60	240/480	85.3	85.1	83.1	10.1
MAXIMUM RATING PER NEMA MG 1 SPECIFICATIONS	CONT	60		208/416				
				230/460				
				240/480				
		50		190/380				
				200/400				
				220/440				
	STAND BY	60		208/416				
				230/460				
				240/480				
		50		190/380				
				200/400				
				220/440				

1800 RPM Motor Starting (Taken on Constant Speed Driver*)
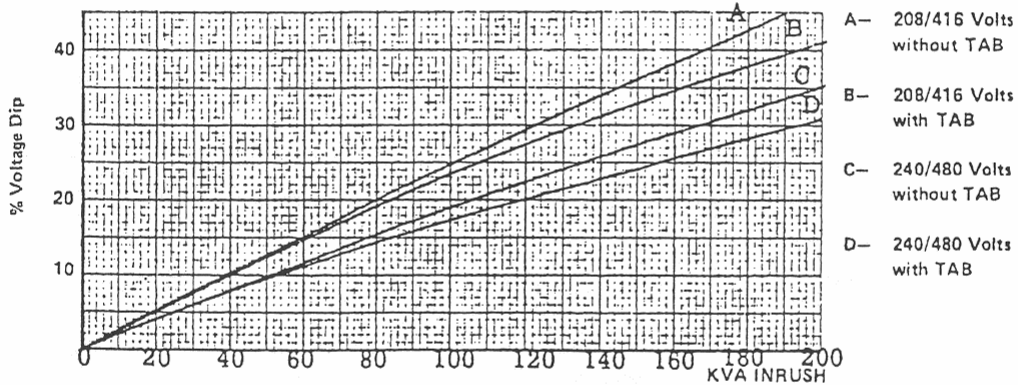
Voltage Dip VS: KVA INRUSH

A— 208/416 Volts without TAB

B— 208/416 Volts with TAB

C— 240/480 Volts without TAB

D— 240/480 Volts with TAB

1500 RPM Motor Starting (Taken on Constant Speed Driver*)

Voltage Dip VS: KVA INRUSH

E— 190/380 Volts without TAB

F— 190/380 Volts with TAB

G— 220/440 Volts without TAB

H— 220/440 Volts with TAB
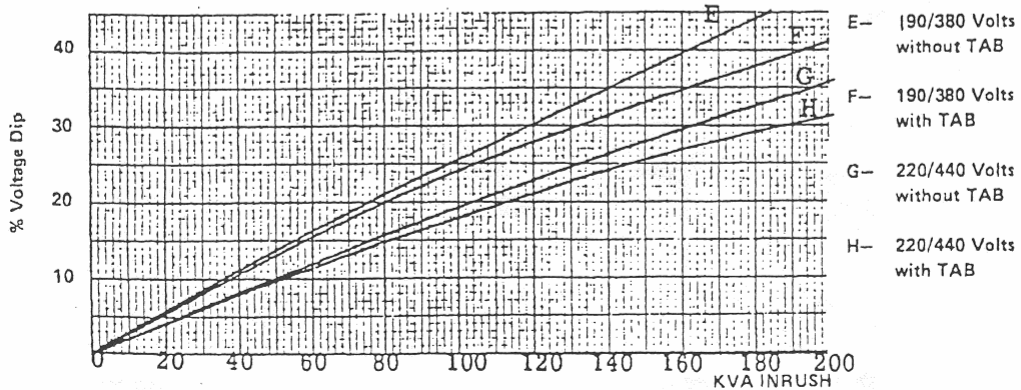
*Engine Droop will effect Voltage Dip

158

PERFORMANCE PARAMETERS
AT NAMEPLATE RATING
EXCEPT WHERE NOTED

DESCRIPTION	VOLTAGE	MAX. TOTAL (%) DELCO	NEMA	MAX. INDIVIDUAL (%) DELCO	NEMA
HARMONIC CONTENT	208/416		No Limit		No Limit
No Load L-L	240/480	1.71	No Limit	1.54	No Limit
WAVE FORM DEV. FACTOR	208/416		10 Max.		
No Load L-L	240/480	4.14	10 Max.		

TELEPHONE INFLUENCE
FACTOR—TIF 39.6

Symbol	Machine Constant @ 480 Volts	Value
Xd	Direct Axis Sync. Reactance	1.81 P.U.
X'd	Direct Axis Transient Reactance	.191 P.U.
X"d	Direct Axis Sub Trans. Reactance	.084 P.U.
Xq	Quadrature Axis Sync. Reactance	1.12 P.U.
X"q	Quadrature Axis Trans. Reactance	.238 P.U.
Xa	Zero Sequence Reactance	.040 P.U.
X2	Negative Sequence Reactance	.161 P.U.
T'do	Open Circuit Time Constant	.967 Sec.
T'd	Short Circuit Time Constant (Transient)	.061 Sec.
T"d	Short Circuit Time Constant (Sub Transient)	.018 Sec.
Zd	Synchronous Impedance	1.81 P.U.

Resistances (Ω) at 25°C

Exciter Fld	50.5
Exciter Arm	.43
Rotating Fld	2.98
Stator	.21

12 Volt Battery
Test @ 1800 RPM

Connected For

Low Voltage	High Voltage
187	374

TAB Model #	H3801RCDA
Resistor Setting	10 Ohms
Tap Selection	4-9 & 10-3

SHORT CIRCUIT DRIVE	208/240	416/480
Three Phase	636.8 Amps	318.4 Amps

EXCITATION REQUIREMENTS

Load		Operating Voltage	Exciter Fld. Amp.	TAB Voltage
No Load		208/416	.242	-1.45
		240/480	.338	-1.5
Full Load	1.0 P.F.	208/416	.504	14.7
		240/480	.532	9.8
	.8 P.F.	208/416	.798	19.6
		240/480	.813	13.0

CFM   Heat Rejection at Max. Nameplate Rating 37, 563 BTU/Hr.

WR² Dwg #   XB-203800-612

Outline Drawing #   2800795

A. C. GEN. DATA E7201L1					SER. NO.	

Type	KVA	Volts	Amps.	Phase	Cycles
NEMA	75	$\frac{208}{416}$ – $\frac{240}{480}$	$\frac{208}{104}$ – $\frac{180}{90}$	3	60

Frame	Temp. - AMB.	P.F.	Poles	Duty	RPM.
#2 B.H.	40°C MAX.	80%	4	CONTINUOUS	1800

Generator

1	Direct Axis Synchronous Reactance (Unsaturated)	Xd	1.81	PER UNIT
2	Quadrature Axis Synchronous Reactance (Unsaturated)	Xq	1.12	" "
3	Direct Axis Transient Reactance (Rated Voltage)	X'd	.191	" "
4	Direct Axis Subtransient Reactance (Rated Voltage)	X"d	.084	" "
5	Quadrature Axis Subtransient Reactance	X"q	.238	" "
6	Zero Sequence Reactance	Xo	.040	" "
7	Negative Sequence Reactance	X2	.161	" "
8	Direct Axis Transient Open Circuit Time Constant	T'do	.967	SECOND
9	Short Circuit Transient Time Constant	T'd	.061	"
10	Short Circuit Sub Transient Time Constant	T"d	.018	"
11	Synchronous Impedance	Z1	1.81	PER UNIT
12				
13	Field Resistance @ 25° C		2.98	OHMS.
14	Field Current @ F/L, Rated PF		20.4	AMPS
15	Field Current @ N/L, Rated Voltage		8.0	"
16	Field Current @ N/L, 550 Volts		13.2	"
17	Continuous Duty Field Voltage		90.5	VOLTS
18	Inherent Regulation		26.0 %	
19	Recommended Field Discharge Resistor	N./A		
20	Wave Form Deviation. No Load Line-Line 4.14 %	Line-Neutral 2.13 %		
21	Wave Form Deviation. Full Load Line-Line 3.06 %	Line-Neutral 2.73 %		
22				
23				

Exciter - Type BRUSHLESS Rpm 1800   Ser.#

1	2.5 KW 100 Volts 25 Amp.				
2	Field Res. @ 25° C 50.5 Ohms.				
3	Recommended Rheostat: —— Plate(s) Ohms. Amps.				
4	Curve No. C-6505-A				

Wales Control System Dump Load Dispatch at the Hybrid Power Test Bed

I.   DUMP LOAD HARDWARE

The dump load at the HPTB can be modelled as (20) 10-kW elements.

II.   DIESEL ON DUMP LOAD DISPATCH

A.   Purpose: If there is at least 1 diesel on-line, the diesel generator's own controls (speed control and voltage regulator) control system frequency and voltage. The Wales Control System PLC will dispatch dump load elements in order to maintain a minimum load on the diesels.

B.   Method: The Wales Control System dispatches dump load elements to maintain instantaneous diesel load values (as read by the PLC every scan) within a certain range defined by maximum and minimum diesel load values. The algorithm uses a modified PID loop to determine the dump load kW required, subtracts the dump load kW currently on to determine the delta dump load kW required, and divides this value by the dump load step size and rounds to determine the number of dump load elements to add or remove. There are several modifications to a standard PID loop: 1) instead of trying to maintain the process value (diesel load) around one setpoint value, we are trying to maintain the process value between an upper and lower setpoint (max and min diesel load values), so the actual setpoint used to calculate the loop error term depends on whether the process value is greater than the upper setpoint, less than the lower setpoint, or in between; 2) the proportional and derivative terms are combined into one by using a predicted error term; and 3) the derivative term is modified in two ways: a) since there is a large deadband during which the error equals zero, the derivative term is based on the derivative of the process value rather than the derivative of the error term (we can do this because the setpoints are constant), and b) the derivative term is also based on a 310 ms interval rather than the PID loop sample rate to account for the 3-per ripple imposed on the diesel kW values by a 3-bladed turbine. The PID Loop algorithm is defined below.

PID Loop Algorithm:

$$M_j = K_c \times PE_j + K_c \times \frac{T_s}{T_i} \times ES_{j-1}$$

M_j = Control Output (Dump Load Required) [kW] for sampling period j
PE_j = Predicted Error [kW]for sampling period j
E_j = Error [kW] for sampling period j
ES_j = Error Sum [kW]for sampling period (See below) j
K_c = Proportional Gain: 1.50

T_s = Sampling Interval: 40 ms
T_i = Integral Time: 80 ms

Limit Control Output if it goes out of bounds:

$$M_j = M_j \text{ if } 0 < M_j < M_{max}$$
$$= 0 \text{ if } M_j \leq 0$$
$$= M_{max} \text{ if } M_j \geq M_{max}$$

M_{max}= Maximum Control Output Allowed (Total DL kW Available): 200 kW

Error Term Definition:

$$E_j = SP_L - PV_j \text{ if } PV_j \leq SP_L$$
$$= SP_H - PV_j \text{ if } PV_j \geq SP_H$$
$$= 0 \text{ if } SP_L < PV_j < SP_H$$

PV_j = Process Value (Diesel Load) [kW] for sampling period j
SP_L = Lower Setpoint (Minimum Diesel Load) [kW]
 = 10% of current diesel capacity on line
SP_H = Upper Setpoint (Maximum Diesel Load) [kW]
 = 50% of current diesel capacity on line OR 34 kW, whichever is greater

Predicted Error Term Definition:

$$PE_j = SP_L - PPV_j \text{ if } PPV_j \leq SP_L$$
$$= SP_H - PPV_j \text{ if } PPV_j \geq SP_H$$
$$= 0 \text{ if } SP_L < PPV_j < SP_H$$
$$PPV_j = PV_j + K_r \times \left[\frac{PV_j - PV_{j-310ms}}{T_d} \right] \times T_s$$

PPV_j = Predicted Process Value (Predicted Dsl Load) [kW] for sampling period j
$PV_{j-310ms}$ = Process Value (Predicted Dsl Load) [kW] 310 ms BEFORE time of
 sampling period j
T_d= Derivative Period: 310 ms
K_r= Derivative Gain: 2.00

Error Sum Definition:
Freeze Error Sum if last Control Output (before limiting) was out of bounds:

$$ES_j = ES_{j-1} + E_j \text{ if } 0 < M_j < M_{max}$$
$$= ES_{j-1} + MAX(E_j, 0) \text{ if } M_j \leq 0$$
$$= ES_{j-1} + MIN(E_j, 0) \text{ if } M_j \geq M_{max}$$

Documentation for RPM-SIM at NREL's National Wind Technology Center

This CD-ROM contains two directories, 'disclaimer.wri' file and this 'readme.wri' file. Its structure is shown in Figure D-1.

Directory RPMSim_DST has the following simulator modules/components:

> BAT.vsm
> BB_RC.vsm
> DG_INV_CTRL.vsm
> DG_m.vsm
> DL.vsm
> INV.vsm
> NO_DIESEL.vsm
> PCC_m.vsm
> PV_ARRAY.vsm
> PV_INV.vsm
> VL.vsm
> WIND_SPEED.vsm
> wtg_base_m.vsm
> WTG_m.vsm

Directory RPMSim_LIB has the structure shown in Figure D-2 and contains the following subdirectories:

- C_stds

    Contains executable VisSim files for all case studies presented in the manual. The file names used are self-explanatory. These are the following files:

    C_Sn.vsm with n = 1,2,…,7
    C_S8_rc_HPTB_AOC_Mode1.vsm
    C_S8_rc_HPTB_AOC_Mode2.vsm
    C_S8_rc_HPTB_AOC_Mode3.vsm
    C_S9_FURL_BAT_PPT.vsm
    C_S9_FURL_INV_PPT.vsm
    C_S9_FURL_INV_PPTm.vsm
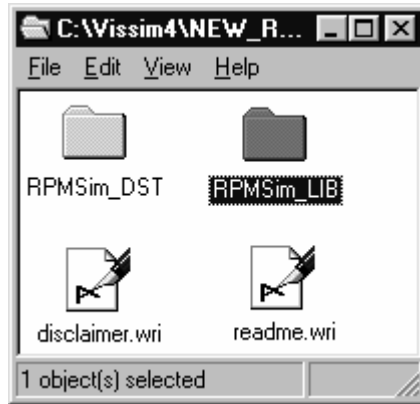
Figure D-1. Structure of the documentation for RPM-Sᴵᴹ
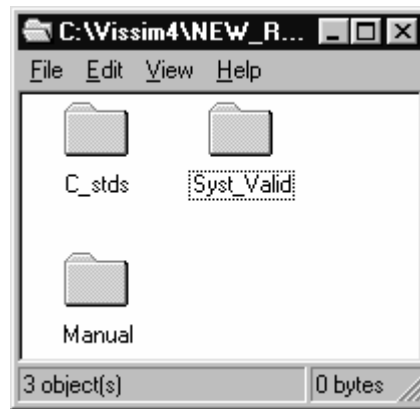
Figure D-2. Subdirectories of the directory RPMSim_LIB

- Syst_Valid

  Contains executable VisSim files, listed below, for system validations described in the manual.

hybrid_casea.vsm	Used to obtain Figure 11-3
hybrid_caseb.vsm	Used to obtain Figure 11-4
hybrid_stup.vsm	Used to obtain Figure 11-5
hybrid_stld.vsm	Used to obtain Figure 11-6
hybrid_s-shd.vsm	Used to obtain Figure 11-7
dl_casea_mod.vsm	Used to obtain Figure 11-10
dl_stup_mod.vsm	Used to obtain Figure 11-11
dl_stld_mod.vsm	Used to obtain Figure 11-12
dl_shd_mod.vsm	Used to obtain Figure 11-13

D-2

- Manual

  Contains the RPM-S<small>IM</small> manual in the form of Microsoft Word files.

NOTE:

All executable files are ready to run under Professional VisSim 4.0 available from Visual Solutions, Inc., 487 Groton Road, Westford, MA 01886, phone (978) 392-0100, fax (978) 692-3102. The Web site is **www.vissim.com**.